

AD-A078 039

COLT INDUSTRIES INC PITTSBURGH PA CRUCIBLE MATERIALS--ETC F/6 11/6  
CONSOLIDATION OF TITANIUM POWDER TO NEAR NET SHAPES.(U)

MAY 78 J H SCHWERTZ , V K CHANDHOK

F33615-74-C-5114

UNCLASSIFIED

AFML-TR-78-41

NL

1 OF 4

AD  
A078039



AD A 078039

18 19  
AFML-TR-78-41

LEVEL #2

6  
CONSOLIDATION OF TITANIUM POWDER TO NEAR NET SHAPES.

10  
J. H. Schwertz, V. K. Chandhok  
V. C. Peterson, V. R. Thompson

Crucible Research Center, Colt Industries  
P. O. Box 88 Pittsburgh, Pennsylvania 15230 *See inside cover*

11  
May 1978

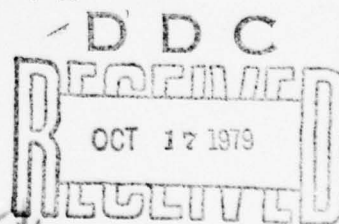
12 333

9  
Final Report. 1 February 1974 - 1 March 1978

15 F 33615-74-C-5114

Approved for Public Release; Distribution Unlimited

MANUFACTURING TECHNOLOGY DIVISION  
AIR FORCE MATERIALS LABORATORY  
AIR FORCE SYSTEMS COMMAND  
WRIGHT PATTERSON AIR FORCE BASE, OHIO 45433



405698

79 10 16 008



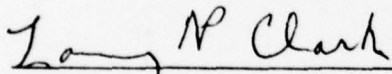
# NOTICE

When Government drawings, specifications, or other data are used for any purpose other than in connection with a definitely related Government procurement operation, the United States Government thereby incurs no responsibility nor any obligation whatsoever; and the fact that the government may have formulated, furnished, or in any way supplied the said drawings, specifications, or other data, is not to be regarded by implication or otherwise as in any manner licensing the holder or any other person or corporation, or conveying any rights or permission to manufacture, use, or sell any patented invention that may in any way be related thereto.

Copies of this report should not be returned unless is required by security considerations, contractual obligations, or notice on a specific document.

This final report was submitted by Colt Industries, Crucible Materials Research Center, Pittsburgh, PA, under Contract F33615-74-C-5114, Manufacturing Methods Project 171-4, "Consolidation of Titanium Powder to Near Net Shapes." Mr. Larry P. Clark, AFML/LTM, was the Laboratory Project Engineer.

This technical report has been reviewed and is approved for publication.



LARRY P. CLARK  
Project Engineer

FOR THE COMMANDER



HENRY A. JOHNSON  
Chief, Metals Branch  
Manufacturing Technology Division

SECURITY CLASSIFICATION OF THIS PAGE (When Data Entered)

REPORT DOCUMENTATION PAGE		READ INSTRUCTIONS BEFORE COMPLETING FORM															
1. REPORT NUMBER AFML-TR-78-41	2. GOVT ACCESSION NO.	3. RECIPIENT'S CATALOG NUMBER															
4. TITLE (and Subtitle)  CONSOLIDATION OF TITANIUM POWDER TO NEAR NET SHAPES		5. TYPE OF REPORT & PERIOD COVERED Final Technical Report Feb. 1, 1974/March 1, 1978															
		6. PERFORMING ORG. REPORT NUMBER															
7. AUTHOR(s) J. H. Schwertz V. K. Chandhok V. C. Peterson and V. R. Thompson		8. CONTRACT OR GRANT NUMBER(s)  F33615-74-C-5114															
9. PERFORMING ORGANIZATION NAME AND ADDRESS CRUCIBLE RESEARCH CENTER - COLT INDUSTRIES P. O. Box 88 Pittsburgh, Pennsylvania 15230		10. PROGRAM ELEMENT, PROJECT, TASK AREA & WORK UNIT NUMBERS															
11. CONTROLLING OFFICE NAME AND ADDRESS Air Force Materials Laboratory Air Force Systems Command Wright-Patterson Air Force Base, Ohio 45433		12. REPORT DATE May 1978															
		13. NUMBER OF PAGES															
14. MONITORING AGENCY NAME & ADDRESS (if different from Controlling Office)		15. SECURITY CLASS. (of this report)  UNCLASSIFIED															
		15a. DECLASSIFICATION/DOWNGRADING SCHEDULE															
16. DISTRIBUTION STATEMENT (of this Report)  Approved for Public Release; Distribution Unlimited																	
17. DISTRIBUTION STATEMENT (of the abstract entered in Block 20, if different from Report)																	
18. SUPPLEMENTARY NOTES General Electric (GE); Aircraft Engine Group, Cincinnati, Ohio; and McDonnell Aircraft Company (MCAIR), St. Louis, Missouri acted as major sub-contractors and conducted testing, machining, and inspection activities for development of production specification.																	
19. KEY WORDS (Continue on reverse side if necessary and identify by block number)																	
<table border="0"> <tr> <td>Ti-17 Alloy</td> <td>Atomization</td> <td>Cost Analysis</td> </tr> <tr> <td>Titanium - Ti-6-4 Alloy</td> <td>Ceramic Molds</td> <td>Material Specifications</td> </tr> <tr> <td>Powder Metallurgy</td> <td>Mechanical Properties</td> <td>Process Specifications</td> </tr> <tr> <td>Hot Isostatic Pressing</td> <td>Inclusions</td> <td></td> </tr> <tr> <td colspan="3"><u>Near Net Shape</u></td> </tr> </table>			Ti-17 Alloy	Atomization	Cost Analysis	Titanium - Ti-6-4 Alloy	Ceramic Molds	Material Specifications	Powder Metallurgy	Mechanical Properties	Process Specifications	Hot Isostatic Pressing	Inclusions		<u>Near Net Shape</u>		
Ti-17 Alloy	Atomization	Cost Analysis															
Titanium - Ti-6-4 Alloy	Ceramic Molds	Material Specifications															
Powder Metallurgy	Mechanical Properties	Process Specifications															
Hot Isostatic Pressing	Inclusions																
<u>Near Net Shape</u>																	
20. ABSTRACT (Continue on reverse side if necessary and identify by block number) This program was conducted to develop the technology necessary to establish a cost effective approach to the production of titanium alloy parts for both aircraft engine and airframe applications. This approach was based on a PM <sup>HIP</sup> near-net shape process utilizing ceramic mold techniques in conjunction with Hot Isostatic Pressing to a minimum machining envelope. Program objectives included: (1) the optimization of an existing PM process for the HIP of near-net shapes of titanium using low-cost tooling; (2) the																	

DD FORM 1 JAN 73 1473

EDITION OF 1 NOV 65 IS OBSOLETE

SECURITY CLASSIFICATION OF THIS PAGE (When Data Entered)

405-698

20.

ABSTRACT cont.

reduction of the process to an efficient, cost effective, manufacturing procedure; and (3) thorough characterization of the end product.)

In cooperation with General Electric (GE) and McDonnell-Douglas (MCAIR) as sub-contractors, representative components and alloys were selected for this program. These were a Ti-17 compressor stub shaft and a Ti-6-4 keel splice former. Both parts were applicable to current Air Force requirements. Crucible Materials Research Center (CMRC) conducted the iterative shape development and production of actual parts for evaluation by GE and MCAIR.

Hot Isostatic Pressing parameters were optimized for both the Ti-17 and Ti-6-4 alloy using the ceramic mold process. SiO<sub>2</sub> was chosen as the most promising mold material.

The ability to produce near-net shapes of both engine and airframe components was successfully demonstrated. Both parts exhibited comparable properties to cast and wrought material with the exception of Low Cycle Fatigue requirements on the engine stub shaft. This problem was primarily attributed to non-metallic inclusions from the powder atomization process and also microstructural effects. Efforts to resolve this problem are being considered in future programs.

A cost analysis on both the engine stub shaft and the keel splice former was performed based on both experimental P/M powder price and projected powder price on a production level. The results indicate that a potential exists for the HIP process to reduce both input material and machining costs compared to current cast and wrought product.

Tentative material and process specifications have been developed and revised to reflect the latest technology for P/M manufacture of Ti-17 and Ti-6-4 alloy parts.

Accession For	
NTIS GRL&I	<input checked="" type="checkbox"/>
DDC TAB	<input type="checkbox"/>
Unannounced	<input type="checkbox"/>
Justification	
By _____	
Distribution/ _____	
Availability Codes	
Dist	Avail and/or special
A	

## PREFACE

This final technical report covers the work performed under Air Force Contract F33615-74-C-5114 during the period of February 1, 1974 through March 1, 1978. The work conducted under this contract was technically monitored by Mr. L. P. Clark, Manufacturing Technology Division (AFML/LTM), Air Force Materials Laboratory (AFSC), Wright-Patterson Air Force Base, Ohio.

This report was prepared by Crucible Materials Research Center (CMRC), Pittsburgh, Pa., as prime contractor. Mr. V. R. Thompson (CMRC) was the program manager and Mr. J. H. Schwertz (CMRC) was the principal investigator. The shape development was carried out by Mr. V. K. Chandhok (CMRC), the titanium physical metallurgy by Mr. V. C. Peterson (CMRC), and the powder characterization by Mr. C. F. Yolton (CMRC). Major sub-contractors on this program were General Electric Company (GE); Aircraft Engine Group, Cincinnati, Ohio; McDonnell Aircraft Company (MCAIR), St. Louis, Missouri; and Battelle's Columbus Laboratory (BCL), Columbus, Ohio. At GE, the overall activity was under the direction of Mr. T. K. Redden with Messrs. R. Peebles and E. Young providing technical support. Mr. H. Turner directed the MCAIR effort; he was assisted by Messrs. R. Kotfila and W. Richards. At BCL, Mr. J. Mueller was responsible for their portion of the program.

Mr. J. N. Fleck was originally the principal investigator on the program and responsible for most of the technical direction. The authors, in behalf of Mr. Fleck, would like to express their appreciation of all the above mentioned personnel for their interest and cooperation during the course of this program.

The data contained herein are published for informational purposes only and do not necessarily represent the recommendations, conclusions, or approval of the Air Force.



## TABLE OF CONTENTS

SECTION	PAGE
I. INTRODUCTION	1
1.1 General Background	1
1.2 Program Goals and Approach	2
II. PROGRAM PLAN	6
2.1 Objectives and Philosophy	6
2.2 Powder Production (Phase I, Task I)	6
2.3 Preferred HIP Parameters (Phase I, Task II)	8
2.4 Shape Making Evaluation (Phase I, Task III)	10
2.5 NDI of Trial Shapes (Phase I, Task IV)	16
2.6 Preliminary Specifications (Phase I, Task IV)	16
2.7 Engine Stub Shaft Evaluation (Phase II, Task I)	16
2.8 Airframe Keel Splice Former Evaluation (Phase II, Task II)	17
2.9 Specifications, Economic Analysis, Data Sheet (Phase II, Task III)	17
III. RESULTS AND DISCUSSION	20
3.1 Phase I - Shape Development	20
3.1.1 Task I - Powder Production	20
3.1.2 Task II - Preferred HIP Parameters	32
3.1.3 Task III - Shape Making Evaluation	109
3.1.4 Task IV - Non-destructive Inspection (NDI) of Trial Shapes	139
3.2 Phase II - Component Development	150
3.2.1 Task I - Engine Stub Shaft Evaluation	150
3.2.2 Task II - Airframe Keel Splice Former Evaluation	197
3.2.3 Task III - Economic Analysis and Tentative Material and Process Specifications	237
IV. CONCLUSIONS AND RECOMMENDATIONS	242
4.1 Conclusions	242
4.2 Recommendations	243



# TABLE OF CONTENTS (cont'd)

	PAGE
APPENDIX A Summary of all electrode shipped to Nuclear Metals for conversion to powder	245
APPENDIX B Test Data for Ti-17	248
APPENDIX C Test Data for Ti-6-4	254
APPENDIX D Dimensional Analysis	257
APPENDIX E Crack Growth Data for Ti-17	267
APPENDIX F Tentative Specification No. 5114-1 Prealloyed Titanium Powder	271
APPENDIX G Tentative Specification No. 5114-2 Hot Isostatic Pressing (HIP) of Titanium Alloy Powder	280
APPENDIX H Tentative Specification No. 5114-3 Premium Quality, Powder Metallurgy As-Hot Isostatic Pressed (HIP) Ti-6-4 Titanium Base Alloy Parts	289
APPENDIX I Tentative Specification No. 5114-4 Premium Quality, Powder Metallurgy As-Hot Isostatic Pressed (HIP) Ti-6-4 Titanium Base Alloy Parts	300
REFERENCES	310

## LIST OF ILLUSTRATIONS

FIGURE		PAGE
1	Isolated view of Ti-17 stub shaft location in F-101 Engine.	4
2	Target shape for keel splice fitting.	5
3	Location of two keel splice fittings in F-15 fuselage structure.	5
4	Program plan.	7
5	Task II HIP matrix.	9
6	Subscale stub shaft.	11
7	Target Dimensions-Keel splice former for F-15 aircraft.	12
8	Schematic diagram of containerization system used in the Crucible Ceramic Mold Process for P/M parts.	13
9	Flow Diagram of the Crucible Ceramic Mold Process for P/M parts.	15
10	Full-sized stub shaft.	18
11	Finished stub shaft.	19
12	CMRC's Ti PM clean room.	23
13	Particle size distribution of Ti-6-4 powder.	26
14	Particle size distribution of Ti-17 powder.	27
15	S.E.M. photographs of Ti-6-4, Lot 2.	28
16	S.E.M. photographs of Ti-6-4, Lot 3.	29
17	S.E.M. photographs, Ti-17, Lot 5.	30
18	S.E.M. photographs, Ti-17, Lot 6.	31
19	Tungsten inclusion in as-HIP Ti-6-4.	33
20	Microstructure of as-HIP Ti-17.	33

# LIST OF ILLUSTRATIONS (continued)

FIGURE		PAGE
21	Task II HIP matrix.	36
22	Crucible's production autoclave.	37
23	Battelle's 27-inch I.D. autoclave.	37
24	Typical Ti-17 experimental compact.	40
25	Beta-transus series (100X).	43
26	Typical structures, 1550°F BCL HIP (250X).	47
27	Typical structures, 1600°F CSMD (HIP (250X).	48
28	Duplex structure in Ti-17 (250X).	50
29	Typical structures, 1600°F BCL HIP (250X).	51
30	Typical structures, 1750°F BCL HIP (250X).	52
31	Typical structures, 1750°F CSMD HIP (250X).	53
32	Typical Ti-17 surface structures (250X).	54
33	High SiO <sub>2</sub> inclusion (250X).	55
34	Iron inclusion (250X).	55
35	Apparent Beta fleck due to iron inclusion (250X).	55
36	Typical tungsten inclusions.	57
37	Structure of duplex treated Ti-17.	59
38	Inclusion containing Si, Ca, Cr, and Mn.	59
39	Iron inclusion in tensile specimen SM-250.	60
40	Low-cycle fatigue of Ti-17.	66
41	Typical LCF fractures.	67
42	High-cycle fatigue of Ti-17.	69
43	SiO <sub>2</sub> inclusion of HCF fracture-Compact SM-270 (~25X).	70
44	Typical microstructures of 1750°F BCL HIP Ti-6-4 (250X).	73

# LIST OF ILLUSTRATIONS (continued)

FIGURE		PAGE
45	Typical microstructures of 1750°F CSMD HIP Ti-6-4 (250X).	74
46	Typical surface (edge) microstructures of Ti-6-4 (250X).	76
47	G. E. specimen T1, duplex STA.	86
48	G. E. specimen FT, triplex STA.	86
49	SEM surface images in neckdown area of broken G. E. tensile specimen FT.	87
50	SEM surface images in neckdown area of broken CMRC tensile specimen C4.	88
51	LCF data for Ti-17.	90
52	Low-cycle fatigue of CMRC bar.	91
53	Effect of beta-HIP temperature on low-cycle fatigue results.	94
54	Effect of heat-treatment on low-cycle fatigue results.	96
55	Effect of HIP thermal cycle on low-cycle fatigue results.	99
56	Effect of grain boundary alpha on low-cycle fatigue results.	100
57	Effect of re-HIP on low-cycle fatigue results.	101
58	Analysis of an inclusion found on LCF break in SM-357-B.	102
59	Effect of container material on low-cycle fatigue results.	104
60	Ti-17 and Ti-6-4 LCF comparison.	105
61	First shape trial on subscale stub shaft.	110
62	Actual vs Target Shape of first trial (SM-295).	111
63	Second shape trial on sub-scale stub shaft.	113
64	Actual vs Target Shape of second trial (SM-324).	115
65	Comparison of HIP cycles used for first (SM-295, BCL) and second (SM-324, IMT) shape trials.	116

# LIST OF ILLUSTRATIONS (continued)

FIGURE		PAGE
66	Third shape trial on sub-scale stub shaft (SM-337) after re-HIP.	117
67	Actual vs Target Shape of third trial (SM-337).	118
68	Actual vs Target Shape of fourth trial (SM-357).	119
69	Notched low-cycle fatigue of SM-357.	121
70	Actual versus target shape of Fifth Iteration (SM-384).	123
71	Sub-Scale shafts SM-384 and SM-385.	124
72	Low-cycle fatigue results on SM-384.	127
73	Effect of sub-transus HIP on low-cycle fatigue results.	131
74	F-15 Keel Splice Fitting.	133
75	First shape iteration on F-15 keel splice fitting.	134
76	Second shape iteration on F-15 keel splice fitting.	135
77	Third shape iteration on F-15 keel splice fitting.	136
78	Dimensional analysis of keel splice fitting SM-355.	137
79	Ultrasonic test specimens.	140
80	Ti-17 low-cycle fatigue.	157
81	Ti-17 low-cycle fatigue.	158
82	LCF comparison.	159
83	Ti-17 Spin Test Disc Configuration.	161
84	Drive arbor assembly for model discs.	162
85	Cross Sectional View of Spin Pit.	163
86	Spin Pit Test Disc #1.	170
87	Spin Pit Test Disc #2.	171
88	Spin Pit Test Disc #3.	172



# LIST OF ILLUSTRATIONS (continued)

FIGURE		PAGE
89	Fracture Origin - Disc #1.	173
90	Crack Growth Rate Data - SM-557.	174
91	First Shape Trial on Full-Sized Stub Shaft.	176
92	Actual versus target shape on stub shaft compact SM-494.	177
93	Final Shape Trial on Three Full-Size Stub Shafts.	178
94	Target versus actual shape of Part SM-556.	179
95	Target versus actual shape of Part SM-555.	180
96	Target versus actual shape of Part SM-557.	181
97	Low-Cycle Fatigue Results - Ti-17 Full-Scale Stub Shaft (SM-557).	188
98	Low-Cycle Fatigue Results - Ti-17 Full-Scale Stub Shaft (SM-557).	189
99	Notched Low-Cycle Fatigue - Ti-17 Full-Scale Stub Shaft.	190
100	Notched Low-Cycle Fatigue - Ti-17 Full-Scale Stub Shaft.	191
101	Smooth Bar High-Cycle Fatigue.	193
102	Notched Bar High-Cycle Fatigue - Rotating Beam.	193
103	Notched fatigue strength of HIPed Ti-6Al-4V.	201
104	Crack growth rate for WOL specimen S1-1, L-T.	203
105	Crack growth rate for WOL specimen S1-2, L-T.	204
106	Crack growth rate for WOL specimen S2-1, LT-L.	205
107	Microstructure of HIP shape.	207
108	As-HIP keel splice former from pilot run (SM-417).	208
109	Test assembly.	212
110	Set-up for spectrum fatigue testing of forged and hot isostatic pressed keel splice formers 68A333019-2007.	213

# LIST OF ILLUSTRATIONS (continued)

FIGURE		PAGE
111	Hot isostatic pressed and machined keel splice former failed in static test.	216
112	Hot isostatic pressed and machined keel splice former with enlarged holes failed in spectrum fatigue test; life, 14,240 hrs.	217
113	Spectrum fatigue life - flange thickness relationship of keel splice former 68A333019-2007.	218
114	Sketch of a compact tension fracture toughness specimen.	220
115	Low and high magnification views of (a) forged and (b) HIPed Ti-6Al-4V in area of initial crack growth showing dimples of mixed sizes and depth.	221
116	Fracture appearance at intermediate location in a compact tension specimen of (a) forged and (b) HIPed Ti-6Al-4V showing dimples of varying size and depth.	222
117	Low and high magnification views of (a) forged and (b) HIPed Ti-6Al-4V fracture in area of rapid crack growth showing dimples of varying size and depth.	223
118	Fracture surface of a forged and machined keel splice former after spectrum fatigue test.	225
119	Fracture surface of HIP keel splice former after spectrum fatigue test.	226
120	Enlargement of fractograph in Areas A, B, and C of a forged keel splice former shown in Figure 116.	227
121	Enlargement of fractograph in Areas A, B, and C of a HIP keel splice former shown in Figure 117.	228
122	250X microstructure of prolongation from keel splice formers SM-409 and SM-411 annealed at 1300 F, 2 hours, air cooled.	231
123	250X microstructure of prolongation from keel splice formers SM-412 and SM-415 annealed at 1300 F, 2 hours, air cooled.	232
124	Tensile specimen geometry.	234

LIST OF ILLUSTRATIONS (continued)

FIGURE		PAGE
125	Microstructure of keel splice formers.	236
D-1	Dimensional Reference Points - Sub-Scale Stub Shaft.	264
D-2	Dimensional Reference Points - Keel Splice Former.	265
D-3	Dimensional Reference Points - Full-Size Stub Shaft.	266
H-1	Notched Low-Cycle Fatigue Test Specimen.	299
I-1	Notched Low-Cycle Fatigue Test Specimen.	309

# LIST OF TABLES

TABLE		PAGE
1	Tensile Property Specifications	14
2	Chemistry of Titanium Ingots (%)	21
3	Material Inventory	22
4	Summary of Powder Chemistry	24
5	Powder Density Data	25
6	Summary of Flow Rate Determination	25
7	Size Distribution of Ti-17 Powder	34
8	Compaction Data, Ti-17	39
9	Summary of Ti-6-4 Specimens	41
10	Compaction Data, Ti-6-4	41
11	Ti-17 Beta Transus Determination	42
12	Density Measurements, Ti-17	44
13	Chemistry Summary, Ti-17	45
14	Ti-17 Structure Study	46
15	Summary of Mechanical Properties, Ti-17	58
16	Effect of Variables, Ti-17, Sub-Transus HIP	62
17	Effect of Variables, Ti-17, beta-HIP	64
18	Density Measurements, Ti-6-4	71
19	Chemistry Summary, Ti-6-4 (Weight %)	71
20	Ti-6-4 Structure Study	72
21	Summary of Tensile Properties, Ti-6-4	77
22	Effect of Variables, Ti-6-4	78

# LIST OF TABLES (continued)

TABLE		PAGE
23	Summary of Ti-17 Powder Characterization	82
24	Summary of Ti-6-4 Powder Characterization	84
25	Properties of Ti-17 HIP at 1650°F	85
26	Properties of Bar Stock	92
27	Properties of Beta Heat Treated Shaft	95
28	Tensile Results - SM-357	98
29	Summary of Non-Metallic Inclusions	98
30	Tensile Properties of As-HIP Ti-6-4	106
31	Properties of HIP + Anneal 0.166% O <sub>2</sub> Ti-6-4	107
32	Mechanical Properties of Sub-Scale Shaft SM-295	114
33	Properties of Sub-Scale Shaft SM-357	120
34	Dimensional Analysis of SM-384 and -385	125
35	Properties of Sub-Scale Shaft SM-384	125
36	Low Cycle Fatigue Tests - SM-384	126
37	Properties of Re-Heat Treated SM-384	126
38	Metallographic Examination of LCF Specimens from SM-384	128
39	Tensile Data for $\alpha$ - $\beta$ HIP Shaft	129
40	Fracture Toughness Data for $\alpha$ - $\beta$ HIP Shaft (Slow Bend Pre-Cracked Charpy)	130
41	Dimensional Analysis - Third Shape Iteration (SM-355)	138
42	Velocity Measurements	141
43	Noise Measurements	141
44	Noise Analysis of Test Billets	142
45	Ultrasonic Inspection Record: Sub-Scale Shaft SM-401	148



LIST OF TABLES (continued)

TABLE		PAGE
46	Summary of Ti-17 Powder Characterization (Lot 4280)	151
47	Identification of Specially Handled Ti-17 Compacts	154
48	Ti-17 HIP Experiment - Low-Cycle Fatigue Results	155
49	Initial Mechanical Properties - 6" Dia. Spin Test Discs	164
50	Spin Pit Disc Test Results	168
51	SM-561 2" Dia. Log - Tensile Results	182
52	Gas Analysis Results	184
53	Tensile Properties of Ti-17 Shaft SM-557	186
54	Low-Cycle Fatigue Results - Ti-17 Full-Scale Stub Shaft (SM-557)	187
55	High-Cycle Fatigue of Ti-17 Shaft SM-557	192
56	High-Cycle Fatigue Results - Ti-17 Full-Scale Stub Shaft (SM-557)	195
57	Pre-Cracked Charpy Toughness Results - Ti-17 F-101 HIP Stub Shaft: S/N SM-557	195
58	Density of Ti-6-4 Test Panels	198
59	Ti-6-4 Tensile Test Results	198
60	Ti-6-4 Fatigue Test Results	200
61	Ti-6-4 Fracture Toughness Test Results	202
62	Dimensional Analysis of HIP Keel Splice Formers	209
63	Static Test Results, Forged and "HIP" Keel Splice Formers, 68A333019-2007	215
64	Spectrum Fatigue Data, R-4 Horizontal Tail Spectrum (F-15) Keel Splice Formers, 68A333019-2007, Design Limit Load - 2,200 lbs.	215
65	Tensile Test Data for Prolongations from HIP Keel Splice Formers	230

# LIST OF TABLES (continued)

TABLE		PAGE
66	Tensile Test Data for Specimens Removed from Keel Splice Formers	235
67	F-101 Engine Titanium Components	238
68	Cost Analysis for the Keel Splice Former 68A333019-2007 Fabricated by Forging and by Powder-HIP Process	240
A-1	Ti-6-4 Electrode Summary	246
A-2	Ti-17 Electrode Summary	247
B-1	Room Temperature Properties of Sub-Transus HIP Ti-17 Alloy (BCL Autoclave)	249
B-2	Room Temperature Properties of Sub-Transus HIP Ti-17 Alloy (CSMD Autoclave)	250
B-3	Room Temperature Properties of Beta-HIP Ti-17 Alloy	251
B-4	Low-Cycle Fatigue Results	252
B-5	High-Cycle Fatigue Results	253
C-1	Tensile Properties of Annealed ELI Ti-6-4 (CMRC)	255
C-2	Tensile Properties of Annealed ELI Ti-6-4 (MCAIR)	256
D-1	Dimensional Analysis of Sub-Scale Stub Shaft - First Iteration - SM-295	258
D-2	Dimensional Analysis of Sub-Scale Stub Shaft - Second Iteration - SM-324	258
D-3	Dimensional Analysis of Sub-Scale Stub Shaft - Third Iteration - SM-337	259
D-4	Dimensional Analysis of Sub-Scale Stub Shaft - Fourth Iteration - SM-357	259
D-5	Dimensional Analysis of Sub-Scale Stub Shaft - Fifth Iteration - (SM-368, -384, and -385)	260

# LIST OF TABLES (continued)

TABLE		PAGE
D-6	Detailed Dimensional Analysis of a Production Run of Four Keel Splice Formers	261
D-7	Dimensional Analysis of Full-Size Stub Shaft - First Iteration - SM-494	262
D-8	Dimensional Analysis of Full-Size Stub Shafts - Final Iteration - (SM-555, -556, and -557)	263
E-1	Crack Growth Data (Room Temperature)	268
E-2	Crack Growth Data (Room Temperature	269
E-3	Crack Growth Data (Test Temperature 600°F)	270
F-1	Composition of Alloys	279
I-1	Properties of Heat Treated Parts	308
I-2	Properties of Annealed Parts	308

## SUMMARY

This program was conducted to optimize an existing process for the Hot Isostatic Pressing (HIP) of near-net shapes for both a typical engine part and an airframe part. The ceramic mold-HIP process for production of near-net shapes of titanium alloy was established as a cost effective manufacturing procedure. The program was designed to establish processing parameters for HIP, including both shape and consolidation procedures. Tolerance control, surface integrity, reproducibility and non-destructive inspection methods were investigated and refined to assure adequate inspection of the complex shapes.

In cooperation with General Electric (GE) and McDonnell-Douglas (MCAIR), acting as sub-contractors, representative components and alloys were selected for the program. A Ti-17 compressor stub shaft from GE's F-101 engine and a Ti-6-4 keel splice former from MCAIR's F-15 aircraft were the particular items chosen as applicable to current Air Force requirements. Crucible Materials Research Center (CMRC) conducted an iterative shape development for the purpose of producing actual parts for evaluation by General Electric and MCAIR.

The program was organized into two phases, with Phase I progressing from materials acquisition through parameter optimization to Phase I shape development. Phase II consisted of scale-up to a full-size stub shaft to be subjected to engine test and component testing of the keel splice former in preparation for flight test. Final material and processing specifications were developed for the PM approach to these alloy systems.

This program was structured to minimize the time required to apply the technology developed, by involving material and manufacturing engineers, as well as design engineers, from both engine and airframe users, at the outset of the study.

During the Phase I study, powder of both alloys manufactured by the Rotating Electrode Process (REP) was evaluated for application to HIP parameters and



shape trials. The REP powder, as received, contained tungsten, iron, and other inclusions. Iron can, for the most part, be separated out, as can most of the larger impurities during screening. The other inclusions decrease significantly with decreasing mesh size. The presence of these inclusions, while undesirable, would not have a major impact on the primary objective of the program, which is shape making. On this basis, recommendations were made to proceed with the next task.

The HIP studies of Ti-17 resulted in the successful bracketing of optimum parameters of 1650°F - 8 hours, heated autoclave with silica mold material. Property goals were met with the exception of low cycle fatigue values. Additional experiments were designed based on the observation that non-metallic inclusions were responsible for the low cycle fatigue results. All potential causes for degraded fatigue performance were considered and evaluated and the major source for the poor LCF results continued to point inclusions in the powder coupled with microstructure. In discussions with design engineering, the LCF fatigue life of Ti-17 (which was equivalent to Ti-6-4) was satisfactory for this part. However, since the fatigue behavior would not be adequate for fan and discs used at higher stress levels, it is obvious that additional work (beyond the scope of this program) is required to eliminate the problem.

The HIP studies of Ti-6-4 powder were not as extensive as those of Ti-17 due to prior experience in this area. HIP cycles of 1750°F - 8 hours using SiO<sub>2</sub> mold material was most successful. Low initial oxygen content of the initial powder resulted in lower tensile properties than desired, but a higher oxygen powder batch (0.166%) resolved the tensile property problem.

In the iterative shape development, the Ti-17 near-net shape version of the sonic shape (1/2 scale) for the F-101 compressor stub shaft was established. The effort included a total of five shape iterations to pinpoint shrinkage characteristics. Mechanical properties were evaluated and found to be acceptable with the exception of low fatigue life, which has been a continuing problem with this P/M product. The Ti-6-4 alloy shape development of the keel splice former was accomplished in three shape iterations. The final shape weighed 1.0 lbs. as compared with the 4.67 lb. forging weight carried to this stage.



In the non-destructive inspection of trial shapes, it was determined that X-ray inspection is not particularly suitable for NDI of HIP shapes due to misleading indications from surface irregularities on the as-HIP parts. However, both the sub-scale stub shaft and the keel splice former showed surface-related defects that were essentially eliminated with surface treatment. Harperizing improved the surface, but not all as-HIP defects were removed. Machining of the keel splice eliminated most inclusion-type defects and areas of low density indications. The as-HIP Ti-17 stub shaft can be ultrasonically inspected to the required specifications. The keel splice former parts passed both radiographic and dye-penetrant inspection to MCAIR quality specifications.

In the Phase II effort, a continued study of REP powder was made in attempts to eliminate the non-metallic inclusion problem and the resultant LCF behavior in the Ti-17 alloy. These attempts again proved unsuccessful. The fracture appearance on LCF specimens indicate the continued presence of foreign material inclusions at the fatigue origins. The original Phase II plans were modified by substitution of 6" diameter discs rather than the full-scale stub shaft at the request of F-101 Design Engineering. Due to heat-treat problems, three discs were spin pit tested, two in a high strength condition and one in the normal specification range. The results of the spin pit tests indicated that the PM discs were in the expected burst speed/stress range for their mechanical property level with the exception of Disc #1 which fractured at approximately 10% lower speed. Flat discs of this type in cast and wrought usually fail by instability rather than bursting, and examinations of the fracture surfaces indicated that the fracture origins were at pores or inclusions in the bore area. The lower speed failure of Disc #1 was attributed to a larger inclusion at the fracture origin.

Shape trials were carried out to produce a full-size stub shaft. After the first trial, only minor shape changes were necessary to produce three full-scale stub shafts based on experience gained in the Phase I effort. The second shape trial produced two stub shafts with machining envelopes adequate for producing finish machined parts. All test data was comparable to cast and wrought data with the exception of low cycle fatigue results.

LCF results, in most cases, fell below the three sigma level of cast and wrought data due to the presence of non-metallic inclusions in the test specimens from the powder processing and handling stage.

A pilot lot of HIP shapes of the keel splice former were produced and component tested. These were found to be equivalent to the current forging parts under both static and spectrum fatigue loading. All parts passed MCAIR NDI testing standards.

A cost analysis on both the engine stub shaft and the keel splice former was performed based on both experimental P/M powder price and projected powder price on a production level. The results indicate that a potential exists for the HIP process to reduce both input material and machining costs compared to current cast and wrought product.

Tentative material and process specifications have been written and revised to reflect the latest technology for P/M manufacture of Ti-17 and Ti-6-4 alloy parts.

## SECTION I

### INTRODUCTION

#### 1.1 General Background

Titanium, by virtue of its high strength, low density, and very good corrosion resistance is ideally suited for use in today's high performance aircraft. Despite its high strength to weight ratio and good corrosion resistance, titanium utilization in both engines and airframes is limited by high acquisition cost. Powder metallurgy affords one possible means for the fabrication of net or near-net structural shapes, thereby improving the materials utilization ratio and, hence, reducing the end item cost.

The conventional method of producing structural shapes from titanium is forging, followed by machining. Titanium is not an easy material to forge; thus most forgings have relatively little detail and large machining envelopes. Forging to finished part/weight ratios of 10:1 are not uncommon. Moreover, the current state-of-the-art is such that a very high percentage of the titanium machine shop scrap is relegated to uses in specialty steel making, thus necessitating further imports of titanium sponge or ore into the U. S.

There are several ways to attack such a problem. One method would be more precise forgings. This approach is being explored by isothermal forging investigations through Air Force Sponsored programs. Ladish Co. is developing "Isothermally Forged Titanium Alloy Wheels" under Air Force Contract #F33615-5257. TRW, under contract AF #33615-5386 is involved in a development study of "New and Improved Forging Lubricants". Wyman Gordon, under Contract #F33615-5011 is investigating the "Isothermal Forging of Beta Titanium". In these studies, the feasibility of isothermally forging moderately complex components has been demonstrated. High tooling costs and lubrication remain the most significant deterrants to the immediate use of isothermal forging. In a recent study, the break even point for isothermal forging was found to be approximately 2,000 parts.<sup>1</sup>

Another approach that has received considerable attention from Air Force sponsored programs is direct casting to shape. This is a more challenging alternative because of the severe reactivity of molten titanium. AiResearch Manufacturing Co. under contract #F33615-74-C-5055, "Development of Titanium Alloy Casting Technology" is working toward low cost, high quality titanium castings. TRW under contract #F33615-70-C-1409 and REM Metals Corp. under contract #F33615-70-C-1410 are working on programs to improve the status of titanium casting for use in aerospace systems. TRW is investigating casting procedures for various titanium alloy systems and REM is concentrating on precision casting techniques utilizing consumable electrode skull melting. Pratt and Whitney, under contract #F33615-75-C-5263, "Titanium Alloy Engine Castings" is investigating cost effectiveness that can be achieved in military aircraft engines through the use of large structural components cast in titanium alloy. Through all these programs, improvements have been made to develop a viable casting process.

Until recently, the state-of-the-art of powder metallurgy (PM) processing, i.e. pressing and sintering, was regarded as suitable only for non-critical parts where a certain level of porosity and lack of ductility could be tolerated. Moreover, conventional die pressing has a definite size limitation. The emergence of hot isostatic pressing (HIP) as a production process has obviated these limitations to a large degree. Full density and equivalent to wrought properties have repeatedly been achieved using a variety of alloys. New shape making techniques have been shown to be applicable to structures of interest. Therefore, PM must be regarded as one very promising route to the near-net shape objective.

## 1.2 Program Goals and Approach

The basic goals of this program were very straightforward. To optimize an existing process for the HIP of net/near-net shapes for both a typical engine part and an airframe part. Also, to fully characterize and qualify the parts produced for use by the respective users.

A HIP process capable of generating near-net shapes of titanium using expendable, low-cost tooling already exists. This process must be reduced to an efficient,



cost-effective manufacturing procedure. Simply stated, this is one of the major program objectives. The other objective is of equal importance; the thorough characterization of the end product.

In cooperation with General Electric (GE) and McDonnell-Douglas (MCAIR), representative components and alloys were selected for this program. These were a Ti-17 compressor stub shaft for the F-101 engine and a Ti-6-4 keel splice former for the F-15 aircraft. Crucible was to conduct an iterative shape development, culminating in the production of actual parts for evaluation by GE and MCAIR.

The location of the stub shaft in the F-101 engine is shown in Figure 1. In service, this part operates at  $\sim 19,000$  rpm at  $\sim 600^\circ\text{F}$ . The most severe loading is a hoop tensile stress at the outer rim. The part, which weighs 11.3 pounds, is currently machined from a 170 pound conventional forging.

A photograph of the target shape for an as-HIP keel splice former is shown in Figure 2. The location of two such formers in the F-15 aircraft is shown in Figure 3. This part is subjected to bending, longitudinal tensile, and cyclic transverse tensile-compressive loading. The normal failure mode, however, is shear at a fastener. This 0.4 pound part is currently machined from a 4.7 pound forging.

For both parts, a near-net PM shape will result in a substantial reduction in the input weight, thus conserving material, and a reduction in the amount of machining, thereby reducing both the machining cost and the volume of chips produced.



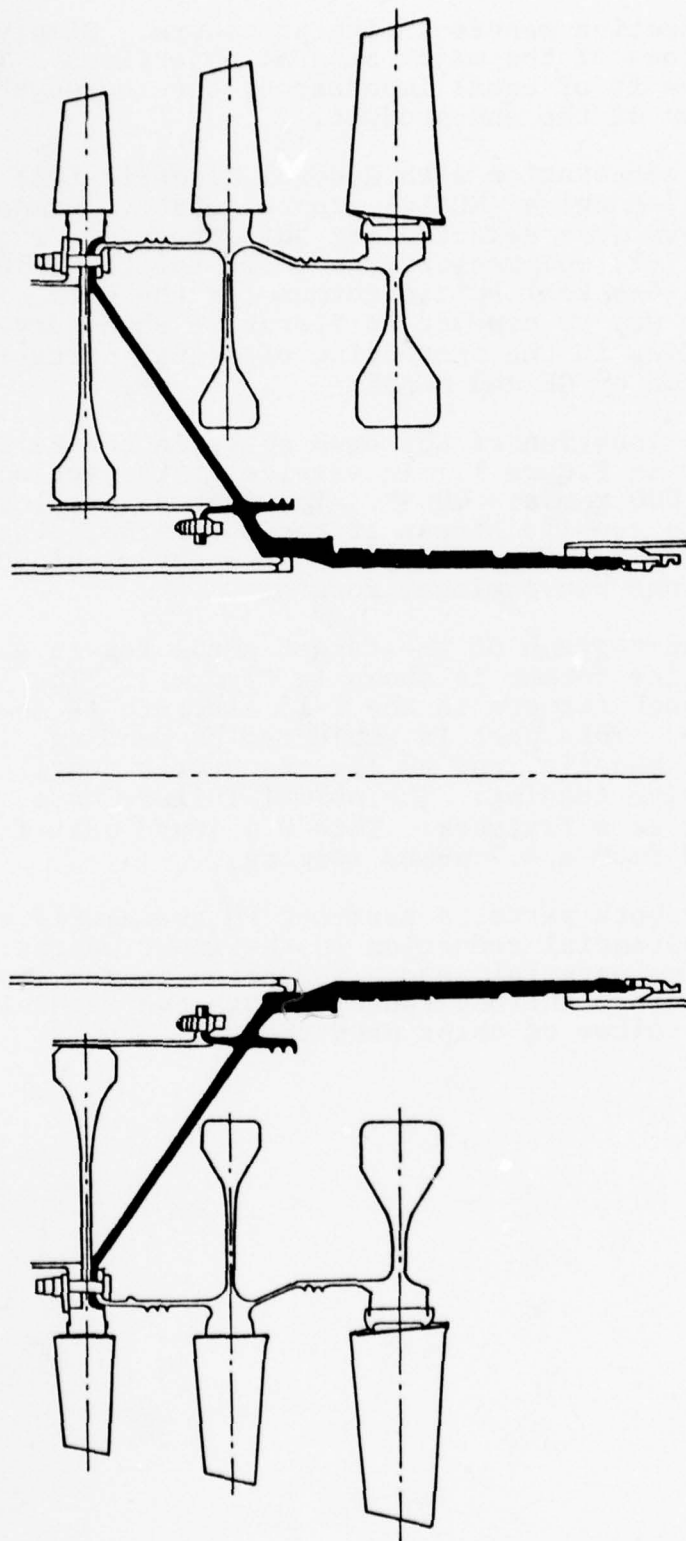


Figure 1. Isolated view of Ti-17 stub shaft location in F-101 Engine.

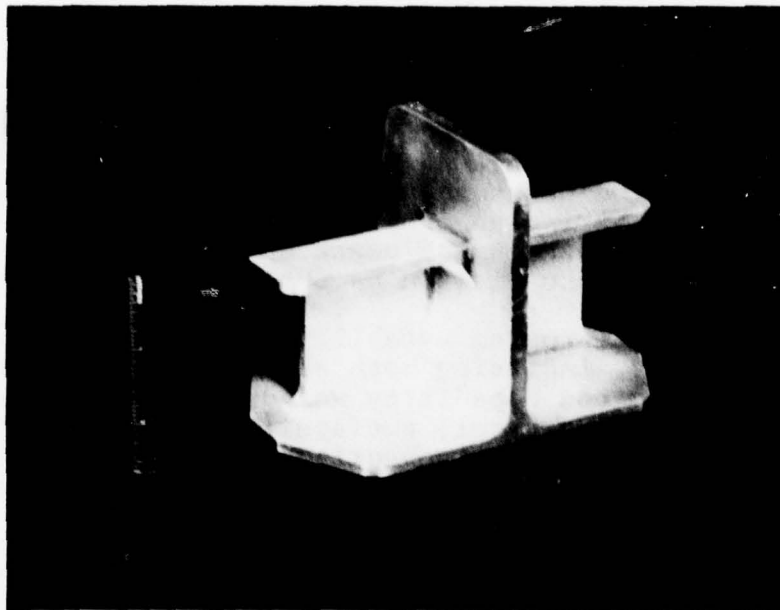


Figure 2. Target shape for keel splice fitting.

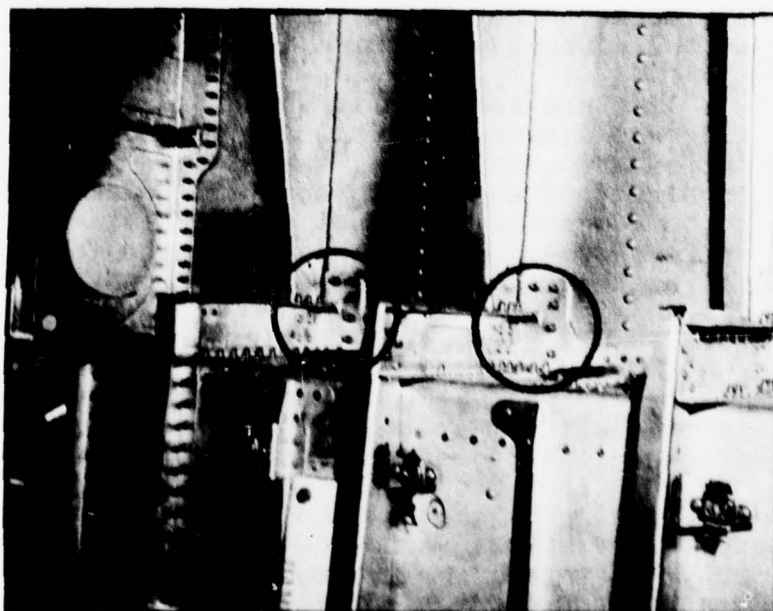


Figure 3. Location of two keel splice fittings in F-15 fuselage structure.

## SECTION II

### PROGRAM PLAN

#### 2.1 OBJECTIVES AND PHILOSOPHY

The exploitation of any new material and/or process requires very close cooperation between the producers and the users. This program was structured to minimize the time required to apply the technology developed by involving materials and manufacturing engineers as well as design engineers from both airframe and engine users at the outset and by maintaining a very close liaison as the study progressed.

The program established optimum processing parameters for HIP, including both shape and consolidation procedures. The process capability was determined in terms of complexity, tolerance control, surface integrity, and reproducibility. Non-destructive inspection methods were investigated and refined to assure adequate inspection of the complex shapes.

A keel splice former from MCAIR's F-15 aircraft and a compressor stub shaft from GE's F-101 engine were to be produced, evaluated, and qualified for use. A sufficient number of parts were to be made to verify the process and to provide an adequate data base for design purposes. A preliminary materials and process specification, including quality control procedures and acceptance/rejection criteria were prepared. Working with the users, the economics of the process was evaluated to determine the cost savings potential compared to the current production methods.

The program plan is shown in Figure 4. The study progressed from materials acquisition through parameter optimization to Phase I shape development. Phase II consisted of a scale-up to a full size stub shaft which was to be subjected to actual engine testing. In addition, keel splice formers were component tested in preparation for flight testing.

#### 2.2 POWDER PRODUCTION (PHASE I, TASK I)

The direct-HIP process to be optimized in this program is most effective with spherical, pre-alloyed powder since no preconsolidation step is used. Therefore, uniform packing and good flow properties in the powder are imperative. Spherical particles afford the best flow and packing characteristics. As of the initiation of this contract, only the rotating electrode process (REP) was in commercial use for the production of titanium powder. Thus, it became the logical selection for Phase I. The REP technique requires as starting material nominally 2-1/2 inch diameter bars. To

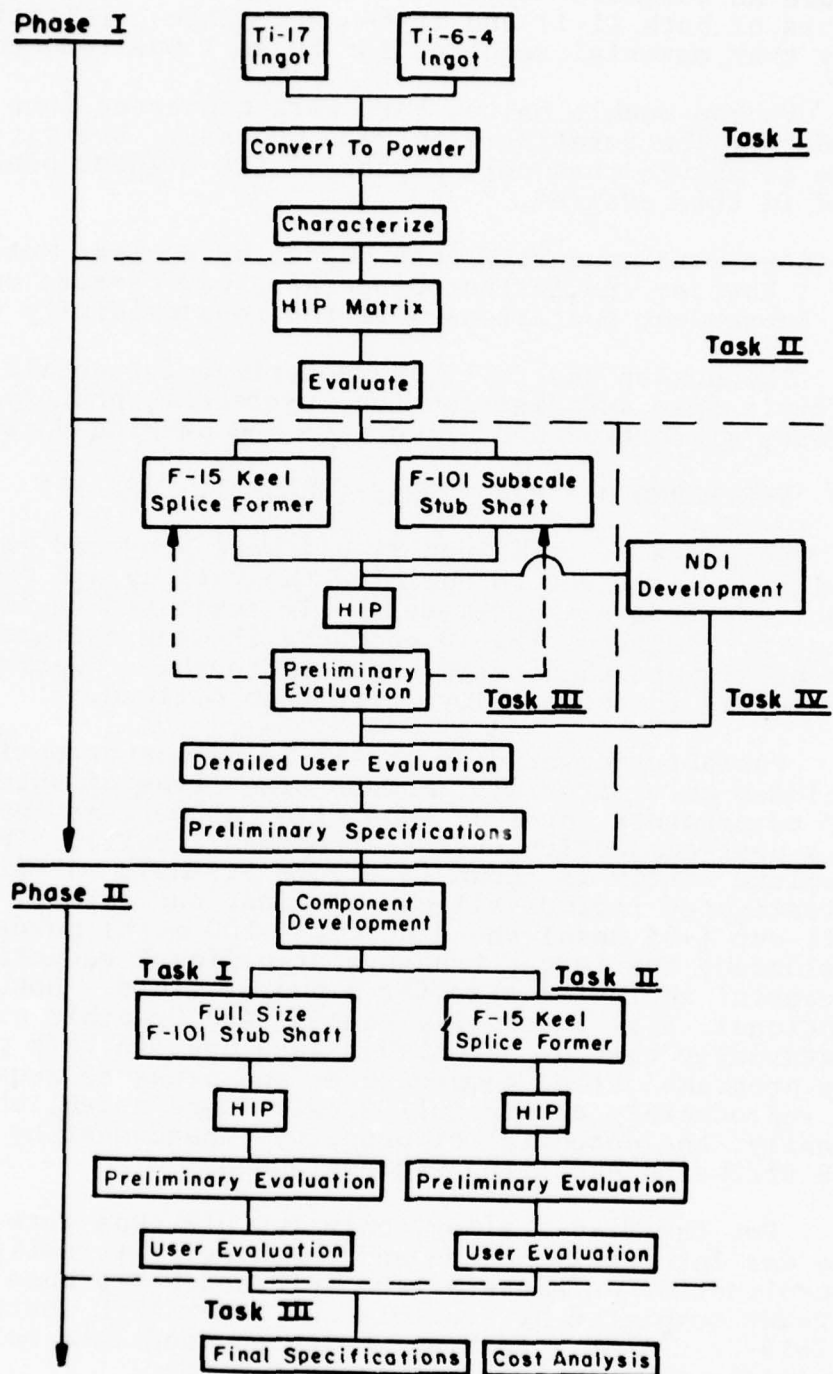


Figure 4. Program plan.



assure an adequate supply of starting material, production ingots of both Ti-17 and Ti-6-4 were made. Initially, only that material required for Phase I was reduced to bars.

Vacuum double melted bars were converted into spherical powder by the rotating electrode process. Every effort was made to assure that only powder of the highest quality was used in this program.

The bars were converted into powder by Nuclear Metals, Inc.; however, no further processing was carried out. All subsequent operations were the responsibility of CMRC.

The powder was fully characterized for chemistry, particle size and distribution, surface morphology, cleanliness, microstructure, flow rate and packing density.

### 2.3 PREFERRED HIP PARAMETERS (PHASE I, TASK II)

Compacts of Ti-17 and Ti-6-4 were produced in a designed experiment to optimize the various HIP parameters. Specimens from all parameters were subjected to limited property testing. The 10 compacts showing the greatest potential were then tested more thoroughly. Optimum HIP parameters for both alloys were then defined.

Variables covered in the Ti-17 parameter optimization included mold materials, powder size, type of autoclave cycle, HIP temperature, pressure and time, as well as the effect of a post-compaction thermal treatment (PCTT). The complete matrix is shown in Figure 5. Mold materials investigated include silica, alumina, and zircon. Both full cut (-35 mesh) and fine cut (-100 mesh) powder were evaluated; the latter trades a significant reduction in potential inclusion size for a poorer yield. Both conventional, i.e. internally heated, and Crucible production (externally heated) autoclaves were used in this phase of the program. Time, temperature, and pressure required to reproducibly attain full density were established. Finally, the potential of property enhancement by post-HIP diffusion annealing was evaluated.

For the Ti-6-4 alloy, only two HIP runs were made. One was internally heated and the other externally heated. Consolidation parameters were selected based upon work already completed by Crucible and under AFML contract F33615-72-C-1449. Each of the three candidate mold materials were included in these two runs.

One compact from each matrix point for both Ti-17 and Ti-6-4 was examined metallographically. In addition, density and room temperature tensile properties were determined. The ten best compacts were further tested

		COMPACTION CONDITIONS			Temperature
					Pressure
		$\frac{1550^{\circ}\text{F}}{15 \text{ ksi}}$	$\frac{1675^{\circ}\text{F}}{15 \text{ ksi}}$	$\frac{1750^{\circ}\text{F}}{15 \text{ ksi}}$	
TIME/AUTOClave CYCLE/POWDER SIZE	5 + 120 min.* CSMD** -35 Mesh	Zircon <sup>#</sup>	SiO <sub>2</sub> <sup>#</sup>	Al <sub>2</sub> O <sub>3</sub> <sup>#</sup>	
	30 + 120 min. BCL -35 Mesh	SiO <sub>2</sub>	Al <sub>2</sub> O <sub>3</sub>	Zircon	
	120 + 0 min. BCL -35 Mesh	Al <sub>2</sub> O <sub>3</sub>	Zircon	SiO <sub>2</sub>	
	30 + 120 min. CSMD -35 Mesh	SiO <sub>2</sub>	Al <sub>2</sub> O <sub>3</sub>	Zircon	
	30 + 120 min. BCL -100 Mesh	SiO <sub>2</sub>	Al <sub>2</sub> O <sub>3</sub>	Zircon	
	30 + 0 min. CSMD -35 Mesh	SiO <sub>2</sub>	Al <sub>2</sub> O <sub>3</sub>	Zircon	

\*The first number is autoclave time, the second is PCTT time.

\*\*CSMD, Crucible production cycle; BCL, Conventional heated autoclave.

<sup>#</sup>Tooling materials.

Figure 5. Task II HIP matrix.

to include slow-bend Charpy and axial fatigue as well as chemical analyses and analyses of surface contamination.

With the results obtained from Task II, the optimum HIP parameters for both Ti-6-4 and Ti-17 were established.

#### 2.4 SHAPE MAKING EVALUATION (PHASE I, TASK III)

In this task, using several iterations of tooling design, fabrication, and evaluation, the sub-scale Ti-17 stub shaft shown in Figure 6 and the Ti-6-4 keel splice former shown in Figure 7 were produced. In each case, it was estimated that from three to six iterations would be required to reproducibly generate the required configuration and to verify tolerances and actual shape capability.

Beginning with a trial pattern, each HIP run was intended to refine the pattern to meet the target dimensions of the engineering drawings for the two shapes under evaluation. During these successive trials, the shape technology was to be optimized to produce the best surface finish, minimum warpage and optimum dimensional tolerances obtainable.

The shape making technology developed by Crucible, using the ceramic mold process, and covered by patents 3,543,345 and 3,700,435 relies basically on the technology developed by the investment casting industry in that the molds are prepared by the "lost wax" method. Specifically, wax patterns are prepared from a dimensionally oversized master drawing or mold pattern using either machined waxes or injection molding techniques, respectively. The resultant wax pattern is then alternately dipped in a refractory slurry and a granular stucco coating to form a thin ceramic shell with an inside shape precisely defined by the shape of the wax pattern. The wax is then melted out and the molds are fired to produce a durable shaped container ready to be filled with metal powder. The powder filled mold is supported in a secondary pressing medium which is contained in a welded steel can. A schematic of a fully loaded container ready for hot isostatic pressing (HIP) is given in Figure 8. Prior to the HIP operation, the loaded steel can is evacuated and outgassed at elevated temperature and sealed.

The HIP operation consists of applying high gas pressure to a heated container inside an autoclave. In this program, heating was performed before placing the container in the autoclave (at CSMD) or after placing the container in the autoclave (at BCL). The secondary pressing medium transmits the applied pressure from the can wall to the ceramic mold

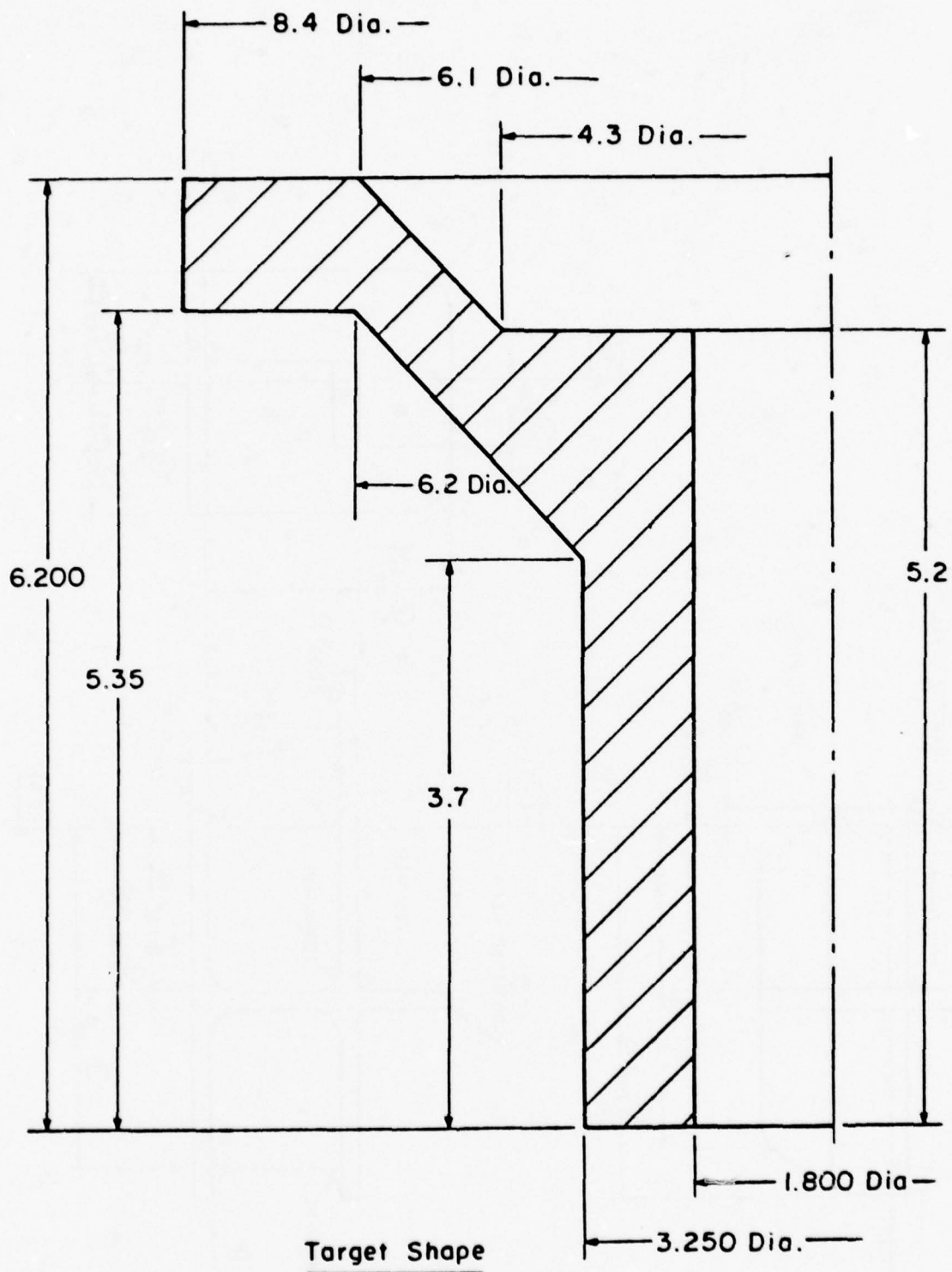


Figure 6. Subscale stub shaft. (All dimensions in inches)



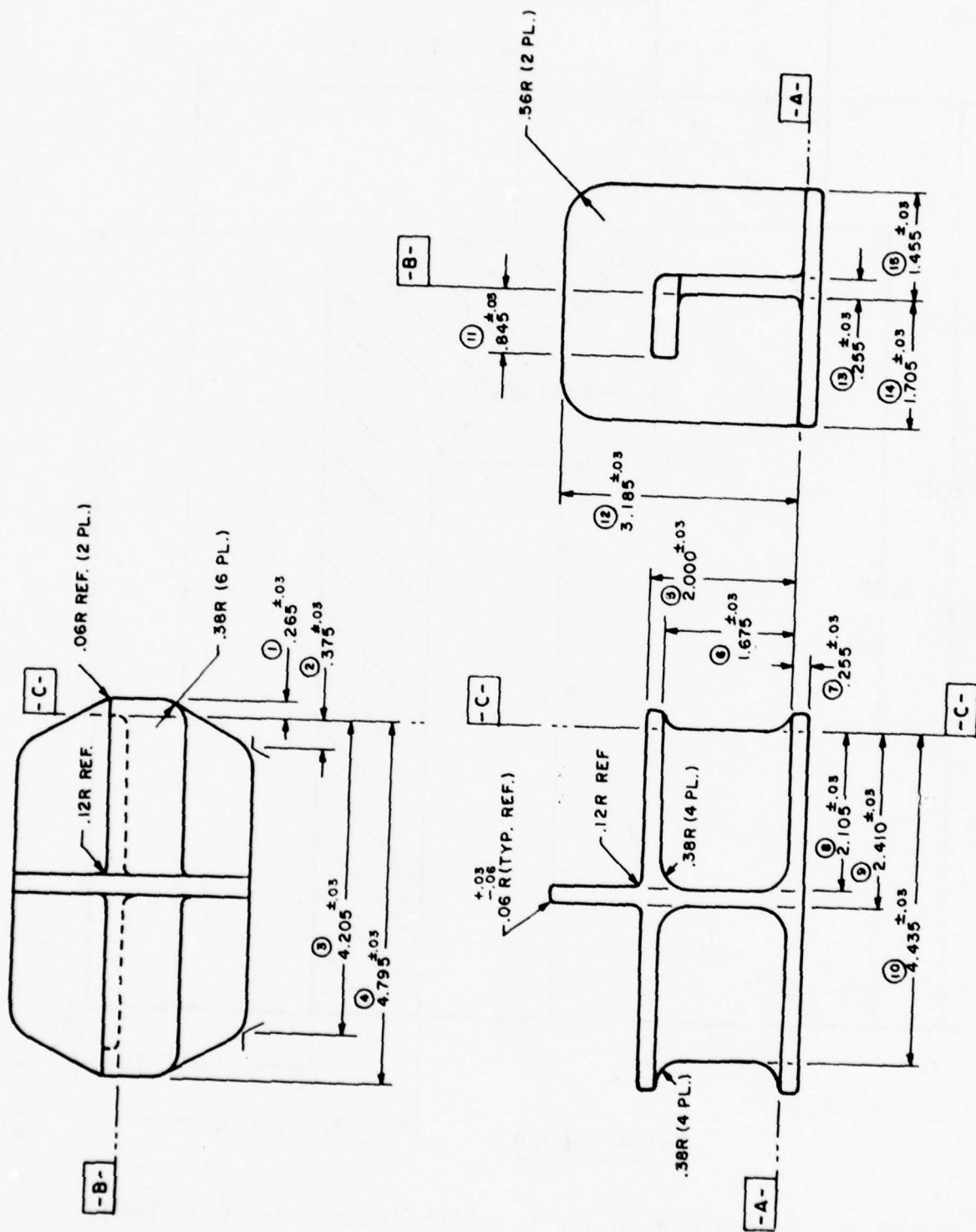


Figure 7. Target Dimensions - Keel splice form for F-15 aircraft.

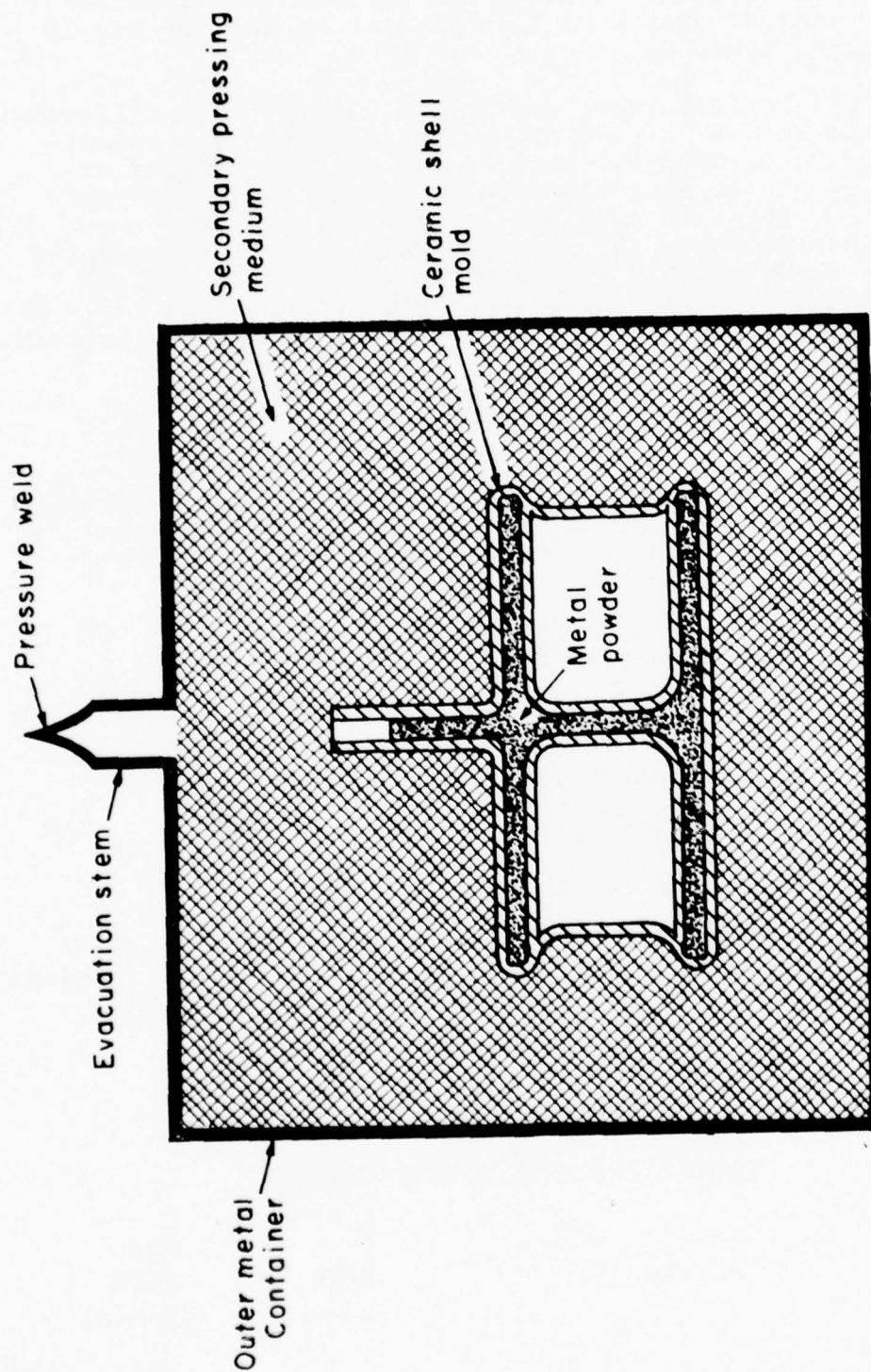


Figure 8. Schematic diagram of containerization system used in the Crucible Ceramic Mold Process for P/M parts.

and, through solid state diffusion of the powder particles, promotes bonding and maximum densification of the target shape. A flow diagram of the process is given in Figure 9.

Unlike investment casting, a large volume difference is experienced between the wax pattern and the consolidated part; however, knowing the packing density of the powder, an approximate calculation of the finished size and shape is possible. For complex parts, such as those proposed for this program, several incremental changes in the mold geometry are required to achieve the desired precision in the final shape. This can be accomplished by changing the shape of the wax pattern.

Optimum mold materials and HIP parameters established during Task II were used during all of the shape trials in Task III.

All parts were completely analyzed dimensionally. In addition, parts from the sub-scale stub shaft and the keel splice former were tested for the following:

- 1) Density
- 2) Microstructure
- 3) Surface Finish
- 4) Mechanical Properties
- 5) Fracture Toughness
- 6) Fatigue Strength

Tensile property requirements for sub-scale stub shaft according to General Electric Brochure for Ti-17 forgings AEG-700, dated January 1973, and for the keel splice per MIL-T-9047 specification are given in Table 1.

TABLE 1  
TENSILE PROPERTY SPECIFICATIONS

<u>Alloy</u>	<u>Strength (ksi)</u>		<u>Elong</u>	<u>Red Area</u>
	<u>F<sub>tu</sub></u>	<u>F<sub>ty</sub></u>	(% min)	(% min)
Ti-17	163/180	153/170	7	15
Ti-6-4	130	120	10	--

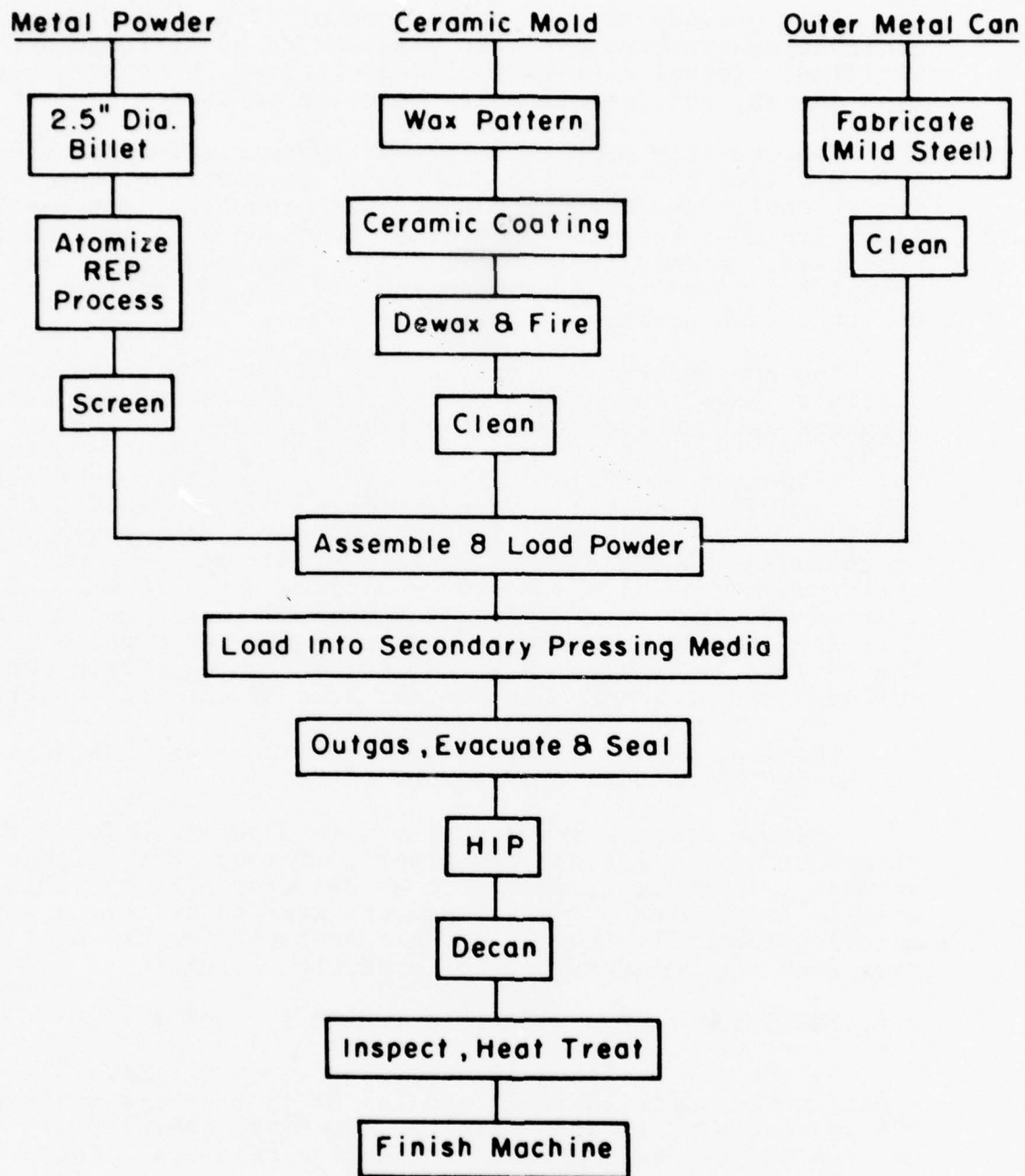


Figure 9. Flow Diagram of the Crucible Ceramic Mold Process for P/M parts.



## 2.5 NDI OF TRIAL SHAPES (PHASE I, TASK IV)

As a prelude to user acceptance of PM near-net shapes, a viable non-destructive test plan had to be designed and verified. Actual testing included reference blocks, prototype shapes, and intentionally defected parts.

Concurrently with Task III, ultrasonic reference blocks were HIP from both Ti-17 and Ti-6-4. In addition, one intentionally defected stub shaft was produced. Anticipated flaws included tungsten particles, iron and/or nickel based particles, ceramic inclusions, cracks, and porosity. All except the porosity were intentionally introduced into the defected stub shaft.

The non-destructive examination of the sub-scale stub shafts employed the normal techniques used on conventional forgings but involved tailoring the techniques to the special limitations of this part. The major consideration for refinement was in the ultrasonic inspection. Initially, the operating conditions were optimized for longitudinal and shear wave inspection. Ultrasonic wave frequency was increased to reduce minimum surface blind zone. It was anticipated that 25 MHZ would be optimum for a 20 mil minimum material envelope and yet have adequate penetration. This frequency might require reduction for penetration in the thicker sections such as the transition zone from the cylindrical portion to the conical area of the stub shaft.

The keel splice fittings were evaluated using state-of-the-art ultrasonic techniques.

Surface defects and porosity were determined for both shapes using fluorescent penetrants. Through the thickness, porosity, inclusions, etc. were to be determined by radiographic inspection. Typical defects were to be cut up and metallographically inspected. A correlation was to be made with the non-destructive inspection results.

## 2.6 PRELIMINARY SPECIFICATIONS (PHASE I, TASK IV)

At the conclusion of Phase I, preliminary materials specifications for PM Ti-17 and for PM Ti-6-4 were prepared. The process specification included quality control procedures as well as acceptance/rejection criteria. These specifications were coordinated with both the users and AFML.

These preliminary specifications will be used in the Phase II portion of this contract.

## 2.7 ENGINE STUB SHAFT EVALUATION (PHASE II, TASK I)

The process was scaled-up to produce full-size F-101 stub shafts to net or near-net shape. The shafts were to be tested by General Electric.

be tested by General Electric.

Additional Ti-17 powder was manufactured from the remainder of the Phase I ingot. The shape making process was scaled to produce the full-size stub shaft shown in Figure 10. This part is 16 inches in diameter at the flange and 12 inches long. A total of 5 parts were to be made; each subjected to the Phase I quality control plan. At least two parts were to be cut up and tested by GE. One instrumented shaft was to be given a component spin test using speed cycles that reproduced the maximum operating cyclic stresses in the stub shaft. At the conclusion of the test, the shaft was to be subjected to an overspeed condition.

An engine endurance test was to be conducted on a full-scale machined part. Testing was to have consisted of approximately 125 hours of running time. Figure 11 shows a conventional finished machined part for engine testing.

## 2.8 AIRFRAME KEEL SPLICE FORMER EVALUATION (PHASE II, TASK II)

Using Ti-6-4 powder remaining from Phase I, a pilot lot of at least 10 keel splice formers were to be produced. In addition, at least four conventional forgings were to be purchased. These parts were to be machined and one (1) HIP and one (1) conventional part were to be statically loaded to failure in a structural test. In addition, three (3) HIP and three (3) conventional parts were to be fatigue tested to failure in a structural test.

## 2.9 SPECIFICATIONS, ECONOMIC ANALYSIS, DATA SHEET (PHASE II, TASK III)

Final materials and process specifications were prepared. A cost analysis, including a comparison with established processes, has been performed. Mechanical property data has been summarized in MIL Handbook V format.

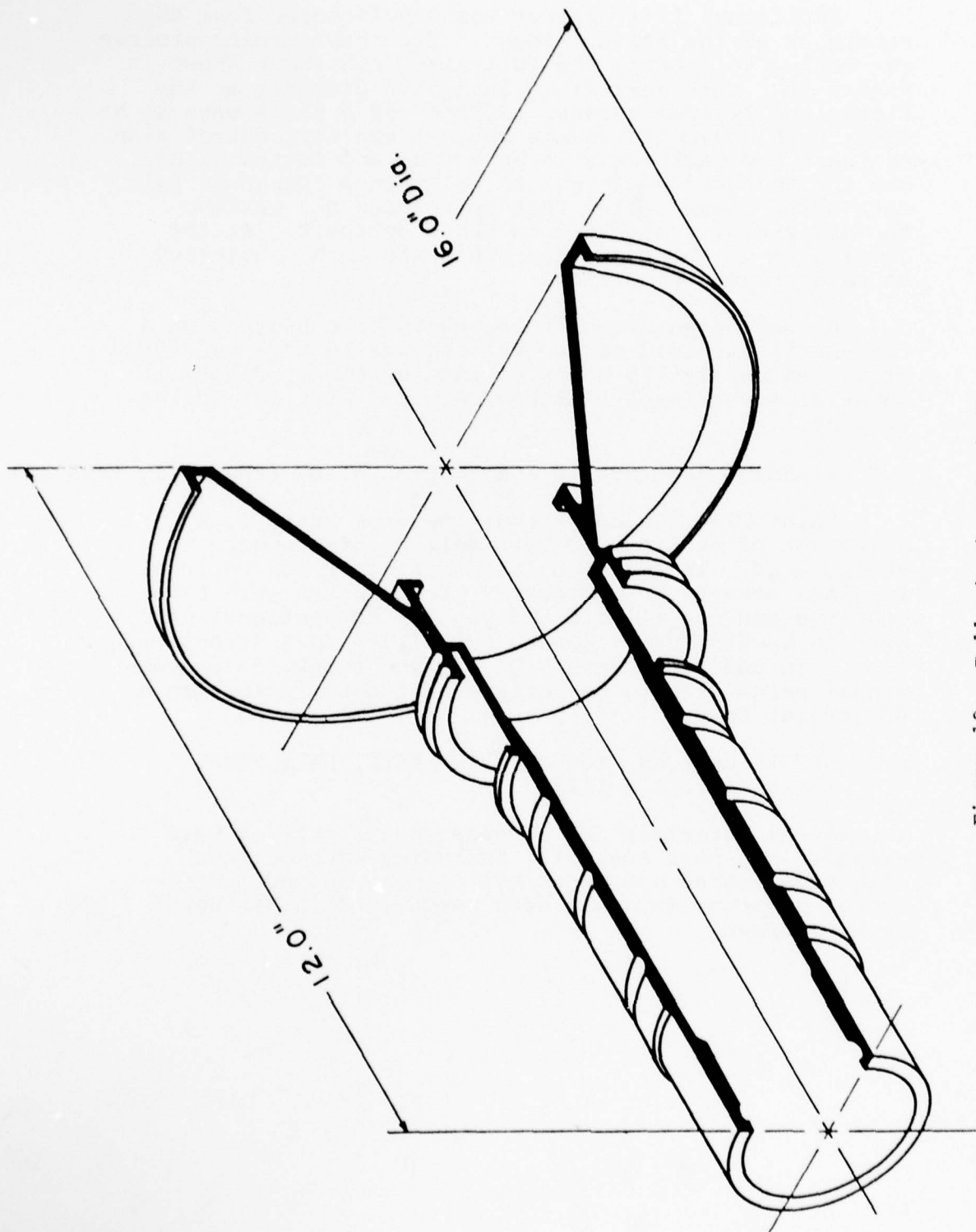


Figure 10. Full-sized stub shaft.

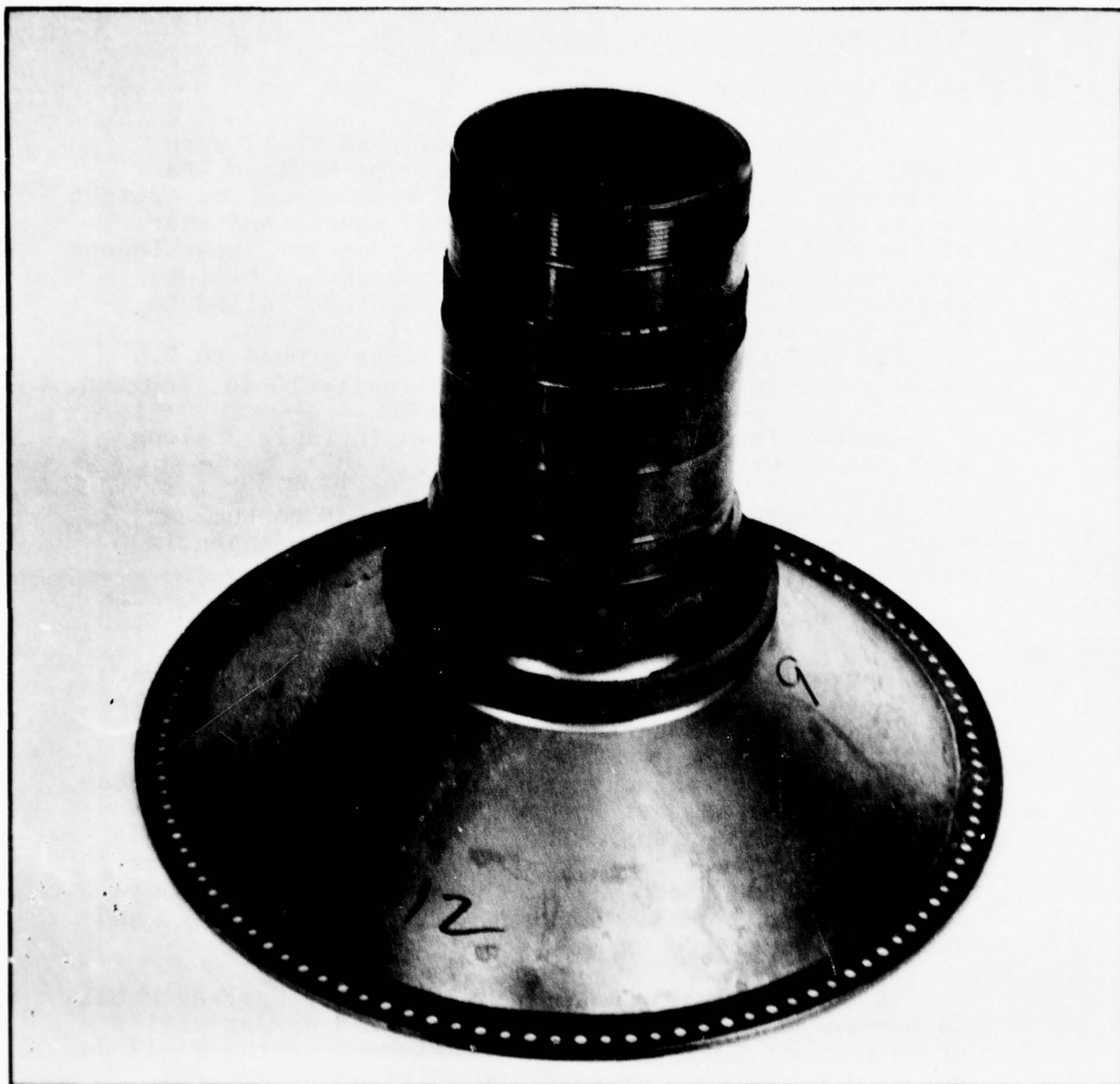


Figure 11. Finished stub shaft.



## RESULTS AND DISCUSSION

### 3.1 PHASE I - SHAPE DEVELOPMENT

#### 3.1.1 Task I - Powder Production

##### 3.1.1.1 Electrode Production

Production ingots of ELI Ti-6-4 and Ti-17 were double vacuum melted by Crucible at the Midland, Pa. production facility. Both were 29 inch diameter. Weight of the Ti-6-4 (Heat R51645) was 4000 pounds and that of the Ti-17 (Heat R51646) was 4060 pounds. These ingots were conditioned and forged to 6 inch square billet. Approximately 1000 pounds of each was then rolled to 2-5/8 inch round. The bars were next annealed, straightened, and turned and centerless ground to 2.5 +0.00 -.003 in. dia. and cut to nominally 10 in. lengths.

Actual ingot chemistry is shown in Table 2 along with the specifications.

A summary of all the electrodes sent to Nuclear Metals for conversion to powder is given in Appendix A to this report.

##### 3.1.1.2 Powder Conversion

Approximately 400 pounds of Ti-17 and 500 pounds of Ti-6-4 were converted into powder by Nuclear Metals Inc. using their rotating electrode process.

Each alloy was converted into powder in three lots as follows: a nominal 25-pound wash heat, followed by two production runs. The Ti-6-4 was run first and followed immediately by the Ti-17. All of the powder was discharged directly from the apparatus into double plastic-lined 5-gallon buckets. These were sealed, and shipped directly to CMRC.

A summary of the material returned by Nuclear Metals is presented in Table 3. The calculated powder yields of 85 percent for Ti-6-4 and 72 percent for the Ti-17 do not include samples of each lot retained by Nuclear Metals at CMRC's request.

Upon arrival at CMRC, the individual cans were cleaned on the outside and moved into a specially constructed titanium PM clean room, as shown on Page 23 before any of the containers were opened.

TABLE 2

## CHEMISTRY OF TITANIUM INGOTS (%)

Ti-6Al-4V ELI (Heat R51645)

	<u>Al</u>	<u>V</u>	<u>Fe</u>	<u>C</u>	<u>N</u>	<u>O</u>
Mil-T-9047						
Specification	5.5/6.75	3.5/4.5	0.25 max	0.08 max	0.05 max	0.13 max
Actual	6.0	3.8	0.05	0.013	0.01	0.094

Ti-17 (Heat R51646)

	<u>Al</u>	<u>Sn</u>	<u>Zr</u>	<u>Mo</u>	<u>Cr</u>	<u>Fe</u>	<u>O</u>
AEI-700 (1/73)							
Specification	4.5/5.5	1.5/2.5	1.5/2.5	3.5/4.5	3.5/4.5	0.30 max	0.08/0.13
Actual	4.7	2.2	2.0	3.8	3.9	0.06	0.086

	<u>N</u>	<u>C</u>
Specification (cont'd)	0.04 max	Not specified
Actual (cont'd)	0.006	0.029

TABLE 3  
MATERIAL INVENTORY

	<u>Ti-6-4 Alloy</u>	<u>Ti-17 Alloy</u>
Material Shipped as 2.5 inch bars	610.19 lb.	577.25 lb.
Material Returned as Raw Powder	Lot 1 24.63 lb. Lot 2 173.38 lb. Lot 3 <u>321.58</u> lb. Total 519.59 lb.	Lot 4 23.81 lb. Lot 5 197.19 lb. Lot 6 <u>194.38</u> lb. Total 415.38 lb.
Material Returned As Stubs and Tops	90.38 lb.	141.20 lb.
Materials Unaccounted for*	0.22 lb.	20.67 lb.
Yield as Raw Powder**	85.1%	71.9%

---

\*Including samples retained by vendor.

\*\*Excluding samples retained by vendor.

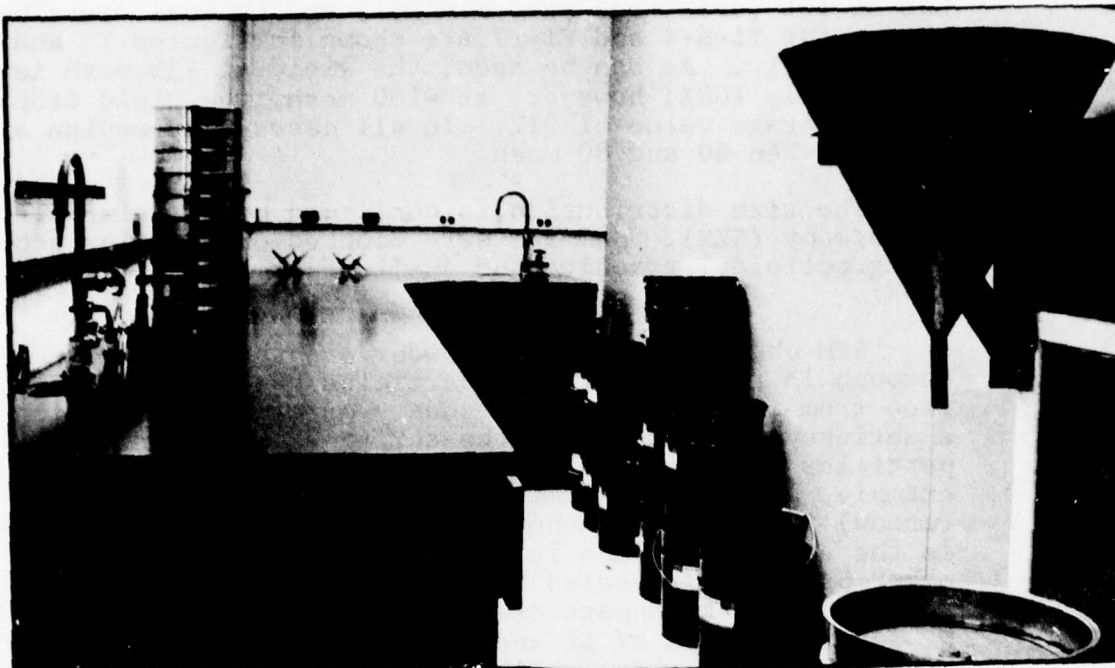


Figure 12. CMRC's Ti PM clean room.

#### 3.1.1.3 Powder Characterization

Powder chemistries were determined for each production lot of each alloy. Results are shown in Table 4. With the exception of a minor discrepancy in carbon for the Ti-6-4, the ingot and powder chemistries are identical. The carbon content of an electrode stub end was rechecked and found to be 0.017 percent, between that originally determined for the ingot (0.013%) and that for the powder (0.024% average).

Densities per ASTM B 212-48 and flow rates per ASTM B 213-48 were determined using -35 and -100 mesh samples from the respective wash heats. Results of the apparent and tap density determinations are shown in Table 5. In the sieve analysis per ASTM B 214-66, the size agreement, i.e., the -35 mesh Ti-6-4 versus Ti-17 and -100 mesh Ti-6-4 versus Ti-17 is excellent. Although the apparent density of the fine powder is low, the tap density agrees quite well with that for full cut powder. Flow rate data are shown in Table 6. Again, size agreement is excellent.



Particle size distribution was determined for each production lot on as-received, i.e., unscreened, powder. Lot to lot variations were minimal, and typical distributions for Ti-6-4 and Ti-17 are shown in Figures 13 and 14, respectively. As can be seen, the yield at -35 mesh is essentially 100%; however, at -100 mesh, the yield drops to an average value of 21%. In all cases, the median size lies between 60 and 80 mesh.

The size distribution is confirmed by scanning electron microscopy (SEM). Samples were mounted on titanium stubs using colloidal graphite and examined at 100, 250, and 500X.

SEM photographs of the powder are shown in Figures 15 through 18. Generally, the particles are spherical and free from flat spots and secondary particles. Occasionally, a shrinkage void opens to the surface. Some foreign particles and non-spherical shapes were observed. For example, an angular aluminum-rich particle is shown (arrow) in Figure 18. However, the other angular particle in the same photograph is Ti-6-4. X-ray analyses of other particles revealed the presence of aluminum, rhodium, slag-type particles containing Ti, Si, Cr, Fe, K, and Ca, oxides of Al and Si, and titanium particles rich in such elements as Al, K, Ca, Fe, and Mn in addition to iron base chips.

TABLE 4  
SUMMARY OF POWDER CHEMISTRY

Ti-6Al-4V Alloy						
	Al	V	Fe	C	N	O
Ingot	6.0	3.8	0.05	0.013	0.01	0.094
Lot 2	6.0	3.8	0.04	0.023	0.008	0.094
Lot 3	6.0	3.9	0.05	0.025	0.008	0.095

Ti-17 Alloy									
	Al	Sn	Zr	Mo	Cr	Fe	C	N	O
Ingot	4.7	2.2	2.0	3.8	3.9	0.06	0.029	0.006	0.086
Lot 5	4.8	2.28	2.20	3.9	3.9	0.06	0.023	0.008	0.093
Lot 6	4.8	2.30	2.20	3.8	3.9	0.06	0.027	0.008	0.094

TABLE 5

POWDER DENSITY DATA  
(per ASTM B 212-48)

Alloy	-35 mesh		-100 mesh	
	Apparent Density*	Tap Density*	Apparent Density*	Tap Density*
Ti-6-4	.0979 lb/in <sup>3</sup>	.1062 lb/in <sup>3</sup>	.0950 lb/in <sup>3</sup>	.1044 lb/in <sup>3</sup>
	60.1%	65.9%	59.0%	64.8%
Ti-17	.1026 lb/in <sup>3</sup>	.1106 lb/in <sup>3</sup>	.1004 lb/in <sup>3</sup>	.1098 lb/in <sup>3</sup>
	61.1%	65.8%	59.8%	65.4%

\*Average of 4 values.

TABLE 6

SUMMARY OF FLOW RATE DETERMINATIONS  
(per ASTM B 213-48)

Alloy	Average Flow Time* (Seconds)	
	-35 mesh	-100 mesh
Ti-6-4	27.5	23.9
Ti-17	26.7	23.5

\*Average of 4 values.

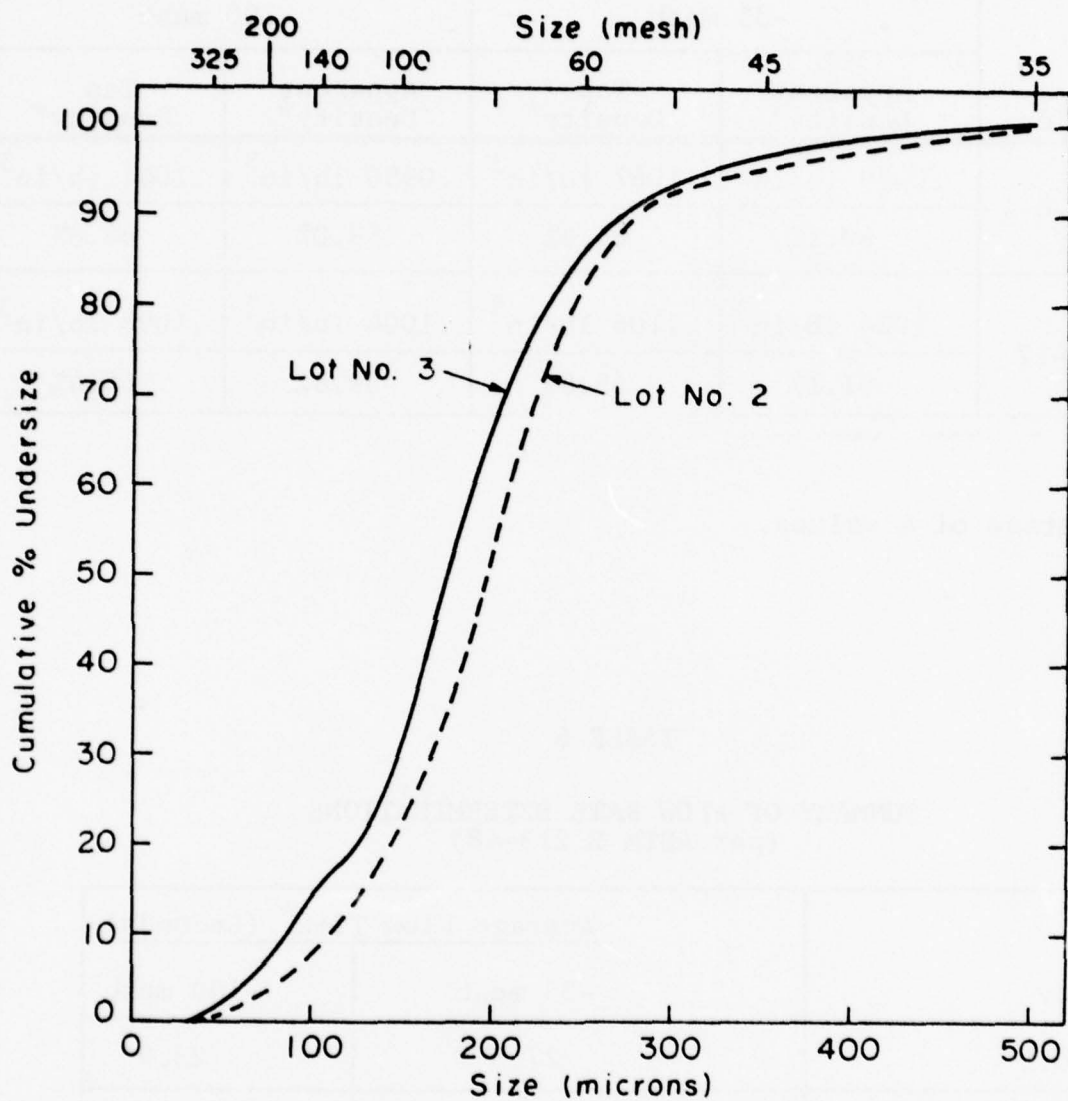


Figure 13. Particle size distribution, Ti-6-4 powder.  
(The two curves represent the two powder lots)

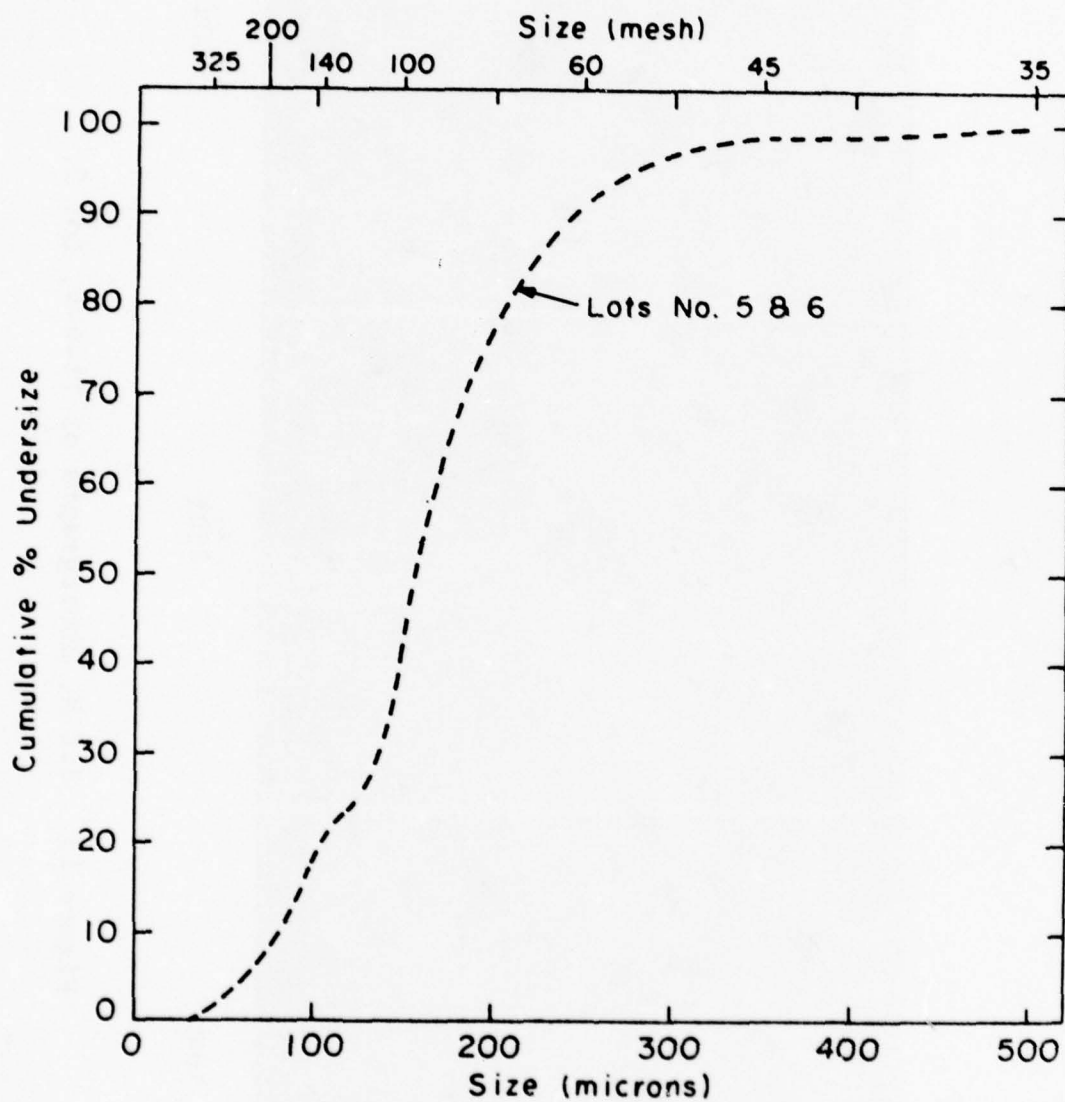
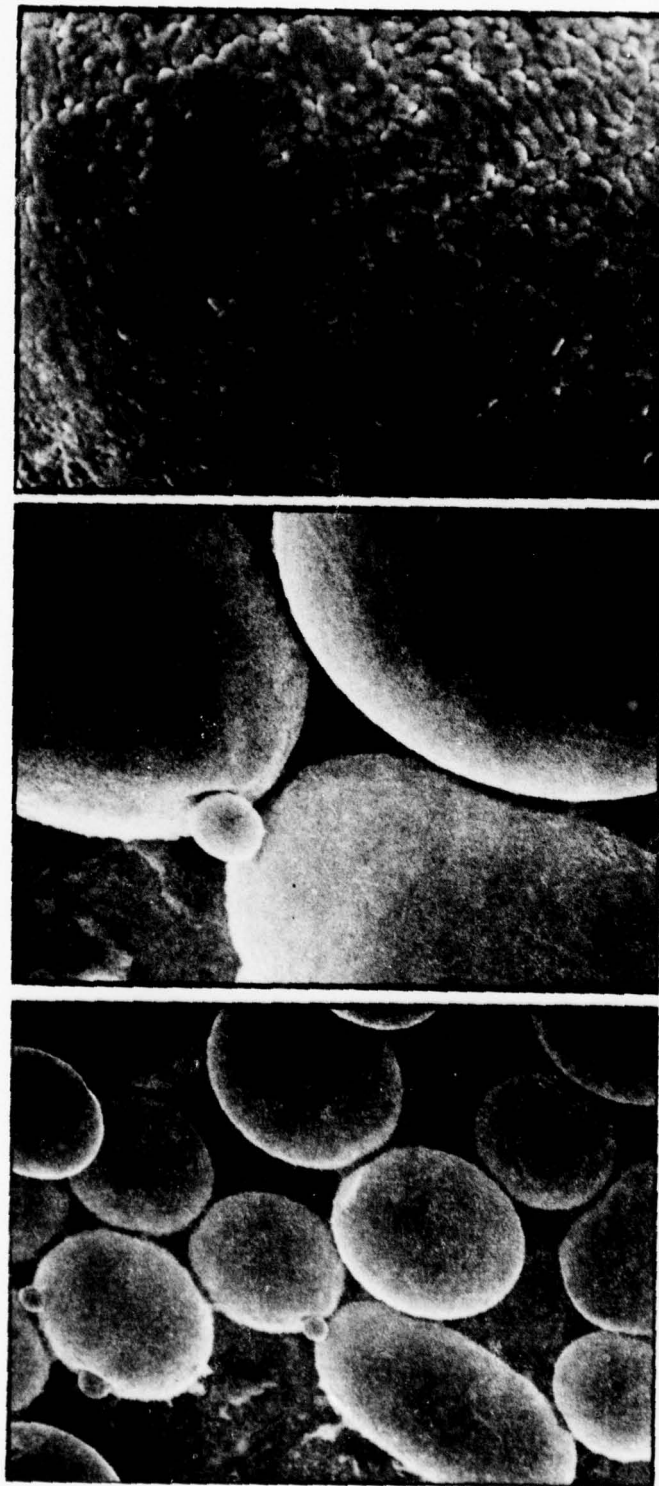


Figure 14. Particle size distribution, Ti-17 powder.  
(Only a single curve is shown as the size distribution of the two powder lots was virtually identical)



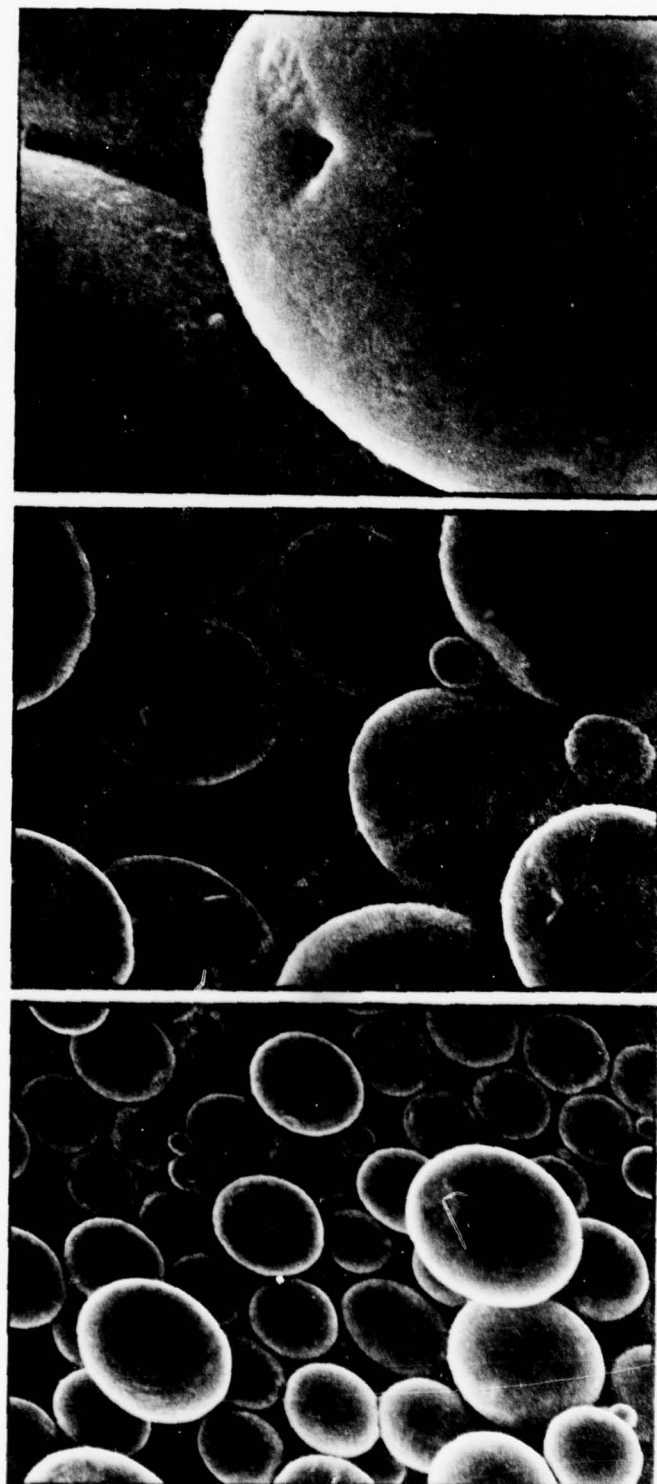


100X

250X

500X

Figure 15. S.E.M. photographs of Ti-6-4, Lot 2.

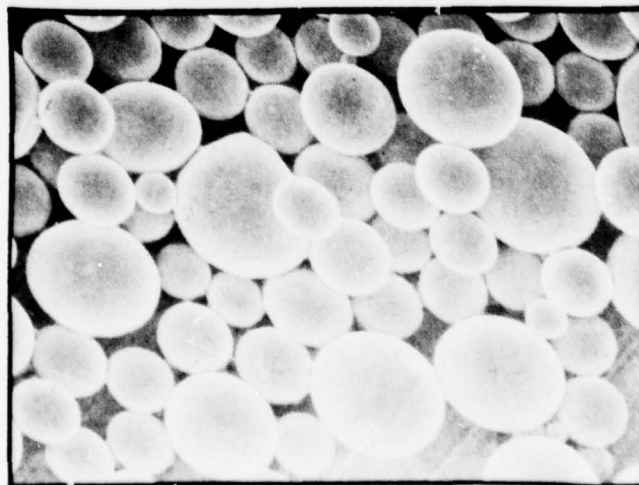


500X

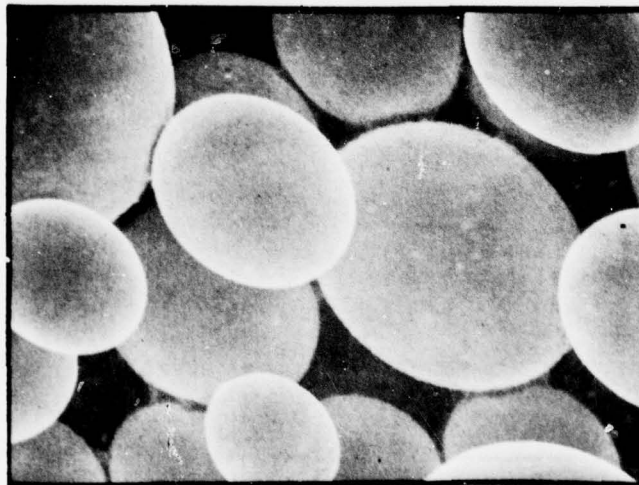
250X

100X

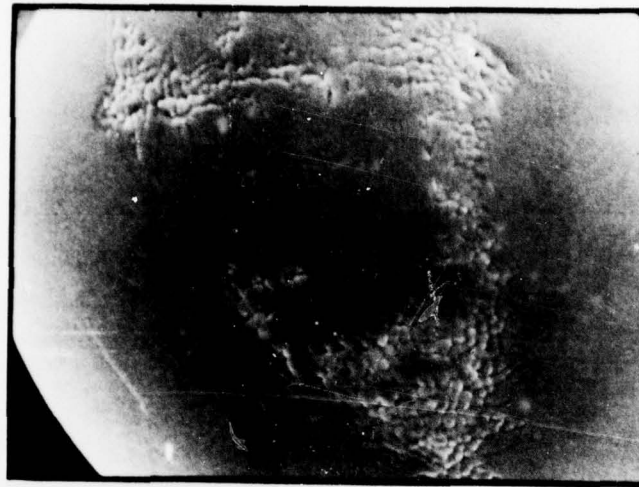
Figure 16. S.E.M. photographs of Ti-6-4, Lot 3.



100X

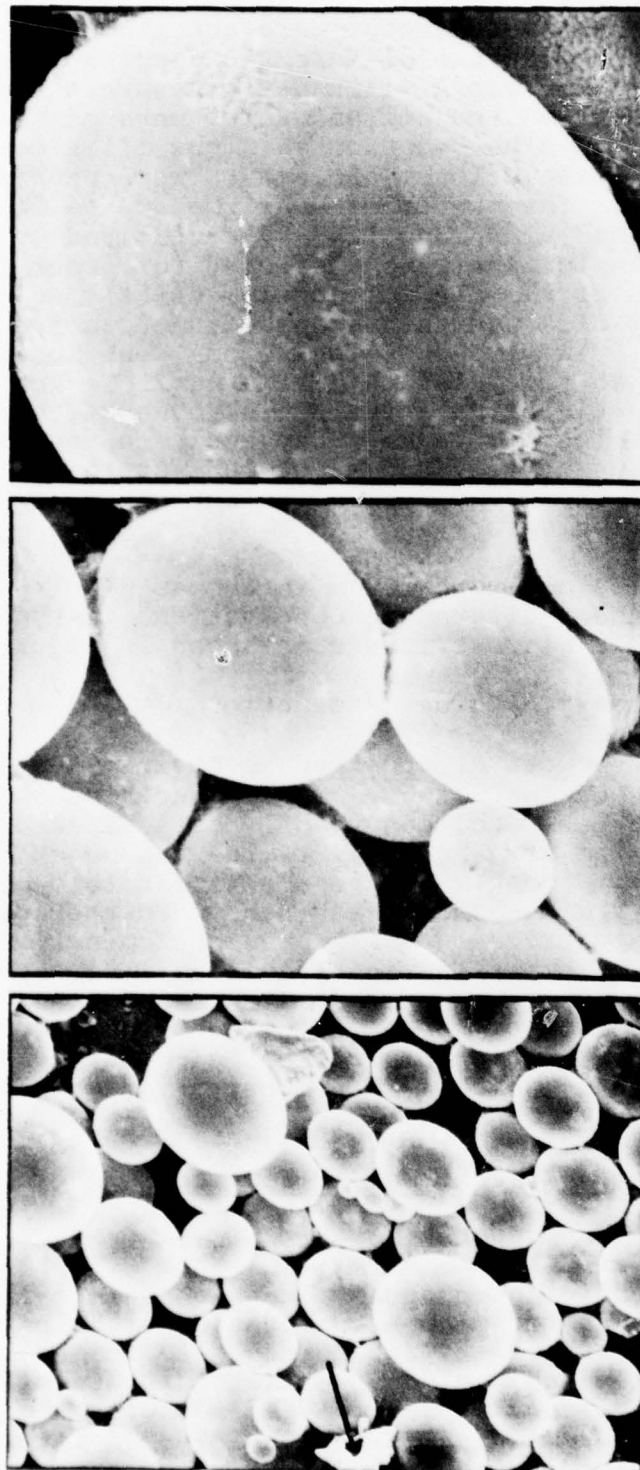


250X



500X

Figure 17. S.E.M. photographs, Ti-17, Lot 5.



500X

250X

100X

Figure 18. S.E.M. photographs, Ti-17, Lot 6.  
 (The particle indicated by the arrow  
 in the 100X photograph was identified  
 as an Al-rich Ti alloy)



Samples of -35 and -100 mesh Ti-6-4, Lot 2, and Ti-17 Lot 5 were encapsulated in carbon steel and HIP at 1750° F and 15,000 psi. One inch thick discs approximately 3 inches in diameter were cut from each compact and radiographed at two different exposures using two double emulsion Class A films per exposure. Each film was scanned at 10X and all anomalies were marked. Only those which could be found on all four films were considered to be inclusions; all others were regarded as film defects. The number of confirmed dense inclusions for the -35 and -100 mesh Ti-6-4 were 24 and 7, respectively. No inclusions were confirmed in either Ti-17 disc. The portion of the HIP compact immediately adjacent to the X-ray disc was then polished and examined metallographically. Two types of inclusions were noted in the Ti-6-4, an irregular chip-like particle and an almost perfectly circular particle. One of the latter is shown in Figure 19. An X-ray analysis revealed that these were essentially tungsten with varying amounts of iron. Thus, the radiographic indications were probably tungsten inclusions.

No inclusions were found in the as-HIP Ti-17, confirming the radiographic observation. A typical Ti-17 beta-HIP microstructure is shown in Figure 20.

#### 3.1.1.4 Summary - Powder Production

The REP powder as received, contained tungsten, iron, and other inclusions. Many impurities such as string, bristles, etc. can readily be separated during screening. The iron-based particles can be extracted magnetically. Those which remain appear to decrease significantly with powder mesh size. Further observation will be carried out by thorough examination of the -100 mesh samples during Task II.

The presence of these inclusions, while undesirable, would not have a major impact on the primary objective of this program, which is a demonstration of net/near-net shape making.

#### 3.1.2 Task II - Preferred HIP Parameters

##### 3.1.2.1 Powder Preparation

As noted in the program plan, several Ti-17 compacts were to be prepared with -100 mesh powder. Therefore, Lots 5 and 6 of powder were screened to remove all of the -100 product which could be separated in a single pass through a vibratory screen. After removing the +35 mesh fraction, the remaining powder was blended into a single lot. Size distribution before and after this operation are shown in Table 7.

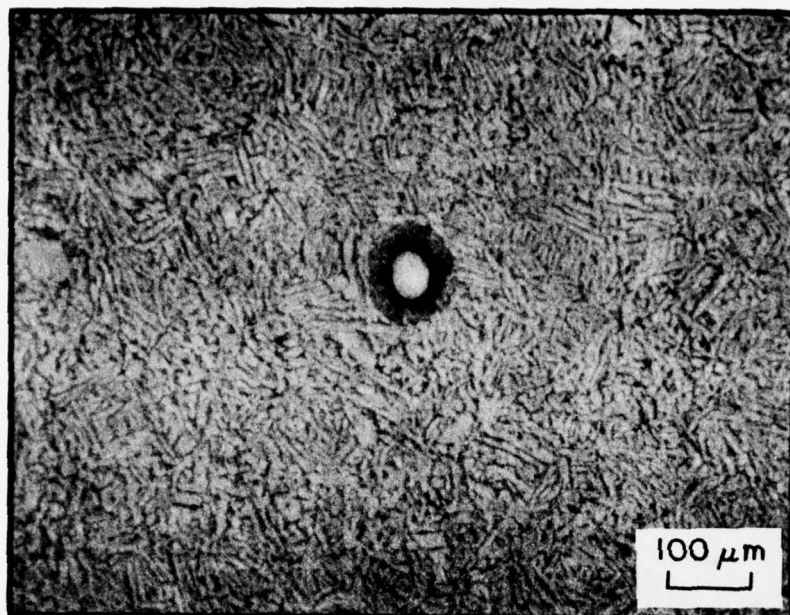


Figure 19. Tungsten inclusion in as-HIP Ti-6-4. (100X)

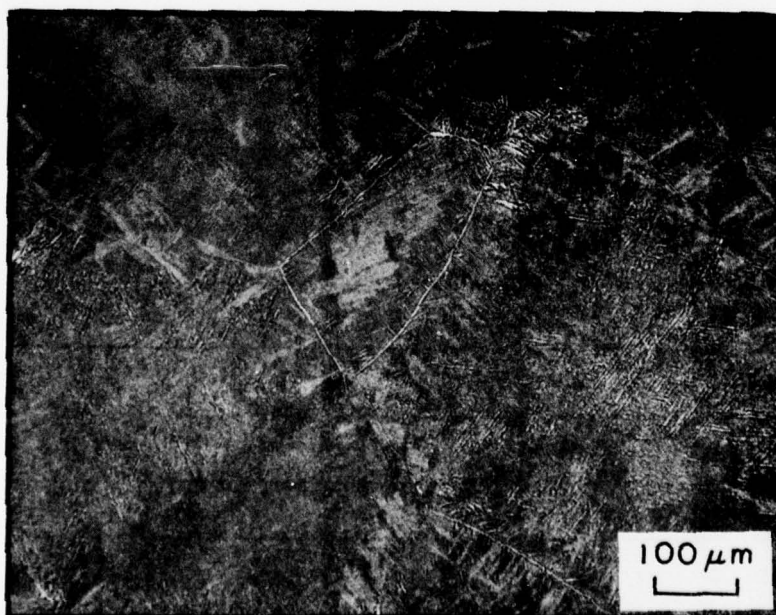


Figure 20. Microstructure of as-HIP Ti-17. (100X)

This truncation of the distribution curve reduced the flow time from 26.7 seconds for the as-received -35 mesh to 24.75 seconds for the modified blend. The apparent densities (61.1 versus 61.0%) and tap densities (65.8 versus 66.4%) were essentially unaffected.

The Ti-6-4 powder was screened to remove only the +35 mesh fraction and then magnetically cleaned. All powder handling was done in air in the clean room shown in Figure 12, Task I.

TABLE 7

SIZE DISTRIBUTION OF Ti-17 POWDER

Mesh Size	As-Received		Master Blend after Removal of some -100 mesh
	Lot 5	Lot 6	
+35	0.73%	0.70%	0%
-35, +45	2.87	2.78	0.62
-45, +60	16.16	14.75	13.74
-60, +80	44.22	39.72	47.51
-80, +100	11.79	14.63	25.47
-100, +120	4.23	5.66	7.52
-120, +200	15.72	16.58	5.08
-200, +325	3.99	4.32	0.05
-325	0.29	0.76	.01

### 3.1.2.2 Ti-17 Specimen Preparation

Cylindrical test specimens nominally 3 inches diameter x 6 inches long were consolidated in a statistically designed experiment to determine the effect of temperature, time, ceramic mold material, type of autoclave, and powder particle size on microstructure and mechanical properties. Temperatures both above and below the Ti-17 beta transus were investigated along with variations in time at temperature and pressure to establish optimum consolidation of compacts. Powder particle size was varied to determine the effect on consolidation efficiency. Two modes of HIPing—one where containers are heated inside the autoclave (at BCL) and the other where containers are heated outside the autoclave (at CSMD)—were evaluated for their effects on properties. Both a hot wall (BCL) and a cold wall (CSMD) autoclave were used to measure the effect of heat cycle variations on the economics and efficiency for optimum consolidation. The experimental HIP matrix for the Ti-17 alloy is shown in Figure 21; assigned specimen codes are included.

Ceramic molds were prepared from silica, alumina, and zircon. These molds were inserted into steel containers, surrounded by a granular ceramic secondary pressing media, and filled with the appropriate size of powder. All specimens were vacuum outgassed at  $\sim 400^{\circ}\text{F}$  to a pressure of less than  $20\mu$  and then hermetically sealed.

Some of the compacts were HIP (hot isostatically pressed) in Crucible's 20-inch I.D. production autoclave (Figure 22) and the remainder in Battelle's 27-inch unit shown in Figure 23.

Prior to initiating this HIP matrix, a ceramic mold compact identical to those assembled for the parameter study was instrumented with a thermocouple and charged into a hot furnace. The time to reach temperature at the center of the titanium powder charge was approximately 8-1/2 hours for both the  $1550^{\circ}\text{F}$  and  $1750^{\circ}\text{F}$  run temperatures. Therefore, the baseline heating time for all of the experimental compacts was set at 8-1/2 hours.



		COMPACTION CONDITIONS			Temperature
					Pressure
		1550°F 15 ksi	1600°F 15 ksi	1750°F 15 ksi	
TIME/AUTOClave CYCLE/POWDER SIZE	5 + 120 min.* CSMD** -35 Mesh	Zircon <sup>#</sup> 254,255	SiO <sub>2</sub> <sup>#</sup> 256,257	Al <sub>2</sub> O <sub>3</sub> <sup>#</sup> 261,262	
	30 + 120 min. BCL -35 Mesh	SiO <sub>2</sub> 227,234	Al <sub>2</sub> O <sub>3</sub> 248,249	Zircon 238,240	
	120 + 0 min. BCL -35 Mesh	Al <sub>2</sub> O <sub>3</sub> 235,236	Zircon 252,253	SiO <sub>2</sub> 237,239	
	30 + 120 min. CSMD -35 Mesh	SiO <sub>2</sub> 265,266	Al <sub>2</sub> O <sub>3</sub> 263,264	Zircon 273,274	
	30 + 120 min. BCL -100 Mesh	SiO <sub>2</sub> 232,233	Al <sub>2</sub> O <sub>3</sub> 250,251	Zircon 243	
	30 + 0 min. CSMD -35 Mesh	SiO <sub>2</sub> 269,271	Al <sub>2</sub> O <sub>3</sub> 268,270	Zircon 275,276	

\*The first number is autoclave time, the second is PCTT time.

\*\*CSMD, Crucible production cycle; BCL, Conventional heated autoclave.

<sup>#</sup>Tooling materials with specimen identification codes.

Figure 21. Task II HIP matrix.

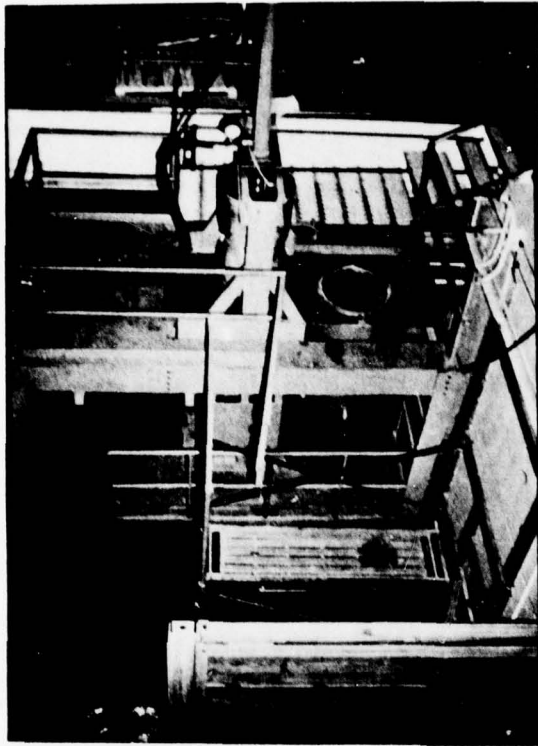


Figure 22.

Crucible's production autoclave. This unit is located at the Specialty Metals Division (CSMD) in Syracuse, N.Y.

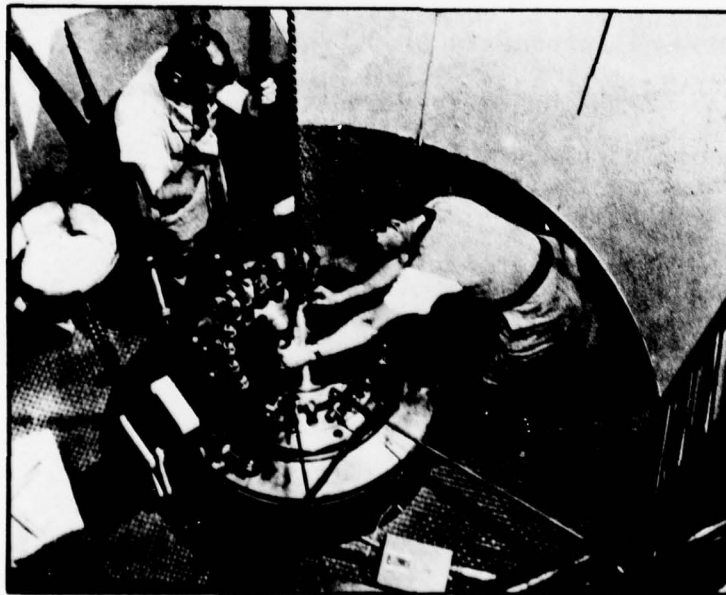


Figure 23. Battelle's 27-inch I.D. autoclave.

Actual HIP cycle data are summarized in Table 8. In the CSMD cycles, the parts were preheated outside the autoclave and held at temperature for the times indicated prior to HIP. At BCL, the parts were heated inside the autoclave and HIP after heating as shown in the table.

After HIP, the parts were decanned. A typical compact is shown in Figure 24. As indicated in Figure 21, some were subjected to a post-compaction thermal treatment (PCTT). This consisted of a 2-hour exposure to the HIP temperature.

### 3.1.2.3 Ti-6-4 Specimen Preparation

Because of the availability of previously generated HIP data,<sup>2,3</sup> a full parametric study was deemed unnecessary. Optimum conditions of 1750°F and a minimum pressure of 10,000 psi were defined. Since 15,000 psi capability existed for all autoclaves used in this program, this higher pressure was selected. Variables included BCL versus CSMD compaction and ceramic mold material. This abbreviated test matrix is shown on page 41. All compacts were nominally 3 inches in diameter by 12 inches long. Half of each was evaluated as-HIP and half HIP plus PCTT.

The HIP cycle data are summarized in Table 10. As with the Ti-17, compacts were heated externally at CSMD and internally at BCL.

### 3.1.2.4 Ti-17 Evaluation

Most of the combinations of processing parameters investigated yielded material which met the specifications for wrought material. Tensile properties and toughness were excellent. Fatigue lives were somewhat low. This is attributed to an inclusion problem. All of the Ti-17 specimens were heat-treated prior to testing at both CMRC and General Electric. The schedules used by CMRC and General Electric were the same except for the solution anneal of 1550°F at CMRC and 1575°F at General Electric with fast air cool.

CMRC  
1550°F/4 hr/AC  
1475°F/4 hr/WQ  
1175°F/8 hr/AC

GE  
1575°F/4 hr/FAC  
1475°F/4 hr/WQ  
1175°F/8 hr/AC

} Duplex only for  
beta-HIP material

TABLE 8  
COMPACTION DATA Ti-17

Specimen Numbers	Temp. (°F)	Pressure, (max.) ksi	Time, hr		
			To Temp. <sup>a</sup>	At Temp. <sup>b</sup>	At Temp. & Pressure
269, 271	1550	14.3	9	14	0.5
254, 255	1550	12.0	7.5	9.7	0.1
265, 266	1550	12.4	9.5	9.0	0.5
263, 264, 268	1600	13.3	9.5	8.5	1.7
270	1600	13.5	8	8.5	0.5
256, 257	1600	12.4	10.8	9.5	0.1
273	1750	13.9	7.5	9	0.5
275, 276	1750	13.4	12.0	9	1.5
261, 262	1750	13.0	11.5	9.5	0.1
248, 249 250, 251	1600	15.0	9.0	-	0.5
252, 253	1600	15.0	9.5	-	2.0
227, 232, 233, 234	1550	15.0	9.0	-	0.5
235, 236	1550	15.0	9.0	-	2.0
238, 240, 243	1600	15.0	9.0	-	0.5
237, 239	1750	15.0	9.0	-	2.0

<sup>a</sup>Outside of container reached desired temperature.

<sup>b</sup>Soak time to heat through the can.  
Note: For BCL cycles, a single time is shown.



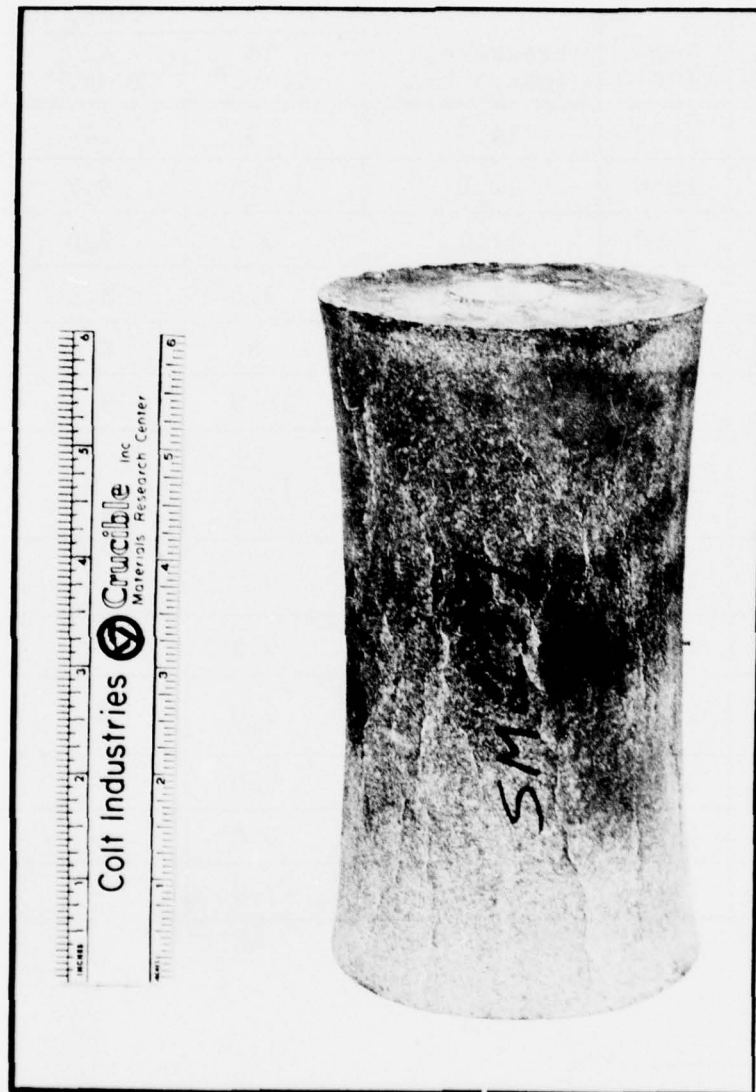


Figure 24. Typical Ti-17 experimental compact.

TABLE 9  
SUMMARY OF Ti-6-4 SPECIMENS

Code	Mold Material	HIP Cycle
277, 278	SiO <sub>2</sub>	CSMD
279, 280	SiO <sub>2</sub>	BCL
281, 282	Al <sub>2</sub> O <sub>3</sub>	CSMD
283, 284	Zircon	CSMD
287, 288	Al <sub>2</sub> O <sub>3</sub>	BCL
292, 293	Zircon	BCL

TABLE 10  
COMPACTION DATA, Ti-6-4

Specimen Numbers	Temp. (°F)	Pressure, (max.) ksi	Time, hr		
			To Temp. <sup>a</sup>	At Temp. <sup>b</sup>	At Temp. & Pressure
277, 278, 283, 284	1740	14.2	16.5	9	0.5
281, 282, 274	1750	13.4	12.0	9	1.5
279, 280, 287, 288, 292, 293	1750	13.6	8.3	-	0.7

<sup>a</sup>Outside of container reached desired temperature.

<sup>b</sup>Soak time to heat through the can.

Note: For BCL cycles, a single time is shown.

For material HIP above the transus, the 1575°F solution anneal was dropped by General Electric but not by CMRC.

The beta transus of specimen SM-227 (HIP at 1550°F) was determined by heating one hour at selected temperatures and water quenching. The results are given in Figure 25 and Table 11. The 1575°F treatment resulted in apparent recrystallization of the beta matrix to an ASTM 6 to 8 grain size. The transus is approximately 1615°F  $\pm$  10°F, which agrees well with previous cast and wrought Ti-17 with the same approximate chemical composition as this material.

Density determinations were carried out on all compacts by water immersion. These are summarized in Table 12. The only specimens which failed to achieve a density equal to or greater than 99% of theoretical were Samples 254, 256, 264, 265, and 269 which were HIP at CSMD at 1550°F and 1600°F. The combination of low temperature and short dwell time of pressure at temperature were responsible for this effect. These were excluded from further evaluation.

TABLE 11

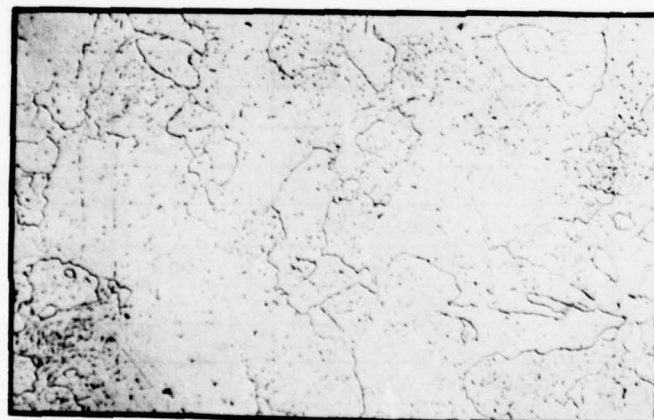
Ti-17 BETA TRANSUS DETERMINATION\*

Heat Treatment	Metallographic Results
1575°F, 1 hr., W.Q.	Below beta transus, 15-20% alpha.
1600°F, 1 hr., W.Q.	Just below transus, 1-2% alpha present.
1625°F, 1 hr., W.Q.	Above beta transus, 3-10 mils grain size, average ~ 6 mils.
1640°F, 1 hr., W.Q.	Above beta transus.

\* Specimen SM-227



1575°F, 1 hr, WQ



1600°F, 1 hr, WQ



1625°F, 1 hr, WQ

Figure 25. Beta-transus series (100X)



TABLE 12

## DENSITY MEASUREMENTS, Ti-17

Compact	Condition	CMRC Data		GE Data	
		Lb/in. <sup>3</sup>	% TD*	Lb/in. <sup>3</sup>	% TD*
227	AH	0.1682	99.88	0.1681	99.8
227	PCTT	.1683	99.94		
233	AH	.1681	99.82	.1672	99.3
233	PCTT	.1683	99.94		
236	AH	.1683	99.94	.1682	99.9
237	AH	.1683	99.94		
237	PCTT	.1684	100	.1684	100
238	AH	.1682	99.88	.1681	99.8
238	PCTT	.1683	99.94		
243	AH	.1683	99.94	.1682	99.9
243	PCTT	.1684	100		
248	AH	.1683	99.94		
248	PCTT	.1683	99.94	.1684	100
250	AH	.1683	99.94	.1683	99.94
250	PCTT	.1683	99.94		
252	AH	.1682	99.88	.1683	99.94
254	AH	.1602	95.13		
254	PCTT	.1592	94.54		
256	AH	.1638	97.27		
256	PCTT	.1654	98.22		
261	AH	.1682	99.88		
261	PCTT	.1683	99.94	.1683	99.94
264	AH	.1651	98.04		
265	AH	.1587	94.24		
265	PCTT	.1601	95.07		
269	AH	.1644	97.62		
270	AH	.1683	99.94	.1683	99.94
270	PCTT	.1683	99.94		
274	AH	.1682	99.88	.1683	99.94
274	PCTT	.1682	99.88		
275	AH	.1682	99.88	.1683	99.94

\*Percent of theoretical density, 0.1684.

TABLE 13  
CHEMISTRY SUMMARY, Ti-17

	Al	Sn	Zr	Mo	Cr	Fe	N	O	C
Ingot	4.7	2.2	2.0	3.8	3.9	0.06	0.006	0.086	-
Powder	4.8	2.29	2.2	3.85	3.9	0.06	0.008	0.094	0.029
SM-270						0.05	0.006	0.100	0.034

A representative specimen (SM-270) was analyzed for interstitials. Results are shown in Table 13. Note that oxygen pick-up is minimal and other residuals are virtually unchanged.

All of the compacts were examined metallographically. The observations are summarized in Table 14. Typical microstructures for the BCL 1550°F HIP are shown in Figure 26. Prior beta grain size is very small and alpha case minimal for all of the mold materials. The maximum depth of penetration by mold fragments is also quite tolerable.

None of the 1550°F compacts HIP at CSMD attained full density. Thus, grain size, alpha case, etc. are of no consequence.

At 1600°F, some of the CSMD compacts attained full density and others did not (see Table 12). The microstructures shown in Figure 27 are typical; some exhibit triple-point porosity and others do not. The as-HIP material shows evidence of a duplex structure. This is possibly a result of a short dwell above the beta transus. This duplex structure persists after heat-treatment. However, after the PCTT at 1600°F (nominal), the structure reverted to beta. Thus, either the transus was slightly lower than 1615°F or the PCTT temperature was excessive. This is shown again in

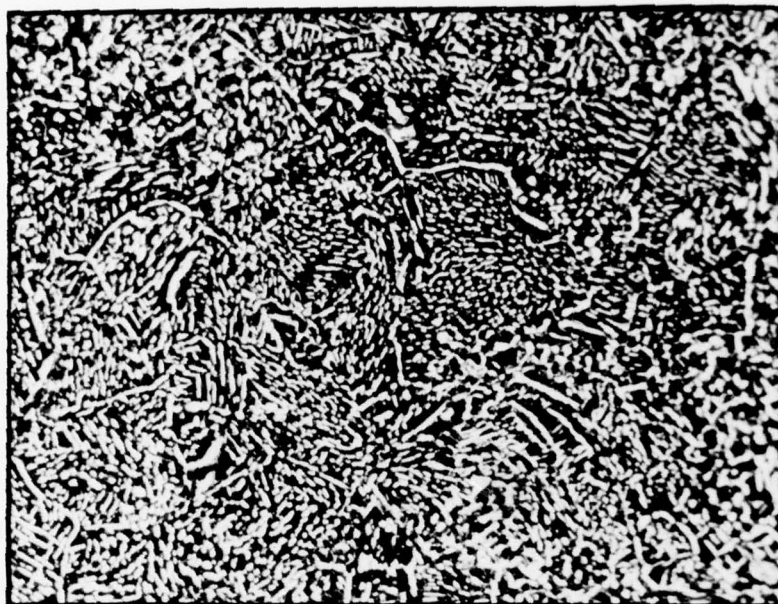
TABLE 14

## Ti-17 STRUCTURE STUDY

HIP Temp. (°F)	Specimen Number and Mold Material	Auto-clave	Heat <sup>a</sup> Treatment Condition	Grain Size, Avg. (in)	Skin Depth (in)	Maximum Mold Fragment Penetration (in)
1550	227 SiO <sub>2</sub>	BCL	TA PT + TA	.002 .0036	.002 .002	.008 .006
	233 SiO <sub>2</sub>	BCL	TA PT + TA	.002 .002	.002 None	None .008
	236 Al <sub>2</sub> O <sub>3</sub>	BCL	TA	.0016	.002	None
	254 Zircon	CSMD	TA PT + TA	Not Fully Dense		
	265 SiO <sub>2</sub>	CSMD	TA PT + TA	Not Fully Dense		
	269 SiO <sub>2</sub>	CSMD	TA	Not Fully Dense		
1600	248 Al <sub>2</sub> O <sub>3</sub>	BCL	TA PT + TA	.0024 .007	.001 .005	.006 None
	250 Al <sub>2</sub> O <sub>3</sub>	BCL	TA PT + TA	.0024 .008	.001 .007	None None
	252 Zircon	BCL	TA	.0028	.003	None
	256 SiO <sub>2</sub>	CSMD	TA PT + TA	.004 .006	.004 .007	None None
	264 Al <sub>2</sub> O <sub>3</sub>	CSMD	TA	.0032	.003	None
	270 Al <sub>2</sub> O <sub>3</sub>	CSMD	TA PT + TA	.005 .009	.001 .002	None .009
1750	237 SiO <sub>2</sub>	BCL	TA PT + TA	.006-.015 .010-.025	.005 .004	None .008
	238 Zircon	BCL	TA PT + TA	.010 .015	.004 .004	None None
	243 Zircon	BCL	TA PT + TA	.008 .014	.005 .005	.005 None
	261 Al <sub>2</sub> O <sub>3</sub>	CSMD	TA PT + TA	.006 .015	.003 .003	None None
	274 Zircon	CSMD	TA PT + TA	.006 .008	.001 .004	None None
	275 Zircon	CSMD	TA	.007	.001	None

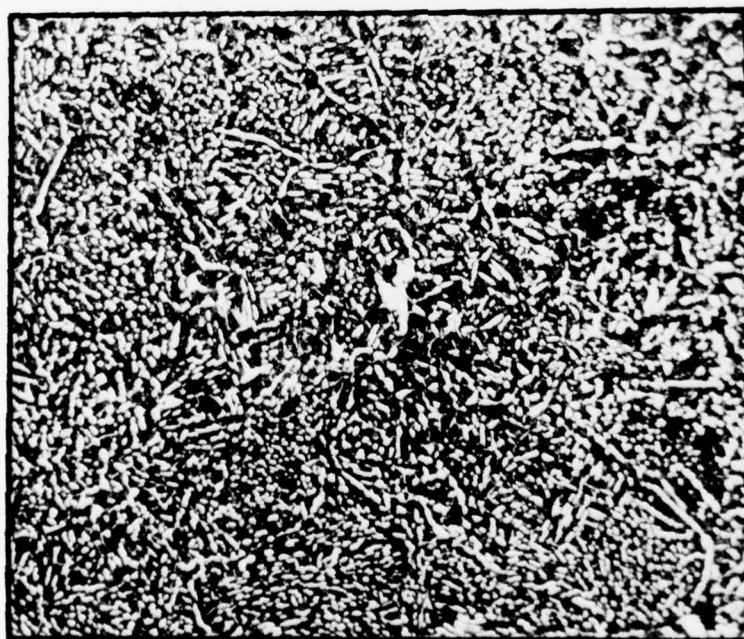
<sup>a</sup>TA = Triplex anneal, 1550 F/4 hr/AC, 1475 F/4 hr/WQ, 1175 F/8 hr/AC.

PT = PCTT, 2 hr at HIP temperature, furnace cool.



26-78

As-HIP + Triplex heat treatment



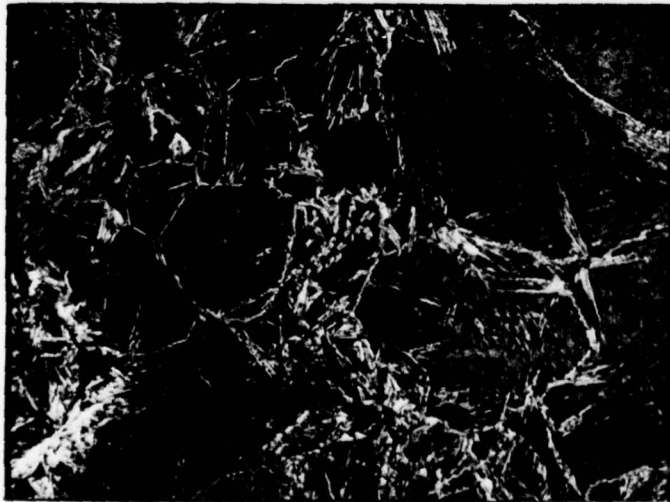
25-78

PCTT + Triplex heat treatment

Figure 26. Typical structures, 1550°F BCL HIP (250X).



11521



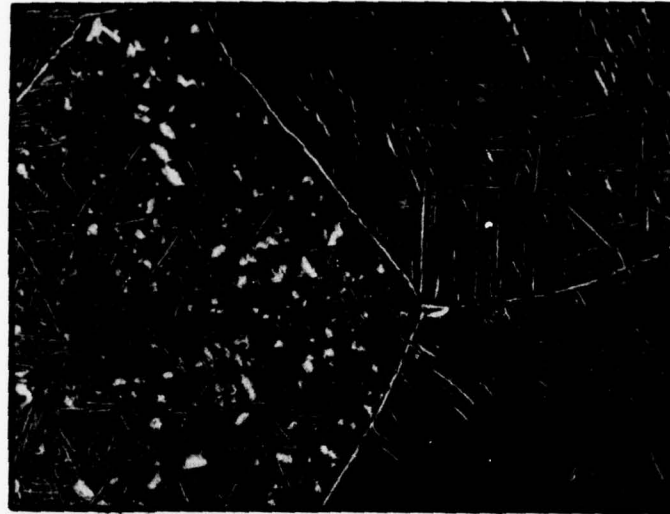
As-HIP

11371



As-HIP + Triplex  
heat treatment

11379



PCTT + Triplex  
heat treatment

Figure 27. Typical structures, 1600° F CSMD HIP (250X).

a heat-treated tensile specimen without a PCTT in Figure 28. Prior beta grain size is quite small and alpha case minimal for this HIP condition.

Typical structures of the BCL 1600°F compacts are shown in Figure 29. As-HIP, the structures are virtually identical with those HIP at 1550°F. Prior beta grain size is slightly larger. Note, however, that the structure reverts to beta after the PCTT. This apparent overtemperature accounts for the increase in alpha case between the as-HIP and HIP + PCTT condition. Again, mold particle penetration is not a problem.

At 1750°F, significant structural differences exist between the BCL and CSMD HIP. These are shown in Figures 30 and 31, respectively. The as-HIP BCL material shows a Widmanstatten transformation beta matrix with grain-boundary alpha. After the triplex heat treatment, the grain-boundary alpha begins to break up and some blunting of the platelets is evident. The PCTT results in still more of this structural refinement.

Beta grain size is more than double that for the sub-transus HIP material, and even more growth occurs during the PCTT. The alpha case is slightly thicker than for the alpha-beta material, but is still of no concern. Mold fragmentation does not pose any problem at this higher temperature.

The CSMD HIP material shows a less well-defined structure because of the short dwell above the transus. This finer structure is more readily broken up during heat-treatment and PCTT. Grain size is smaller and alpha case less than for the BCL HIP material.

As noted in Table 14, mold reaction and/or alpha case is almost independent of the mold material but is a function of temperature. Typical surface structures are shown in Figure 32. At 1550°F, the reaction is minimal. This increases to a few mils at 1600°F and to 10 mils or less at 1750°F. These are all well within the machining allowance planned for the Ti-17 shaft and any other rotating part requiring dynamic balance.

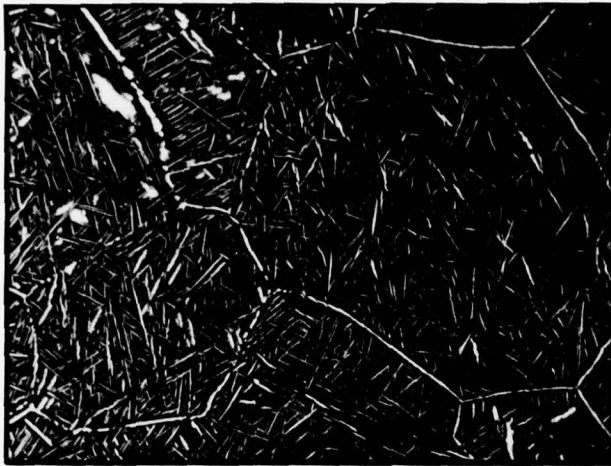
Inclusions also were encountered. These were identified by X-ray analysis and generally of three types, viz. non-metallic (high in SiO<sub>2</sub>), iron, and tungsten. These observations were identical to the Ti-6-4 experience in the Task I Powder Characterization Studies, but now showing up in Ti-17. Typical high SiO<sub>2</sub> and iron inclusions are shown in Figures 33 and 34. The silica-rich particle is from specimen



385-75

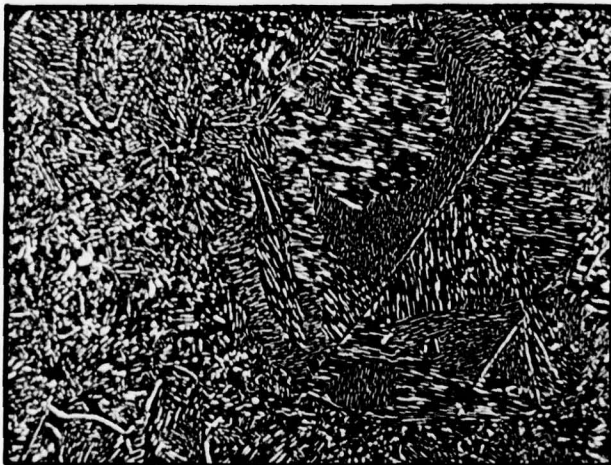
Figure 28. Duplex structure in Ti-17 (250X).  
(This material, SM-270, was HIP at  
CSMD at 1600°F and heat-treated  
without a PCTT)

11520



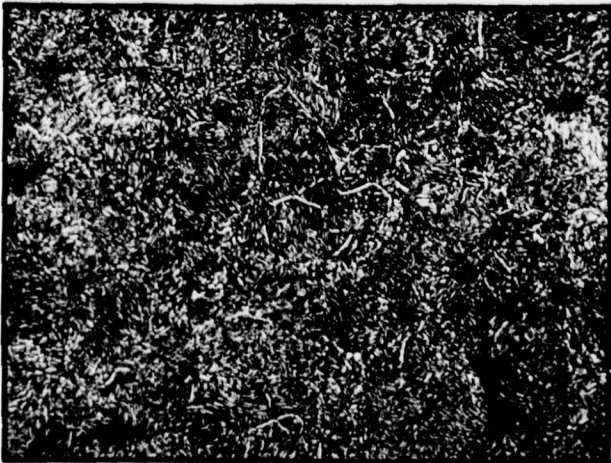
PCTT + Triplex  
heat treatment

11353



As-HIP + Triplex  
heat treatment

11519



As-HIP

Figure 29. Typical structures, 1600°F BCL HIP (250X).

Note: The as-HIP sample is from a stem;  
the porosity is not typical of 1600°F  
BCL HIP.

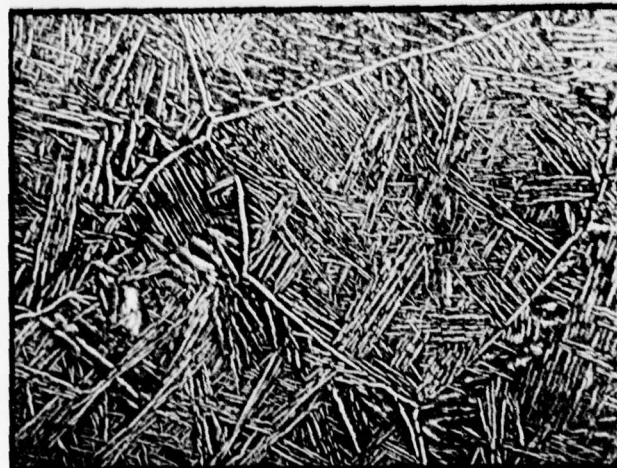


11321



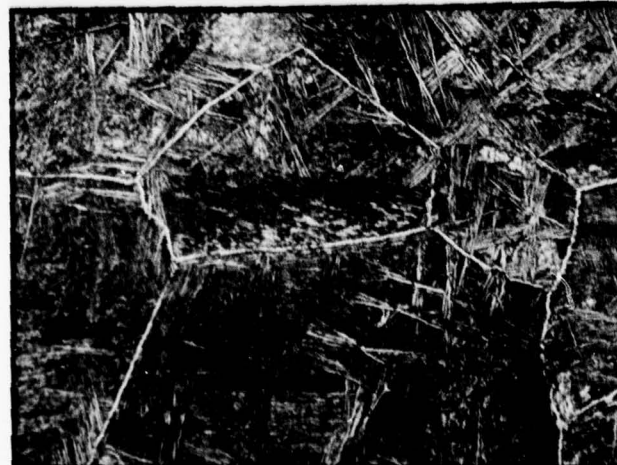
PCTT + Triplex  
heat treatment

11312



As-HIP + Triplex  
heat treatment

11507



As-HIP

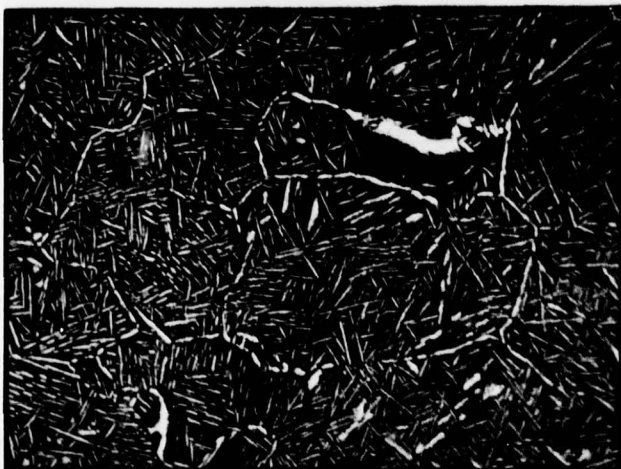
Figure 30. Typical structures, 1750°F BCL HIP (250X).

11383



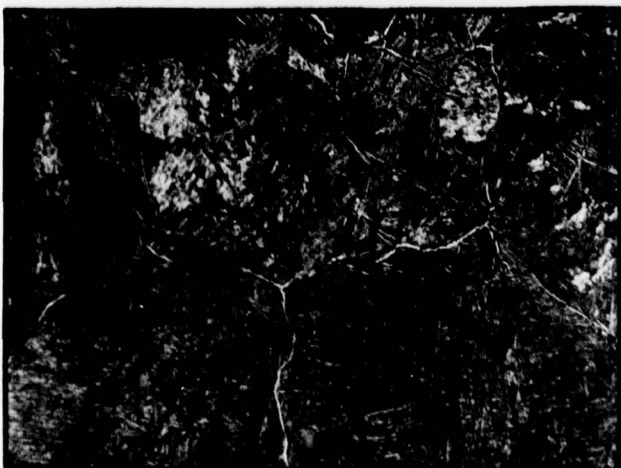
PCTT + Triplex  
heat treatment

11385



As-HIP + Triplex  
heat treatment

11508



As-HIP

Figure 31. Typical structures, 1750°F CSMD HIP (250X).

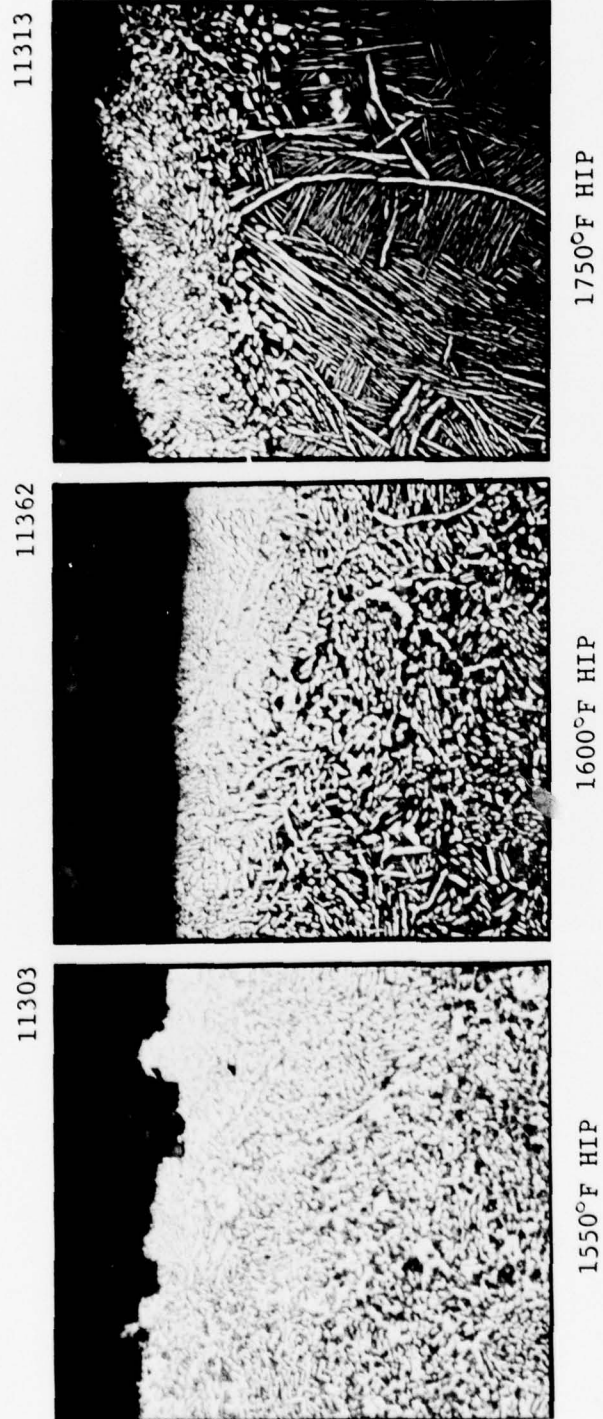


Figure 32. Typical Ti-17 surface structures (250X).

11351

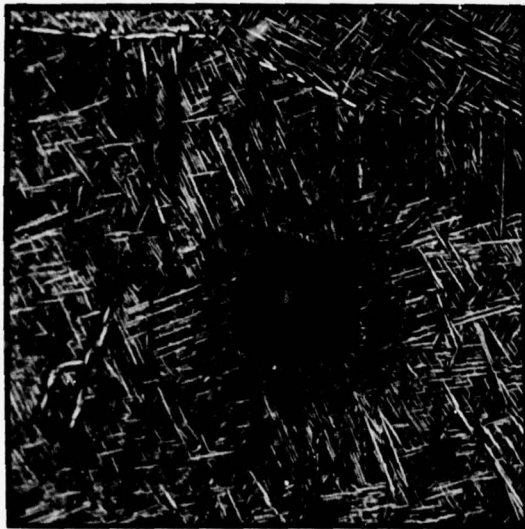


Figure 33. High SiO<sub>2</sub> inclusion (250X).

11345

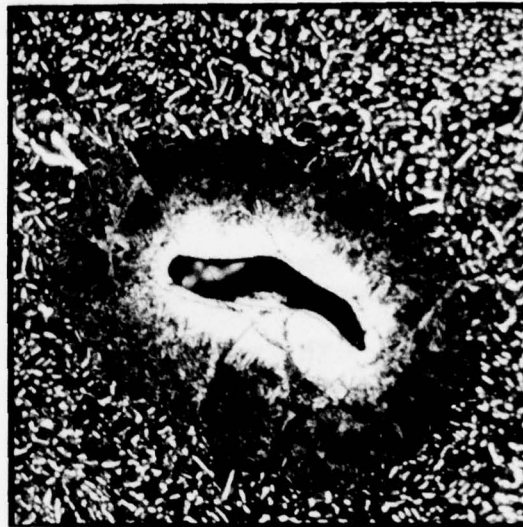


Figure 34. Iron inclusion (250X).

11334



Figure 35. Apparent Beta fleck due to iron inclusion (250X).



SM-243 HIP with a zircon mold and -100 mesh powder. Note the fine structure which results from the use of small particles. The iron inclusions typically have an associated void plus a beta-stabilized area surrounding the particle. A slight sub-surface inclusion gives the appearance of a beta fleck, a problem commonly encountered in Ti-17 due to chromium segregation. However, X-ray analysis conclusively proves iron to be the problem in the case of the PM Ti-17 alloy. The reaction zone from a typical sub-surface iron inclusion is shown in Figure 35.

Two morphologies of tungsten inclusion are shown in Figure 36.

The mechanical properties of the Ti-17 are summarized in Table 15. All of the test data are presented in Appendix B to this report. As-HIP, the alpha-beta material exceed the wrought material specification. The BCL material also meets the specification after a PCTT, whereas the CSMD material does not. This may be due to the micro-structural change noted earlier.

For the 1750°F beta-HIP, the BCL material was marginal, but the CSMD material appears quite satisfactory in the as-HIP condition. Both show appreciable drops in ductility after a PCTT. It is interesting to note that General Electric tended to report lower ductility for the beta-HIP material than did CMRC. This might be attributed to the fact that for the 1750°F material, CMRC continued to use the triplex heat-treatment, whereas General Electric used only a duplex heat-treatment. The triplex treatment was shown earlier to result in blunting of the sharp alpha platelets, but, as is shown in Figure 37, the duplex treatment is less effective in this regard.

Some inclusions were noted on tensile fracture surfaces. Generally, these appear to have little effect on strength or ductility. Tungsten was not found but both iron and non-metallics were. Typical examples are shown in Figures 38 and 39.

#### 3.1.2.5 Ti-17 Data Analysis

The effect of the process variables was examined separately for the alpha-beta and beta-HIP cycles. For sub-transus compaction, the as-HIP BCL averages ( $\bar{X}$ ) from Appendix B to this report were considered baseline values. The standard deviation,  $\sigma$ , where  $t$  designates the total population for these values, is:



388-75

Irregular particle in SM-236

1000X



388-75

Spherical (?) particle in SM-243

1000X

Figure 36. Typical tungsten inclusions.

TABLE 15

## SUMMARY OF MECHANICAL PROPERTIES, Ti-17

HIP	Cycle	PCTT	Strength (ksi)		Elonga- tion (%)	Reduction of Area (%)	Charpy, K <sub>Q</sub> (ksi $\sqrt{\text{in.}}$ )
			F <sub>Tu</sub>	F <sub>Ty</sub>			
Alpha-beta <sup>a</sup>	BCL	No	164.9	158.9	14.3	34.9	48.3
		Yes	166.8	159.3	12.3	25.5	45.3
Alpha-beta <sup>b</sup>	CSMD <sup>d</sup>	No <sup>e</sup>	164.3	156.9	13.6	35.3	46.4
		Yes	161.7	151.2	9.0	15.0	-
Beta <sup>c</sup>	BCL	No	162.8	154.1	6.6	11.9	59.2
		Yes	164.7	156.8	4.6	8.9	49.6
Beta <sup>c</sup>	CSMD	No	165.0	155.2	10.0	21.1	54.2
		Yes	165.4	155.9	5.3	10.4	54.0
<u>Specifications</u>							
Alpha-beta, wrought		No	163 min	153 min	7 min	15 min	30 min
Beta, wrought		No	163 min	153 min	5 min	10 min	50 min

<sup>a</sup>1550 and 1600 F.<sup>b</sup>1600 F.<sup>c</sup>1750 F.<sup>d</sup>Excluding specimens with obvious porosity.<sup>e</sup>Some of these specimens exhibit a beta structure after the PCTT.



100X



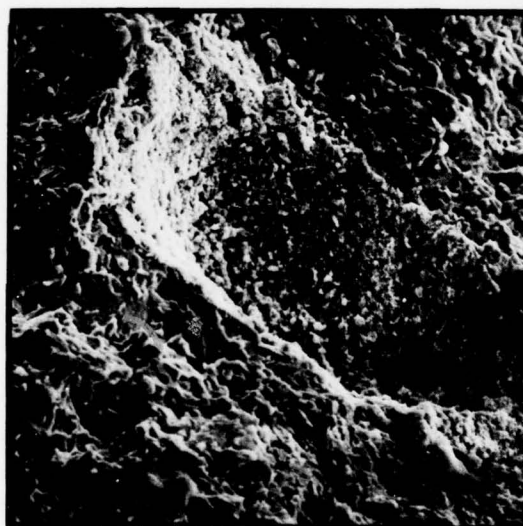
1000X

388-75

Figure 37. Structure of duplex treated Ti-17.



2-1/2X

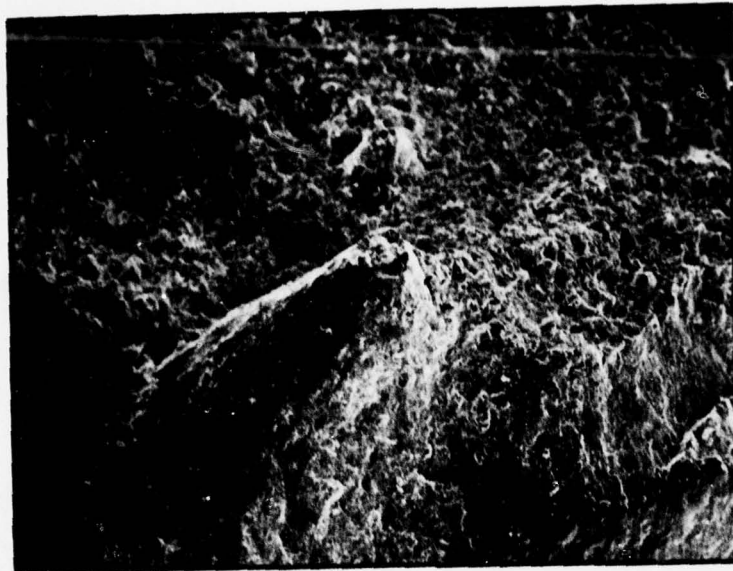


400X

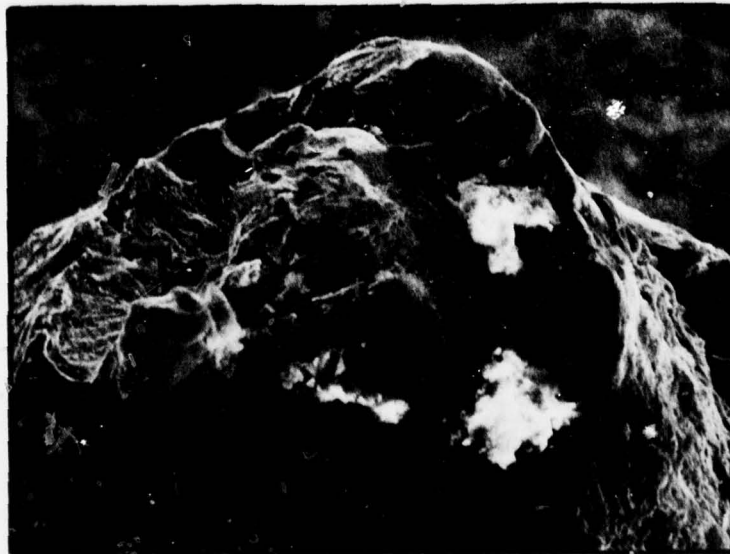
74-1680

Figure 38. Inclusion containing Si, Ca, Cr, and Mn.  
(This is a tensile break on specimen SM-227)





43X



425X

74-1792

Figure 39. Iron inclusion in tensile specimen SM-250.

$F_{tu}$	-	1.8 ksi	El	-	1.3%
$F_{ty}$	-	1.6 ksi	RA	-	3.6%

Individual property averages were then computed for each lot of specimens embodying a given variable. The difference between this average,  $\bar{X}_1$ , and the overall average,  $\bar{X}$ , is termed  $\Delta$ . A value of  $\Delta$  greater than  $\sigma_t$  is assumed to be significant, whereas a  $\Delta$  less than  $\sigma_t$  is considered to fall within the normal data scatter. Throughout this report this method of determining whether groups of values are significantly different will be used. It is recognized that a more rigorous analysis would be to compare the difference between the two means with the standard error of the difference. Using this so-called t test, the probability that two sample groups are drawn from the same population can be defined precisely. That is, the level of significance of a particular difference between the means can be given an exact probability value<sup>4</sup>.

From Table 16, it can be seen that the  $\Delta$  values for all of the mold materials are small. Only those of the strengths with  $\text{SiO}_2$  (marked with an asterisk) exceed  $\sigma_t$ . Note also that only the  $\text{SiO}_2$  molds show a positive  $\Delta$  for ductility. Although tensile test data does not reflect surface defects and reaction zone effects from the mold material, the data indicate no diffusion or compaction problems with any of the mold materials. The data indicate that all mold materials are acceptable, but for convenience, the  $\text{SiO}_2$  system was chosen for future work.

Autoclave hold time below the transus appears to have no effect on properties. As is shown in Table 16, the  $\Delta$  values are very small for both 30 and 120 minute cycles. Here, economy dictates the shortest feasible cycle, so the 30 minute hold should be used in subsequent work.

Although the  $\Delta$  values for HIP temperature are small in comparison with  $\sigma_t$ , there is a definite trend towards higher strength and lower ductility with increasing consolidation temperature below the beta transus.

Fine powder, (-100 mesh) was introduced into this program not necessarily to show a superiority, but an equivalence. If a process capable of making fine titanium powder is developed, it may be possible to

TABLE 16  
EFFECT OF VARIABLES, Ti-17, SUB-TRANSUS HIP

A. Effect of Mold Material					
Variable		$F_{tu}$ (ksi)	$F_{ty}$ (ksi)	Elonga- tion (%)	Reduction of Area (%)
SiO <sub>2</sub>	Avg, $X_1$ $\Delta$	162.7 -2.2*	156.9 -1.7*	15.5 +1.2	36.3 +1.4
Al <sub>2</sub> O <sub>3</sub>	Avg, $X_1$ $\Delta$	165.5 +0.6	159.4 +0.8	14.1 -0.2	34.9 0
Zircon	Avg, $X_1$ $\Delta$	165.5 +0.6	158.2 -0.4	13.6 -0.7	33.6 -1.3
B. Effect of Autoclave Hold Time					
30 min	Avg, $X_1$ $\Delta$	164.9 0	159.0 +0.4	14.4 +0.1	34.5 -0.4
120 min	Avg, $X_1$ $\Delta$	164.9 0	158.0 -0.6	14.2 -0.1	35.4 +0.5
C. Effect of HIP Temperature					
1550 F	Avg, $X_1$ $\Delta$	163.6 -1.3	157.4 -1.2	15.1 +0.8	36.8 +1.9
1600 F	Avg, $X_1$ $\Delta$	166.0 +1.1	159.5 +0.8	13.7 -0.6	33.4 -1.5
D. Effect of Powder Particle Size					
-35 mesh	Avg, $X_1$ $\Delta$	165.0 +0.1	158.3 -0.3	14.5 +0.2	37.3 +2.4
-100 mesh	Avg, $X_1$ $\Delta$	164.7 -0.2	159.1 +0.5	14.1 -0.2	31.5 -3.4
E. Effect of PCTT					
With PCTT	Avg, $X_1$ $\Delta$	166.8 +1.9*	159.3 +0.7	12.3 -2.0*	25.5 -9.4*
F. Effect of Test Procedure					
CMRC Data	Avg, $X_1$ $\Delta$	165.0 +0.1	158.5 +0.1	15.0 +0.7	35.8 +0.9
GE Data	Avg, $X_1$ $\Delta$	164.7 -0.2	158.6 0	11.5 -2.8*	33.1 -1.8
G. Effect of HIP Cycle (1600 F only)					
BCL	Avg, $X_1$ $\Delta$	166.0 +0.4	159.5 +0.6	13.7 -0.2	33.4 -0.5
CSMD	Avg, $X_1$ $\Delta$	163.8 -1.8*	156.3 -2.6*	15.0 +1.1	36.5 +2.6
1600 Baseline	$X_2$ $\sigma^2$ $\sigma_t$	165.6 2.5 1.6	158.9 3.4 1.9	13.9 1.9 1.4	33.9 9.4 3.1

Note: Values marked with asterisk exceed  $\sigma_t$ .

employ a practice which would limit the maximum flaw size as defined by fracture mechanics. The data in Table 16 show no effect of particle size, i.e., all  $\Delta$  values are less than  $\sigma_t$ . The lack of any negative effect, therefore, shows the technical feasibility of such a concept. The economic feasibility remains to be considered.

The PCTT has a significant effect on properties; the  $+\Delta$  for  $F_{tu}$  exceeds  $\sigma_t$ . Unfortunately, so do the  $-\Delta$  values for elongation and reduction of area. The latter is regarded as especially serious and, coupled with economics, is the reason for the decision to discontinue the use of a PCTT step.

The effect of test technique can often be significant. Therefore, this factor was also considered. By our definition, only elongation shows any significance, i.e.,  $\Delta \geq \sigma_t$ . Note, though, that CMRC data show a consistent positive trend as compared with General Electric's data. This inherent variability was the rationale for dividing the testing effort on this contract.

Because of the porosity encountered in the 1550°F HIP cycles, CSMD and BCL compaction can be compared only at 1600°F. This necessitates the use of a new set of baseline values excluding those for 1550°F HIP at BCL. These are shown in Part C of Table 16 along with the respective  $\Delta$  values. The lower strength associated with the CSMD cycle is significant. On the other hand, the CSMD ductilities show positive  $\Delta$  values, but they are less than  $\sigma_t$ . Notwithstanding these comparisons, sub-transus HIP of Ti-17 in a CSMD cycle is regarded as marginal because of the frequency of incomplete consolidation which was encountered.

For the 1750°F. beta HIP cycles, the overall averages,  $\bar{X}$ , and standard deviations,  $\sigma_t$ , are:

Property	$\bar{X}$	$\sigma_t$
$F_{tu}$	164.1	1.7
$F_{ty}$	154.7	1.8
El	8.5	2.5
RA	17.0	7.2

In Table 17, several significant observations are marked with an asterisk with respect to mold material.



TABLE 17

## EFFECT OF VARIABLES, TI-17, BETA-HIP

A. Effect of Mold Material					
Variable		$F_{tu}$ (ksi)	$F_{ty}$ (ksi)	Elongation (%)	Reduction of Area (%)
SiO <sub>2</sub>	Avg, $X_1$ $\Delta$	162.3 -1.8*	153.9 -0.8	5.2 -3.3*	9.1 -7.9*
Al <sub>2</sub> O <sub>3</sub>	Avg, $X_1$ $\Delta$	166.4 +2.5*	153.0 -1.7	10.0 +1.5	16.2 -0.8
Zircon	Avg, $X_1$ $\Delta$	164.2 +0.1	155.3 +1.6	9.4 +0.9	19.8 +2.8
B. Effect of HIP Cycle					
BCL	Avg, $X_1$ $\Delta$	163.4 -0.7	154.5 -0.2	7.7 -0.8	15.0 -2.0
CSMD	Avg, $X_1$ $\Delta$	165.4 +1.3	155.1 +0.4	10.9 +2.4	23.3 +6.3
C. Effect of Autoclave Hold Time					
5 min	Avg, $X_1$ $\Delta$	166.4 +2.3*	153.0 -1.7	10.0 +1.5	16.2 -0.8
30 min	Avg, $X_1$ $\Delta$	164.2 +0.1	155.3 +0.6	9.4 +0.9	19.8 +2.8
120 min	Avg, $X_1$ $\Delta$	162.3 -1.8*	153.9 -0.8	5.2 -3.3*	9.1 -7.9*
D. Effect of Particle Size					
-35 mesh	Avg, $X_1$ $\Delta$	164.0 -0.1	154.5 -0.2	9.0 +0.5	18.7 +1.7
-100 mesh	Avg, $X_1$ $\Delta$	164.7 +0.6	155.1 +0.4	8.0 -0.5	13.4 -3.6
E. Effect of PCTT					
2 hr PCTT	Avg, $X_1$ $\Delta$	165.0 +0.9	156.5 +1.8	4.9 -3.6*	9.5 -7.5*
F. Effect of Test Procedure					
CMRC Data	Avg, $X_1$ $\Delta$	163.8 -0.3	153.8 -0.9	8.7 +0.2	15.8 -1.2
GE Data	Avg, $X_1$ $\Delta$	164.4 +0.3	156.6 +1.9	8.2 -0.3	19.5 +2.5

Note: Values marked with asterisk exceed  $\sigma_t$ .

The most important is that, for a 1750°F HIP temperature, SiO<sub>2</sub> appears to be unsatisfactory, whereas the Al<sub>2</sub>O<sub>3</sub> and zircon should both be usable.

Although the comparison of CSMD and BCL 1750°F HIP cycles show no significant values of  $\Delta$ , i.e., none exceed  $\sigma_t$ , it is interesting to note that all BCL  $\Delta$  values are negative and all CSMD values are positive. This probably relates to the microstructural differences noted earlier. Although there is an inclination to favor a CSMD cycle at 1750°F, either should be acceptable.

Unlike the alpha-beta cycles, autoclave hold time is an important variable at 1750°F. Especially noteworthy are the large  $-\Delta$  values at 120 minutes. At 5 minutes, both positive and negative values are seen, but at 30 minutes, all are positive. Thus, a 30 minute cycle is recommended for high-temperature HIP of Ti-17.

Again, particle size appears to have no effect on properties. As noted earlier, -35 mesh was specified until finer powder becomes more cost effective.

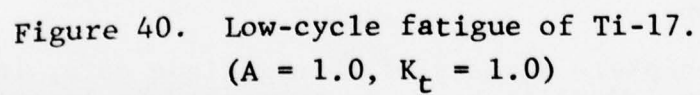
The PCTT shows a significant drop in ductility. This is probably associated with excessive grain growth at 1750°F. This treatment has been discontinued.

For beta HIP Ti-17, the effect of test procedure appears to be random. This is inconsistent with the same comparison on sub-transus HIP material where definite trends were noted.

Low cycle (tension-tension) fatigue curves for the Ti-17 are shown in Figure 40. All of the points fall below the typical wrought material curve. Note, though, that of the five specimens with no obvious inclusions on the fracture surface, only one falls outside the  $3\sigma$  limits. Conversely, of 10 specimens with identified inclusions, five fall below the  $3\sigma$  limit. Note also that, of the four beta-HIP materials tested (see arrows), only one falls below the  $3\sigma$  line and it had an inclusion.

A complete summary of this fatigue data, including inclusion identification, is presented in Appendix B to this report (Table B-4 and B-5). Some typical fracture surfaces are shown in Figure 41. One of these specimens was HIP in an Al<sub>2</sub>O<sub>3</sub> mold and the other in zircon.

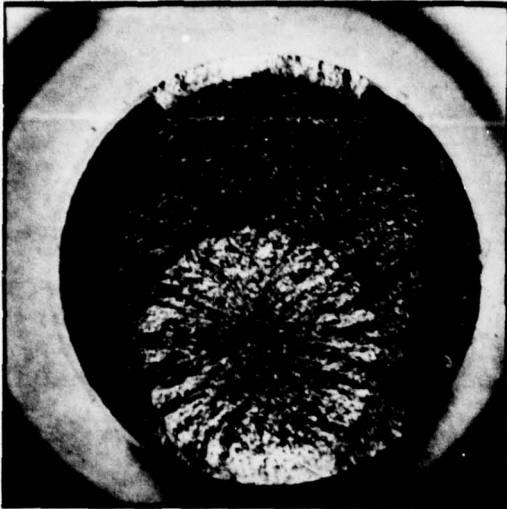
As was the case for the tensile testing, no tungsten inclusions were found on the LCF fractures.



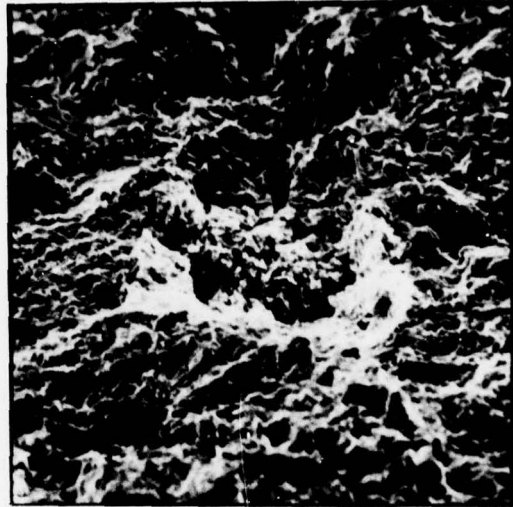
66

390-75

381-75



8.5X



285X

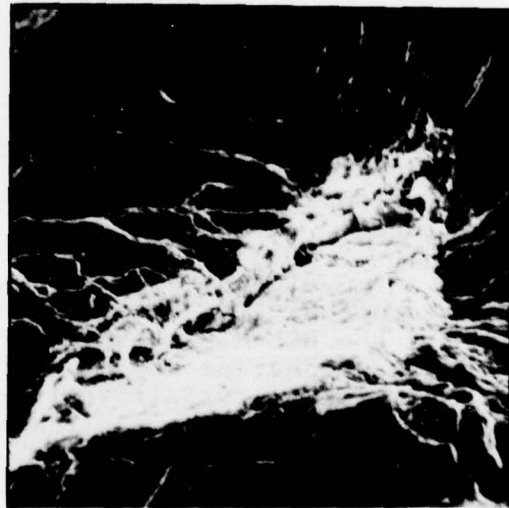
A. Inclusion containing Fe, Mn, K, Ca, and Si in compact SM-233.

382-75

382-75



68X



725X

B. High Si, Ca, K inclusion in compact SM-275.

Figure 41. Typical LCF fractures.



The inclusion problem makes it difficult to draw meaningful conclusions. Further testing with cleaned powder was completed during the next task in an attempt to clarify this matter.

For high cycle fatigue, an apparent structural dependence is again shown in Figure 42. Almost all of the alpha-beta HIP material falls below the  $3\sigma$  limits for wrought Ti-17. Note, however, that the BCL beta-HIP material falls within the  $3\sigma$  range and the CSMD beta-HIP material is nearly on the wrought curve.

Because of the fretting associated with rotating beam fatigue failures, fractography is difficult. Nevertheless, some inclusions were observed; a typical one is shown in Figure 43. This compact (SM-270) was HIP in an  $Al_2O_3$  mold.

#### 3.1.2.6 Ti-6-4 Evaluation

Three variables, (1) type of HIP cycle, (2) mold material, and (3) Post Compaction Thermal Treatment (PCTT) were included in the investigation. The PCTT consisted of a 1750°F treatment with a 2 hour hold followed by a furnace cool.

Density determinations were made on samples from all compacts by water immersion techniques. These are summarized in Table 18. Every specimen attained a density of  $\geq 99.7$  percent of theoretical. The PCTT had no effect on density; this indicates that TIP is also not a problem with this alloy.

A representative specimen was analyzed for interstitials. Results are shown in Table 19. With the exception of a minor decrease in iron, the content of residuals is essentially the same as that of the parent ingot.

A microstructural study was performed on the various compacts. These results are summarized in Table 20. All of the BCL-HIP materials exhibit typical coarse plate-like alpha, as can be seen in Figure 44. Note the partial recrystallization, indicative of grain-boundary working, in the as-HIP material. This is most likely due to the nature of the cycle used, i.e., some pressure was applied prior to reaching the 1750°F HIP temperature. The BCL-HIP + PCTT materials show structures typical of sub-transus processed Ti-6-4.

The CSMD-HIP material (Figure 45) shows no recrystallization at the grain-boundaries since all working was

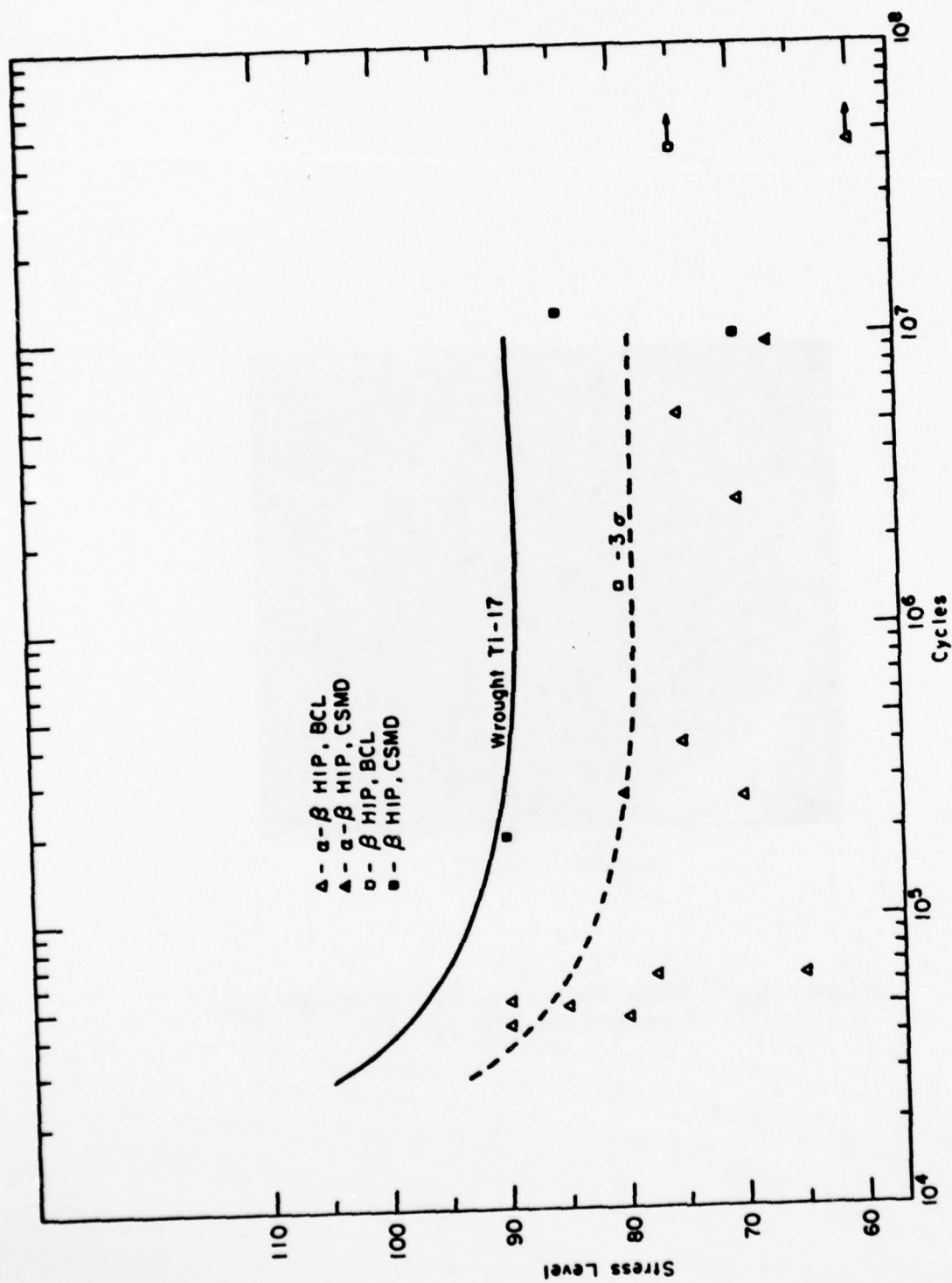
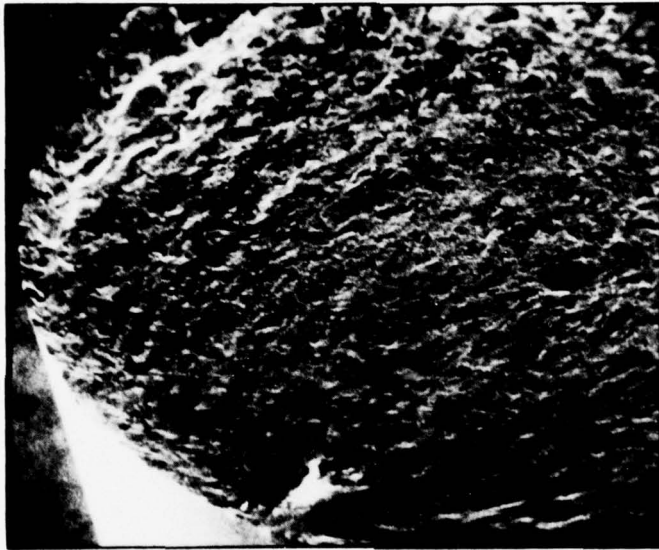


Figure 42. High cycle fatigue of Ti-17.  
 ( $A = \infty$ ,  $K_t = 1.0$ )



Compact SM-270

Figure 43.  $\text{SiO}_2$  inclusion of HCF fracture-  
Compact SM-270 ( $\sim 25\times$ ).

TABLE 18

## DENSITY MEASUREMENTS, Ti-6-4

Compact	Condition	Lb/in. <sup>3</sup>	% TD
277	AH	0.1596	99.94
277	PCTT	.1596	99.94
279	AH	.1597	100
279	PCTT	.1597	100
281	AH	.1595	99.87
281	PCTT	.1596	99.94
284	AH	.1596	99.94
284	PCTT	.1596	99.94
287	AH	.1597	100
287	PCTT	.1597	100
293	AH	.1596	99.94
293	PCTT	.1597	100

TABLE 19

## CHEMISTRY SUMMARY, Ti-6-4 (Weight %)

	Al	V	Fe	C	N	O
Ingot	6.0	3.80	0.050	0.013	0.010	0.094
Powder	6.0	3.85	0.045	0.024	0.008	0.094
SM-279			0.04	0.038	0.006	0.100



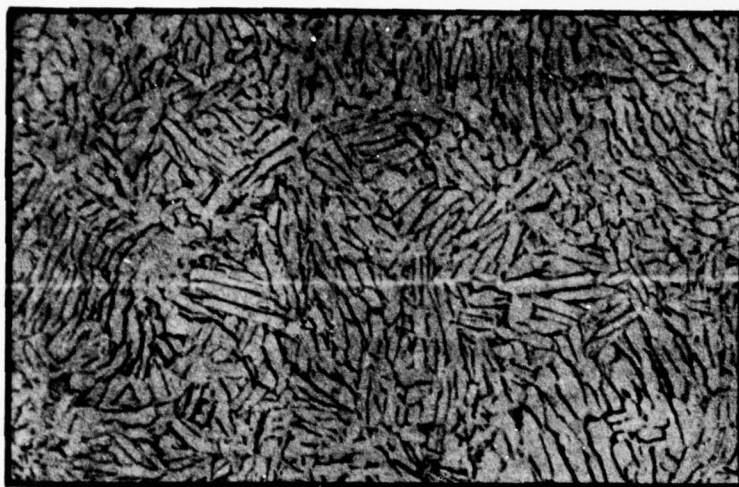
TABLE 20

## Ti-6-4 STRUCTURE STUDY

HIP Temp. (°F)	Specimen Number and Mold Material	Auto-clave	Heat <sup>a</sup> Treatment Condition	Beta Grain Size, Avg. (in)	Skin Depth (in)
1750	279 SiO <sub>2</sub>	BCL	Ann. PT + Ann.	.005 .0056	<.001 <.001
	287 Al <sub>2</sub> O <sub>3</sub>	BCL	Ann. PT + Ann.	.005 .005	<.001 <.001
	293 Zircon	BCL	Ann. PT + Ann.	.004 .005	<.001 <.001
1750	277 SiO <sub>2</sub>	CSMD	Ann. PT + Ann.	.005 .016	<.001 <.008
	281 Al <sub>2</sub> O <sub>3</sub>	CSMD	Ann. PT + Ann.	.006 .016	<.001 .012
	284 Zircon	CSMD	Ann. PT + Ann.	.006 .012	<.001 .008

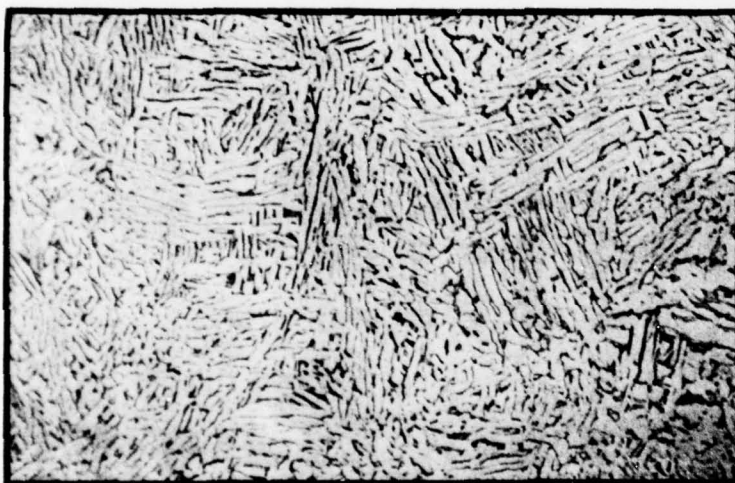
<sup>a</sup>Ann. = 4 h 1450°F, furnace cool to 1100°F, air cool.  
PT = PCTT, nominally 2 h 1750, furnace cool.

11405



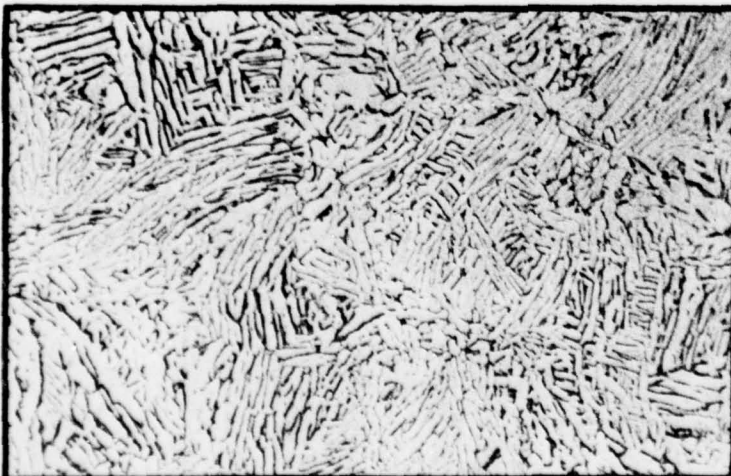
As-HIP + PCTT

11407



As-HIP + Anneal

11517



As-HIP

Figure 44. Typical microstructures of 1750°F BCL HIP Ti-6-4 (250X).

AD-A078 039

COLT INDUSTRIES INC PITTSBURGH PA CRUCIBLE MATERIALS--ETC F/G 11/6  
CONSOLIDATION OF TITANIUM POWDER TO NEAR NET SHAPES.(U)

MAY 78 J H SCHWERTZ , V K CHANDHOK

F33615-74-C-5114

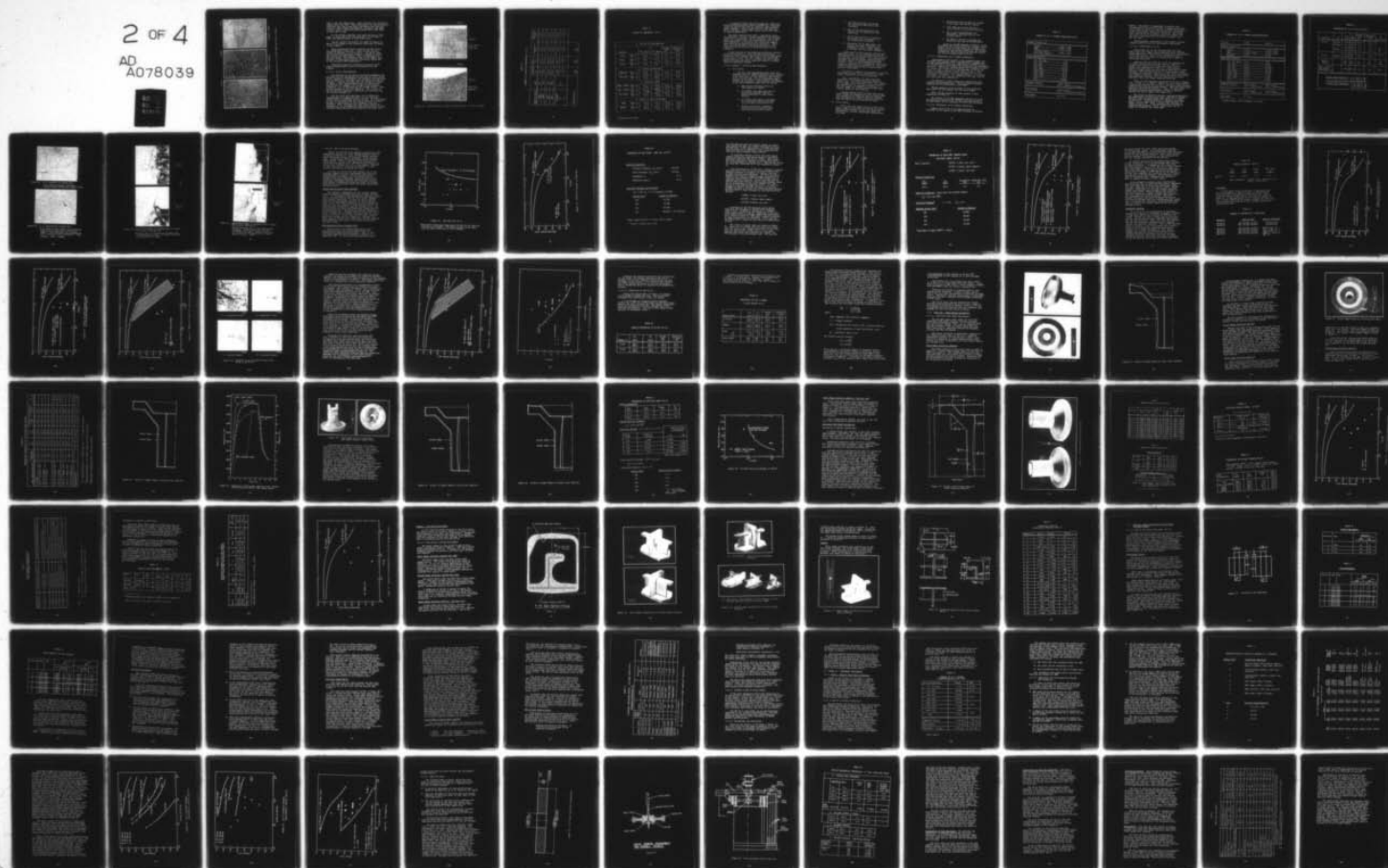
UNCLASSIFIED

AFML-TR-78-41

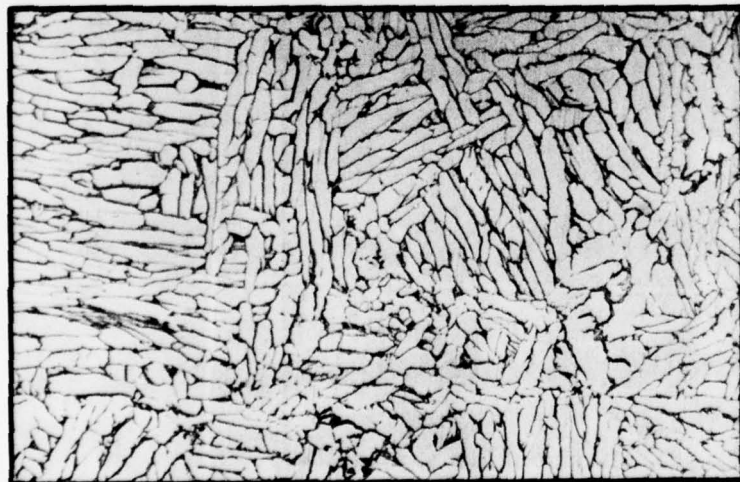
NL

2 OF 4

AD  
A078039

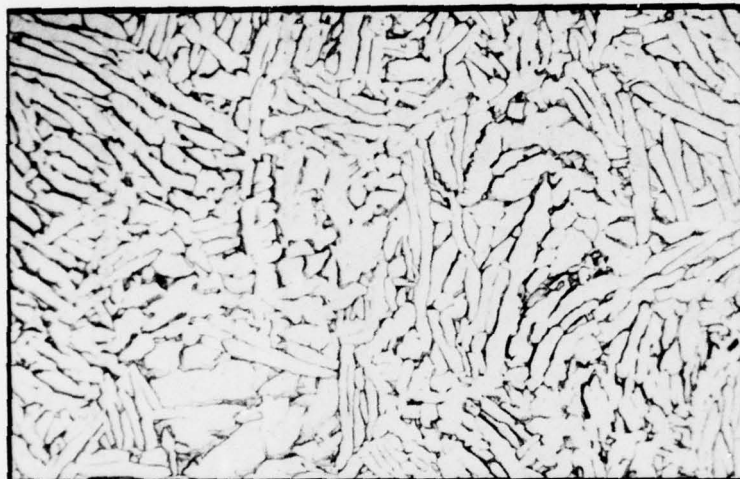


11516



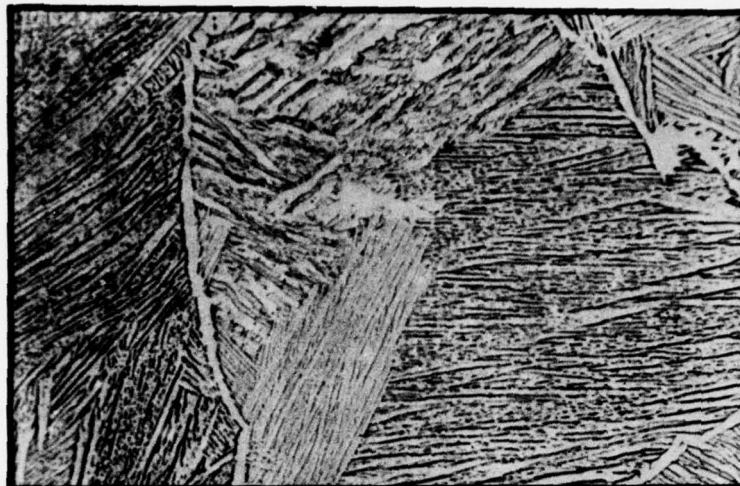
As-HIP

11395



As-HIP + Anneal

11393



As-HIP + PCTT

Figure 45. Typical microstructures of 1750°F CSMD-HIP Ti-6-4 (250X).



done at the HIP temperature. Note, however, the structural change after the PCTT. This transformed beta microstructure indicates that the actual PCTT temperature was above the effective beta transus temperature. Moreover, the CSMD compacts tend to show more grain growth after PCTT than do those HIP at BCL.

In the as-HIP condition, the reaction zone or skin depth is quite small for all materials. Even after a PCTT, the maximum depth is only 0.012 inch.

Typical surface structures are shown in Figure 46. There is no change in the structure from edge to center of the compact.

Room temperature tensile data for the ELI Ti-6-4 are summarized in Table 21. Detailed data are presented in Appendix C to this report. As can be seen, ductilities are excellent; however, strength is below the desired 130/120 minimum. This is attributed to the low oxygen. The ductility drop in the CSMD + PCTT material is associated with the structural change due to the excessive PCTT temperature.

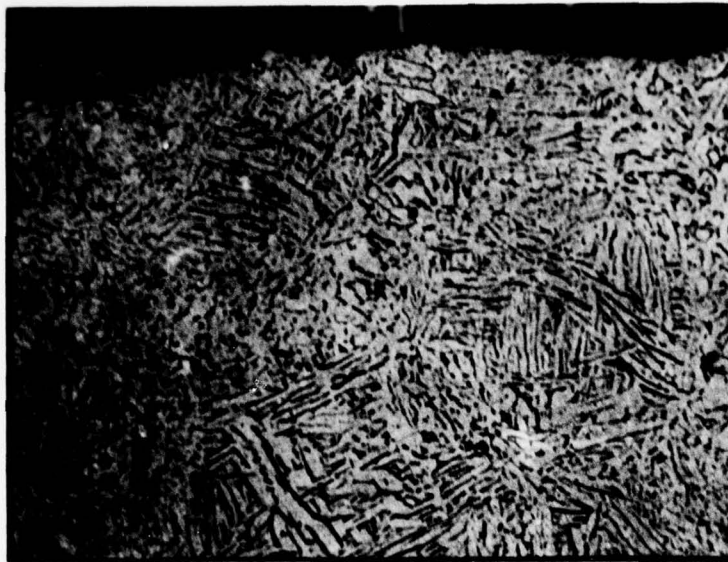
Additional property testing was suspended until higher oxygen powder could be introduced into the program.

### 3.1.2.7 Ti-6-4 Data Analysis

The analysis of the effect of process variables was performed in the same manner as that for the Ti-17 alloy. Of the variables investigated, for example, mold material, type of HIP cycle, and PCTT, only the latter proved significant. Property averages for the variables, listed in Table 22 were compared with those for the overall population, for example, the average  $\bar{X}$  and standard deviation,  $\sigma_t$ , of the data for all as-HIP Ti-6-4. This overall average is noted in Table 21. The  $\Delta$  value is the difference between the individual lot averages,  $X_1$ , and overall averages,  $\bar{X}$ .

For the three mold materials, all  $\Delta$  values are insignificant in comparison with  $\sigma_t$ , but the SiO<sub>2</sub> system shows a consistent positive trend. In the previous section it was noted that the zircon molds were suspect because of penetration of mold fragments into the titanium. Thus, although the Al<sub>2</sub>O<sub>3</sub> system should be satisfactory, we recommend the SiO<sub>2</sub> molds because of more extensive experience with this material and lower cost.

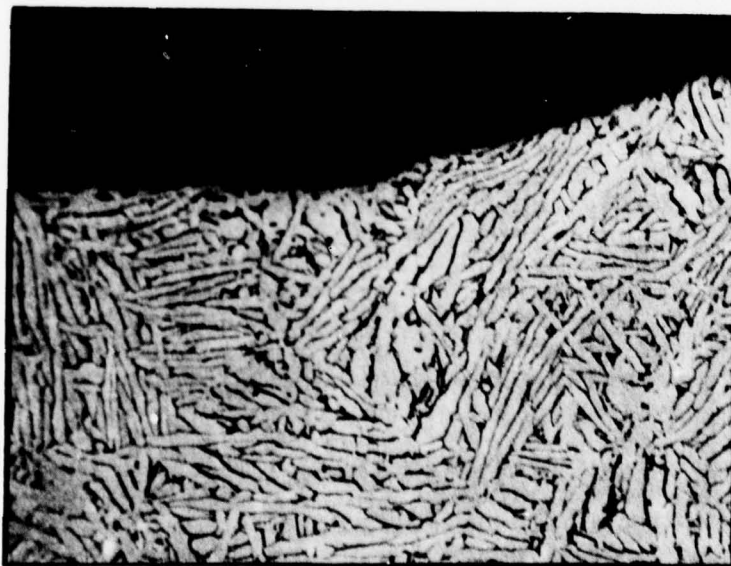
11404



SM-287

$\text{Al}_2\text{O}_3$  Mold  
BCL HIP

11388



SM-277

$\text{SiO}_2$  Mold  
CSMD HIP

Figure 46. Typical surface (edge) microstructures of Ti-6-4 (250X).

TABLE 21

## SUMMARY OF TENSILE PROPERTIES, Ti-6-4

Type of Cycle	PCTT	Strength (ksi)		Elongation (%)	Reduction of Area (%)
		F <sub>tu</sub>	F <sub>ty</sub>		
CSMD	No	122.9	111.3	17.7	44.4
CSMD	Yes	122.3	110.5	14.7	33.4
BCL	No	125.7	116.0	17.3	44.2
BCL	Yes	121.3	109.8	17.0	43.6
Average	} No	124.3	113.7	17.5	44.3
$\sigma^2$		6.7	8.3	1.4	1.5
$\sigma_t$		2.6	2.9	1.2	1.2
Specification		130 min	120 min	10 min	

TABLE 22

EFFECT OF VARIABLES, Ti-6-4

A. Effect of Mold Material					
Variable		$F_{tu}$ (ksi)	$F_{ty}$ (ksi)	Elonga- tion (%)	Reduction of Area (%)
SiO <sub>2</sub>	Avg, $X_1$ $\Delta$	124.4 +.1	113.8 +.1	17.5 0	44.6 +.3
Al <sub>2</sub> O <sub>3</sub>	Avg, $X_1$ $\Delta$	124.3 0	113.5 -.2	17.7 +.2	44.1 -.2
Zircon	Avg, $X_1$ $\Delta$	124.2 -.1	113.7 0	17.3 -.2	44.2 -.1
B. Effect of HIP Cycle					
CSMD HIP	Avg, $X_1$ $\Delta$	122.9 -1.4	111.3 -2.4	17.7 +.1	44.4 +.1
BCL HIP	Avg, $X_1$ $\Delta$	125.7 +1.4	116.0 +2.3	17.3 -.2	44.2 -.1
C. Effect of PCTT					
CSMD + PCTT	Avg, $X_1$ $\Delta$	122.3 -2.0	110.5 -3.2*	14.7 -2.8*	33.4 -10.9*
BCL + PCTT	Avg, $X_1$ $\Delta$	121.3 -3.0*	109.8 -3.9*	17.6 +.1	43.6 -0.7
All PCTT	Avg, $X_1$ $\Delta$	121.8 -2.5	110.2 -3.5*	16.2 -1.3*	38.5 -5.8*
D. Effect of Test Procedures					
CMRC	Avg, $X_1$ $\Delta$	121.8 -2.5	112.5 -1.2	18.8 +1.3*	45.8 +1.5*
MCAIR	Avg, $X_1$ $\Delta$	125.6 +1.3	114.3 +0.6	16.8 -0.7	43.5 -0.8

\* $\Delta$  values exceed  $\sigma_t$ .



In comparing CSMD versus BCL compaction, CSMD gives better ductility and BCL better strength due to the variation in heat-up rate and its effect on grain boundary alpha formation. The  $\Delta$  values are also less than  $\sigma_t$ . Still, the data indicate that either type of HIP could be used satisfactorily.

The PCTT treatment does have a significant effect on properties. All the  $\Delta$  values marked with an asterisk exceed  $\sigma_t$ ; furthermore, all are negative. Even a PCTT below the transus causes some grain growth and, if the PCTT temperature is excessive, the structural changes noted earlier can adversely affect properties. Therefore, we conclude that a PCTT is detrimental to the properties of Ti-6-4 HIP at 1750°F and should be discontinued.

A less obvious but nevertheless significant variable is testing procedures. Note that CMRC consistently measures a lower strength and higher ductility than MCAIR. In the case of ductility, the  $\Delta$  values are significant with respect to  $\sigma_t$ . This is probably typical of multi-facility testing and merely shows the value of a modest amount of duplicate testing.

### 3.1.2.8 Summary - Preferred HIP Parameters

#### A. Ti-17 Alloy

The Ti-17 HIP experiment proved to be well designed since the optimum parameters were successfully bracketed. Viable alpha-beta and beta-HIP cycles were defined. The property goals stated earlier in the text were met, although fatigue results were marginal. Specifically, the findings on the HIP Parameter studies were as follows:

1. Only heated autoclave cycles are satisfactory at 1550°F.
2. For 1600°F, the CSMD autoclave is considered marginal, whereas a heated autoclave is quite satisfactory.
3. At 1750°F, both types of autoclave are acceptable although the CSMD cycle provides better ductility.
4. Tensile and fracture toughness characteristics of as-HIP alpha-beta and beta material compare

5. The PCTT is neither necessary nor beneficial and can be discontinued.
6. Any of the mold materials considered are acceptable for use with Ti-17.
7. Use of fine powder is technically acceptable but, at present, is not economically feasible.
8. Inclusions in the REP powder constitute the major difficulty encountered to date. Their effect on fatigue was especially damaging.

Based upon the observations from the HIP Parameter study, it was recommended that the REP apparatus be investigated for any source of Si-Ca-K type of inclusions. Discussions with personnel at Nuclear Metals indicated that a possible source of contamination had been located. Based on their evaluation, additional powder was produced to determine if corrective measures would satisfactorily control these types of inclusions.

In order to complete the parameter selection, additional fatigue tests should be run using powder relatively free from inclusions.

Also, evaluation of a lower beta-HIP temperature in a heated autoclave should be carried out. The short dwell above the transus in the CSMD cycles resulted in good ductility. The feasibility of upgrading ductility of a BCL-HIP sample by dropping the beta-HIP temperature should be investigated.

Further duplex versus triplex heat treatments should be compared since the tensile data for beta-HIP Ti-17 indicate that the triplex heat treatment may result in better ductility than the duplex used by General Electric.

#### B. Ti-6-4 Alloy

Due to the low oxygen levels in the Ti-6-4 alloy, tensile properties were below the target values stated earlier in the text (Page 14). Nevertheless, several significant observations were made.

1. Mechanical property data for as-HIP Ti-6-4 show very little scatter.
2. Both CSMD and heated autoclave cycles result in excellent material.
3. Any of the mold materials are acceptable, although SiO<sub>2</sub> is the primary choice.
4. The PCTT is neither necessary nor beneficial and can be discontinued.

Based on the HIP Parameter studies, it was determined that additional Ti-6-4 powder with a higher oxygen content should be purchased and evaluated in the as-HIP condition. All further testing was deferred until the 130/120 tensile and yield strength goals were met.

#### 3.1.2.9 Additional Ti-17 Powder Production

Approximately 100 pounds of the original ingot were converted into powder after a non-metallic component in the REP apparatus which was regarded as a possible source of Si-Ca-K type of inclusions was replaced by an alternative material. Powder was examined under the scanning electron microscope and treated in tetrabromethane to remove all particles with a density of less than 2.9 g/cc. This latter treatment had previously isolated the silicon-containing inclusions. In a random sample of 1.3 pounds of powder from this new lot (4026-3B), only one silicon base inclusion was identified.

In addition, a small sample was consolidated and examined metallographically. This procedure revealed tungsten but no non-metallic inclusions.

Oxygen analyses given in Table 23 are consistent with those for the initial lots of Ti-17 powder.

Other characterization of this powder is also summarized in Table 23.

The changes in the REP apparatus appeared to have successfully eliminated the Si-Ca-K type inclusions in the New Powder lot as indicated in the tests performed.

#### 3.1.2.10 Additional Ti-6-4 Powder Production

Higher oxygen Ti-6-4 was produced from two different Ti-6-4 ingots by the REP technique at Nuclear

TABLE 23

## SUMMARY OF Ti-17 POWDER CHARACTERIZATION

<u>Oxygen Content (%)</u>	
Vendor	0.083, 0.084
CMRC	0.097, 0.100
Previous value from same ingot(2)	0.094, 0.095
<u>Size Distribution</u>	
-35, +45 mesh	1.3%
-45, +60	4.9%
-60, +80	37.1%
-80, +100	28.4%
-100, +120	9.1%
-120, +200	18.4%
-200, +325	0.8%
-325	Trace
<u>Apparent Density</u>	.1019 lb/in <sup>3</sup> 60.4 % theoretical density
<u>Tap Density</u>	.1048 lb/in <sup>3</sup> 62.7 % theoretical density
<u>Flow Rate</u>	26.9 sec.



Metals. The powder is comparable in quality and characteristics to the ELI Powder evaluated previously. As is shown in Table 24, there is a slight discrepancy between the oxygen values reported by the vendor and those determined by Crucible. Hereafter, the median value will be used to describe these two powder lots. All other characteristics of these two powder lots are the same.

Metallographic examination of the powder revealed tungsten particles but no non-metallic inclusions.

### 3.1.2.11 1650°F HIP of Ti-17

During Task II, it was observed that the short dwell above the transus in the CSMD HIP cycle produced better ductility values than were achieved in conventional 1750°F HIP cycles. Thus, it was recommended that a lower beta HIP temperature be explored as a means of increasing ductility.

Material HIP at 1650°F from both the original lot of powder (Part SM-295) and the new lot, 4026-3, of powder (Part SM-357) were heat-treated and tested. Results are summarized in Table 25. Both exhibit higher strengths than were previously attained at 1750°F. However, using General Electric's standard duplex heat-treatment for beta-processed Ti-17, only SM-357 exhibited the enhanced ductility. When SM-295 was given the triplex heat-treatment normally used for alpha-beta processed material, this also showed improved ductility.

There are two plausible explanations for this observation. First, as is shown in Figure 47, the typical 1650°F + duplex STA material has a nearly continuous grain-boundary alpha network and sharp alpha needles. Both microstructural features could reduce ductility. After a triplex STA, the grain boundary alpha begins to break up and the needles are not as sharp<sup>5</sup> (see Figure 48).

The second possibility involves specimen preparation. SEM examination of failed specimens returned by General Electric show circumferential tool marks, as is shown in Figure 49. Fracture appears to initiate from these marks. On the other hand, a failed CMRC specimen is shown in Figure 50. These specimens were finished by longitudinal grinding. These scratch marks do not appear to influence the crack path.

TABLE 24

## SUMMARY OF T1-6-4 POWDER CHARACTERIZATION

Lot No.	4026-1	4026-4
Oxygen Content (%)		
Vendor	0.130	0.150, 0.159
CMRC	0.140, 0.154	0.178, 0.182
Nominal*	0.142	0.166
Size Distribution		
-35, +45 mesh	0.3%	0.4%
-45, +60	3.3%	5.97%
-60, +80	30.0%	52.34%
-80, +100	29.1%	25.15%
-100, +120	13.8%	8.57%
-120, +200	19.9%	7.45%
-200, +325	3.5%	0.03%
-325	0.1%	0.02%
Apparent Density	.0976 lb/in <sup>3</sup> 60.9 % theoretical	.0961 lb/in <sup>3</sup> 60.0 % theoretical
Tap Density	.1059 lb/in <sup>3</sup> 66.2 % theoretical	.1048 lb/in <sup>3</sup> 65.5 % theoretical
Flow Rate	24.1 sec	

\*Median Value, used in balance of report.

TABLE 25

## PROPERTIES OF Ti-17 HIP AT 1650°F

Specimen	HT	F <sub>tu</sub> (ksi)	F <sub>ty</sub> (ksi)	Elonga- tion (%)	Reduction of Area (%)	K <sub>Q</sub> (ksi in. <sup>1/2</sup> )
SM-295	As-HIP	154.1	140.7	16.5	30.7	-
	Triplex	171.7	161.9	9.5	17.4	-
	Duplex	176.5	168.5	5.5	9.2	40.3
		174.4	165.5	4.4	10.1	44
SM-357	Duplex	170.6	159	10.5	17.9	50.6
		168.9	158	8.6	16.7	-
Specifi- cation		163 min	153 min	5 min	10 min	50 min
Avg., 1750 F HIP heated autoclave (3)		162.8	154.1	6.6	11.9	59.2
<p><u>Duplex Heat Treatment:</u> 4 hr 1475 F, WQ 8 hr 1175 F, AC</p> <hr/> <p><u>Triplex Heat Treatment:</u> 4 hr 1550 F, AC 4 hr 1475 F, WQ 8 hr 1175 F, AC</p>						



570-75

Figure 47. G. E. specimen T1, duplex STA.  
(G.B. alpha is nearly continuous.  
Primary alpha needles are sharp. 250X)



Figure 48. G. E. specimen FT, triplex STA.  
(G.B. alpha is more broken up and primary  
alpha more blunted than in the above  
figure. Both structures are typical for  
their respective heat treatments - 250X)  
Etchant: 2%HF - 15% $\text{HNO}_3$





↔  
Tensile  
Stress

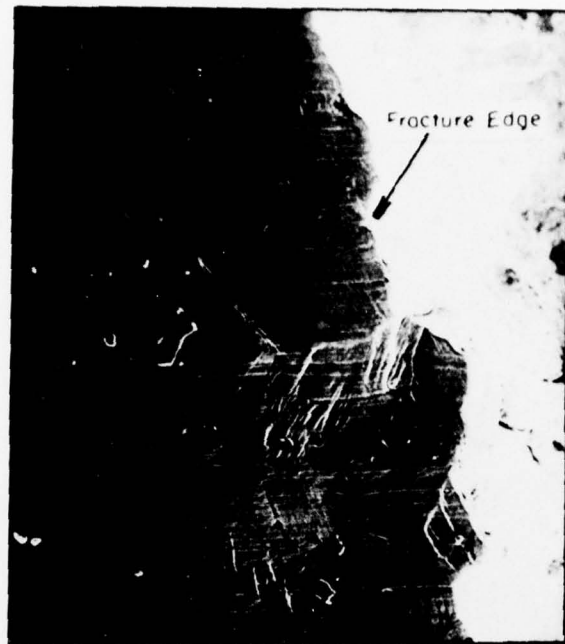
571-75



↔  
Tensile  
Stress

Figure 49. SEM surface images in neckdown area of broken G. E. tensile specimen FT.

(Fracture path is observed to initiate from circumferential machine tool marks resulting in low ductility - 100%)



←→  
Tensile  
Stress

572-75



←→  
Tensile  
Stress

Figure 50. SEM surface images in neckdown area of broken CMRC tensile specimen C4.

(Finish machining was by fine longitudinal grinding. Scratch marks here did not influence crack path. Improved ductility is evidenced by the appearance of shear bands or twins - 100X)

### 3.1.2.12 Ti-17 Low Cycle Fatigue

During the initial investigations on preferred HIP parameters, erratic low cycle fatigue behavior was encountered in HIP Ti-17. Most of the fatigue fracture faces contained inclusions, generally of the Si-Ca-K type. It was hoped that clean powder would eliminate this problem. However, LCF tests from compacts prepared from new powder still exhibited this scatter, as can be seen in Figure 51. Yet, fractographic analyses in this case did not indicate the presence of non-metallic inclusions as initiation sites.

In order to resolve the LCF problem, all of the possible reasons for poor performance were noted and systematically evaluated. These included inherent problems with the parent heat, microstructure as influenced by both compaction parameters and by heat treatment, inadequate bonding, and inclusion sources from either contamination associated with the ceramic mold process or associated with the powder production/handling process.

#### Properties of Parent Heat (R51646)

One possible explanation for the erratic fatigue behavior would be a problem with the original heat of Ti-17. To investigate this possibility, LCF and tensile tests were performed on the bar stock which remained after powder conversion. It must be noted, however, that the optimum forging practice for Ti-17 was not used in this expedient processing of the electrode bar prior to testing. Figure 52 gives the LCF results of this material compared to cast and wrought Ti-17. All of the points are above the minus three sigma data for beta-processed Ti-17 and about average for alpha-beta processed material. Tensile data for this bar stock is given in Table 26 and exhibit strengths near the lower end of the normal range, thus LCF strengths slightly below the average are to be expected. However, the data range is considerably higher than the HIP material which indicates that there is no basic problem with the parent heat.

#### Microstructure Versus Fatigue Life

For the Ti-17 cast and wrought alloy, beta processing results in superior fatigue life as compared with alpha-beta processing. Thus, it was felt that beta-HIP should likewise be superior to alpha-beta HIP. In the earlier HIP parameter study,

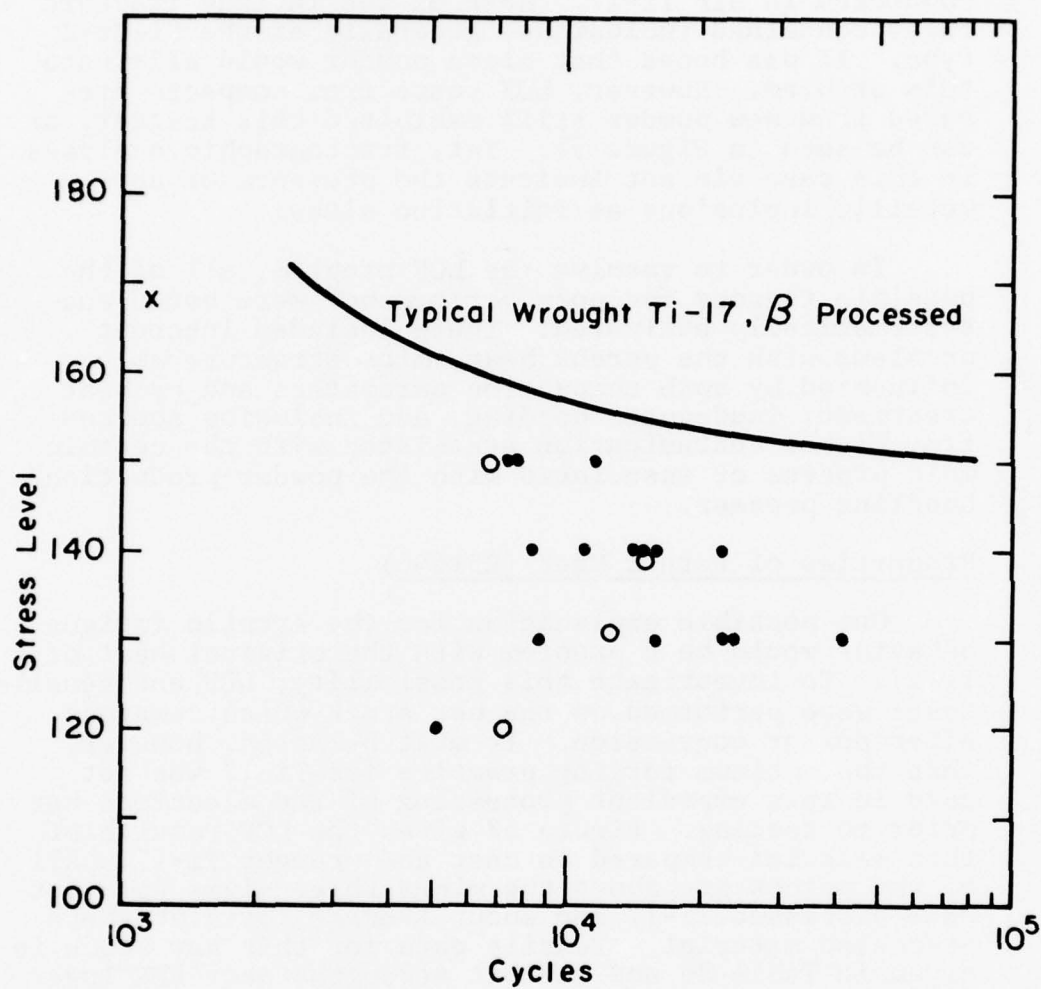


Figure 51. LCF data for Ti-17.

(The solid circles are data points for HIP Ti-17 from the initial lot of powder. The open circles are new data from the most recent lot of Ti-17 powder)



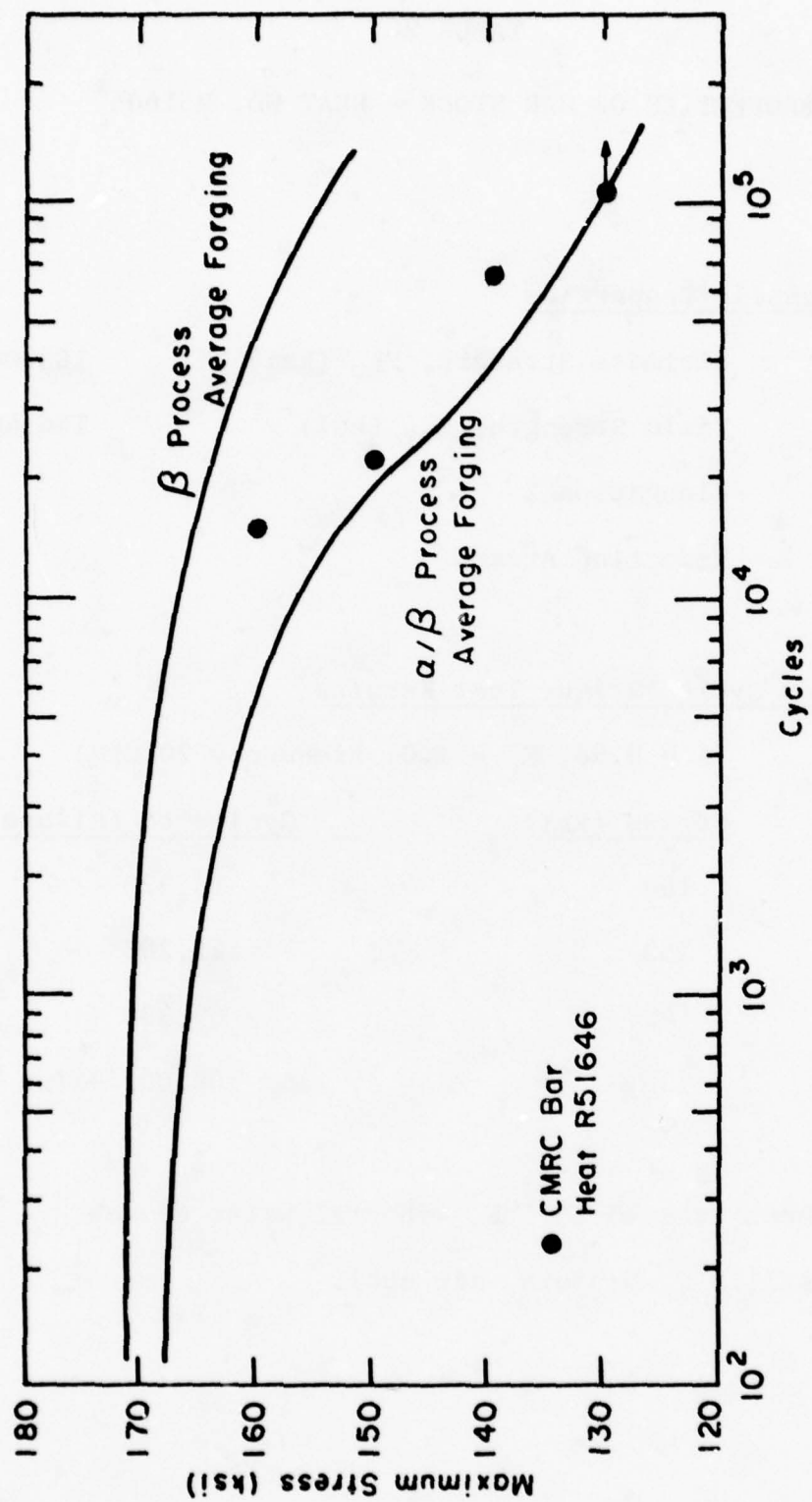


Figure 52. Low-cycle fatigue of CMRC bar.

TABLE 26

PROPERTIES OF BAR STOCK - HEAT NO. R51646\*

Tensile Properties

Ultimate Strength, $F_{tu}$ (ksi)	163,000
Yield Strength, $F_{ty}$ (ksi)	154,400
Elongation %	14.3
Reduction Area %	27.9

Low Cycle Fatigue Test Results(A = 0.98,  $K_t = 1.0$ , Frequency 20 CPM)

<u>Stress (ksi)</u>	<u>Cycles to Failure</u>
160	15,320
150	22,288
140	69,300
130	108,000 + (no failure)

\*Heat treated 1475°F, 4 hours, water quench

+ 1175°F, 8 hours, air cool.

the beta-HIP material did exhibit higher  $K_q$  values than alpha-beta HIP, but fatigue life was no better. At that time, a HIP temperature of 1750°F was used. This resulted in a relatively coarse grain with an extensive grain-boundary alpha network.

To determine whether a lower but still supertransus compaction temperature would be beneficial, additional material was HIP at 1650°F. This lower beta-HIP temperature resulted in enhanced ductility but no improvement in fatigue life. Typical LCF curves for 1650 and 1750°F HIP Ti-17 are compared in Figure 53.

The microstructure of HIP Ti-17 exhibits a coarser alpha platelet size and more continuous alpha grain-boundary networks as compared to typical cast and wrought beta processed material. The beta processed material also has an elongated grain structure as a result of hot working, while the HIP product has an equi-axed grain structure. It has been reported by others<sup>6</sup> that some forms of coarse grain-boundary alpha can be detrimental to low cycle fatigue, but this has never been demonstrated for Ti-17. In order to attempt to simulate the HIP structure in cast and wrought material a section of a beta processed forging has been given a heat treatment in the beta field as follows:

1650°F, 1 hour, air cool  
+1475°F, 4 hours, water quench  
+1175°F, 8 hours, air cool

A section of the HIP sub-scale shaft SM-357 from Task III was given a similar heat treatment (1625 + 1475 + 1150°F) in an attempt to produce a finer alpha platelet size for comparison to the beta heat-treated cast and wrought sample described above. As is shown in Table 27, this heat treatment resulted in high strength but low ductility. Thus, the LCF specimens were re-aged for four hours at 1200°F prior to test.

The results of these tests are shown in Figure 54. First, it is evident that the above heat treatment did offer a very slight improvement in LCF life over the conventional duplex cycle. It is also apparent that this heat treatment did degrade the LCF strength of the beta-forged disk. The data for

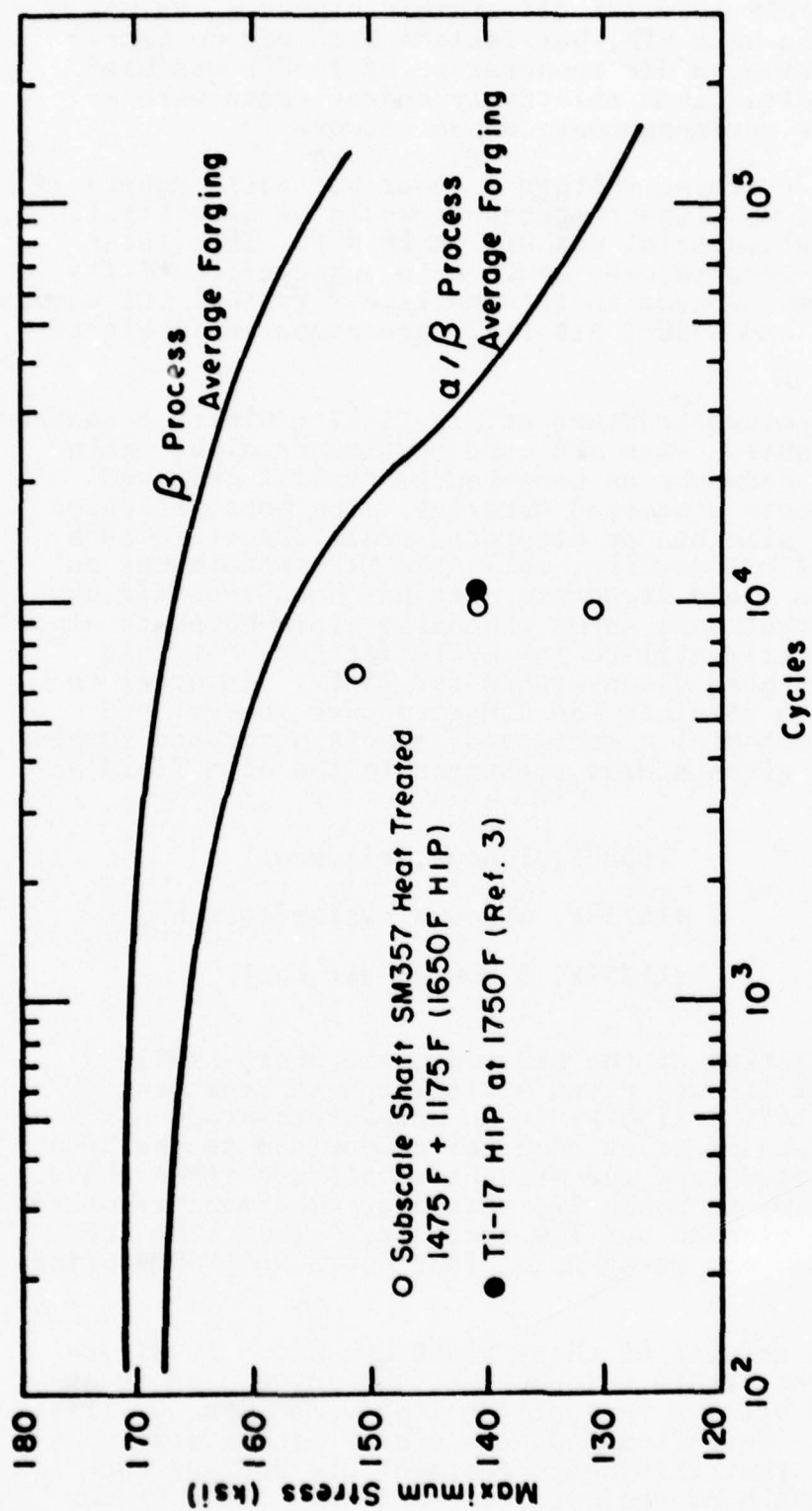


Figure 53. Effect of beta-HIP temperature on low cycle fatigue results.



TABLE 27

## PROPERTIES OF BETA HEAT TREATED SHAFT

## SUB-SCALE SHAFT, SM-357

Heat Treatment: 1625°F, 1 hour, air cool +  
 1475°F, 4 hours, water quench +  
 1150°F, 8 hours, air cool

Tensile Properties

$F_{tu}$ (ksi)	$F_{ty}$ (ksi)	Elongation (%)	Reduction Area (%)
181.8	180.6	4.5	9.3

Fracture Toughness (Slow Bend Pre-cracked Charpy)

$$K_Q = 36.4 \text{ ksi} \sqrt{\text{in.}}$$

Low Cycle Fatigue\*

$$A = 1.0, \quad K_t = 1.0$$

Maximum Stress (ksi)Cycles to Failure

120	16,604
120	19,577
140	16,102
130	15,535

\*Specimens re-aged 1200°F, 4 hours

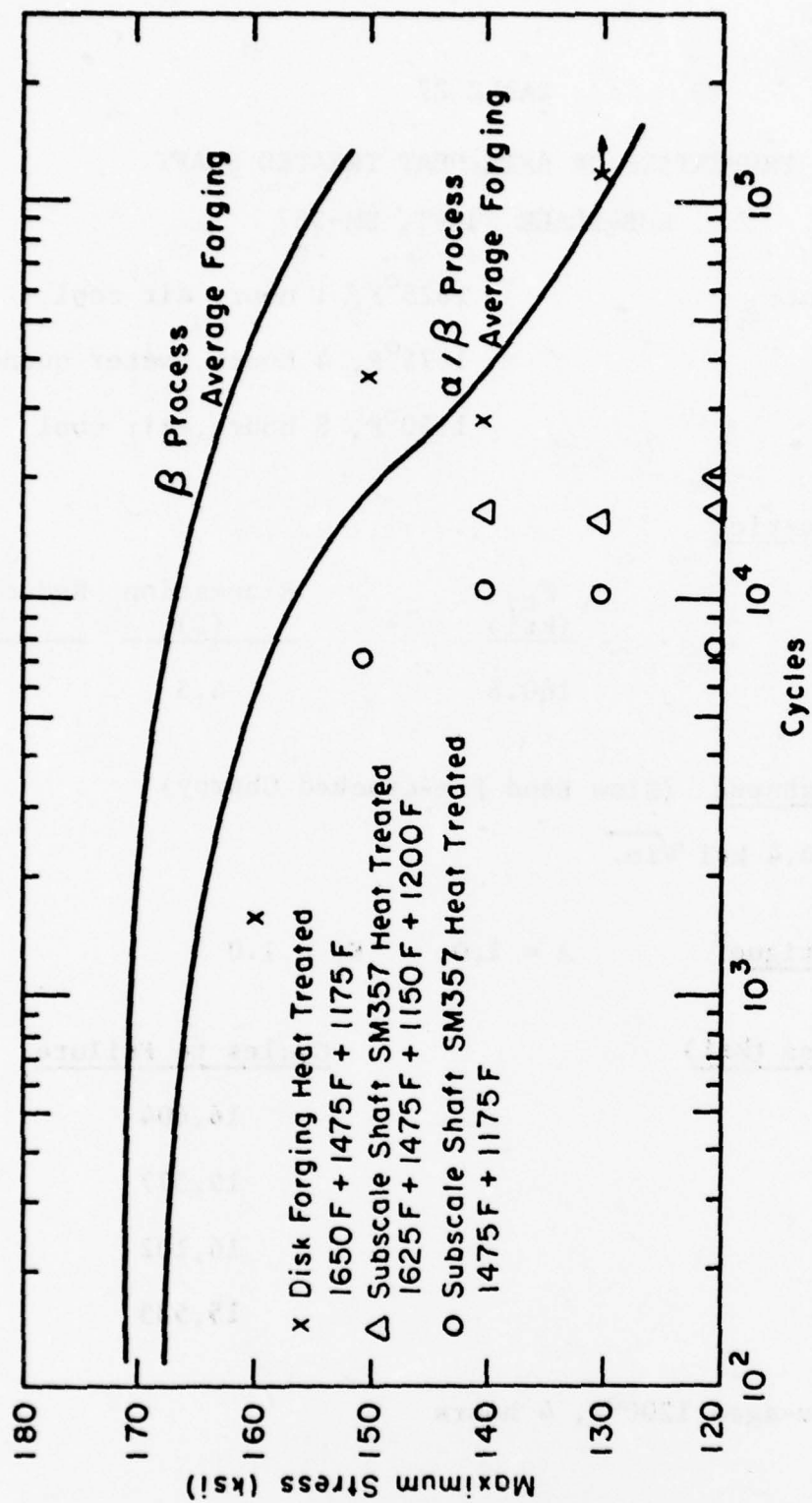


Figure 54. Effect of heat-treatment on low-cycle fatigue results.

the beta-rolled bar stock, which was noted earlier, is also plotted again. It is noteworthy that the two wrought materials as tested here have microstructures similar to the beta-HIP material. Thus, these results tend to discount microstructure as the sole cause of the poor fatigue properties in the HIP Ti-17.

To further evaluate the microstructural effect on LCF, tests were run on a beta-forged disk provided by General Electric. A portion of this same disk was then subjected to a 1650°F HIP cycle, heat-treated, and tested again. Results are plotted in Figure 55. These data show that the type of microstructure which arises from a standard 1650°F HIP cycle can degrade the LCF life somewhat, but certainly not to the extent encountered in the HIP product. Nevertheless, some work in microstructural refinement was initiated. This is summarized later in this report.

In an attempt to produce a beta heat-treated microstructure free of grain boundary alpha, specimens from stub shaft SM-357 were heat-treated at 1650°F, one hour, rapid air cool plus age at 1250°F. Metallographic examination of the heat treated specimen showed only minimal grain boundary alpha present in the microstructure. Tensile results are given in Table 28, which show higher strength than expected, but accompanied by lower ductility. Low cycle fatigue properties are given in Figure 56 and are the same as obtained with the conventional heat treatment. Although not conclusive, grain boundary alpha does not seem to be a major cause of the low cycle fatigue problem.

#### Inadequate Bonding

To investigate the possibility of inadequate bonding as a cause of low fatigue strength, a portion of stub shaft SM-384 was returned to Crucible for re-HIP. During the rerun, a power failure occurred and the run was aborted after reaching temperature, but not full pressure. Thus, the cycle was repeated and the part actually experienced three thermal cycles, two with full pressure. This re-HIP material, which by now had a very coarse grain size (some as large as 0.050 inch) was reheat-treated and LCF tested. As is shown in Figure 57, the rerun--probably as a result of excessive grain growth--further degraded the fatigue life of the Ti-17. Although excessive grain size resulted, the data appear to discount the theory that better bonding in the PM material would improve fatigue properties.

TABLE 28  
TENSILE RESULTS - SM-357

	$F_{tu}$ (ksi)	$F_{ty}$ (ksi)	Elong. (%)	Red. Area (%)
SM-357	181.8	176.8	3.6	7.5
Heat treatment: 1650°F, 1 hr, rapid air cool + 1250°F, 8 hrs, A.C.				

#### Inclusions

In concurrent Task III efforts on sub-scale stub shaft development, a high incidence of non-metallic inclusions were encountered in the HIP Ti-17. Those found in sub-scale parts SM-357 and -384 are listed in Table 29. A SEM photograph at the fracture surface of one of these (SM-357-B) is shown in Figure 58. Note that there is some partitioning of the elements within the contaminated area.

TABLE 29  
SUMMARY OF NON-METALLIC INCLUSIONS

<u>Material</u>	<u>Type of Test</u>	<u>Type of Inclusion</u>
SM-384-A	LCF (59,074 cycles)	Silica-rich
SM-384-D	LCF (14,894 cycles)	Silica-rich
SM-357-A	LCF (16,604 cycles)	High in Si, Zr
SM-357-B	LCF (19,577 cycles)	Ca, P, Mg, Si, Al
SM-357-C	LCF (16,102 cycles)	High in Si, Zr
SM-357-D	LCF (15,535 cycles)	High Si, plus Zr, Mg, Ca



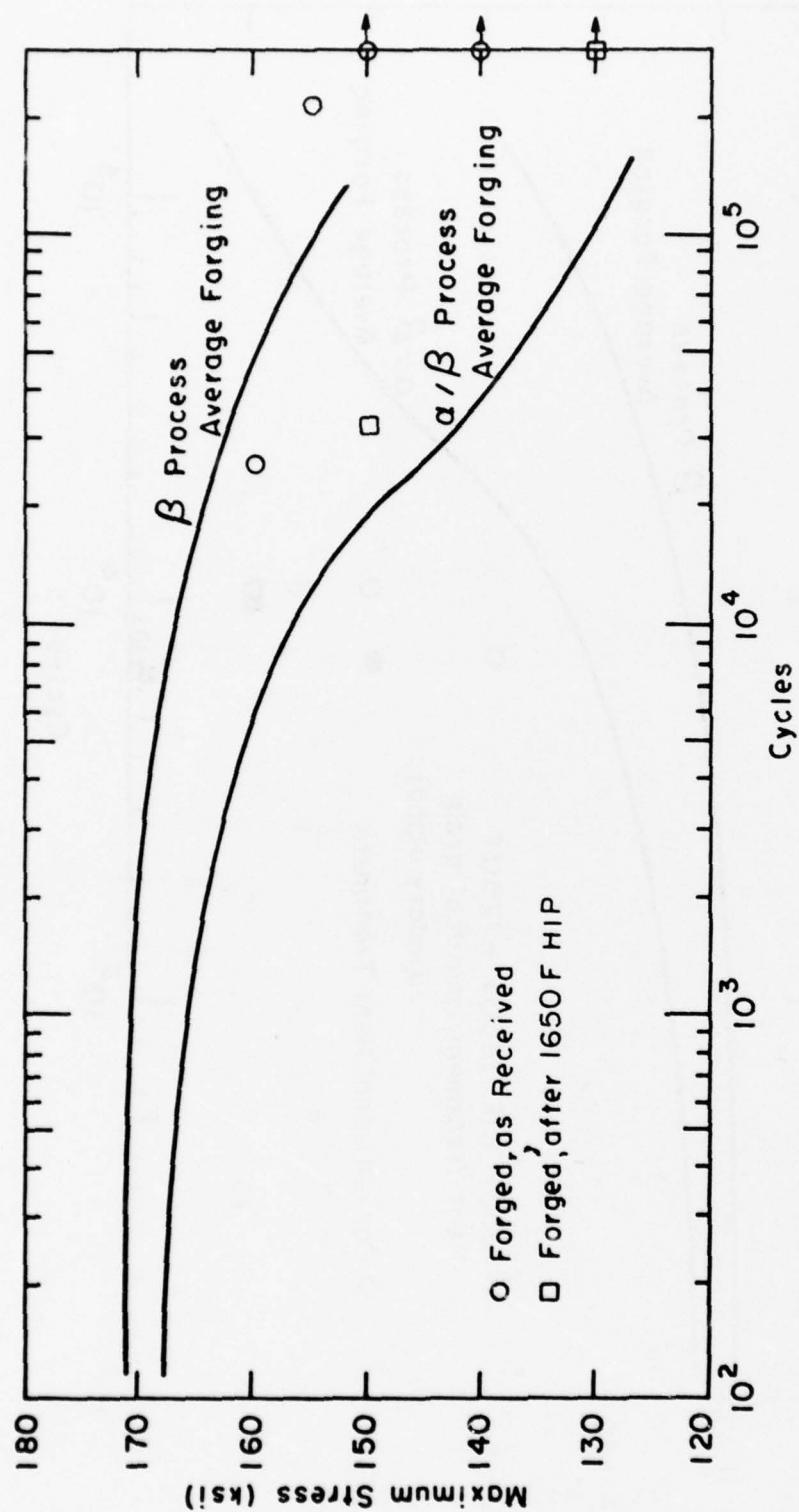


Figure 55. Effect of HIP thermal cycle on low-cycle fatigue results.

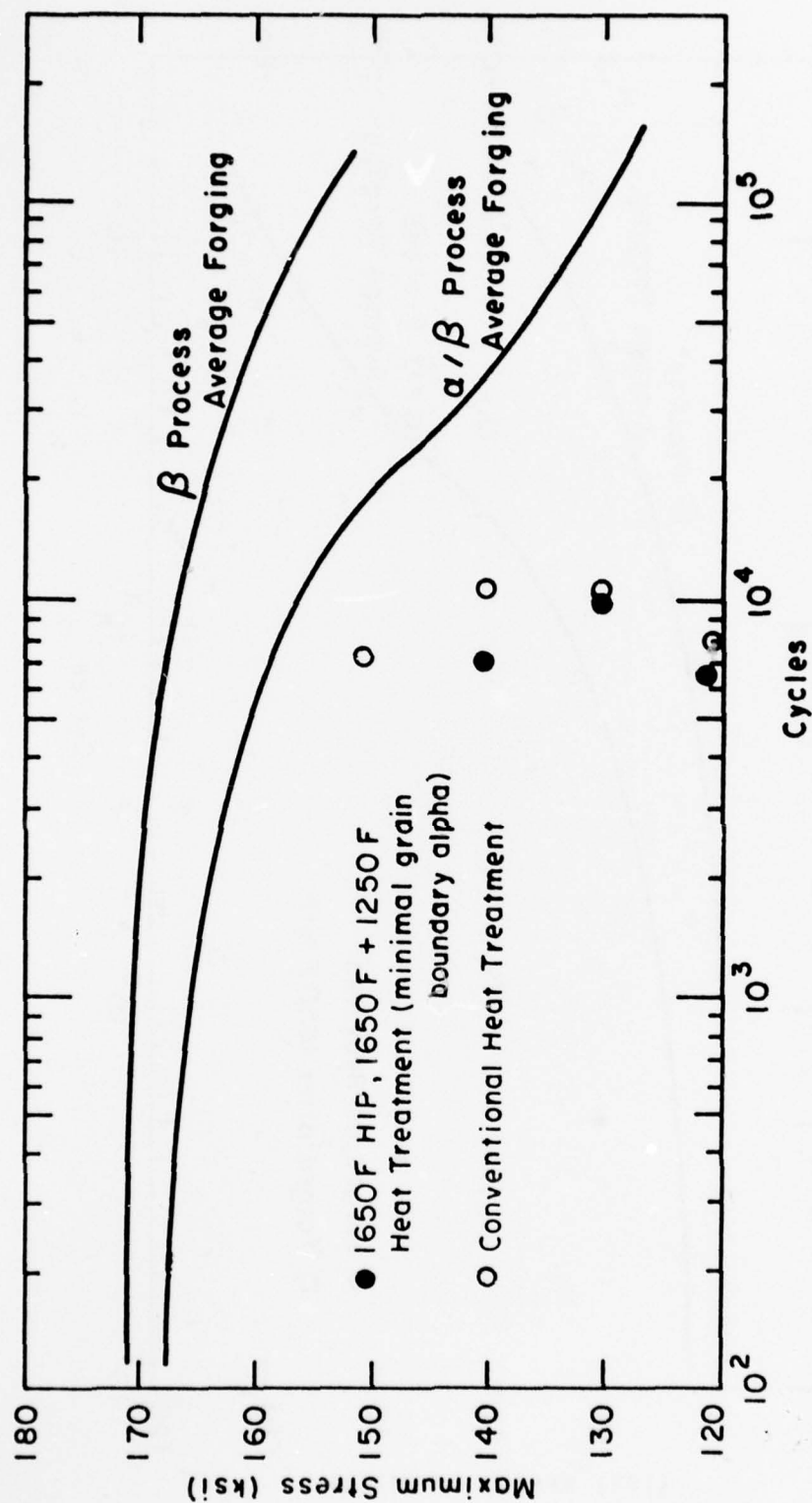


Figure 56. Effect of grain boundary alpha on low-cycle fatigue results.

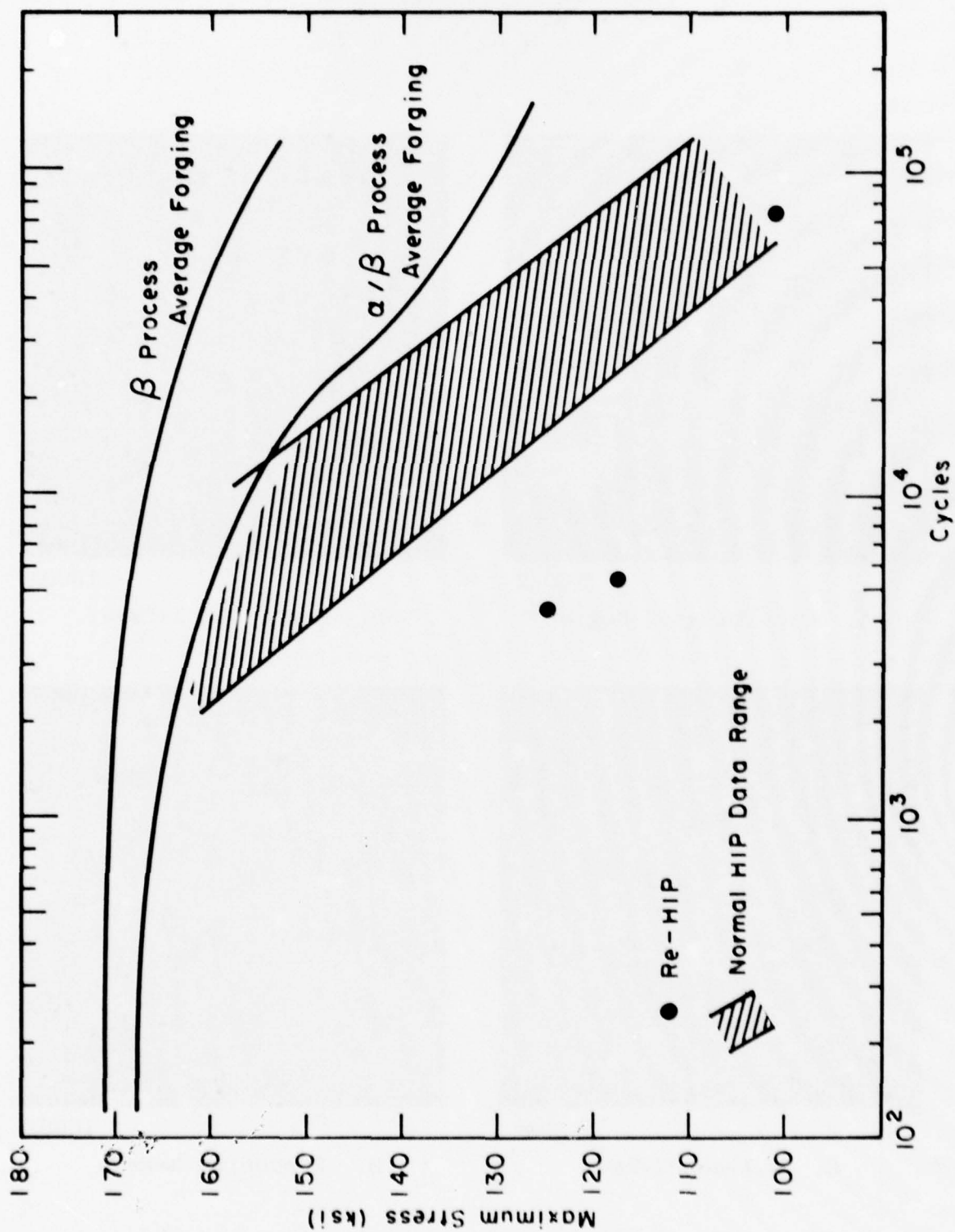
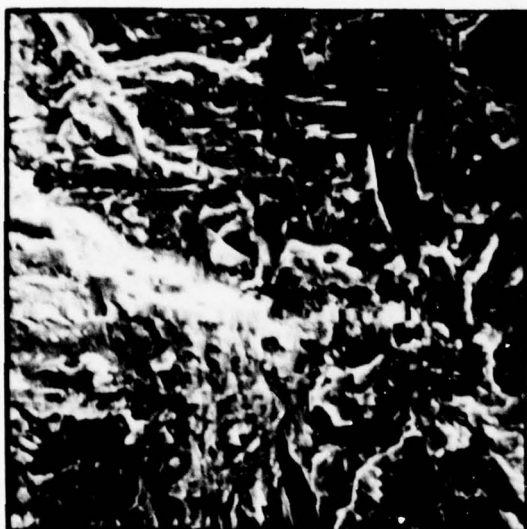
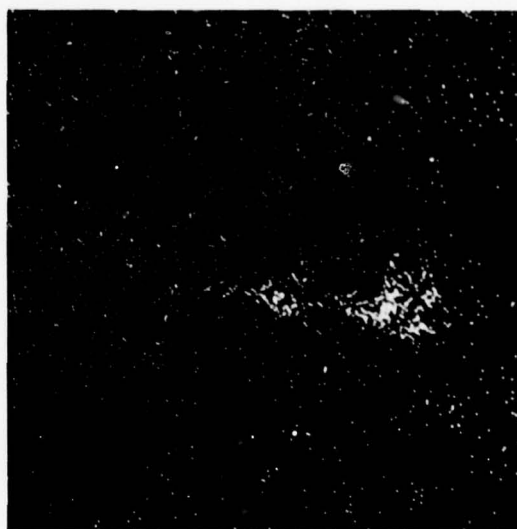


Figure 57. Effect of re-HIP on low-cycle fatigue results.



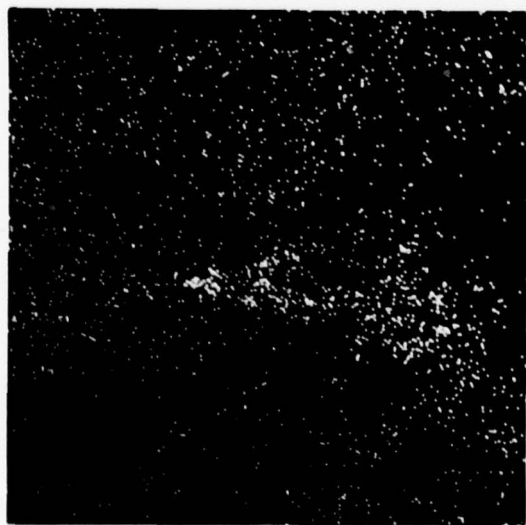
1000X

A. Contaminated Region



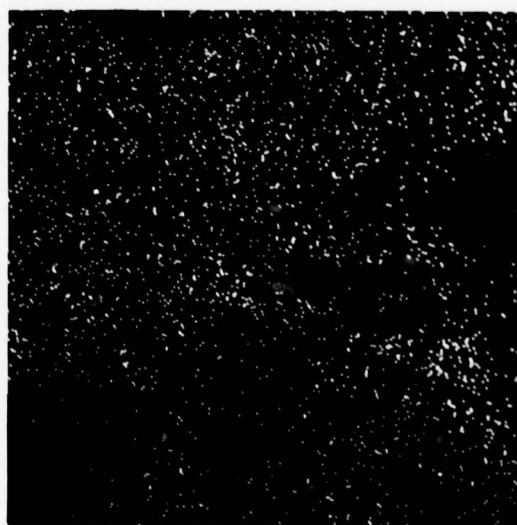
1000X

B. Magnesium X-Rays



1000X

C. Silicon X-Rays



1000X

D. Zirconium X-Rays

Figure 58. Analysis of an inclusion found on LCF break in SM-357-B.



Based on the above results, the existence of non-metallic inclusions in the HIP Ti-17 cannot be disputed. However, the composition of these inclusions is not constant except for the presence of silicon. This makes identification of a contamination source extremely difficult.

One obvious possibility as a contamination source is the silica mold system used by Crucible to produce the shapes. Two critical experiments were performed to investigate this possibility. First, pieces of actual molds were examined qualitatively on the SEM. Only silicon was found in every case; there was no evidence of any of the additional elements listed in Table 29. In another experiment, the Ti-17 powder was HIP at 1650°F in a metal (carbon steel) can, heat-treated and tested. The LCF results are shown in Figure 59 together with the range of values encountered on beta-HIP Ti-17 in ceramic molds. These results show no improvement for metal can processed material. It is therefore concluded, that the ceramic mold process is not responsible for the poor fatigue properties in the Ti-17.

Since all potential causes for degraded fatigue performance were considered and evaluated, the only potential source for the low LCF is non-metallic inclusions in the powder. Furthermore, as has been noted previously in this report, such inclusions have been found in the as-received REP powder. Based on these findings, a current AF program F-33615-77-C-5421 is in progress to eliminate the source of non-metallic inclusions in REP powder. However, further tests were carried out in the Task III effort on this program to verify this conclusion.

Although the smooth bar load controlled LCF tests conducted to date have all been below the average Ti-17 cast and wrought data, and some below the minus three sigma limit of these data, the data does show lives above the average Ti-6Al-4V data for this test as shown in Figure 60. The overall results of the testing conducted to date were reviewed with F-101 Design Engineering with the aim of determining the advisability of proceeding with the full-scale compressor shaft manufacturing in Phase II. The results of this discussion indicate that the properties obtained will be adequate for the F-101 mission, since the low cycle fatigue life equivalent to Ti-6-4 is satisfactory for this part.

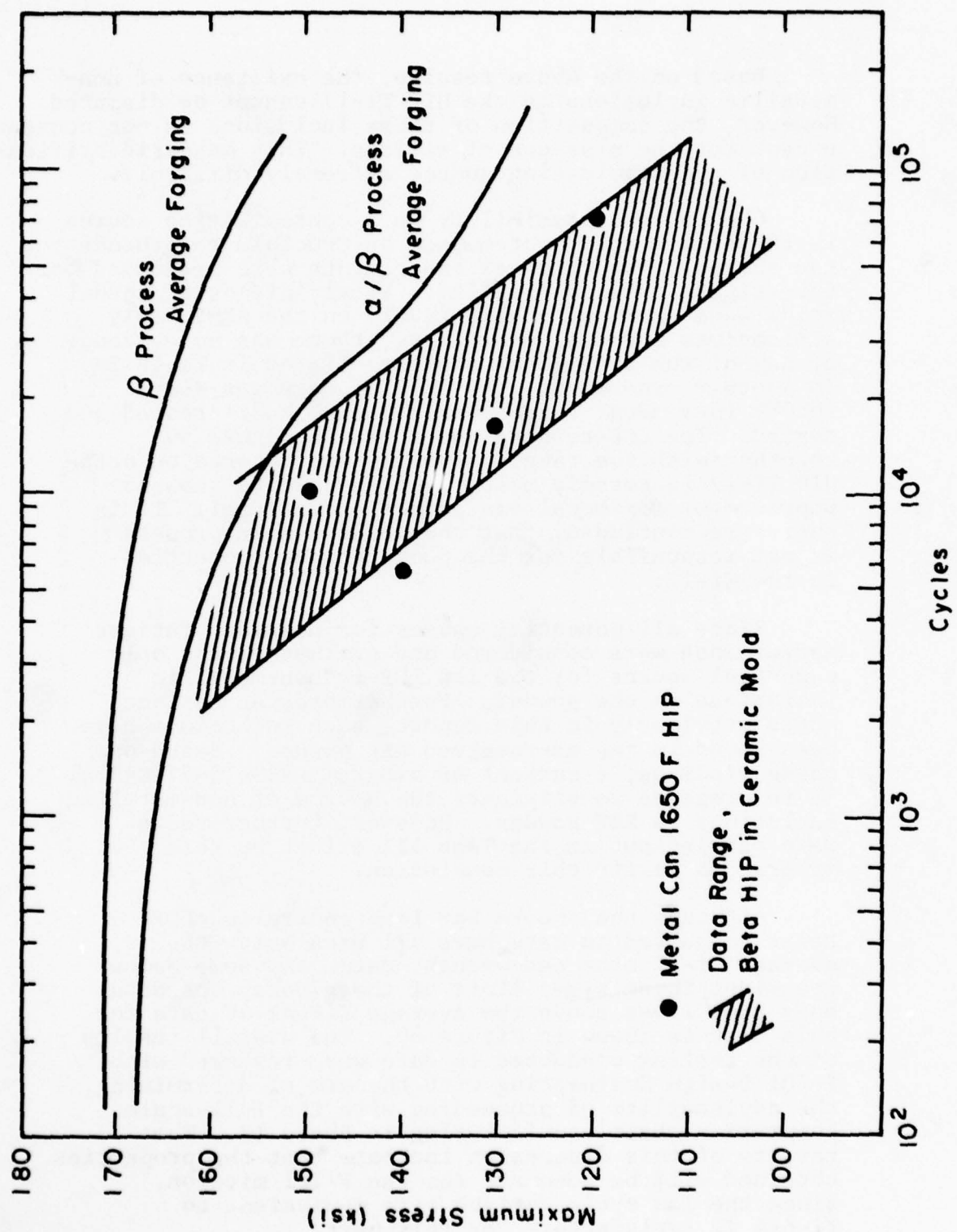


Figure 59. Effect of container material on low-cycle fatigue results.

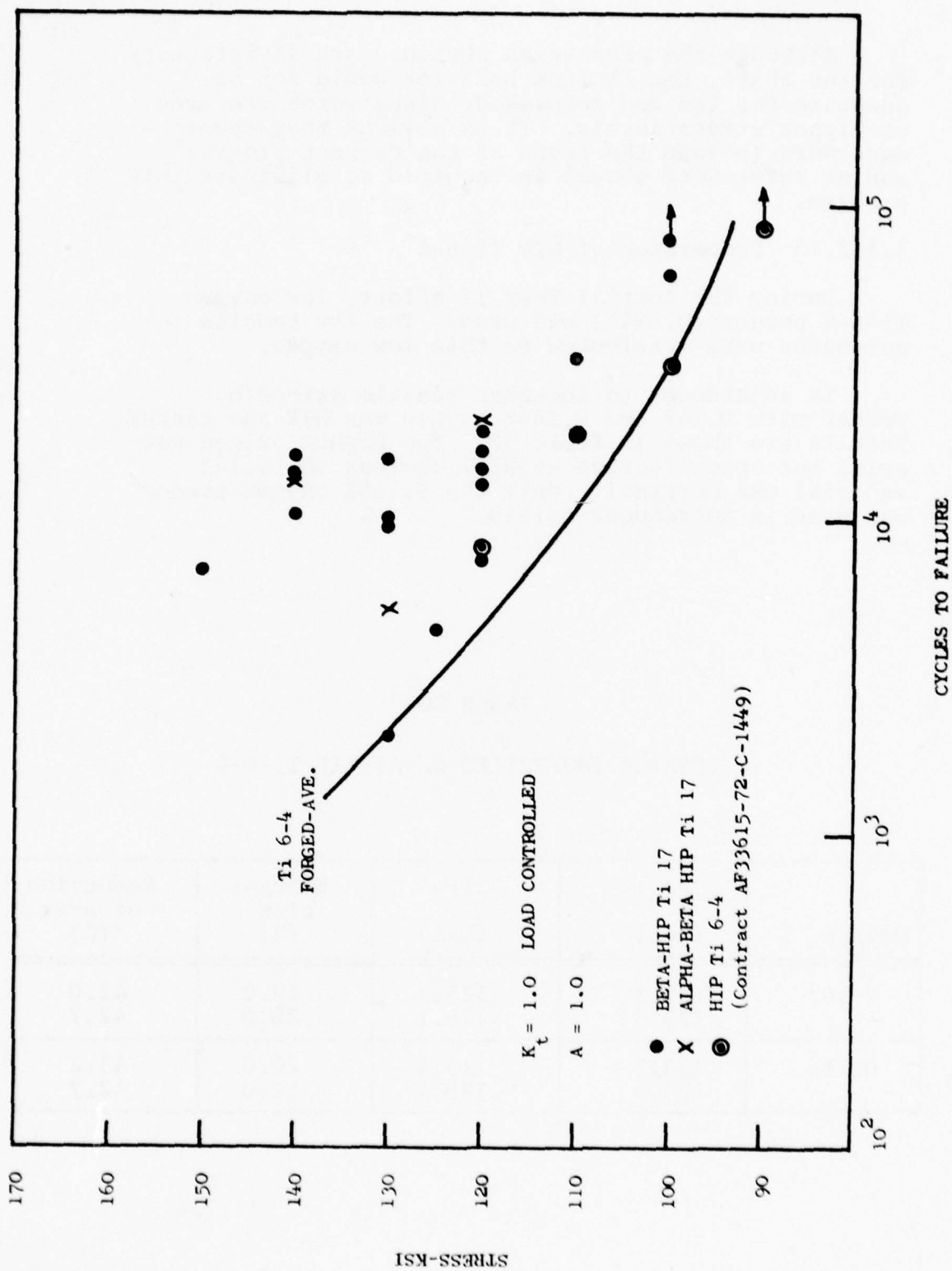


Figure 60. Ti-17 and Ti-6-4 LCF comparison.

Although the properties obtained are satisfactory for the shaft, the fatigue behavior would not be adequate for fan and compressor disks which are used at higher stress levels. It is obvious that development work (beyond the scope of the current program and as referenced above) is required to eliminate this problem.

### 3.1.2.13 Properties of HIP Ti-6-4

During the initial Task II effort, low oxygen Ti-6-4 powder (0.094%) was used. The low tensile strengths were attributed to this low oxygen.

In an attempt to increase tensile strength, powder with 0.142 and 0.166% oxygen was HIP and tested. Results are shown in Table 30. The higher oxygen material met specification as-HIP, whereas the 0.142 material was marginal. Only the 0.166% oxygen powder was used in subsequent trials.

TABLE 30

### TENSILE PROPERTIES OF AS-HIP Ti-6-4

Oxygen, %	F <sub>tu</sub> (ksi)	F <sub>ty</sub> (ksi)	Elonga- tion (%)	Reduction of Area (%)
0.142	129.3 129.5	115.2 116.1	19.0 20.0	42.0 42.7
0.166	133.3 133.6	119.4 120.4	20.0 19.0	43.2 42.7



Billets were produced using SiO<sub>2</sub> mold material and a 1650°F - 8 hr HIP cycle. Samples were annealed and evaluated by both MCAIR and Crucible. Results are summarized in Table 31. Note that these values all exceed specification minimums.

TABLE 31  
PROPERTIES OF HIP + ANNEAL  
0.166% OXYGEN Ti-6-4

Data Source	F <sub>tu</sub> (ksi)	F <sub>ty</sub> (ksi)	Elonga- tion (%)	Reduction of Area (%)
Crucible	135.6 135.8	126.8 123.1	20.0 19.0	43.9 39.2
MCAIR	139.0 139.0	128.0 126.0	18.0 18.0	44.6 45.4
Avg.	137.4	125.9	18.8	43.2
$\sigma^2$	3.6	4.3	0.9	7.8
$\sigma_t$	1.9	2.1	1.0	2.8
MIL-T-9047	130 min	120 min	10 min	25 min

The apparent fracture toughness was determined at MCAIR using a slow-bend Charpy specimen. This is not a valid test for toughness but provides an estimate of its value for comparative purposes. The test method used is a modification of that described by Pierce et al in AFML-TR-70-311<sup>7</sup>. The Charpy specimens were pre-cracked using a load ratio of 0.10 and cyclic rate of 30 Hertz. A load of 1000 pounds was used to initiate the crack and the last 0.050 inches of crack growth was made with a load of 500 pounds. After precracking, the specimens were fractured in three point bending using a ram travel rate of 0.1 inches per minute and a span length of 2.0 inches. An autographic plot of ram travel vs. load was obtained for each specimen. The fracture face of each specimen was photographed. The fractured area (area not initially fatigue cracked) and the area of the shear lips on each fracture face on the photograph was measured using a planimeter. A toughness value,  $K_{FF}$  (K flat fracture) based on energy per unit area of flat fracture was calculated using the following formula:

$$K_{FF}^2 = \frac{E (W/A)_{FF}}{2 (1 - \mu^2)}$$

where

$K_{FF}$  = apparent flat fracture toughness

$E$  = Young's modulus

$W/A$  = energy per unit area of flat fracture where  $W$  =  
energy measured in load displacement curve

$\mu$  = Poisson's ratio (0.3)

The results were as follows:

$$87.7 \text{ ksi}\sqrt{\text{in}}$$

$$79.0 \text{ ksi}\sqrt{\text{in}}$$

There was not a sufficient number of specimens tested to establish a correlation between a valid  $K_{IC}$  test per ASTM 72-399 and the Charpy method described above and therefore, the values listed must be considered estimates of fracture toughness<sup>5</sup>. According to the DMIC Ti-6Al-4V Handbook,  $K_{IC}$  for the annealed alloy ranges from 40 ksi  $\sqrt{\text{in}}$ .

(corresponding to mill anneal) to 90 ksi  $\sqrt{\text{in.}}$   
(corresponding to beta anneal) at a yield strength  
of 125 ksi.

Two notched ( $K_t = 3$ ) fatigue bars were tested  
at 65 ksi,  $R = 0.1$  and 1800 cycles per minute. Lives  
were 11,000 and 22,000 cycles. These compare favorably  
with MIL-HDBK-5 data for notched, annealed bar.

Based on the results of previous Task II eval-  
uation of HIP parameters, a higher oxygen content  
from 0.094 to 0.166% was produced to increase strength  
levels. Mechanical property requirements of MIL-T-9047  
were met with HIP + annealed Ti-6-4 powder containing  
0.166% oxygen.

The Ti-6-4 alloy did not display the fatigue  
problems encountered with the Ti-17 alloy. Based on  
the results of the Task II efforts on Ti-6-4, it was  
recommended that work proceed with the component test  
program for the F-15 keel splice fitting.

### 3.1.3 Task III - Shape Making Evaluation

#### 3.1.3.1 Sub-Scale Stub Shaft Development

The one-half scale sonic shape for the F-101  
compressor stub shaft consists of three sections,  
(1) a hollow cylindrical shaft, (2) a truncated cone,  
and (3) an outer flange. The size was reduced by  
one-half in Phase I and the target shape was some-  
what simplified to facilitate process development,  
testing, and NDI development.

Each shape iteration is graphically compared to  
the original target shape in the text. Complete  
dimensional analysis of each sub-scale shaft itera-  
tion with comparison to target shape reference dim-  
ensions are given in Appendix D to this report (Tables  
D-1 through D-5).

#### First Shape Iteration (SM-295)

The shape produced in the first trial is shown in  
Figure 61. Actual versus target shape of this part is  
shown in Figure 62. The cylindrical portion of the  
stub shaft was not fully dense; up to 0.3% of residual  
porosity existed after HIP at 1650°F. Therefore, all  
of the mechanical property testing was restricted to  
the flange and cone areas.

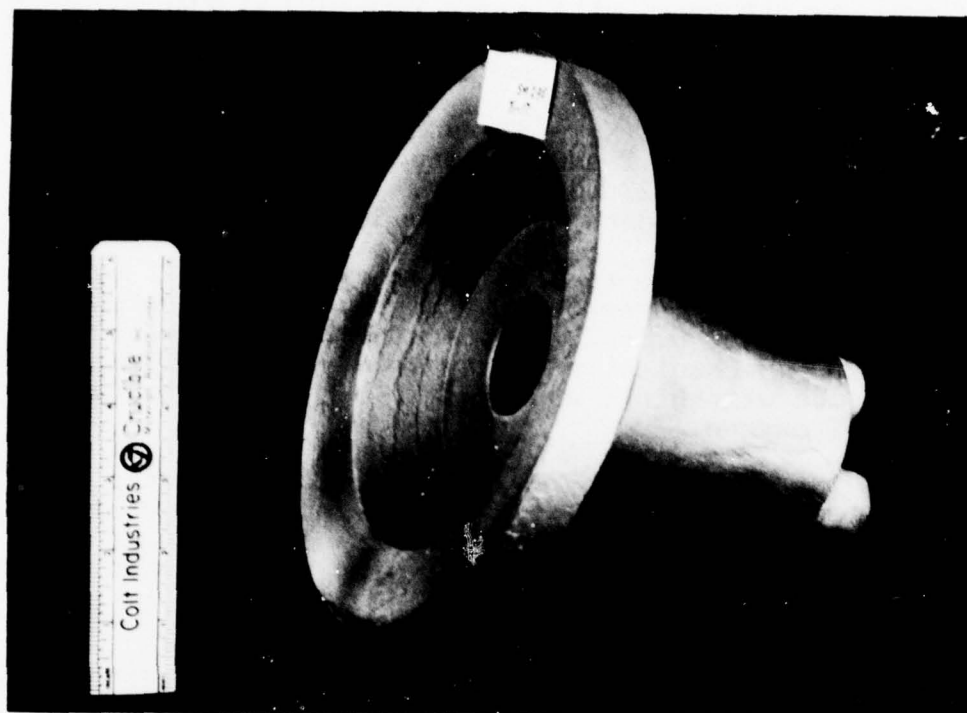


Figure 61. First shape trial on subscale stub shaft.



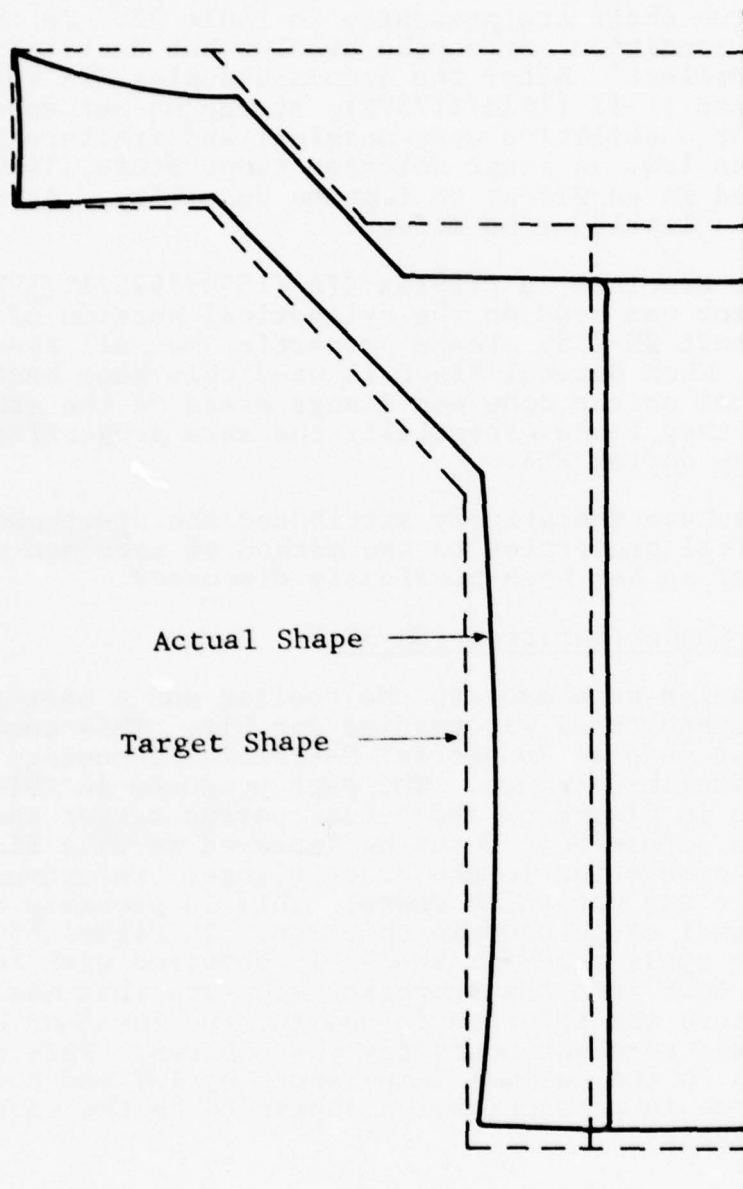


Figure 62. Actual vs Target Shape of first trial (SM-295).

Metallographic examination of a sample from the flange area indicated a typical beta-HIP structure with a prior beta grain size which ranged from 3 to 10 mils and averaged about 6 mils. Mechanical property data from this stub shaft are presented in Table 32. In the as-HIP condition, strengths are low but ductilities are excellent. After the standard duplex STA for beta-processed Ti-17 (1475/1175°F), strengths met specification but ductilities were marginal and fracture toughness was low. A lower solution temperature, 1450°F, was used in an effort to improve ductility. As shown, this had little or no effect.

At Crucible, a triplex STA (1550/1475/1175°F) treatment was used on the cylindrical portion of stub shaft SM-295. These properties met all specifications. When General Electric used this same heat-treatment on the cone and flange areas of the stub shaft, they found essentially the same properties as with the duplex STA.

We have tentatively attributed the discrepancy in mechanical properties to the method of specimen preparation, as has been previously discussed.

#### Second Shape Iteration (SM-324)

Changes were made to the tooling and a part for the second shape trial was readied for HIP. This compaction cycle was made at Industrial Materials Technology rather than Battelle-Columbus. The part produced in this trial is shown in Figure 63 and actual versus target shape is given in Figure 64. Note the improved surface finish and shape reproduction in the outer flange. Unfortunately, this part was not fully dense. This is probably due to the thermal cycle used in this run. In Figure 65, the Battelle cycle used for SM-295 is compared with this IMT cycle. Note from the temperature curves that maximum temperature was attained in the IMT run for four hours as opposed to eight hours for the BCL run. This slower approach to the maximum temperature by IMT and the difference in pressurization appear to be the cause of lower density.

#### Third Shape Iteration (SM-337)

This trial was essentially a rerun of the second iteration incorporating a tooling change to eliminate the residual porosity in the cylindrical portion of the stub shaft. During the HIP cycle, the container leaked and full consolidation was not achieved. An

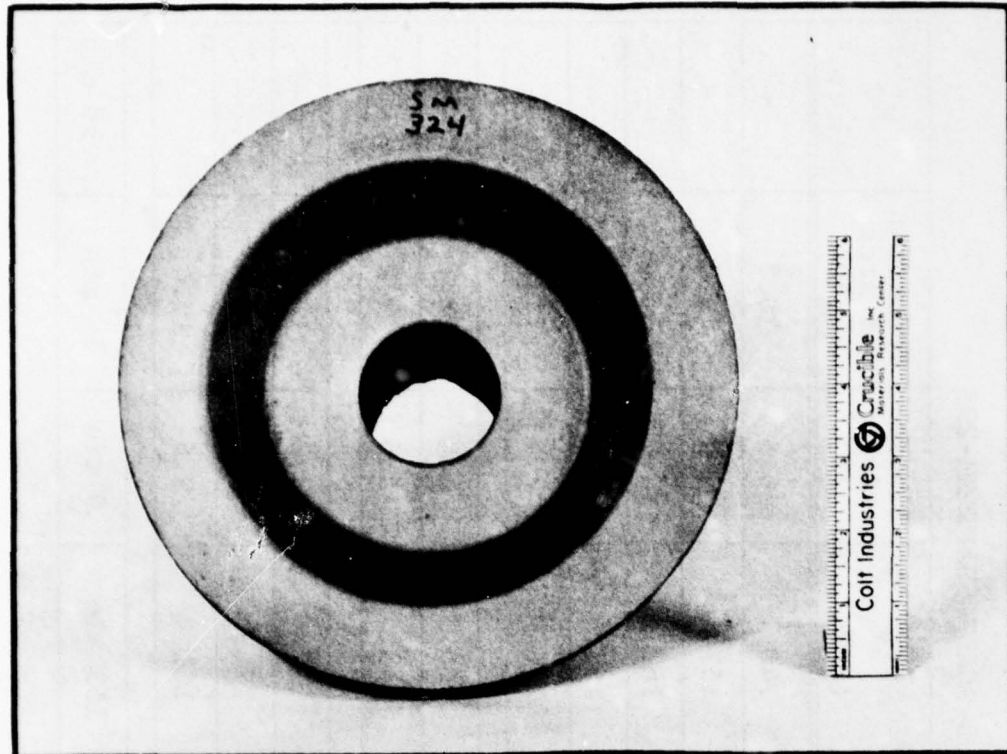


Figure 63. Second shape trial on sub-scale stub shaft.

examination of the part failed to show any contamination, so it was re-HIP. The final shape is shown in Figure 66. As expected, this is essentially the same as SM-324. The actual versus target shape is shown in Figure 67.

After the re-HIP, the part was fully dense but the reaction zone was thicker than in the previous trials. Because of the double HIP cycle, this part was relegated to use in fixturing and NDI development.

#### Fourth Shape Iteration (SM-357)

This iteration successfully accomplished full densification of the stub shaft and resulted in some additional dimensional refinement. The overall appearance was essentially the same as SM-337 (Figure 66). Actual versus target shape of this part is shown in Figure 68.

TABLE 32

## MECHANICAL PROPERTIES OF SUB-SCALE SHAFT SM-295

Heat Treat Condition	Specimen <sup>1</sup> Location <sup>1</sup>	F <sub>tu</sub> (ksi)	F <sub>ty</sub> (ksi)	Elonga- tion (%)	Reduction of Area (%)	K <sub>Q</sub> $\frac{1}{2}$ ksi in. <sup>2</sup>
As-HIP	C <sup>2</sup>	154.1	140.7	16.5	30.7	-
1450 F, 4 hours, WQ +	T	170.6	157.1	5.5	13.5	-
1175 F, 8 hours	F	176.3	162.0	4.7	10.9	-
1175 F, 8 hours	T <sup>3</sup>	179.9	168.4	4.2	13.8	-
	F <sup>3</sup>	176.9	166.9	2.3	11.5	-
1475 F, 4 hours, WQ +	T	174.4	165.5	4.4	10.1	44.0
1175 F, 8 hours	F	176.5	168.5	5.5	9.2	40.3
1550 F, 4 hours, AC +	T	178.0	159.0	3.2	10.4	-
1475 F, 4 hours, WQ +	F	180.5	174.8	4.1	10.7	-
1175 F, 8 hours, AC	C <sup>2</sup>	171.7	161.9	9.5	17.4	-
Specification		163 min	153 min	5 min	10 min	50 min

<sup>1</sup>T = Conical section, F = Flange section, C = Cylindrical section.

<sup>2</sup>Tested by Crucible, all others tested by General Electric.

<sup>3</sup>Head speed increased after yield was reached.



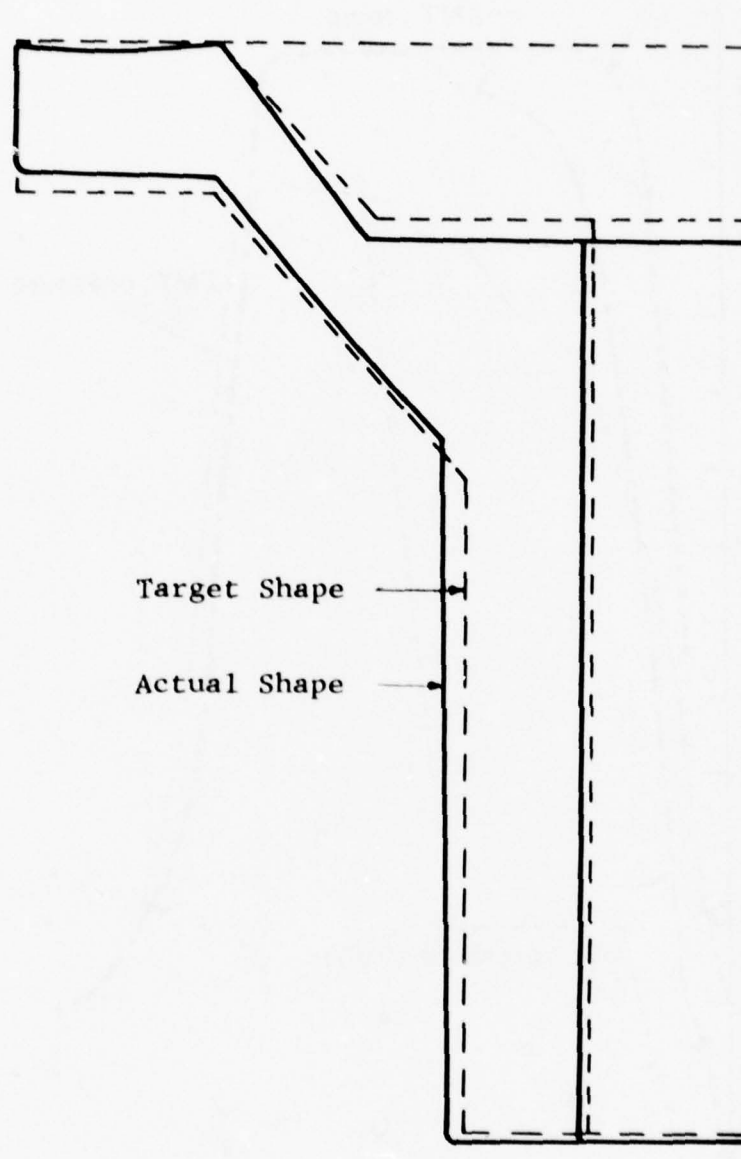


Figure 64. Actual vs Target Shape of second trial (SM-324).

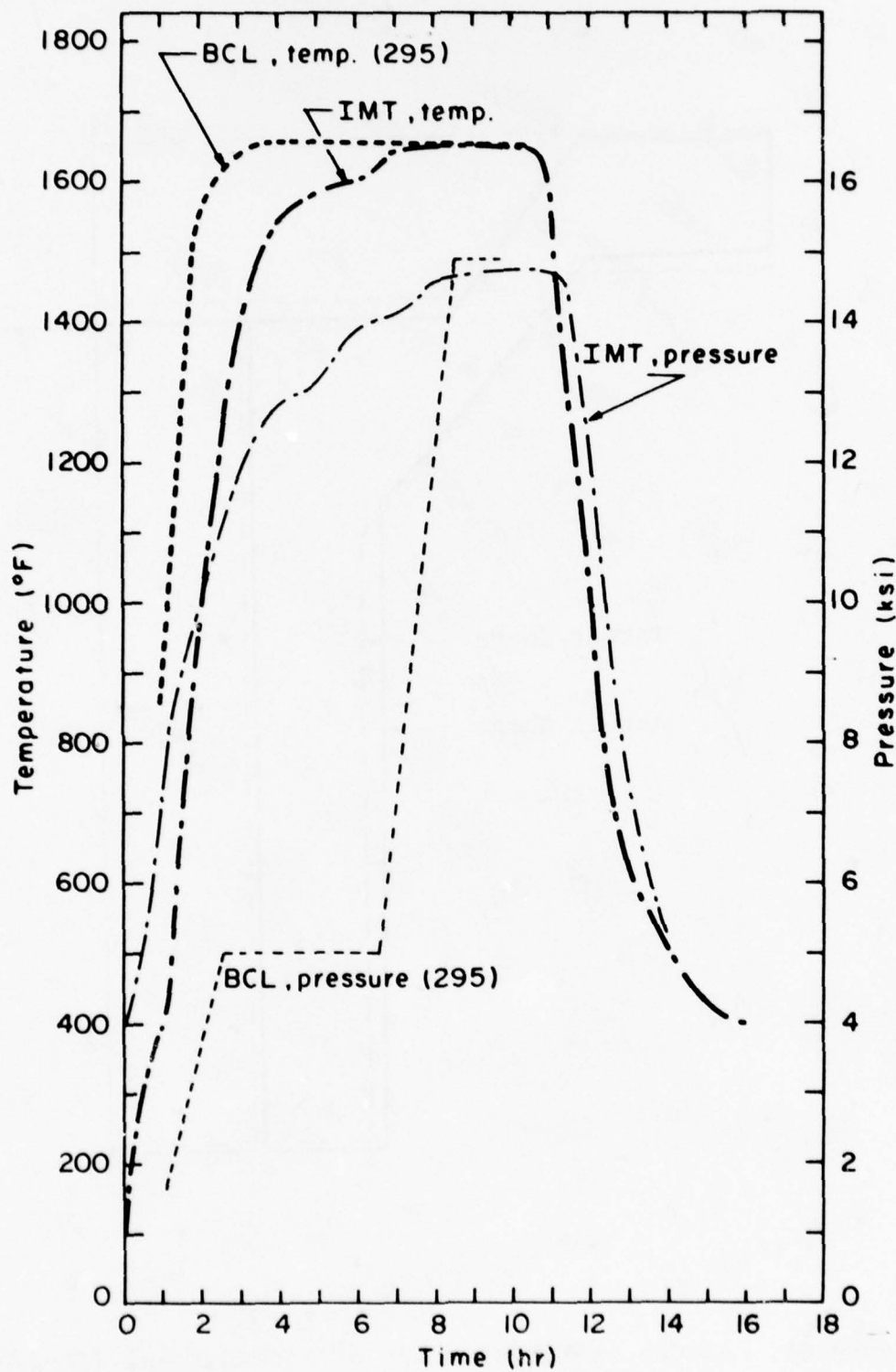


Figure 65. Comparison of HIP cycles used for first (SM-295, BCL) and second (SM-324, IMT) shape trials.

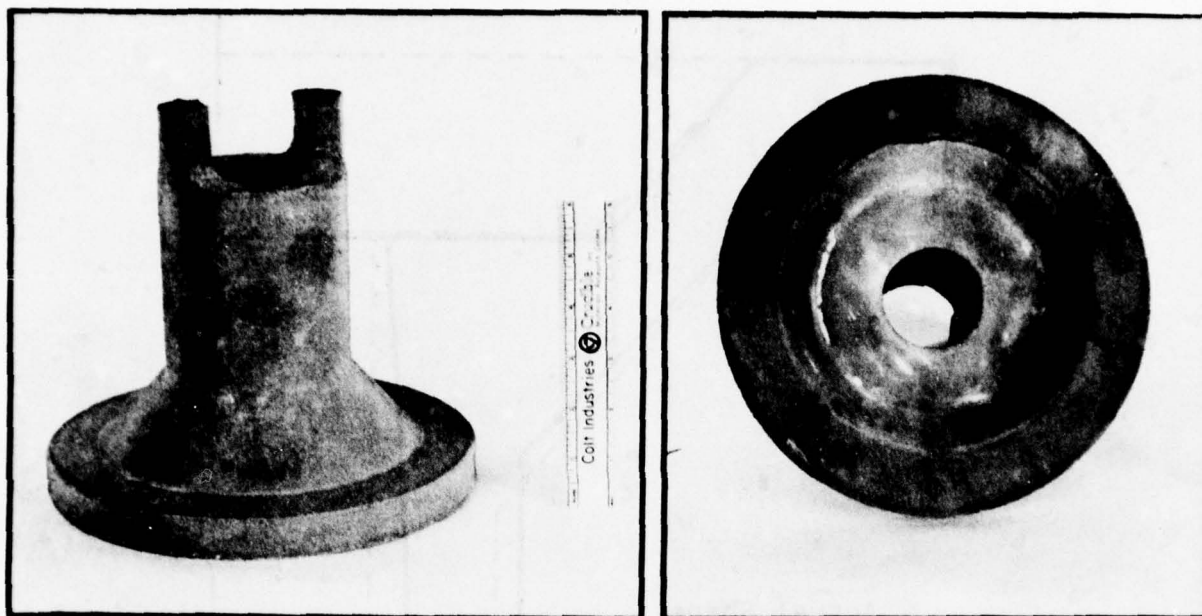


Figure 66. Third shape trial on sub-scale stub shaft (SM-337) after re-HIP.

Comprehensive mechanical property tests were performed on this HIP shape following a 4 hr/1475°F plus 8 hr/1175°F duplex heat treatment. The tensile properties, as shown in Table 33, exceed specification minimums and the notch tensile strength and notch-time-fracture behavior are typical of cast and wrought Ti-17. The smooth bar low cycle fatigue results are low, as previously reported. Notched low cycle fatigue tests at a  $K_t = 2.0$  were also run and properties comparable to cast and wrought were obtained. A curve is shown in Figure 69. This notched specimen, of course, localizes the maximum stress volume at the notch whereas smooth bar specimen provides a large volume stressed at about the same level. One might rationalize these results, therefore, on the basis that the smooth bar specimens permit areas of weakness due to voids, poor bonding, or inclusions to act as sites for early crack initiation and growth, whereas the notch bar specimens will yield "normal" life unless a defective area happens to be present at the notched area.

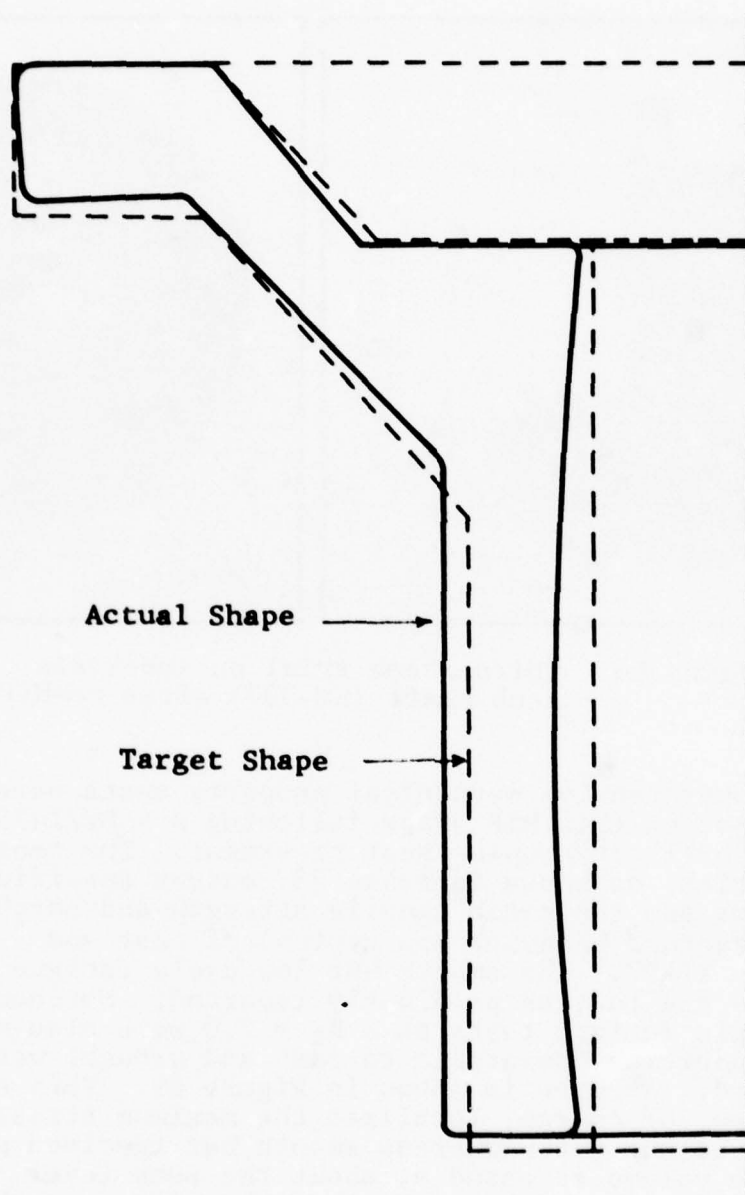


Figure 67. Actual vs Target Shape of third trial (SM-337).



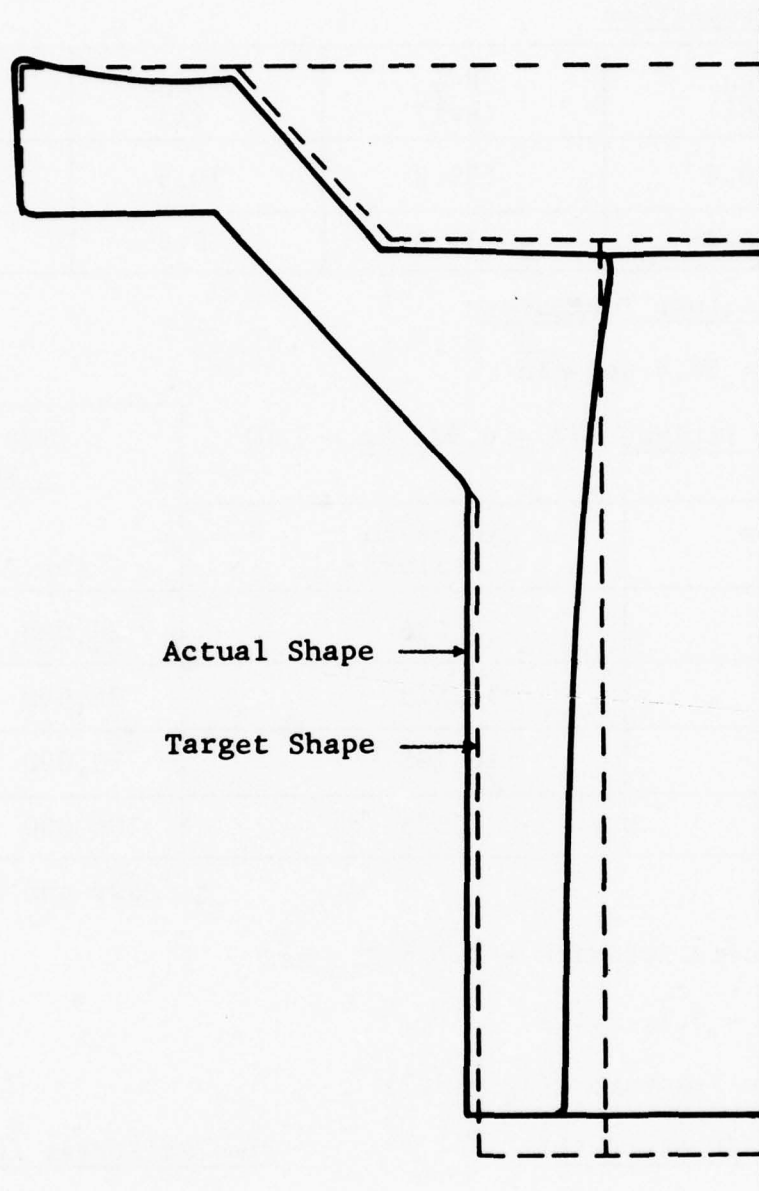


Figure 68. Actual vs Target Shape of fourth trial (SM-357).

TABLE 33

## PROPERTIES OF SUB-SCALE SHAFT SM-357

Tensile Properties

F <sub>tu</sub> (ksi)	F <sub>ty</sub> (ksi)	Elong. (%)	RA (%)
170.6	159.0	10.5	17.9
168.9	158.0	8.6	16.7

Charpy Fracture Toughness

$$K_C = 50.6 \text{ ksi} \sqrt{\text{in.}}$$

Low Cycle Fatigue (A = 0.98, K<sub>t</sub> = 1.0)

Stress (ksi)	Cycles to Failure	<u>Typical Cycles to Failure*</u>	
		Ave.	
			-30
150	7,086	20,000	-
140	10,523	35,000	2,000
130	10,195	70,000	19,000
120	7,535	100,000	35,000

\*Cast and wrought Ti-17

Notch Tensile Strength = 227.6 F<sub>tu</sub> ksi(K<sub>t</sub> = 3.7, R.T.)Notch-Time-Fracture (K<sub>t</sub> = 3.7)

<u>Stress (ksi)</u>	<u>Time at Stress (hours)</u>
160	5.1
170	17.0
180	7.2
190	16.1
200	6.9 (no failure, test stopped)
	52.3 hours

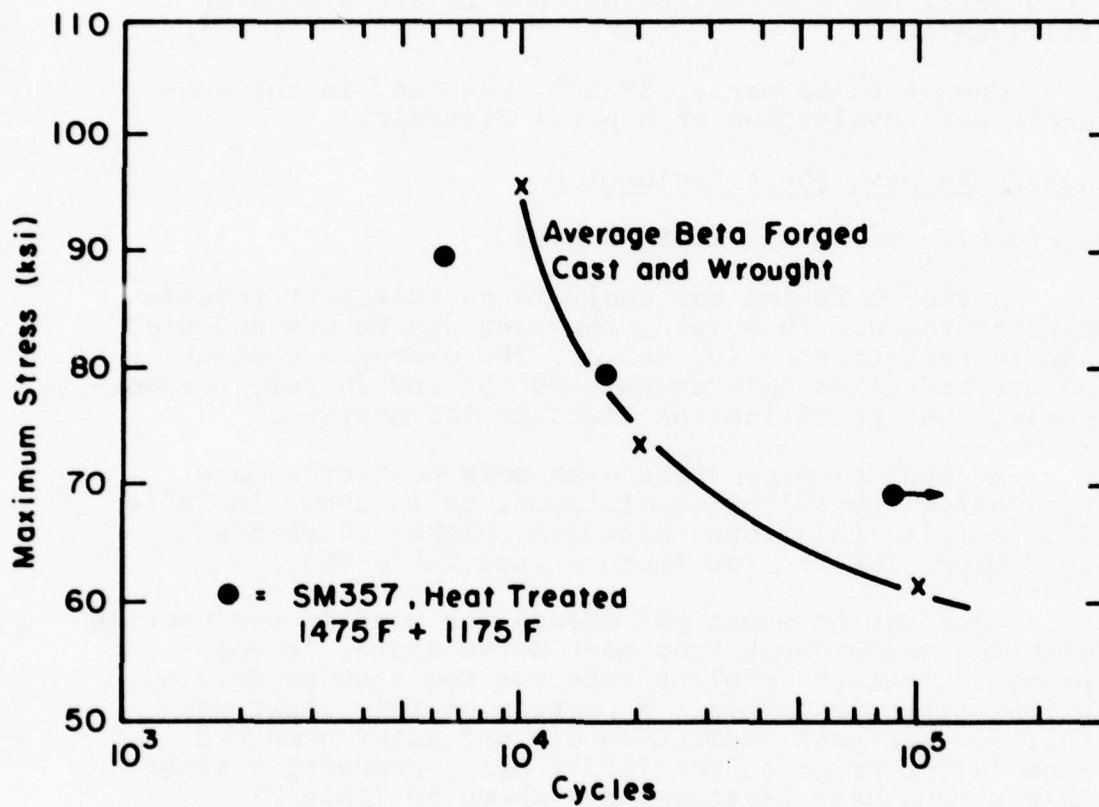


Figure 69. Notched low-cycle fatigue of SM-357.

### Fifth Shape Iteration (SM-368, -384 and -385)

Three parts were made using identically machined waxes. The actual versus target shape for SM-384 is shown in Figure 70, and two of the parts are shown in Figure 71. A dimensional analysis is presented in Table 34. With the exception of the shaft inner diameter, dimensional reproducibility is generally within  $\pm 1$  percent, i.e.,  $\pm 0.01$  inch per inch between each part, but some deviation from target dimension still exists.

One of these parts, SM-384, was used in the sub-scale part evaluation at General Electric.

### Sub-Scale Stub Shaft Evaluation

#### Evaluation of SM-384 (1650°F HIP)

A vacuum fusion gas analysis on this part revealed high hydrogen. Thereupon, the part was vacuum annealed and re-heat treated in vacuum. The hydrogen content before and after this anneal was 361 and 74 ppm, respectively. The specification limit is 125 maximum.

Mechanical properties with this heat treatment fall below specification minimums, as is shown in Table 35. Despite this lower strength, higher toughness condition, LCF did not improve (see Table 36).

Although an inert gas quench was used in conjunction with the vacuum heat treatment noted above, it was presumed that the cooling rate was too slow to develop normal strength levels. A portion of this shaft was therefore re-heat treated in air and water quenched from 1475°F prior to the 1175°F age. Properties after this second heat treatment are shown in Table 37. Strength increased very slightly and is still below the specification minimum. Low cycle fatigue data for the two heat treatments are compared in Figure 72. Results of a fractographic examination of these test specimens are summarized in Table 38. Again, LCF is well below wrought values and the fractographic examination indicate that non-metallic inclusions are the reason for the poor LCF results. Earlier in the program, similar data was recorded on a group of specimens where approximately half the fracture surfaces exhibited no detectable inclusions even though low LCF values were experienced. Table 38 shows similar results with two fracture surfaces having no detectable inclusions. The data suggest that inclusions affect LCF behavior even below detection limits of SEM and EDAX on surface fractures.



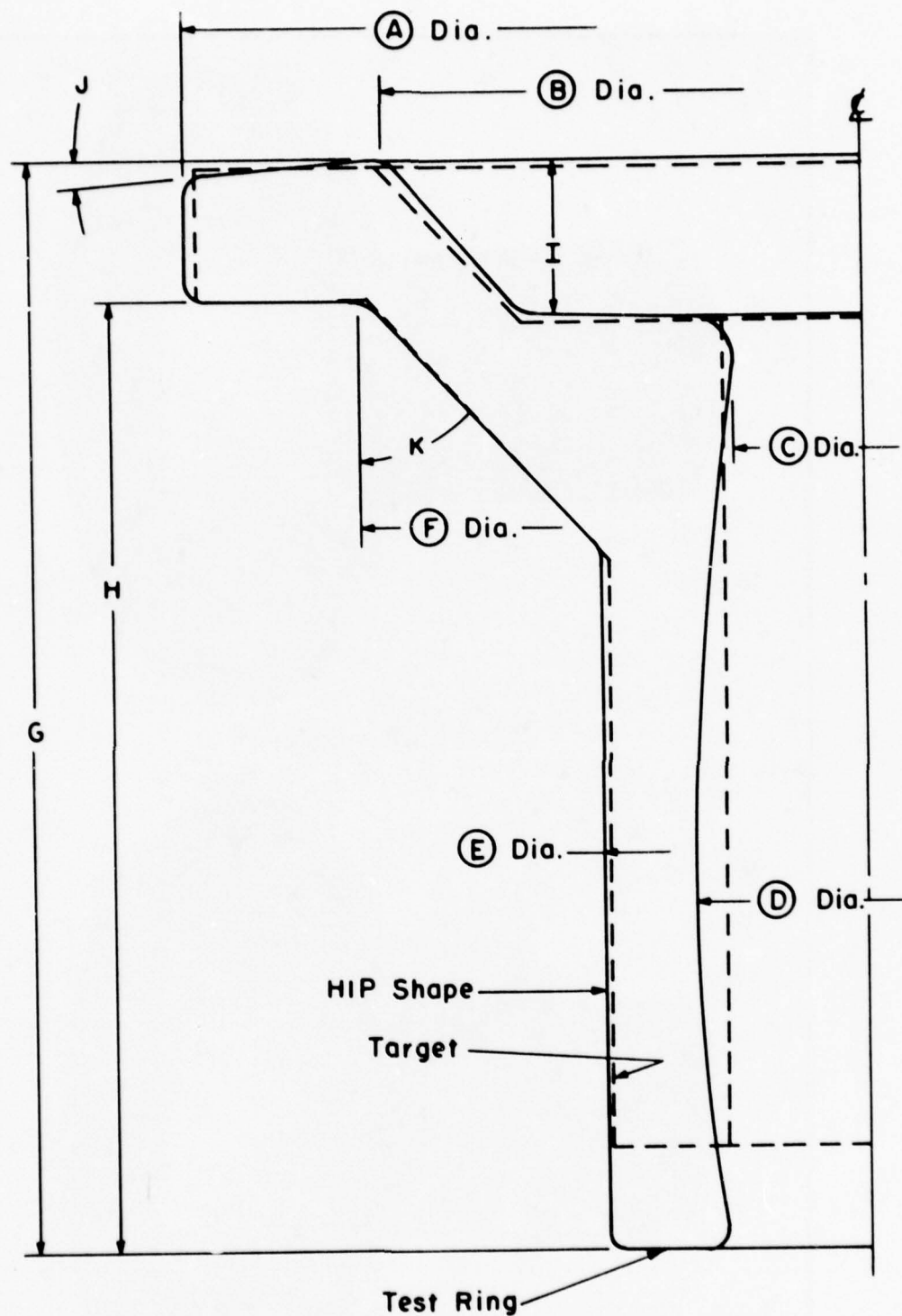


Figure 70. Actual versus target shape of Fifth Iteration (SM-384).



Figure 71. Sub-Scale shafts SM-384 and SM-385.

TABLE 34  
DIMENSIONAL ANALYSIS OF SM-384 AND 385

Dimension	SM-384 (in)	SM-385 (in)	$\Delta$		Target Dim. (in)	$\Delta$	
			Actual (in)	%		Actual (in)	%
A	8.51	8.50	0.01	0.1	8.40	.11	1.3
B	6.00	5.99	0.01	0.2	6.10	.11	1.8
C	1.68	1.73	0.05	3	1.8	.11	6.1
D	2.14	2.26	0.12	5.5	1.8	.40	22.2
E	3.30	3.32	0.02	0.6	3.25	.06	1.8
F	6.27	6.24	0.03	0.5	6.20	.06	.97
G	6.89	6.98	0.09	1.3	6.20	.73	12.1
H	5.98	6.01	0.03	0.5	5.35	.65	12.1
I	0.98	0.97	0.01	1.0	1.0	.03	3.0
J	5 deg	6 deg	1 deg	20	0.0	6 deg	--
K	43 deg	43 deg	0 deg	0	43.2	.2	.46

TABLE 35  
PROPERTIES OF SUB-SCALE SHAFT SM-384

TENSILE PROPERTIES (1)

Test Temp.	$F_{tu}$ (ksi)	$F_{ty}$ (ksi)	EI (%)	RA (%)
75°F	158.4	147.9	10.5	25.8
	155.1	144.1	8.8	23.2
Spec. Min.	163.0	153.0	5.0	10.0
400°F	135.9	115.0	10.1	26.9
600°F	130.7	105.4	10.4	29.5

FRACTURE TOUGHNESS RESULTS (1) (2)

Specimen No.	$K_Q$ (ksi $\sqrt{\text{in}}$ )
1	67
2	66

Notes: (1) Heat treatment 1475°F, 6 hrs vacuum, helium cool to 500°F, re-heat in vacuum to 1175°F, 8 hrs, vacuum cool.

(2) Pre-cracked cherry bars.

TABLE 36  
LOW-CYCLE FATIGUE TESTS - SM-384\*

A = 1.0, K = 1.0

Specimen No.	Stress Level (ksi)	Cycles to Failure
384-A	100	59,074
384-B	130	2,077
384-C	Cracked in inertia weld during machining	
384-D	120	14,894

\*Tested in high-toughness, low-strength condition.

TABLE 37  
PROPERTIES OF RE-HEAT TREATED SM-384

Heat Treated 1475°F, 4 hrs, vacuum helium quench  
+ 1175°F, vacuum, 8 hrs + 1475°F, 4 hrs, air, water  
quench + 1175°F, 8 hrs, air, air cool.

Test Temperature	F <sub>tu</sub> (ksi)	F <sub>ty</sub> (ksi)	Elong. (%)	Red. Area (%)
75°F	160.3	152.6	8.2	13.8
Spec. Min (75°F)	163.0	153.0	5.0	10.0
400°F	141.1	122.2	11.3	25.6
600°F	134.4	108.7	10.1	22.7
600°F	134.4	107.6	8.6	19.9



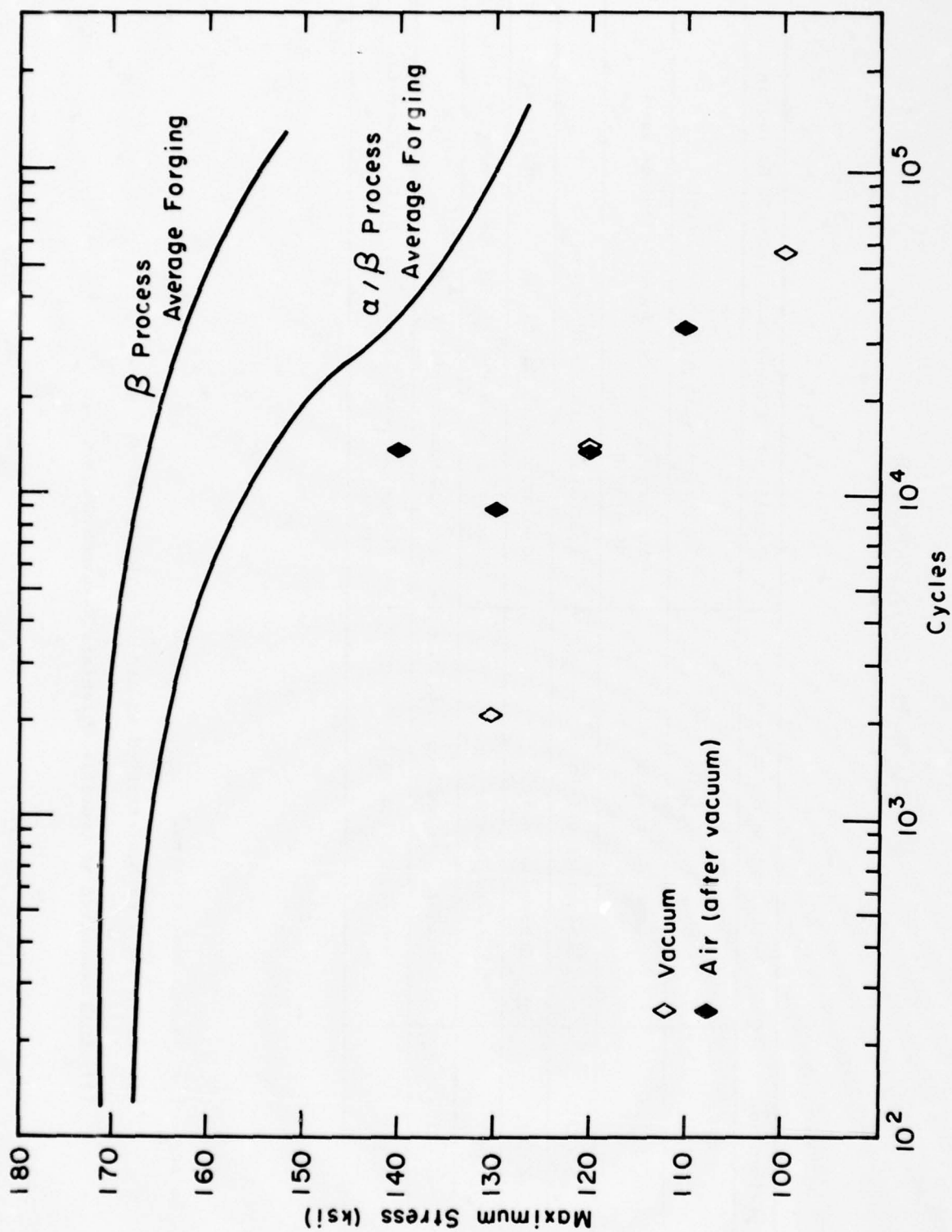


Figure 72. Low-cycle fatigue results on SM-384.

TABLE 38

METALLOGRAPHIC EXAMINATION OF  
LCF SPECIMENS FROM SM-384

Specimen No.	Metallographic Examination	Results of SEM and EDAX Analysis of Origin
A (1)	Subsurface origin	Inclusions with silicon at origin.
B (1)	Subsurface origin	No foreign material found, cleavage area at origin.
D (1)	Subsurface origin	Inclusion with Si at origin
E (2)	Subsurface origin	Inclusion with Mg, Si, K, Ca at origin area. (3)
F (2)	Near-surface origin	Inclusion with Mg, Al, Si, Ca at origin
G (2)	Slightly subsurface origin	No foreign material found
H (2)	Near-surface origin	Inclusions with Na, Al, Si, S, Cl, K and Ca present.

Notes: (1) Vacuum heat treated.

(2) As in (1) + re-heat treated in air and water quenched + age.

(3) EDAX conducted at Crucible Materials Research Center.

## Evaluation of SM-400 (1550°F HIP)

Using the same target shape as SM-384 and -385, an additional sub-scale stub shaft was consolidated using an alpha-beta HIP cycle (1550°F). This run was initiated to investigate 1) position of the ceramic mold and fill tubes relative to the secondary pressing medium, 2) effect of lower HIP temperature on surface and shrink of stub shaft I.D. and 3) effect of lower HIP temperature on mechanical properties.

Although no change in the stub shaft dimensions and surface condition were noted at the lower HIP temperature, mechanical property determinations were made to confirm alpha-beta range properties.

Tensile data for this part are shown in Table 39. These values are typical of cast and wrought Ti-17. Fracture toughness data are listed in Table 40. As is noted in Figure 73, the LCF lives are again below the minus three sigma level for the cast and wrought alloy. Again fractographic analysis confirmed the presence of non-metallic inclusions in three of four failed LCF specimens.

TABLE 39

### TENSILE DATA FOR $\alpha\beta$ HIP SHAFT\*

Mat'l.	Loc.	Spec. No.	F <sub>tu</sub> (ksi)	F <sub>ty</sub> (ksi)	Elong. %	RA %
SM-400	Flange	B5	174.7	166.5	10.3	23.0
SM-400	Shaft	B6	176.4	168.3	10.3	25.9
Spec. Min			163.0	153.0	7.0	15.0

\*Alpha-Beta HIP, Heat Treated 1550°F, 4 hrs, Rapid Air

Cool + 1475°F, 4 hrs, WQ + 1175°F, 8 hrs A.C.

TABLE 40

FRACTURE TOUGHNESS DATA FOR  $\alpha$ - $\beta$  HIP  
SHAFT (SLOW BEND PRE-CRACKED CHARPY)

Mat'l.	Loc.	Spec. No.	W	A	P <sub>Q</sub>	a/w	f(a/w)	K <sub>C</sub> * (ksi $\sqrt{\text{in}}$ )
SM-400	Flange	B7	0.394	0.1795	920	0.456	4.67	35.8
SM-400	Shaft	B8	0.394	0.190	800	0.482	5.03	33.6
Spec. Min.	30							

---

\*Calculated from formula -  $K_C = 8.35 P_Q F(a/w)$



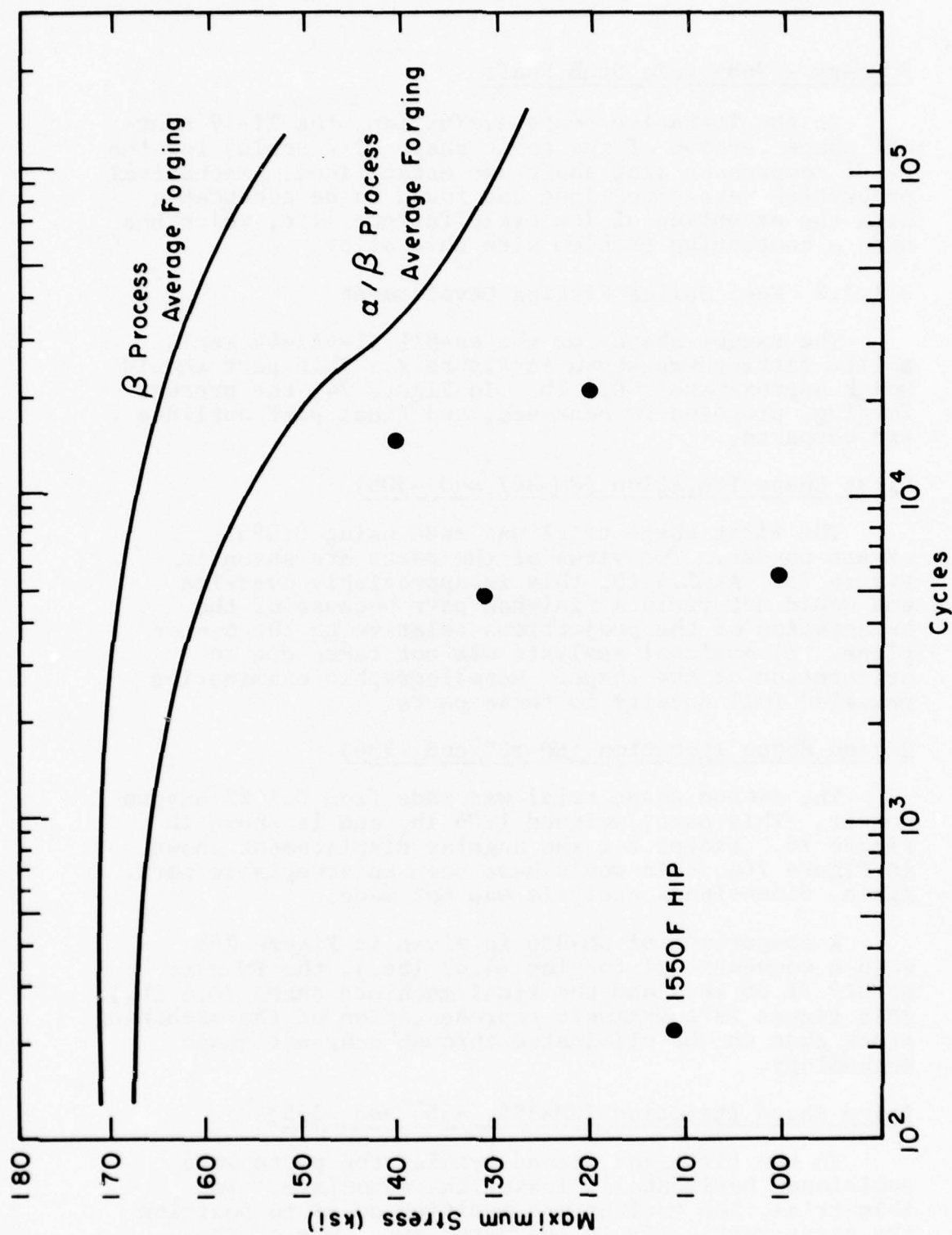


Figure 73. Effect of sub-transus HIP on low cycle fatigue results.

### Summary - Sub-Scale Stub Shaft

In the iterative shape evaluation, the Ti-17 near-net shape version of the sonic shape (1/2 scale) for the F-101 compressor stub shaft was established. Mechanical properties were determined and found to be acceptable with the exception of low cycle fatigue life, which has been a continuing problem with this alloy.

#### 3.1.3.2 Keel Splice Fitting Development

The target shape for the as-HIP Ti-6Al-4V keel splice fitting was shown in Figure 2. This part should weigh approximately 0.8 lb. In Figure 74, the present forging, proposed PM near-net, and final part outlines are compared.

#### First Shape Iteration (SM-307 and -308)

The first shape trial was made using 0.095% oxygen powder. Two views of the parts are shown in Figure 75. At 1.4 lb, this is appreciably oversize and would not yield a finished part because of the orientation of the projections relative to the center plane. Dimensional analysis was not taken due to orientation of the shape. Metallographic examination revealed full density in these parts.

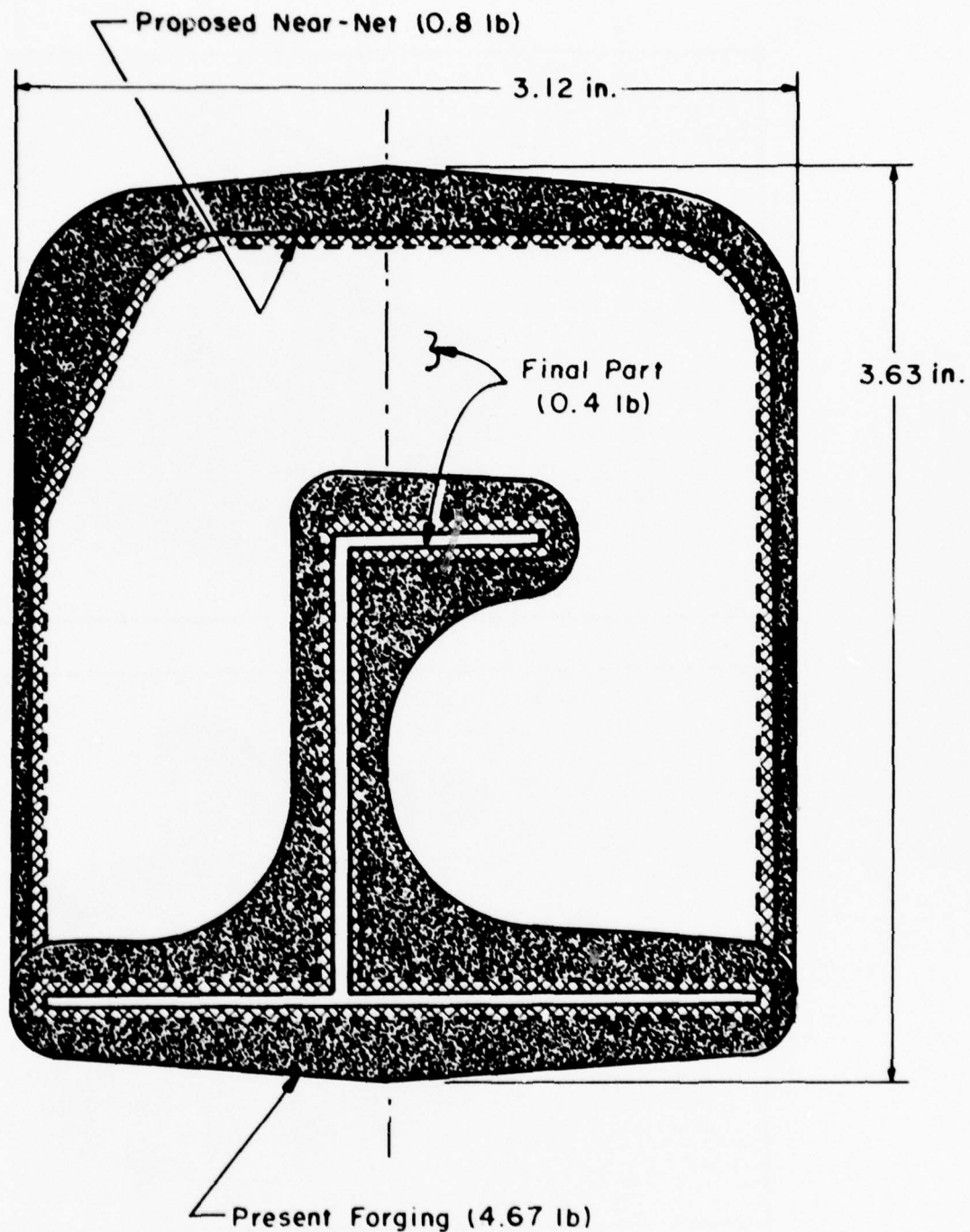
#### Second Shape Iteration (SM-335 and -336)

The second shape trial was made from 0.142% oxygen powder. This part, weighed 1.06 lb, and is shown in Figure 76. Except for the angular displacement shown in Figure 76a, this would have been an acceptable part. Again, dimensional analysis was not made.

A comparison of SM-336 is given in Figure 76b with a conventional forging (4.67 lbs.), the PM part as-HIP (1.06 lb.) and the final machined shape (0.4 lb.). This figure is a dramatic representation of the machining stock that can be eliminated through near-net shape technology.

#### Third Shape Iteration (SM-353, -354 and -355)

In the first and second trials, the parts were positioned horizontally inside the autoclave. In this trial, the tooling was modified so as to position the parts vertically in the autoclave. One of the



### F-15 Keel Splice Fitting

Figure 74.

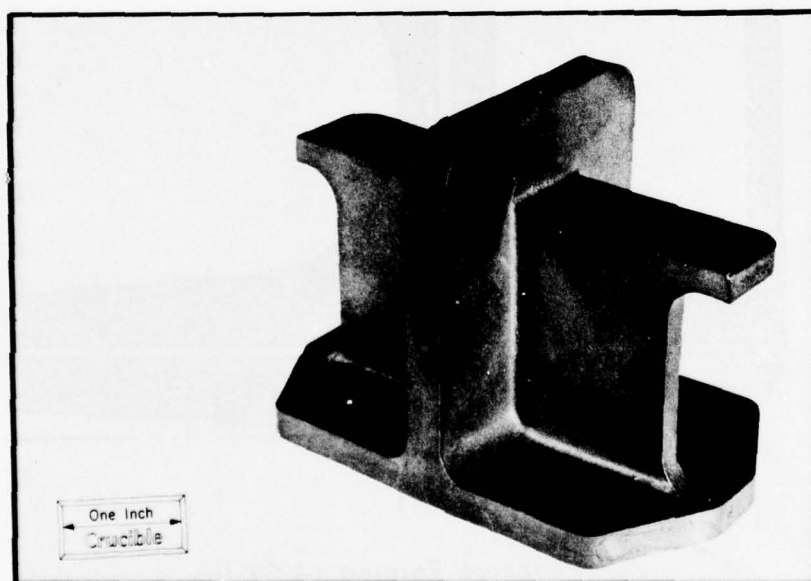
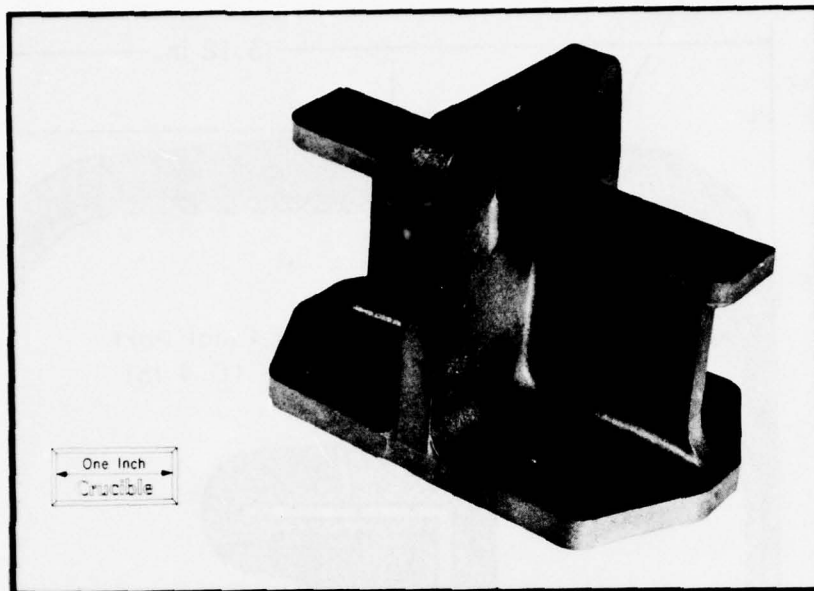
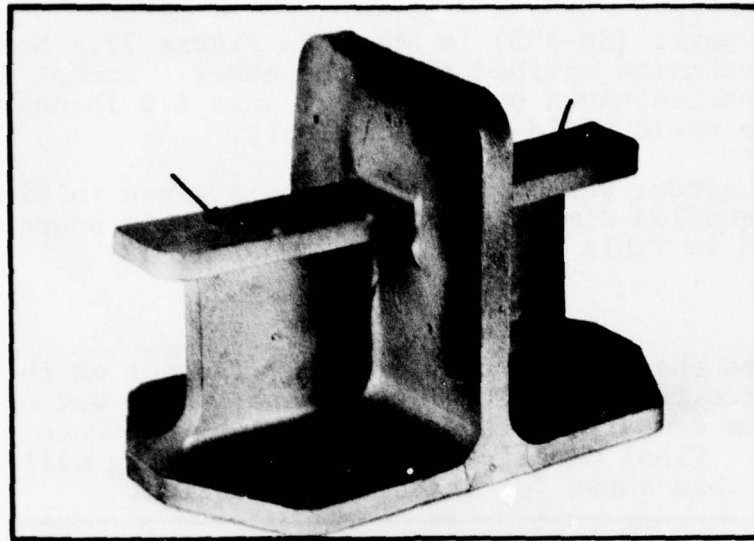
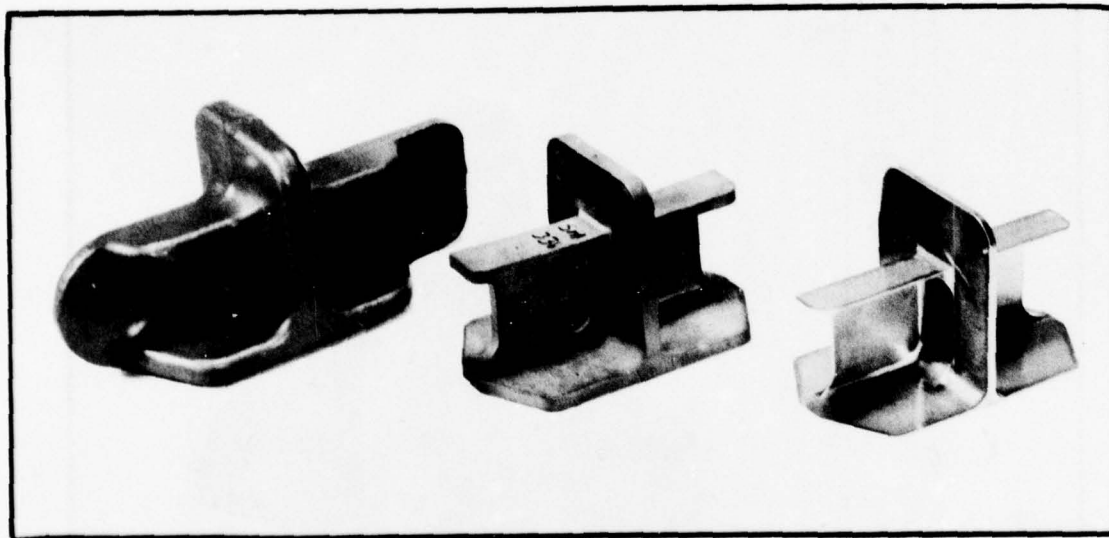


Figure 75. First shape iteration on F-15 keel splice fitting.





(a) Part SM-336. Arrows denote misaligned surfaces.



(b) From left: Conventional 4.67 lb forging, 1.06 lb PM Part (SM-336), and 0.4 lb final shape.

Figure 76. Second shape iteration on F-15 keel splice fitting.

finished parts (SM-355) is shown in Figure 77. Note the layout marks scribed along the edges. Except for the depression shown by the arrow, this 1.0 lb near-net shape would yield a finished part.

The actual versus finish shape is given in Figure 78. A detailed dimensional analysis of this shape is presented in Table 41.

#### Summary

Three shape iterations were carried out on the keel splice fitting. The final shape, which weighs 1.8 lb, as compared with a 4.67 forging, has been produced. Final modifications to the tooling will optimize this shape for Phase II evaluation.

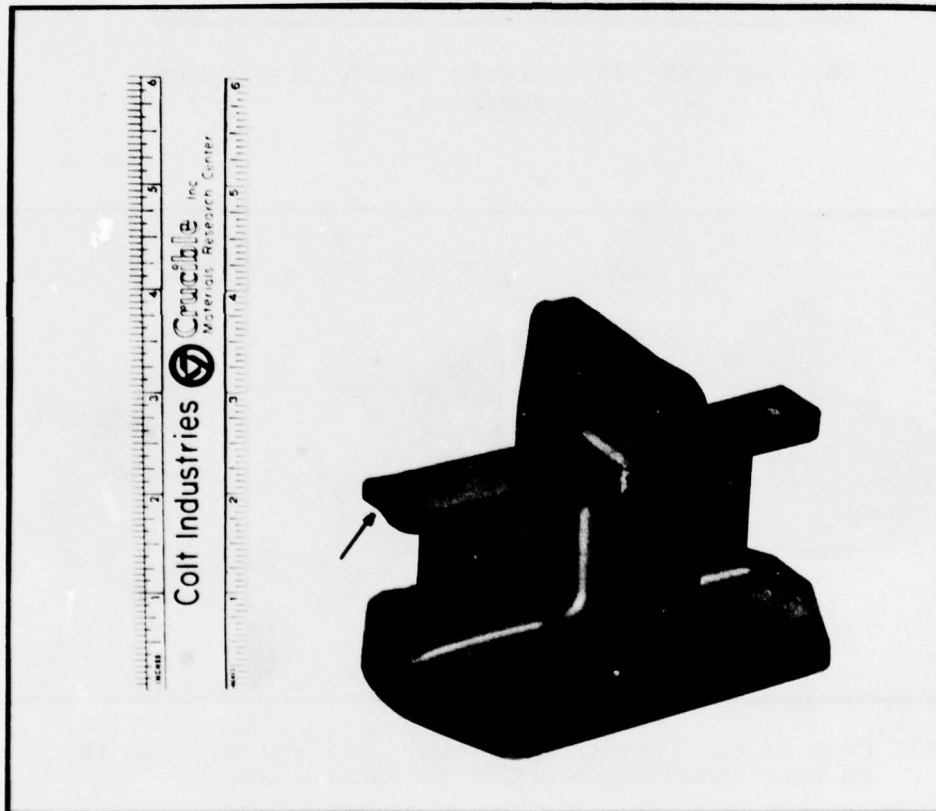


Figure 77. Third shape iteration on F-15 keel splice fitting.

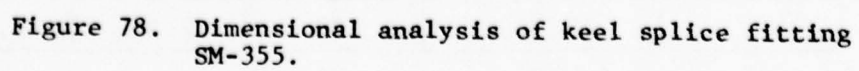


TABLE 41

DIMENSIONAL ANALYSIS  
THIRD SHAPE ITERATION (SM-355)

Dimension	SM-355	Target	Finish	
1	5/16R	5/16R	.41R	--
2	1.190	---	1.05	1.17
3	.820	---	.65	.86
4	3.100/3.170	3.020	2.770	2.89
5	4.780	4.910	4.180	4.79
6	26°	27°56'	---	---
7	5/16R	3/8R	.38R	.38
8	2.255	2.330	2.09	2.33
9	1.770	1.820	2.09	1.82
10	3.732	3.760	4.18	3.64
11	.310	.224	.090	.15
12	1/8R	1/8R	.12R	.12
13	9/32R	5/16R	---	---
14	.880	.880	.860	.750
15	3.363/3.407	3.320	---	---
16	2.145/2.190	2.125	2.02	2.00
17	.155/.210	.180	.065	.055
18	1.210	1.180	---	---
19	1/8R	1/8R	.12R	.12R
20	.170/.200	.174	.065	.050
21	10°	9°56'	---	---
22	1/2R	1/2R	---	.50
23	.150/.195	.180	.065	.050
24	1.900	2.120	2.300	2.000



### 3.1.4 Task IV - Non-Destructive Testing (NDI) Of Trial Shapes

#### 3.1.4.1 NDI of Sub-Scale Stub Shaft (Ti-17)

The NDI procedures called for on full-scale F-101 conventional cast and wrought forgings include ultrasonic testing of the forging after machining to a designated ultrasonic shape. After final machining, the part is also penetrant inspected. X-ray examination is not called out on most titanium cast and wrought materials now since the incidence of porosity and high density inclusions has been found to be extremely low. However the incidence of tungsten inclusions in REP powder is relatively high and X-ray examination was evaluated on the sub-scale shafts.

#### Preliminary Trials

Portions of test billets 236 and 237 were heat-treated and machined to the configuration shown in Figure 79. Evaluation consisted of ultrasonic attenuation and noise level measurements in order to obtain a preliminary idea of the response of HIP Ti-17 to ultrasonic examination. Since a HIP Ti-17 standard was not yet available, the results are compared to Ti-6-4.

There was a 2% difference in ultrasonic longitudinal velocity between the length of the bar and the two short dimensions. Both samples exhibited this difference, as is shown in Table 42.

Both samples exhibited low ultrasonic noise levels at standard gain levels (Table 43). The highest noise levels were exhibited in the shear mode. At high sensitivity gain levels, both samples exhibited high noise levels in the longitudinal mode along the length of the bar. Excessive noise levels were exhibited in the shear mode.

In order to evaluate the noise characteristics further, the ultrasonic instrument gain was increased until the peak noise level reached 80% FSA (full usable oscilloscope amplitude) or until maximum gain was reached. Two types of ultrasonic noise were noted: exponential (where the peak noise is inside the surface) and banded (where the peak noise is inside the material). No banded type noise was found in either sample in the long dimension for longitudinal mode (Table 44).

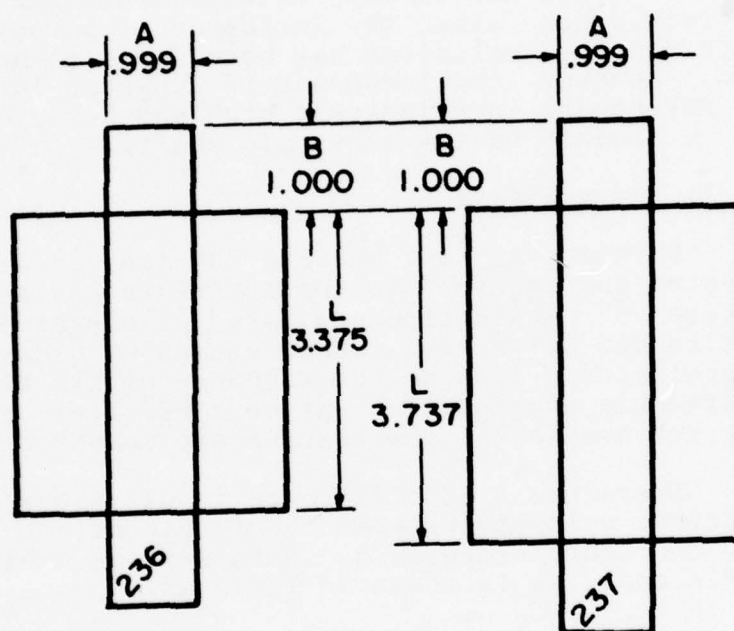


Figure 79. Ultrasonic test specimens.

TABLE 42

VELOCITY MEASUREMENTS

Direction	Mode	Velocities $\alpha/\beta$ -HIP   $\beta$ -HIP #236   #237 (inches per microsecond)	
A	Long.	.241	.241
B	Long.	.242	.242
L	Long.	.236	.237

TABLE 43

NOISE MEASUREMENTS

Direction	Mode	Type	Noise (% FSA)			
			$\alpha/\beta$ -HIP #236		$\beta$ -HIP #237	
			P3TF1	+12 db	P3TF1	+12 db
A	Long.	Exp.	0	6	3	18
B	Long.	Exp.	0	6	0	8
L	Long.	Exp.	4	21	7	36
A	Long.	Band	0	3	7	7
B	Long.	Band	0	3	7	7
L	Long.	Band	--- Data Not Available ---			
A	Shear	Exp.	2	43	6	32
B	Shear	Exp.	3	23	6	36
L	Shear	Exp.	11	18	6	32
A	Shear	Band	4	39	11	57
B	Shear	Band	4	31	7	47
L	Shear	Band	6	43	11	53

TABLE 44

## NOISE ANALYSIS OF TEST BILLETS

Direction	Mode	Type	$\alpha/\beta$ -HIP #236			$\beta$ -HIP #237		
			Gain	Noise (% FSA)	$\Delta$ db	Gain	Noise (% FSA)	$\Delta$ db
A	Long.	Exp.	1000	26	22.2	1000	46	22.2
B	Long.	Exp.	1000	19	22.2	1000	54	22.2
L	Long.	Exp.	1000	60	22.2	900	80	21.2
A	Long.	Band	1000	21	22.2	1000	36	22.2
B	Long.	Band	1000	21	22.2	1000	46	22.2
L	Long.	Band	----- DATA NOT AVAILABLE -----					
A	Shear	Exp.	780	80	11.8	960	80	13.6
B	Shear	Exp.	1000	64	14	880	80	12.9
L	Shear	Exp.	1000	57	14	950	80	13.5
A	Shear	Band	1000	71	14	800	80	12
B	Shear	Band	1000	62	14	980	80	13.8
L	Shear	Band	1000	57	14	890	80	13

For the longitudinal mode, maximum gain was reached before 80% FSA noise levels, except for one direction on sample #237. For the shear mode, maximum gain was reached before 80% FSA noise levels on sample #236 except for one direction. However, on sample #237, 80% FSA noise levels were reached before maximum gain in every case.

Sample #236 was less attenuative than sample #237, requiring a 16-19 db gain reduction (from the 1/4" deep hole on a P3TF1 block) to reduce the back surface signal to 80% FSA. Sample #237 required only 12-13 db reduction in the shorter dimensions and 6 db reduction in the long dimension. No significant indications were recorded during the scanning of the two samples.

The stub shaft is required to meet the ultrasonic requirements of General Electric specification P3TF1. Based on the results reported here, both the



alpha-beta and beta-HIP compacts could be inspected to this level. However, at high sensitivity levels (+12 db of Table 43) the noise level in shear becomes excessive indicating near-surface inspectability would be difficult, if not impossible. This "near surface" noise is due to surface porosity and roughness from the HIP operation. Sensitivity requirements above the P3TF1 specification level are sometimes called out for highly critical jet engine parts but are not a requirement for the stub shaft. HIP Ti-17 therefore appears to be inspectable to the levels required for the present program.

#### Ultrasonic Standards

The standard calibration block required by the P3TF1 specification was HIP, heat-treated (1475°F 4 hours, WQ + 1175°F, 8 hours) and machined. The surface finish of the calibration block (after machining by grinding) was 8-9 RMS on one side and 6-8 on the other.

The Ti-17 calibration block has been evaluated in a comparison with similar blocks of Ti-6Al-4V alloy and cast and wrought alpha-beta processed Ti-17. A directly comparable standard for beta processed cast and wrought Ti-17 is not available. The results are given below.

- 1) The Ti-17 HIP standard was inspected by the General Electric Metrology Laboratory to determine the block's dimensional conformance to AEG Dwg. #9062M21. The standard was found dimensionally acceptable.
- 2) The ultrasonic evaluation was conducted using a linear Branson Sonoray 600, 623 Ts P/R, 610 UIN Time Base, 9' RG 62 B/U Coax Cable and two 0.75" diameter lead metaniobate transducers. One transducer was a 10 mhz compound lens wide beam ( > .200") and the other a 5 mhz simple lens narrow beam ( < .200"). The ultrasonic evaluation consisted of comparing hole responses, attenuation and noise between the standards.
- 3) Attenuation was measured by two methods. One method compared the loss of amplitude of the first back reflection from the standards in the longitudinal mode. This provides a rough

estimate of the relative attenuation characteristics of the material when compared with a known standard. These measurements were done in two directions and with two transducers; results from both were very comparable. The Ti-17 HIPed standard was up to 3.5 and the Ti-17 wrought 2.5 db per inch more attenuative than the Ti-6-4 standard and within 1 db per inch of each other. In percentage, the variation between the Ti-17 standards was approximately 9% while the Ti-17 average was 14% to 16% per inch more attenuative than the Ti-6-4 alloy standard. It should be noted that these measurements would be indicative of the longitudinal mode only.

- 4) The second method of assessing attenuation effects was to compare hole responses by means of constant gain curves. A curve was established for each standard and transducer and then these curves were compared against each other.
- 5) In the longitudinal mode Ti-6-4 displayed the least attenuation, followed by Ti-17 wrought and then the Ti-17 HIPed. Depending upon transducers, the Ti-17 wrought measured 1-2 db and the Ti-17 HIPed 2-3 db more attenuative than Ti-6-4 at the 1.5" (38.1 mm) depth; at the 2.875" (73 mm) depth the Ti-17 wrought measured 2 db and the Ti-17 HIPed 3-4 db more attenuation.
- 6) In the shear mode Ti-6-4 was again the least attenuative; however, the Ti-17 HIPed was less attenuative than the Ti-17 wrought. Depending upon transducer, at the 1.5" (38.1 mm) depth, the Ti-17 HIPed was 9 db and the Ti-17 wrought 10-12 db more attenuative than Ti-6-4. This significantly higher attenuation would forewarn of penetration and noise problems in attempting thick sections of the alloy in the shear mode.
- 7) There was significantly different structural noise between the Ti-17 HIPed and the other surveyed standards. In the longitudinal mode, a minimal difference (3%) in noise was noted. However, in the shear mode the differences were significant. At the 1.5" scanning gain for each transducer, the Ti-6-4 standard displayed minimal baseline noise, the Ti-17 wrought

5%, while the Ti-17 HIPed showed noise up to 20%. It is felt this noise can be attributed to structure as all other test parameters had remained constant and all surface finishes were comparable.

The overall results indicate beta-HIP Ti-17 is "noisier" than Ti-6-4 or alpha-beta processed Ti-17. However, some data on beta processed cast and wrought forgings indicate that it is "noisier" than alpha-beta processed Ti-17. The present results are therefore not surprising. Based on these results, it appears that HIP Ti-17 can be inspected at the normal sensitivity level to GE specifications. However, inspection at higher sensitivity levels would be difficult due to the relatively high noise level present. The higher noise level might be compensated somewhat by DAC techniques or changes in transducers, etc., if inspectability proves to be a problem later.

#### Sub-Scale Shaft SM-337

This shaft was run twice through the HIP cycle since the can leaked in the first run. Due to this, it was not cut up for test, but was used for NDI studies.

The shaft was heat-treated (1475°F, 4 hours, WQ + 1175°F, 8 hours) and grit blasted (grit size 150) to remove the surface oxide. It was then submitted for ultrasonic inspection since this would be the preferred manufacturing sequence for a production HIP part. Preliminary machining prior to sonic inspection would be an added expense. Inspection was carried out in both longitudinal and circular shear modes on the flange area by immersion inspection. In the as-grit-blasted condition, the noise level was excessive in both inspection modes and inspection to P3TFl limits could not be accomplished. An area of the flange was hand polished with abrasive paper to ~10 RMS finish and inspection appeared possible by both longitudinal and circular shear modes. The surface roughness was 130-170 RMS in the as-grit-blasted condition. These results indicate that some surface conditioning will be required prior to sonic inspection. A similar condition has been found to exist on nickel-base alloy HIP products and a Harperizing treatment (essentially a tumbling operation) has been identified which produces a surface finish of ~20 RMS.



After Harperizing, the overall surface finish was improved from 130-170 RMS to 25-30 RMS. However, some pits and seams remained from cracks in the mold. Most of these were on the inside diameter of the shaft but some were present on the OD and on the flange area. Ultrasonic examination after Harperizing indicated that the shaft was inspectable to the General Electric P3TF1 specification limits required for this part in the longitudinal mode. At an increased gain of + 6 db, it was also inspectable, but at + 12 db, increased sensitivity of the noise level made inspection questionable at this gain level. Some rounding of corners occurred during the Harperizing treatment, but it does appear to be a useful process for improving the surface finish of HIP Ti-17 shapes.

X-ray inspection of Part SM-337 was also conducted. This was done using one exposure to X-ray the flange and conical section and multiple strip film exposures to inspect the shaft area. The laps on the inside surface of the shaft were revealed by this inspection. No defects were found in the shaft or the conical section. One apparent defect was found in the shaft section near the transition to the conical section. This appeared to be a void or low density inclusion and was  $\sim 0.025'' \times 0.075''$  in size. No evidence of tungsten or other high density inclusions was found, however, this is not surprising since prior metallographic evidence indicated that the tungsten inclusions present were only 1 mil or less in size. This is well below the limit of detectability in X-ray examination. The one low density area found appeared to be related to a surface protrusion on the as-HIP shaft which indicates there may be a void beneath this protrusion. The shaft was Harperized and X-rayed again. The Harperizing treatment removed the surface protrusion and, apparently, the defect along with it. Based on the overall X-ray results, this does not appear to be a useful inspection method for PM shapes.

#### Intentionally Flawed Shaft (SM-401)

One sub-scale shaft, SM-401, was produced from Ti-17 powder into which the following were intentionally added:

2 pieces	0.02 inch (nominal)	superalloy powder
2 pieces	0.02 inch (nominal)	silica sand ( $\text{SiO}_2$ )
1 piece of	$\text{SiO}_2$ -coated titanium sheet.	



The first two are intended to simulate powder cross-contamination and non-metallic contamination, respectively. The coated sheet is intended to simulate an internal crack.

The sub-scale shaft was surface conditioned by tumbling in an abrasive slurry solution (Harperizing). This treatment produces a very smooth surface. However, seams caused by mold cracks and other surface defects such as depressions, protrusions, etc. were not removed by this surface treatment.

The sub-scale shaft was X-rayed in General Electric facilities using a 1.1 million volt X-ray unit powered by a Van de Graaff generator. Separate films were taken of the flange area, the conical section and the straight shaft section. No defects were indicated in any of the films.

The shaft was next ultrasonically inspected by water immersion using the parameters given in Table 45, and the ultrasonic traces were recorded using a grey scale "C" scan. As indicated in Table 45, no indications identifiable as defects were found. Some of the inspection modes showed indications which were obviously a result of the defects which were visible on the surface of the HIP part (depressions, protrusions, seams, etc.).

It appears that the defects which were seeded into this sub-scale shaft are not detectable by normal inspection methods. However, some of the inspection modes proved inconclusive as a result of the indications shown due to surface irregularities on the as-HIP surface. A more regular surface free of depressions, protrusions and seams would be necessary for inspection of critical components.

#### NDI of Keel Splice Former

Radiography and penetrant inspections were the principal methods of non-destructive examination. The parts were X-rayed according to MCAIR process specification P.S. 21206 Quality Level 2-IT which is standard NDI technique for the keel splice former. This quality level is defined as follows:

Maximum penetrameter thickness, 2%  
(expressed as percentage of the  
material thickness)

TABLE 45

ULTRASONIC INSPECTION RECORD: SUB-SCALE SHAFT SM-401  
Ultrasonic Conditions (1)

Area of Shaft	Table Speed (RPM)	Grain	Mode	Sensitivity (2)	Results
Conical Section	7	20 X 10	Longitudinal	+ 12 db	No indications
Conical Section	12	106	Radial Shear	+ 6 db	Indications of surface defects
Conical Section	12	106	Circum. Shear	+ 6 db	Indications of surface defects
Flange	12	114	Circum. Shear	+ 6 db	Few surface indications
Flange	12	114	Radial Shear	+ 6 db	No indications
Flange	7	20 X 10	Longitudinal	+ 12 db	No indications
Straight Shaft Section	7	106	Axial Shear	+ 6 db	No indications
Straight Shaft Section	7	106	Circum. Shear	+ 6 db	No indications
Straight Shaft Section	7	148	Longitudinal	+ 12 db	No indications

Notes: (1) All at 5 MHZ Frequency

(2) Sensitivity as compared to normal inspection sensitivity.

Minimum perceptible hole diameter, 1T  
(expressed as multiple thickness of  
image quality indicator T)

Equivalent penetrameter sensitivity, 1.4%

All films were double loaded to minimize artifacts. The parts were shot in three orthogonal views before and after machining.

Examination of the film for the as-HIP condition showed dense inclusions less than 0.030 inch diameter and areas of low density. The latter type of defect was thought to be surface type defects. The examination of the film for the fully machined condition showed a decrease in a number of inclusions; in addition, the areas of low density were eliminated. No other abnormalities which would hinder performance were detected.

The parts were routinely inspected after machining using penetrant per MCAIR specification P.S. 21202, Class L. This class permits rounded indications, however, no linear indications are acceptable. All parts passed this penetrant inspection.

#### 3.1.4.3 Summary of NDI of Trial Shapes

It has been determined that X-ray inspection is not particularly suitable for non-destructive inspection of HIP shapes. Seams, laps, indentations, etc. on the as-HIP surface of both the sub-scale stub shaft and the keel splice former showed up as defects that were essentially eliminated with surface treatment. Harperizing improved surface, but not all as-HIP defects were removed. Machining of the keel splice eliminated most inclusion-type defects and areas of low density.

The HIP Ti-17 stub shaft can be ultrasonically inspected to the required specifications. The keel splice former parts passed both radiographic and penetrant inspection, after machining, to MCAIR quality specifications.

#### 3.1.4.4 Preliminary Specifications

Based on the results of the Phase I effort on the Ti-17 alloy and the shape evaluation of the sub-scale stub shaft, preliminary specifications were prepared for use in the Phase II effort.

Similarly, based on the results of the Phase I effort on the Ti-6-4 alloy and the keel splice former, preliminary specifications were prepared for use in the Phase II effort.

The preliminary specifications were included in the appendices of the fourth interim report on this contract, and covered material and processing areas for 1) Prealloyed Titanium Powder, 2) "Hot Isostatic Pressing (HIP) of Titanium Alloy Powder", 3) "Premium Quality Powder Metallurgy As-Hot Isostatic Pressed (HIP) Ti-17 Titanium Base Alloy Parts", and 4) "Premium Quality Powder Metallurgy As-Hot Isostatic Pressed (HIP) Ti-6-4 Titanium Base Alloy Parts".

### 3.2 PHASE II - COMPONENT DEVELOPMENT

#### 3.2.1 Task I - Engine Stub Shaft Evaluation

Based on the results of the Phase I effort, additional investigation was planned to identify the source of non-metallic inclusions in pre-alloyed titanium powder. New titanium powder was necessary for the Phase II effort and particular pains were taken to incorporate the most favorable atomization and handling conditions. Test samples of the resultant powder were consolidated under varying conditions in order to evaluate the effect on LCF properties. These steps were investigated prior to the application of powder to the manufacture of full-scale stub shafts.

##### 3.2.1.1 New Ti-17 Powder Production

Nuclear Metals initiated a new run of Ti-17 powder with emphasis on powder cleanliness. The powder was made in the REP #2 machine which was modified to remove all ceramic materials from the machine except for the sight ports. The sight port portion of the machine was moved out ~8" by welding in an extension section. The extension moved the sight ports further from the arc zone and powder path. In addition, Lexan plastic shields were placed between the arc zone and the sight ports so that any powder entering the extension would strike the plastic and not the silica (quartz) sight ports. The electrical insulation in the machine have either been removed by re-design, or replaced with an organic (plastic) material which would decompose to carbon, hydrogen, and oxygen and, it is presumed, would be less harmful



than the glassy ceramic materials which have been found to reduce the fatigue properties of Ti-17. A summary of Powder Lot 4280 Characterization is given in Table 46.

The major portion of powder was allowed to collect in the stainless steel transfer canister affixed to the bottom of the REP chamber. Once the powder was cooled, the canister was detached from its O-ring seal and all further processing, i.e., crushing of the sintercake, screening to -35 mesh, magnetic separation, and sample splitting took place in air.

TABLE 46

SUMMARY OF Ti-17 POWDER  
CHARACTERIZATION (LOT 4280)

Size Distribution	Vendor	CMRC
-35, +45 mesh	7.63%	10.90%
-45, +60	17.59%	15.7%
-60, +80	30.40%	50.2%
-80, +120	28.81%	
-120, +170	10.60%	22.6%
-170, +230	3.57%	
-230, +325	1.09%	0.6%
Pan	0.31%	
Apparent Density	2.66 g/cc	2.66 g/cc
Tap Density	3.33 g/cc	2.92 g/cc
Flow Rate - 50 gms *	50.0 sec	31.5 sec

\*(0.1" Hall)

The chamber was cleaned after the stainless steel canister was removed and a 4-liter Erlenmeyer flask was attached to the chamber bottom, through use of a special adapter plate. The last three electrodes were then converted to powder, which was removed from the chamber under helium. The flask was transferred to a glovebox, which was evacuated and back filled with argon, after which the powder was removed from the flask, screened to -35 mesh, and distributed into containers as follows:

- 1) Two steel cans via evacuation tubes for HIP.
- 2) One steel can for extrusion to rod.
- 3) One polyethylene bag for HIP in ceramic mold.

All containers were sealed after inert/vacuum handling and shipped to CMRC.

#### 3.2.1.2 Additional LCF Investigations Through HIP Parameters

In order to assess the quality and nature of inclusions, if any, in the most recent lot of REP Ti-17 powder (Lot 4280), a series of tests were conducted according to the following plan:

- 1) NMI would inert/vacuum handle two (2) samples of the additional Ti-17 powder to be made for Phase II of the contract. Each sample should be at least five (5) pounds. One sample would be loaded into a steel can, the other into a ceramic mold. NMI would load and seal the steel can while the other sample would be provided to CMRC for inert/vacuum handling and loading of the ceramic mold. Both compacts would be HIP consolidated at the established 1650°F HIP cycle.
- 2) A sample of the new powder would be handled by conventional methods, loaded into a steel can and HIP at 1650°F.
- 3) A sample of the new powder would be handled by conventional methods, loaded into a ceramic mold and HIP at 1650°F.
- 4) The Ti-17 powder "swirls" used to clean and to verify the cleanliness of the ceramic molds would be retained and when a sufficient quantity had been accumulated, loaded in a steel can and HIP at 1650°F.

- 5) The HIP compacts would be cut in half, CMRC would retain one half and provide the other half to AFML for microstructural examination and machining of LCF specimens. A minimum of five (5) specimens would be machined from each compact and provided to CMRC for LCF testing. Test conditions would be the same as used for all previous tests, i.e.  $R=0.1$ , 1800 cpm. Two (2) specimens of each type would be tested at 140 ksi stress. Stress levels for further tests would be determined after examining the results of the initial tests. Also, all fractures would be examined to determine origin of failure using fractographic analysis, SEM, microprobe and metallographic techniques, as required.
- 6) In addition to the above, CMRC would provide AMFL, with two (2) pound samples of each of the first two (2) lots of Ti-17 powder produced by NMI and a two (2) pound sample of the powder to be produced for completing the work in Phase II. This powder would be characterized using the AFML swage tube evaluation technique. Also, CMRC would provide to AFML all of the fractured LCF specimens used to generate the data and each specimen would be identified as to its fatigue life and processing history. AFML would examine each specimen in detail and determine whether any modification of thermal treatments to get improved microstructure of the HIP product is necessary.

The test specimens were HIP at Battelle in the large autoclave system (LAS). The processing conditions are shown in Table 47. Nuclear Metals, CMRC, and AFML processed the materials, AFML heat-treated the material and machined LCF specimens and General Electric performed the LCF tests. As received by General Electric, the specimens were identified only as shown in Table 48 by specimen number, the code identification in Table 47 was revealed by AFML only after testing was completed.

The LCF test results and remarks regarding LCF fatigue origin, appearance and location are given in Table 48. One specimen of each group was also examined metallographically at General Electric after test.

TABLE 47

## IDENTIFICATION OF SPECIALLY HANDLED Ti-17 COMPACTS

<u>SERIES CODE*</u>	<u>PROCESSING PROCEDURE</u>
A	Nuclear Metals inert/vacuum handle, Phase II powder, steel can, beta HIP.
B	Conventionally handle, steel can, beta HIP.
C	Conventionally handle, ceramic can, beta HIP.
D	AFML swage, Phase I powder.
E	AFML swage, Phase II powder.
F	CMRC "swirls", steel can, beta HIP.
G	AFML swage, Phase IA powder.

<u>* Code</u>	<u>Crucible Identification</u>
A	533-51A, -51B
B	533-47
C	SM-542
F	533-49



TABLE 48

## T1-17 HIP EXPERIMENT - LOW-CYCLE FATIGUE RESULTS

A=0.95, F=30 CPM  $K_T=1$ 

Spec. No.	STRESS		CYCLES TO FAILURE	FATIGUE ORIGIN LOCATION	FRACTURE LOCATION IN GAGE	"BULLS-EYE" DEFECT @ ORIGIN
	MAX (KSI)	MEAN (KSI)				
A1	140	71.8	68.2	Internal	Off Center	Yes
A2	130	66.7	63.3	Internal	Off Center	Yes (2)
A3	120	61.5	58.5	Internal	Off Center	Yes
A4	110	56.4	53.6	Run-out	-	-
B1	140	71.8	68.2	Internal	Off Center	Yes
B2	130	66.7	63.3	Internal	At Center	Yes
B3	120	61.5	58.5	Surface	Off Center	No
B4	110	56.4	53.6	Surface	Off Center	No
C1	110	56.4	53.6	Sub-Surface	At Center	Yes
C2	120	61.5	58.5	Near Surface	Off Center	Small one
C3	100	51.3	48.7	Not Detectable	At Center	No
C4	90	46.2	43.8	Near Surface	Off Center	No
D1	140	71.8	68.2	Surface	At Center	No
D2	130	66.7	63.3	Surface	Off Center	No
D3	120	61.5	58.5	Surface	Off Center	Yes (Small)
D4	110	56.4	53.6	Run-out	-	-
E1	125	----	----	To Be Run	-	-
E2	110	56.4	53.6	Near Surface	Near Center	No
E3	120	61.5	58.5	Run-out	-	-
E4	150	76.9	73.1	Sub-Surface	Off Center	Yes (Small)
F1	140	71.8	68.2	Internal	At Center	Yes
F2	130	66.7	63.3	Near Surface	Far Off Center	No
F3	120	61.5	58.5	Near Surface	Off Center	No
F4	110	56.4	53.6	Run-out	-	-
G1	140	71.8	68.2	Surface	Center	No
G2	130	66.7	63.3	Sub-Surface	Far Off Center	Yes
G3	120	61.5	58.5	Run-out	-	-
G4	150	76.9	73.1	Surface	Off Center	No

Although no SEM work was conducted on these specimens, the "bulls-eye" fracture appearance noted in Table 48 has previously been indicative of the presence of foreign material inclusions at the fatigue origin. Eylon and Birla<sup>8</sup> indicated that inclusions of the type found in the present work were also present at fatigue origins in solution treated and aged powder metallurgy Beta III alloy compacts made with REP powder. Their data indicated that smooth fatigue specimens with lower life had sub-surface initiation sites with traces of SiO<sub>2</sub> as well as other non-metallic inclusions. They observed there may be several sources by which a powder may be contaminated with SiO<sub>2</sub> particles (ceramic electrical insulator, ceramic bricks, quartz viewing ports or machine shop dust), and at this stage the origin is not yet clear. Also, their fatigue failure analysis showed that although REP titanium powders may be clean enough from non-metallic inclusions to provide good tensile and fracture toughness properties, they still may have sufficient inclusions to reduce the smooth high cycle fatigue life. Therefore, more careful powder production and powder handling procedures may be necessary in order to maintain fatigue life of the alloy. This tends to confirm that such inclusions are detrimental to the high strength solution treated and aged titanium alloys but are relatively innocuous in the lower strength alloys similar to annealed Ti-6Al-4V.

The data of Table 48 are plotted in Figures 80 and 81. Figure 82 shows earlier data on various HIP compacts and sub-scale stub shafts produced by CMRC. Data for cast and wrought Ti-6Al-4V and for the Ti-17 bar stock used to produce the powder for this program are shown for comparison. All of the Ti-17 materials were in the solution treated and aged condition, the Ti-6Al-4V data are for annealed material.

None of the various processing conditions produced LCF behavior as good as cast and wrought material. The "C" series was incompletely consolidated as evidenced by porosity in the metallographic specimen. This was in the HIP run which had problems at BCL. The "C" series also had the poorest LCF behavior, falling well below the Ti-6Al-4V data. The AFML swaged materials exhibited considerable scatter in results. The overall results from the test series indicate that handling procedures, outside of the powder production and processing step do not have a serious effect on LCF behavior. However, inclusions from the

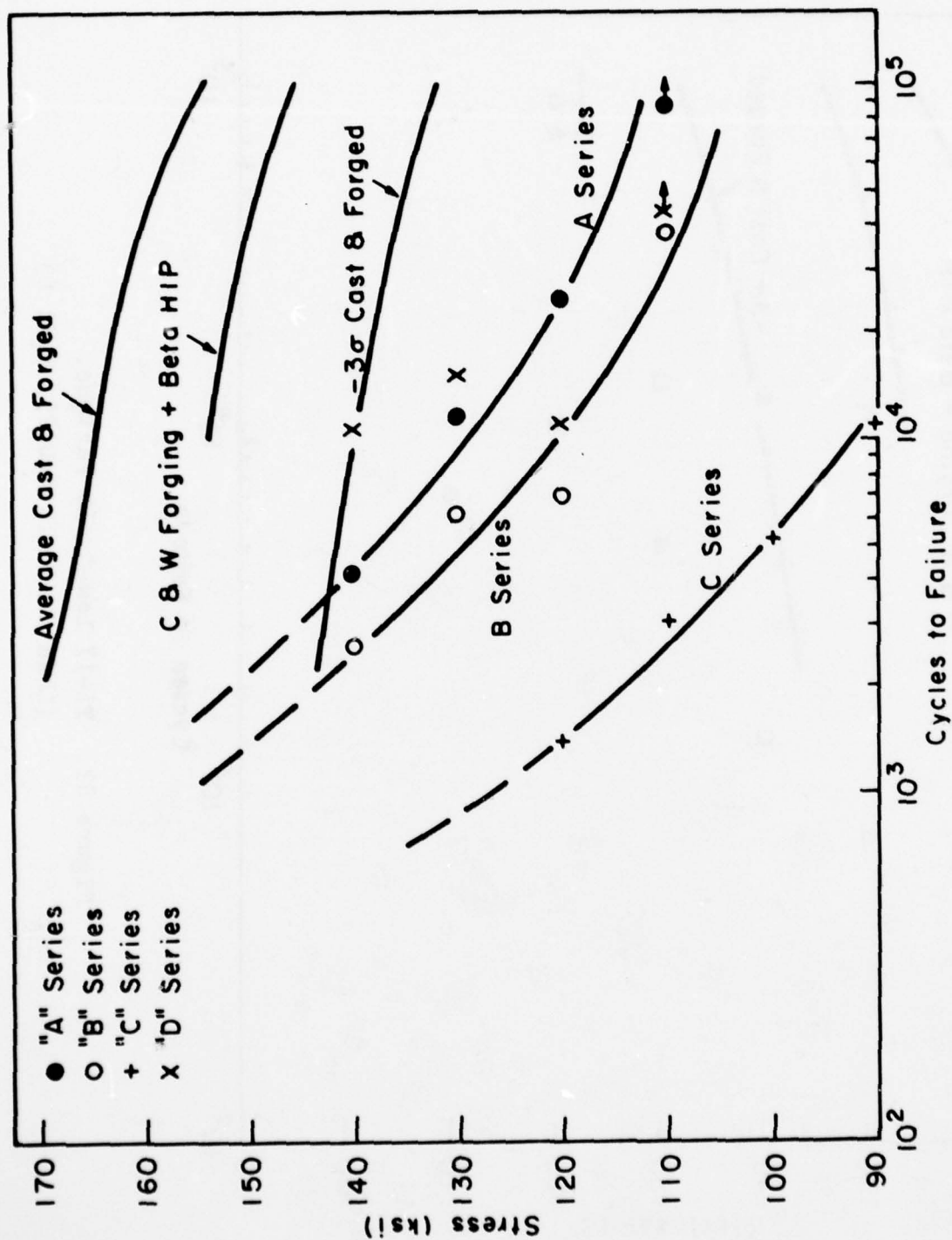


Figure 80. Ti-17 Low-Cycle Fatigue.  
(Load Control,  $A=0.95$ ,  $K_t=1.0$ )

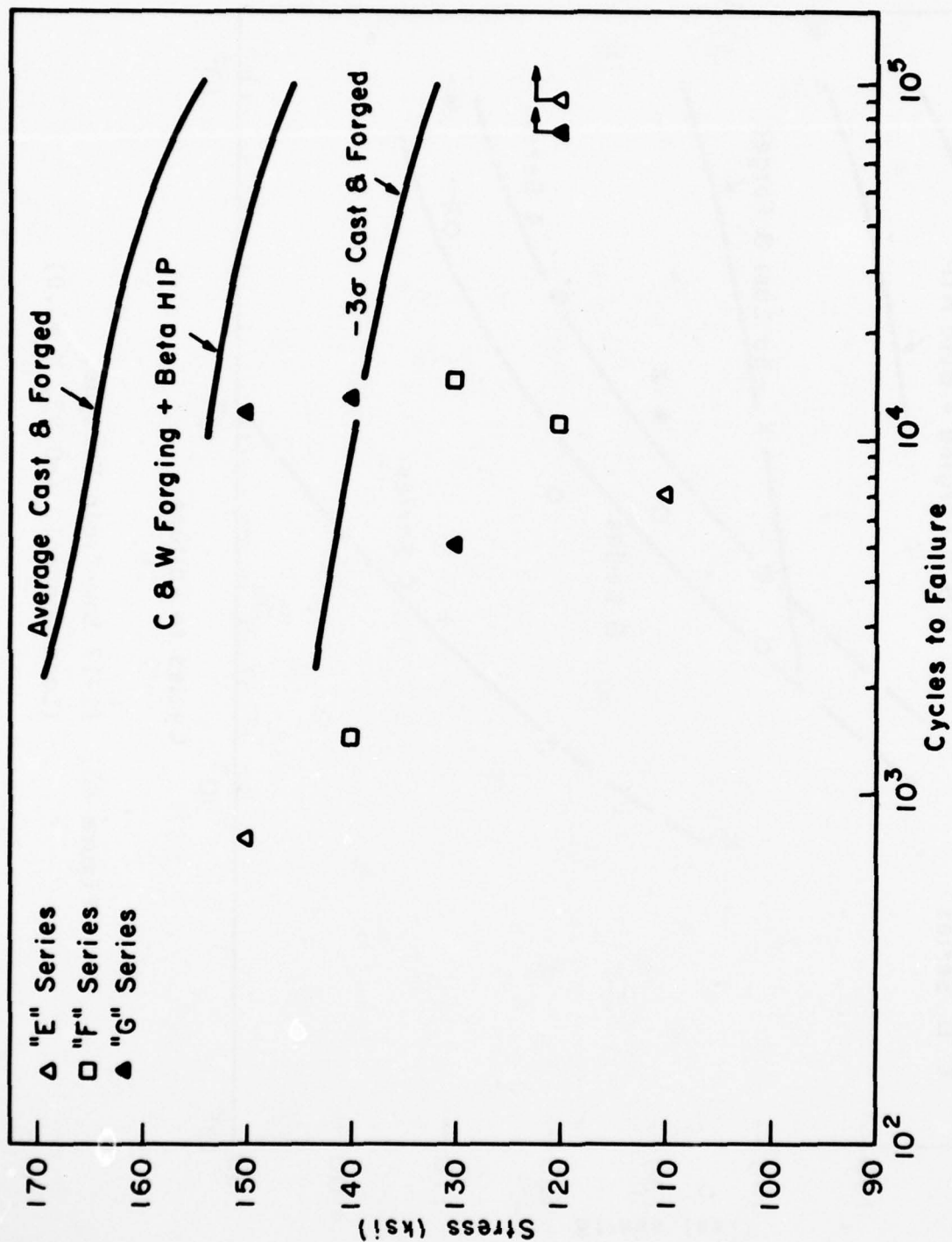


Figure 81. Ti-17 Low-Cycle Fatigue.  
(Load Control,  $A=0.95$ ,  $K_t=1.0$ )



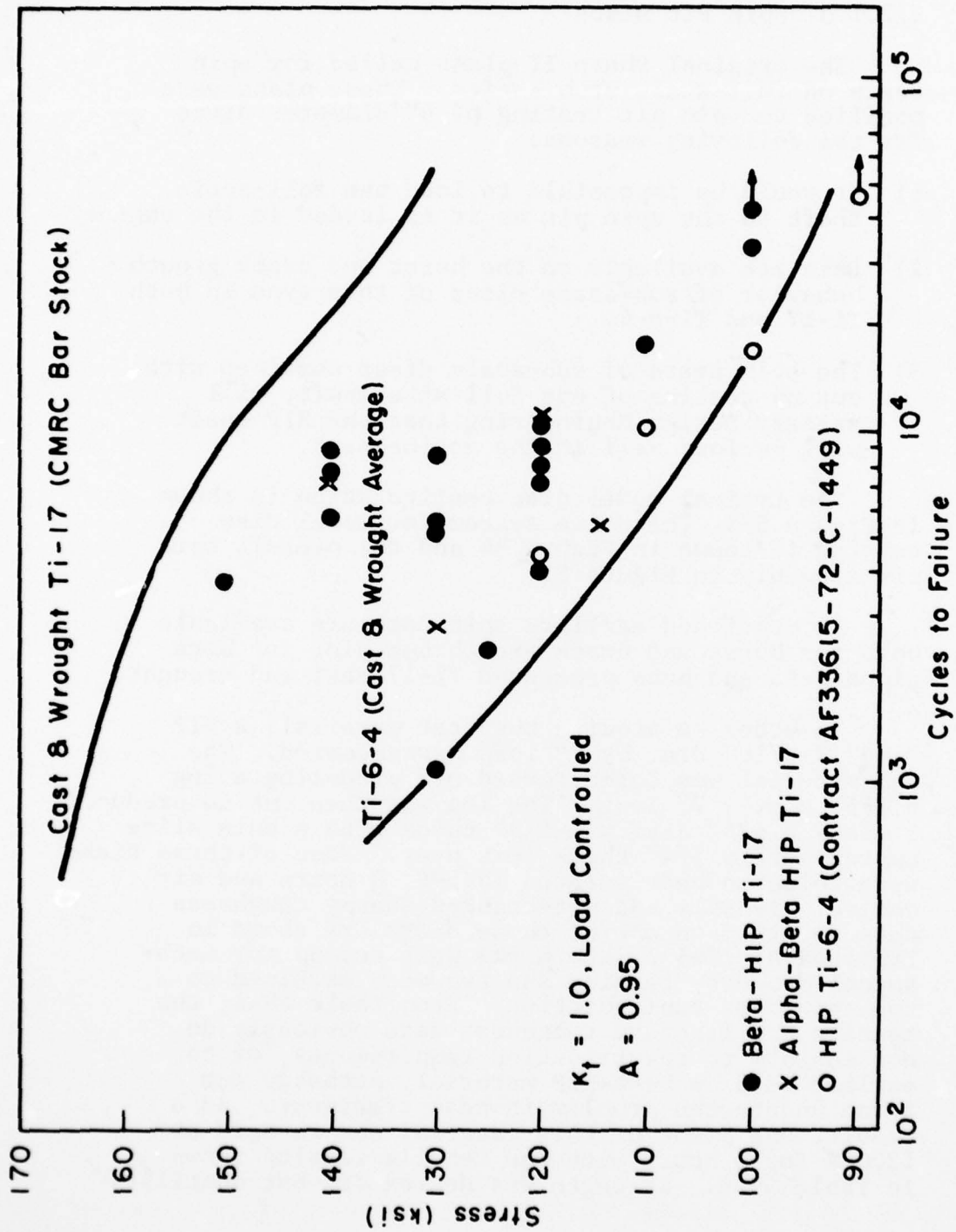


Figure 82. LCF Comparison.

powder processing are still present and detrimental to LCF results.

### 3.2.1.3 Spin Pit Discs

The original Phase II plans called for spin tests on full-scale stub shafts. These plans were modified to spin pit testing of 6" diameter discs for the following reasons:

- 1) It would be impossible to load the full-scale shaft in the spin pit as it is loaded in the engine.
- 2) Data are available on the burst and crack growth behavior of sub-scale discs of this type in both Ti-17 and Ti-6-4.
- 3) The spin tests of sub-scale discs combined with cut up testing of one full size shaft, will satisfy Design Engineering that the HIP shaft will perform well in the engine test.

The typical model disc configuration is shown in Figure 83. The drive system for model disc testing is shown in Figure 84 and the overall spin pit assembly in Figure 85.

As mentioned earlier, spin data are available both for burst and crack growth behavior for both alpha-beta and beta processed Ti-17 cast and wrought.

In order to acquire the test material, a HIP "log" 7-5/16" dia. by 7" long was prepared. The can material was lathe turned off producing a log 6.675" dia. x 7" long. The log was then cut to produce 5 disks 6.675" dia. x 1-1/8" thick with a thin slice approximately 3/4" thick left over. Four of these disks were solution heat treated 1475°F, 8 hours and air cooled. Tensile and pre-cracked Charpy toughness data obtained on one of these disks are shown in Table 49-A. Two of the disks were cut up for mechanical property testing and two were machined to the spin disk configuration. From Table 49-A, the tensile and fracture toughness data obviously do not conform to specification requirements, or to earlier data on beta-HIP material, probably due to an undetected problem in heat treatment. As a result, one piece of this material was re-aged at 1200°F for 8 hours with the tensile results shown in Table 49-B. Strength was decreased, but ductility

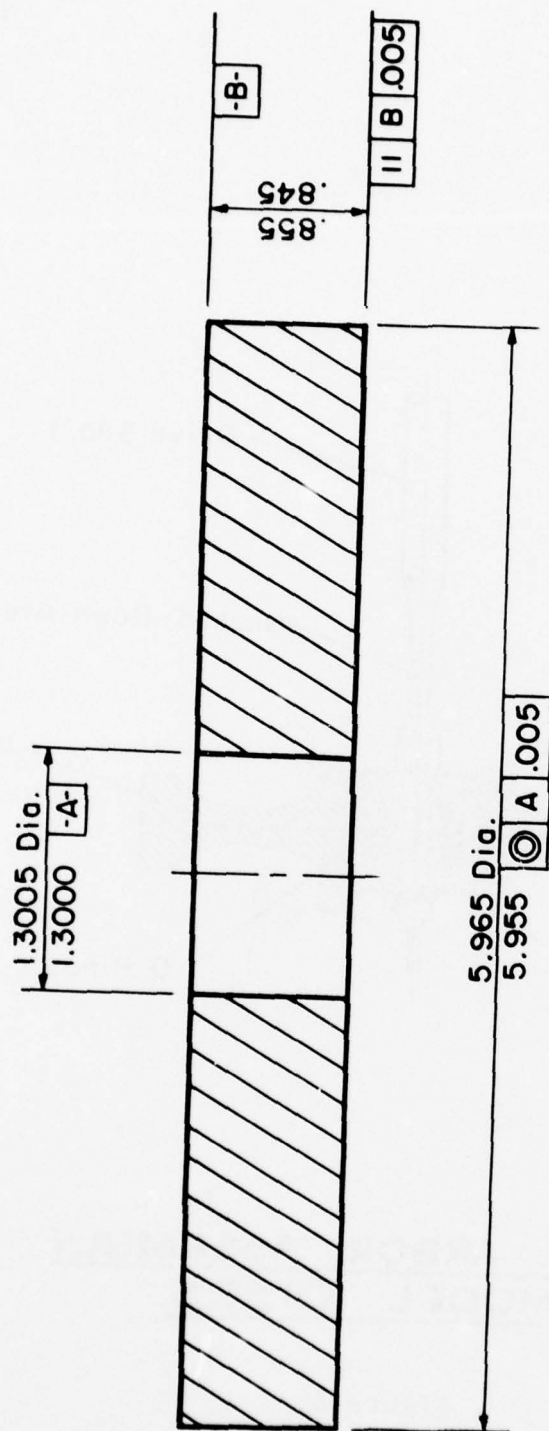
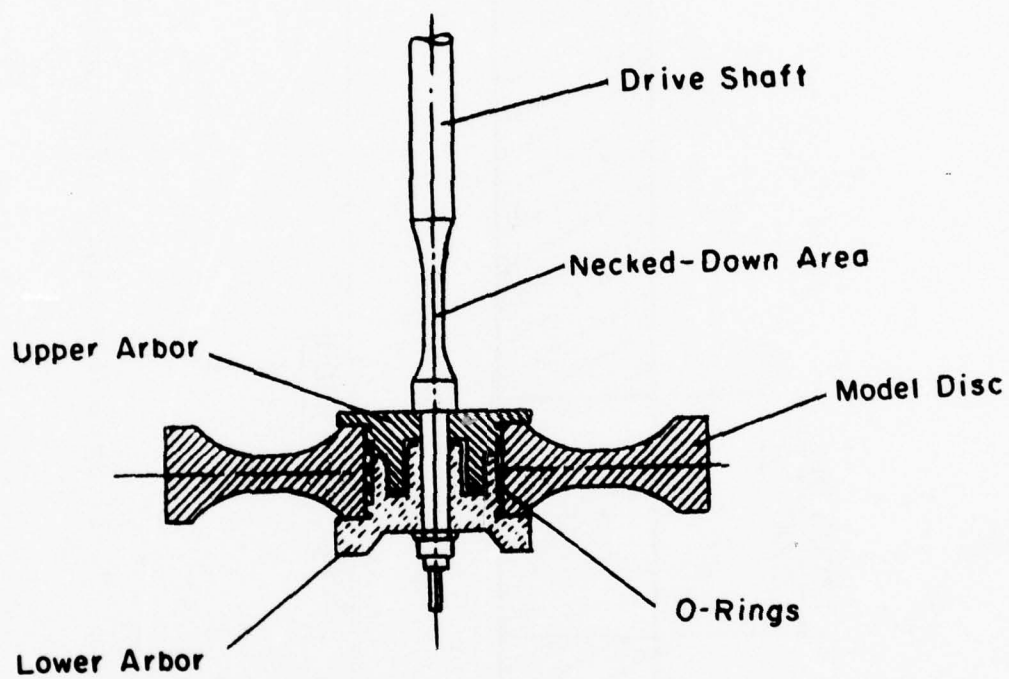


Figure 83. Ti-17 Spin Test Disc Configuration.



**DRIVE ARBOR ASSEMBLY**  
**FOR MODEL DISCS.**

Figure 84



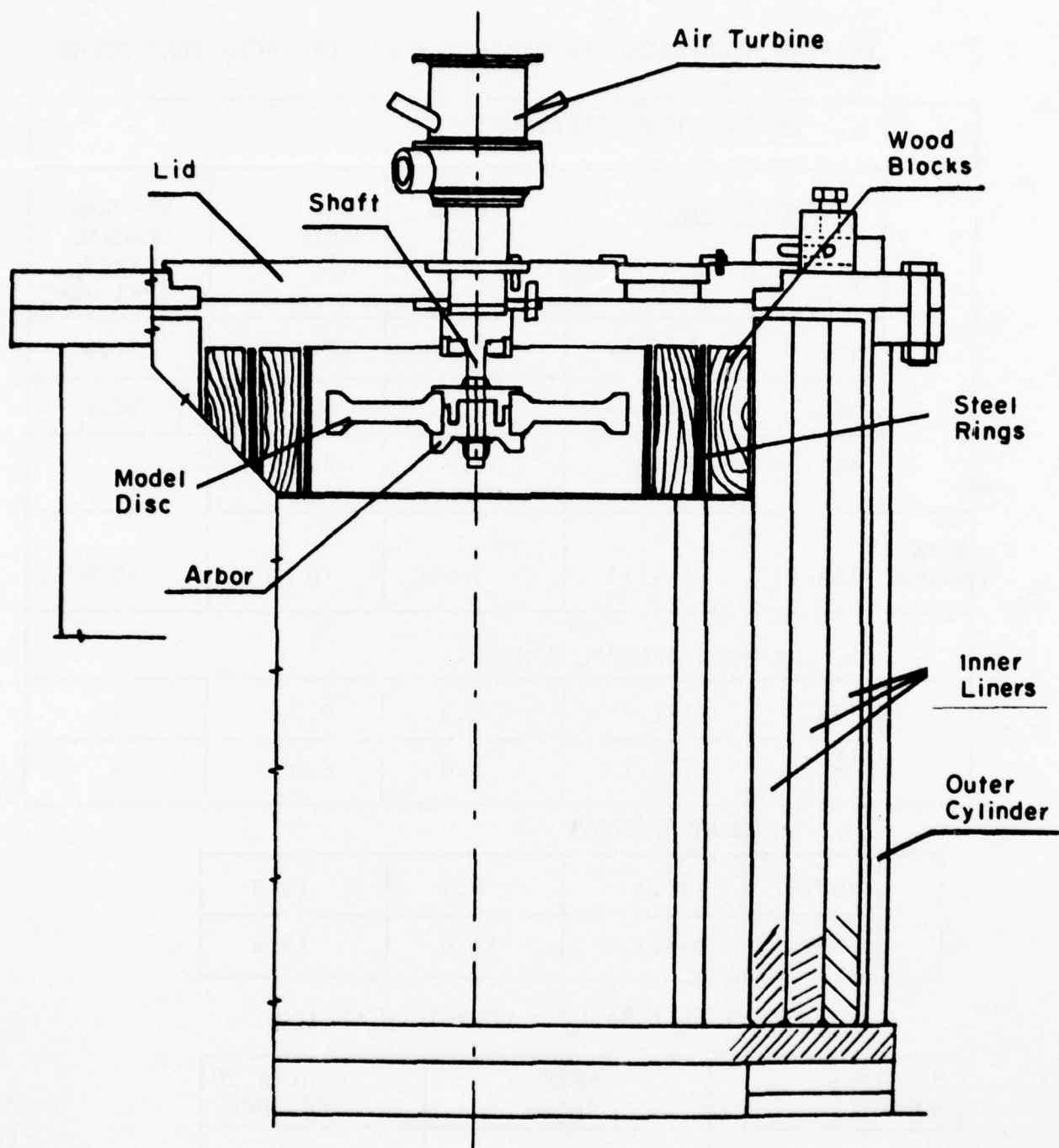


Figure 85. Cross Sectional View of Spin Pit.

TABLE 49

## INITIAL MECHANICAL PROPERTIES - 6" DIA. SPIN TEST DISCS

A. INITIAL HEAT TREATMENT					
	STRENGTH (ksi)		ELONG (%)	RED AREA (%)	Kc-PRE-CRACKED CHARPY (ksi $\sqrt{\text{in}}$ )
	F <sub>tu</sub>	F <sub>ty</sub>			
	187.5	181.9			
	185.5	180.0			
	186.9	180.9			
SPEC RANGE	163-183	153-173	5 MIN.	10 MIN.	50 MIN.
B. RE-AGED 1200°F, 8 HOURS					
	177.8	172.7	6.3	9.3	-
	180.0	172.1	5.0	8.0	-

C. RE-HEAT TREATED				
	163.9	159.3	9.5	16.0
	164.1	158.7	11.0	15.4

## D. RE-HEAT TREATED - LOW-CYCLE FATIGUE

SPECIMEN SOURCE	STRESS (ksi)	CYCLES TO FAILURE
Spin-Pit Disc	140	4,531
	130	6,397
	120	14,998
	110	32,154

was still lower than desired. Another piece of this material was given a complete re-solution treatment at 1475°F, water quenched and aged 1175°F, 8 hours with the results shown in Table 49-C. Strength was within specification limits, and ductility was improved over the earlier results. Metallographic examination of the first material indicated that the solution temperature was probably about 50°F too high, since very little primary acicular alpha was present, resulting in high strength and low ductility. The fully re-heat treated material had the expected microstructure and strength level. The low cycle fatigue specimens from the first discs were fully re-heat treated and tested with the results given in Table 49-D. The cyclic life of the spin pit disc specimens was about the same as obtained previously on the sub-scale stub shafts. The crack growth data from the compact tension specimens of the re-heat treated disc were analyzed with results indicating somewhat more rapid crack growth rates than for cast and wrought Ti-17. The  $K_{Ic}$  specimen from this disc indicated a value of 43.7 ksi  $\sqrt{\text{in}}$  which is below the 50 ksi  $\sqrt{\text{in}}$  minimum for cast and wrought beta processed Ti-17.

In view of these results, the spare disc was heat treated correctly and machined to spin disc configuration. There were, therefore, two spin discs in the high strength condition and one with strength properties within specification limits. It was decided to spin test all three discs. The high strength discs could not be re-heat treated, since they were in the finish machined condition and the dimensional tolerances were very tight. The spin test procedures and results are given as follows:

Preparation of Disc Specimens - The material was subjected to a complete ultrasonic and X-ray inspection. After machining to the desired shape, the discs were given a thorough dimensional check, critical areas such as the bore and rim dimensions were recorded.

The drive arbor was then assembled to the disc together with a special shaft for use in the dynamic balance machine and a very careful balance was made. It has been found that a close tolerance on the level of imbalance is essential to obtaining a successful high speed test free from vibration problems.

Preparation of Spin Pit Facilities - The drive arbor mechanism used for these spin pit tests is made in two parts, both of which are clamped by the lower part of the drive shaft. Provision is made to disassemble the two parts should it become necessary during the build-up. The drive mechanism is linked to the disk by a series of O-rings contained in the cavity formed between the arbor and the disk bore.

The drive shaft has a necked-down region adjacent to the arbor to ensure that should a vibration or instability problem occur, the shaft will fail in this area and thereby prevent damage to the drive turbine bearings.

The spin pit is comprised of an outer cylinder lined with three separate inner cylinders to guard against penetration by the high energy fragments emanating from a burst disc. The pit contains a heavy lid to which a vertical air turbine is attached. Access to the pit is made by removing this lid. High pressure air is delivered to accelerate the drive turbine and also to decelerate after the test disc has burst. The turbine is capable of driving to 100,000 rpm with a maximum torque of 2.0 in. lb. The disc-arbor-shaft assembly is suspended vertically from the turbine.

The area surrounding the disc in the test configuration is lined with a device to help contain the burst fragments and thereby prevent secondary damage to the fragments.

If a fragment is permitted to reach the walls of the cylinder, considerable secondary damage would be sustained which would negate a post-test examination of the primary fracture surfaces. A means of eliminating this was found by placing a series of mild steel rings interspaced with wooden blocks in the space between the disc and pit wall. Penetration of the rings and compression of the wood is sufficient to minimize secondary damage.

At the commencement of the test, the lid is sealed and the pit evacuated down to approximately 7.0 torr. This is to prevent air friction causing changes in temperature in the disc and thereby influencing the burst speed.



Testing Procedures - Electromagnetic speed pickups are located in the turbine housing that permit several instruments to record the speed during the test. Because the speed measurement is the most critical part of the test, three separate and different instruments are used to record the RPM. Permanent recordings are made by a tape recorder and a Sanborne trace recorder. Also, the speed is displayed on two ATEC digital units and recorded visually.

The disc is driven by the air turbine, the rate of acceleration is controlled manually and not measured. However, an attempt is made to maintain a uniform rate of acceleration. The duration of the test is usually about 15 minutes and consists simply of accelerating the disc until burst occurs. Determination of the point of fragmentation is made from the loud report caused by the impact of fragments with the containment device. The exact point is established from the speed traces, and identified when rapid acceleration of the turbine is detected after the disc has been released.

When the test is complete, the fragments are removed for fractographic analysis. If the test results in disc instability and failure of the arbor, the disc is, of course, not fragmented. However, gross plastic deformation of the disc occurs in these cases and the RPM at the time of arbor failure is considered to be "incipient burst" speed.

Test Results - The spin pit test results are given in Table 50, along with data obtained on a previous program using cast and wrought material taken from F-101 engine disc forgings.

All three PM discs failed by fragmentation, while the two cast and wrought discs grew in size by plastic deformation and caused instability of the system, which caused the drive arbor to fail first. However, the burst speeds for the PM discs were, with the exception of disc (1), in the expected burst speed/stress range for their mechanical property level.

The disc fragments were examined by fractographic methods to determine the locus of fracture origins for the discs. Disc 1 was of particular interest, since it did fail at less than the expected burst speed of about 92,000 RPM. Flat discs of this type

TABLE 50

## SPIN PIT DISC TEST RESULTS

Data	Cast and Wrought Discs (1)		Beta-HIP Discs		
	$\alpha/\beta$ Forged	$\beta$ Forged	Disc 1	Disc 2	Disc 3
Material Type					
Burst Speed (RPM)	89,400	92,600	82,400	92,960	94,020
Type of Failure	Instability	Instability	Fragmented	Fragmented	Fragmented
Pseudo - Elastic Stress at Burst:					
$\sigma$ max.	282.0	301.5	233.6	297.3	304.0
$\sigma$ ave.	143.2	153.7	117.9	150.0	153.5
Material Properties:					
$F_{TU}$ (ksi)	170	175	186	186	164
$F_{TY}$ (ksi)	166	166	181	181	159
Elongation (%)	12	9	4.7	4.7	10
Red. Area (%)	35	20	9.5	9.5	16
Notch Strength Ratio	1.2	1.4	1.2	1.2	1.4
Fracture Toughness ( $K_{IC}$ )	35	55	(Est)(2) 28	(Est)(2) 28	(Est)(2) 44
Max. Bore Distortion	.0615	.0698	(3)	(3)	(3)
Max. Rim Distortion	.0609	.0239	(3)	(3)	(3)

Notes: (1) Data obtained earlier on M&PTL disc burst test program on discs of same design and test procedure as Contract HIP Discs. Test discs were machined from full scale F-101 engine rotor disc forgings.

(2) Notch tensile ratio is estimated from tensile properties, test not yet conducted.

(3) Disc fragmented, measurements not possible.

usually fail by instability and fracture of the drive arbor rather than by fragmentation, so fracture analysis of all three discs was of interest.

Photographs of the burst 6" diameter spin pit discs are shown in Figures 86, 87, and 88. Discs 2 and 3 burst at about the expected speed, but Disc 1 fractured at ~10% lower speed than Discs 2 and 3. Examination of the fracture surfaces indicated that the fracture origins for all three discs were near the bore, but slightly below the surface. Macro examination indicated that the fracture origins were at inclusion sites. Disc 1 appeared to have a larger void at the fracture origin as compared to discs 2 and 3. This is illustrated by the macro photograph in Figure 89. The arrow indicates the fracture origin with an apparent defect present.

The crack growth rate data for specimens taken from a disk heat treated in the same manner as spin test disc #3 are given in tabular form in Appendix D to this report. The data are shown graphically in Figure 90 which is a computer plot of all three crack growth tests. The 750°F and 600°F data fell within the same data scatter band. Figure 90 also shows a comparison of the HIP Ti-17 crack growth data with data for a cast and wrought beta processed forging. The reason for the poorer crack growth behavior of the HIP product is not known. However, high hydrogen content of the specific disc tested could adversely affect crack growth rate, since it is known to do so in other alloys.

AD-A078 039

COLT INDUSTRIES INC PITTSBURGH PA CRUCIBLE MATERIALS--ETC F/6 11/6  
CONSOLIDATION OF TITANIUM POWDER TO NEAR NET SHAPES.(U)

MAY 78 J H SCHWERTZ , V K CHANDHOK

F33615-74-C-5114

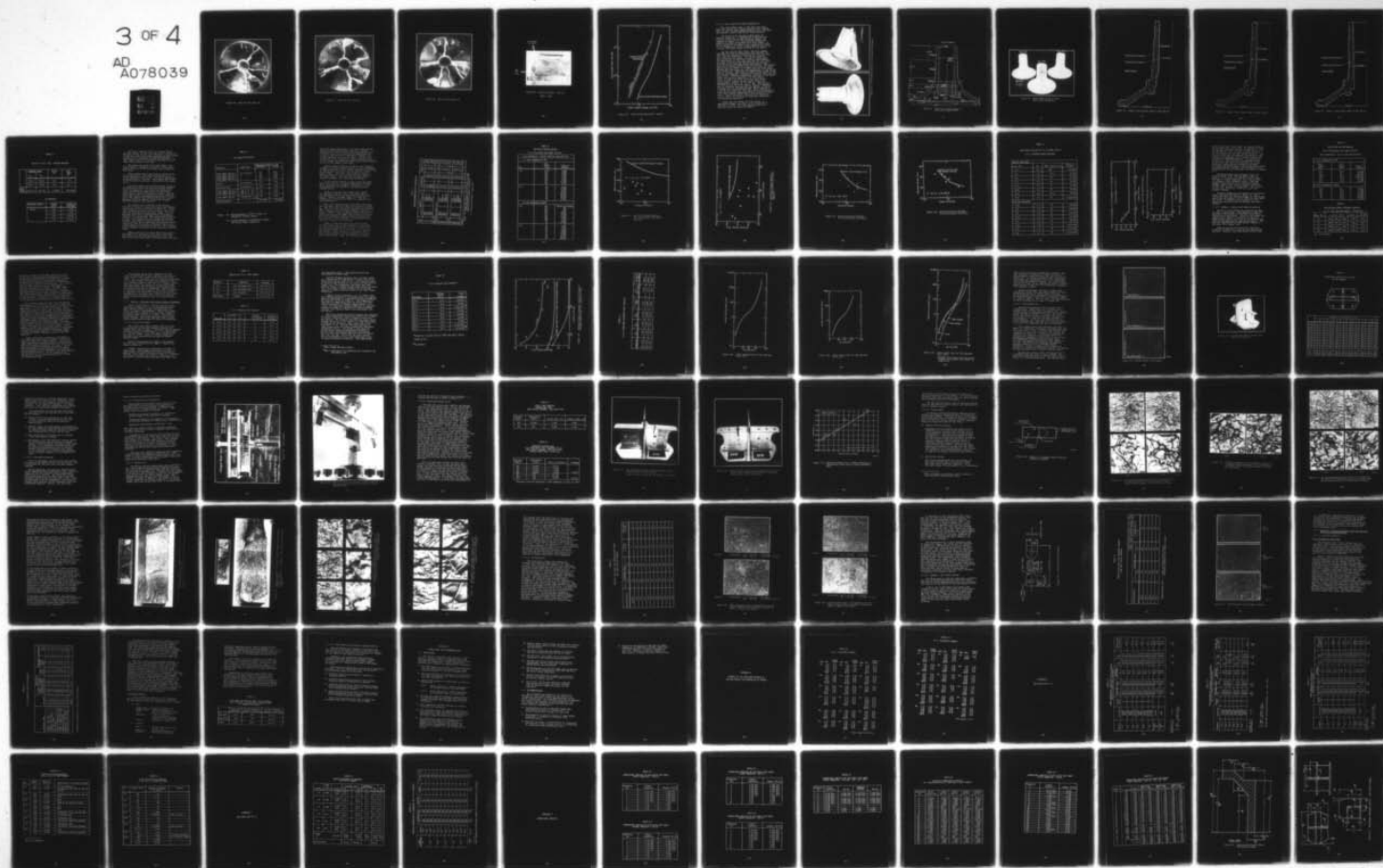
UNCLASSIFIED

AFML-TR-78-41

NL

3 OF 4

AD  
A078039





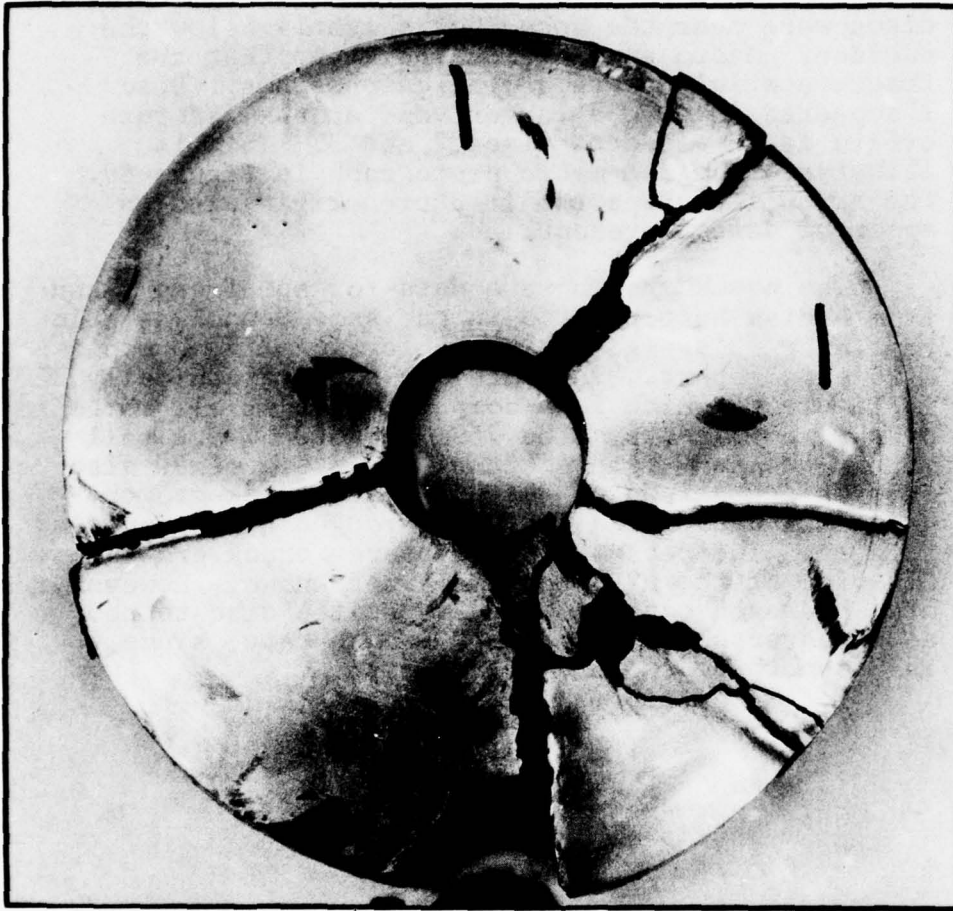


Figure 86. Spin Pit Test Disc #1.

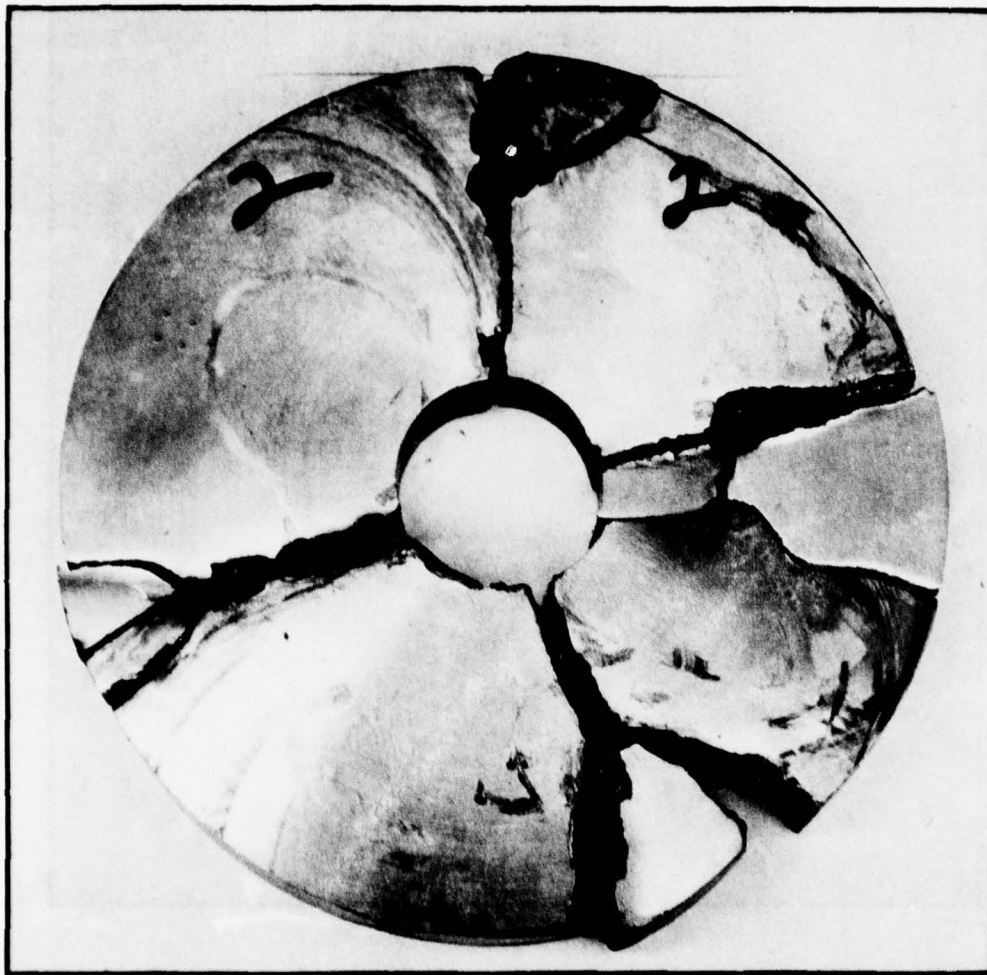


Figure 87. Spin Pit Test Disc #2.

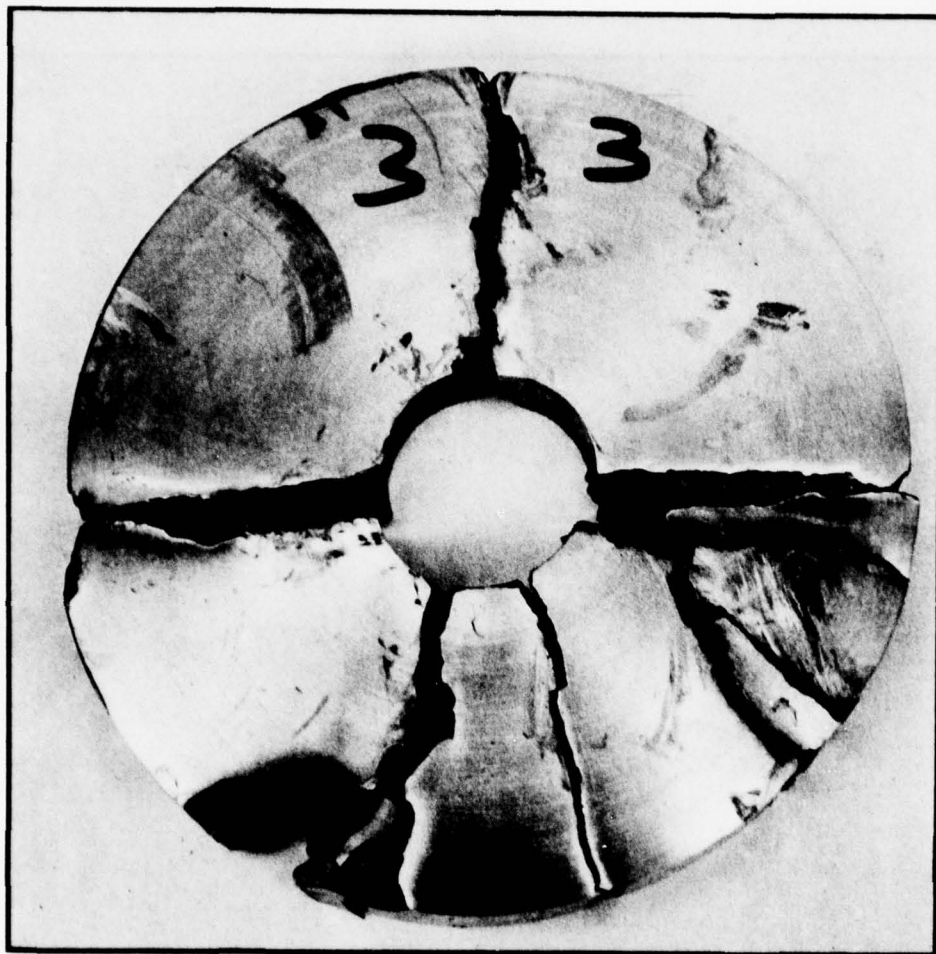


Figure 88. Spin Pit Test Disc #3.

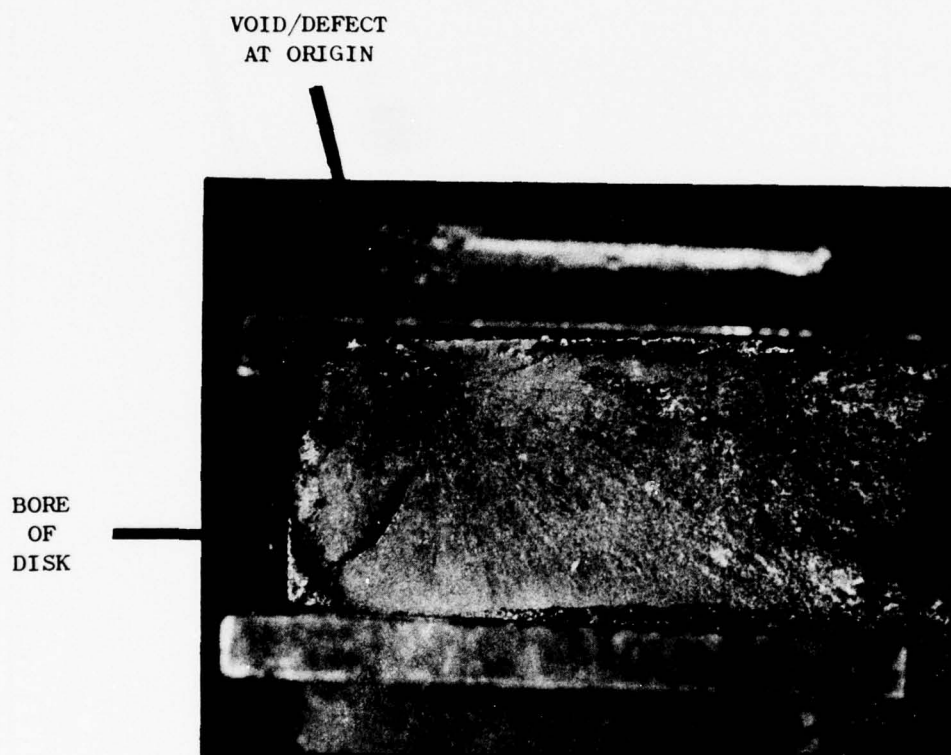


Figure 89. Fracture Origin - Disc #1.  
(Mag. 1.9X)



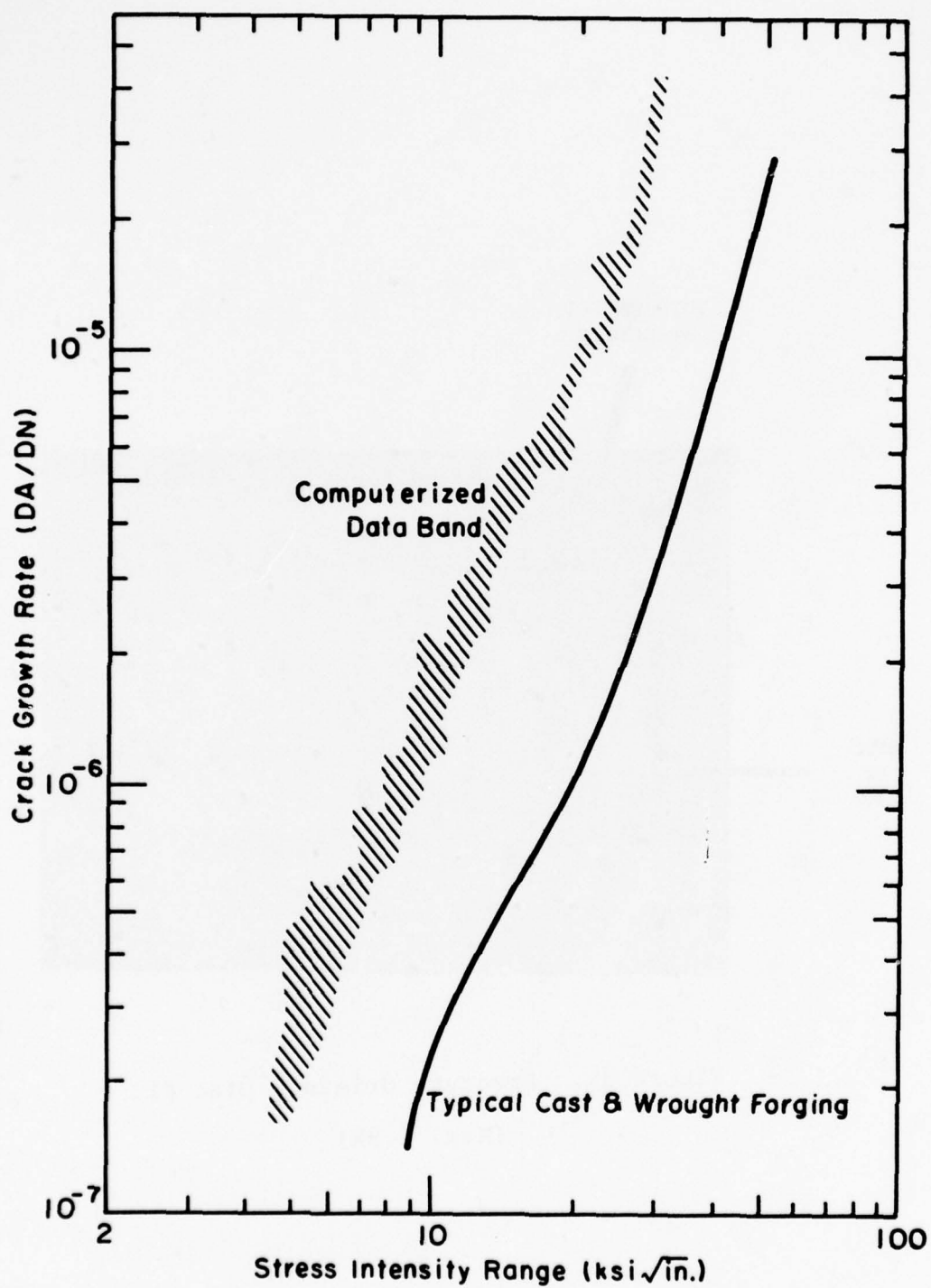


Figure 90. Crack Growth Rate Data - SM-557.

#### 3.2.1.4 Full Scale Stub Shaft Manufacture

The first shape trial on the full size stub shaft was carried out using remaining Ti-6-4 powder since it was for shape making purposes only, and alloy type wouldn't affect dimensional data generated.

Two views of the initial as-HIP shape are shown in Figure 91. A dimensional inspection was carried out and the actual and target shapes are compared in Figure 92. The complete dimensional analysis is given in Appendix D to this report. A minor correction was made to the starting mold shape in the flange area for the second shape iteration to overcome off-target shape as shown in the figure.

For the second shape trial, new Ti-17 powder from NMI was used in conjunction with material for test discs as requested previously for spin pit test discs and LCF evaluation. The second iteration was carried out to produce a total of three parts for application to the final contract requirements. The three (3) parts plus material for the test discs were HIP in the same LAS (large autoclave system) cycle as the trial compacts for LCF studies. The results showed the stub shafts in ceramic molds were not dense whereas the test discs in a metal can were fully dense. This problem was caused by low temperatures in the bottom zone of the LAS. The three (3) shafts were re-HIP in the LAS and metallographic examination revealed that they were fully dense. Detailed dimensional analyses of the three shafts are given in Appendix D to this report. Figure 93 shows the three full size stub shafts after re-HIP. Target versus actual shapes are summarized in Figures 94, 95, and 96. Note that P/N 9940 M50 is the F-101 shaft. This configuration will be obtained from part SM-556 readily. Careful indexing will be required for part SM-555 and SM-557 to obtain the final P/N 9940 M50. Since VSE cut-up tests on the final part were required for qualification stub shaft compact number SM-557 was chosen for these tests. SM-557 would have been the most difficult part to index for clean up to final part dimensions as observed in Figure 96.

Along with the three (3) stub shafts, an additional compact was HIPed in the re-HIP cycle. This was a 2" dia. x 8" long compact which gave tensile results as shown in Table 51.



Figure 91. First Shape Trial on Full-Sized Stub Shaft.

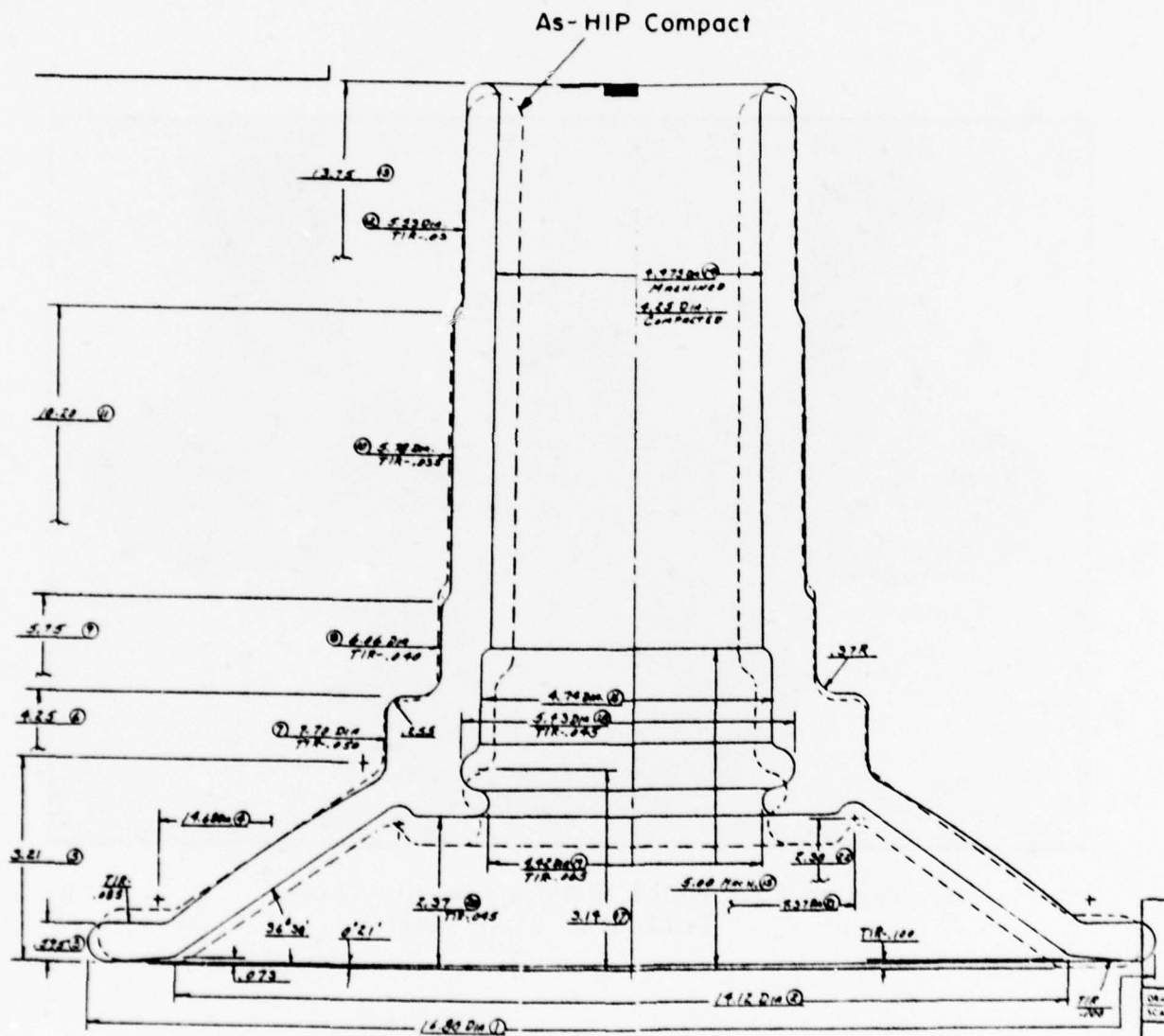


Figure 92. Actual versus target shape on stub shaft compact SM-494.



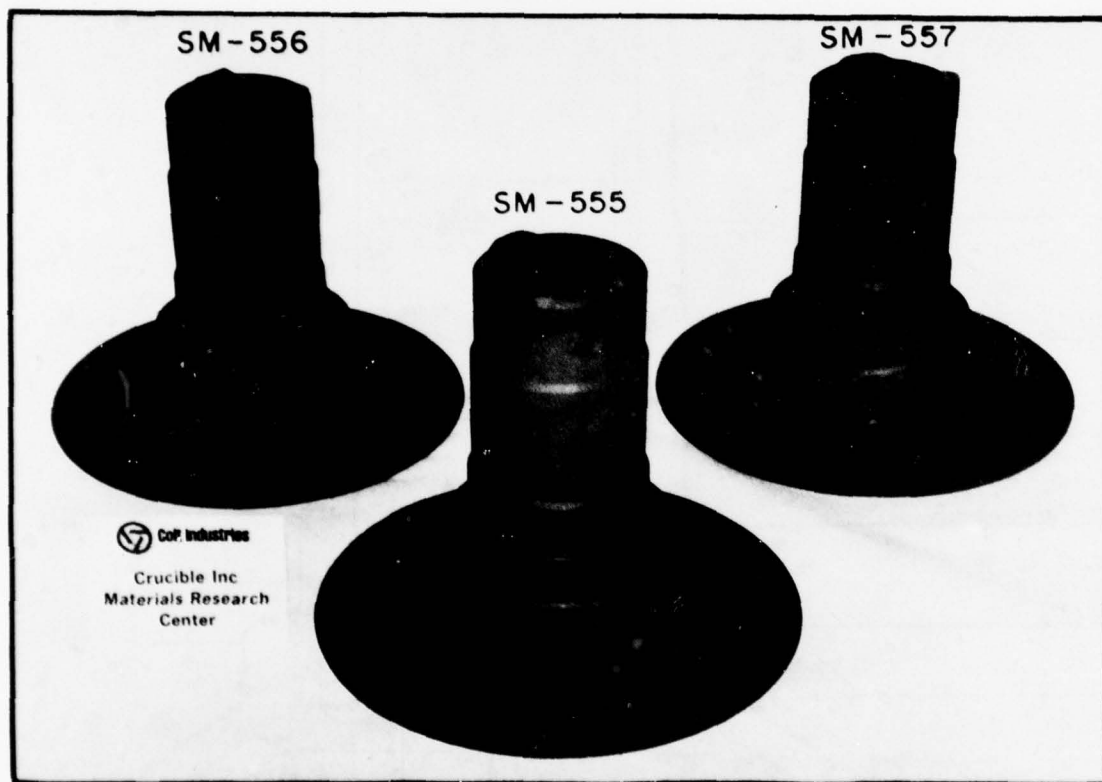


Figure 93. Final Shape Trial on Three Full-Size Stub Shafts.

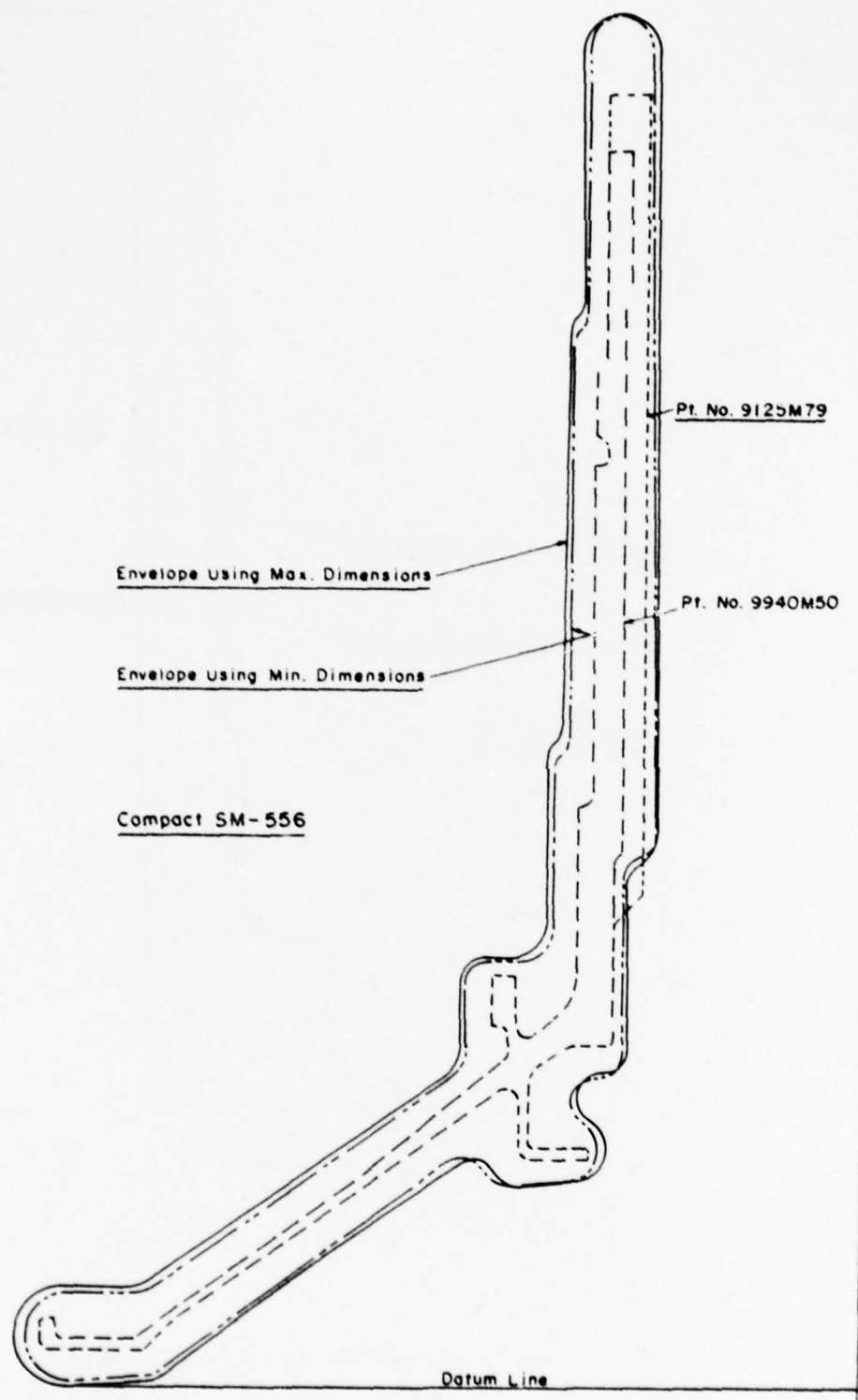


Figure 94. Target versus actual shape of Part SM-556.

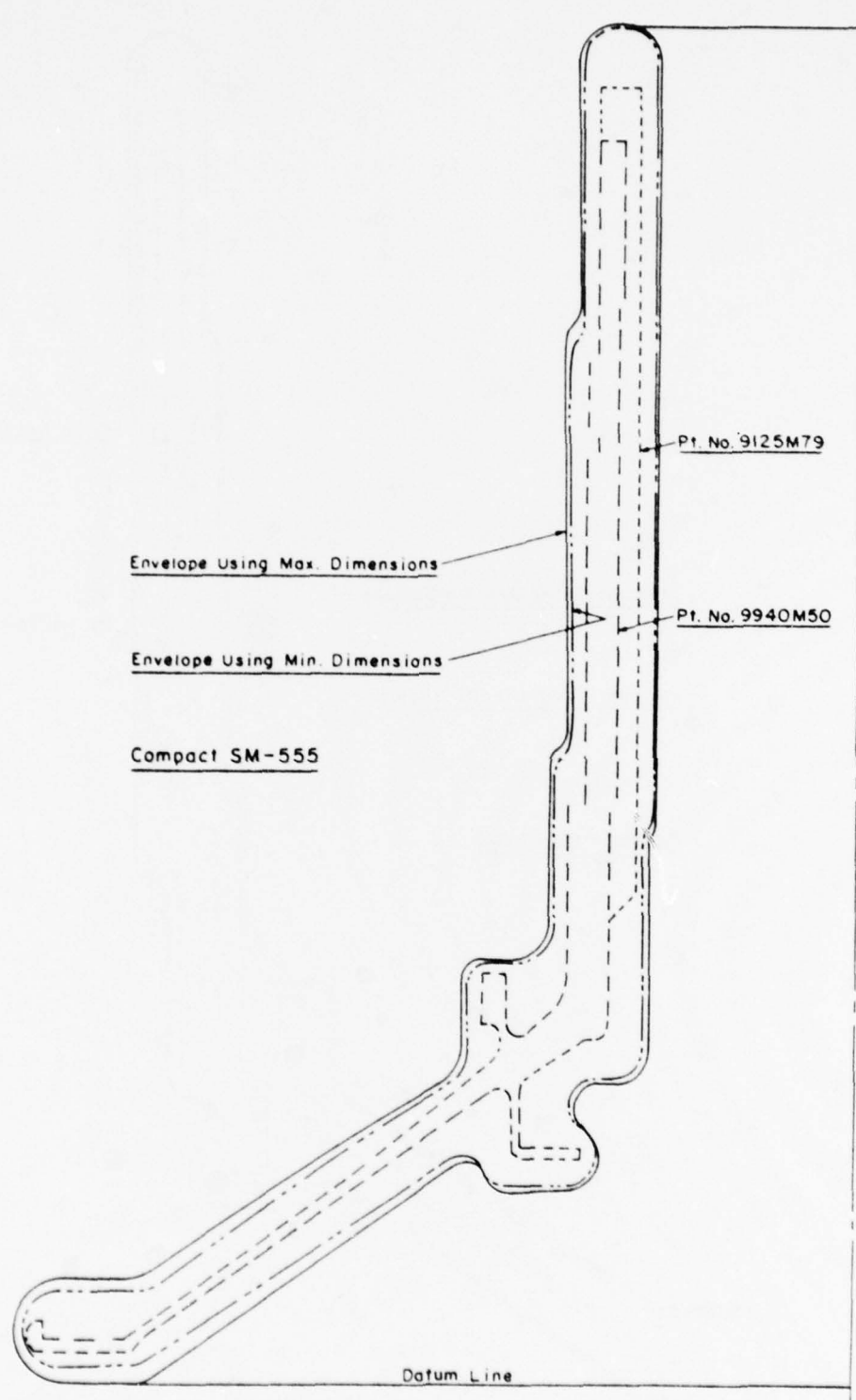


Figure 95. Target versus actual shape of Part SM-555.

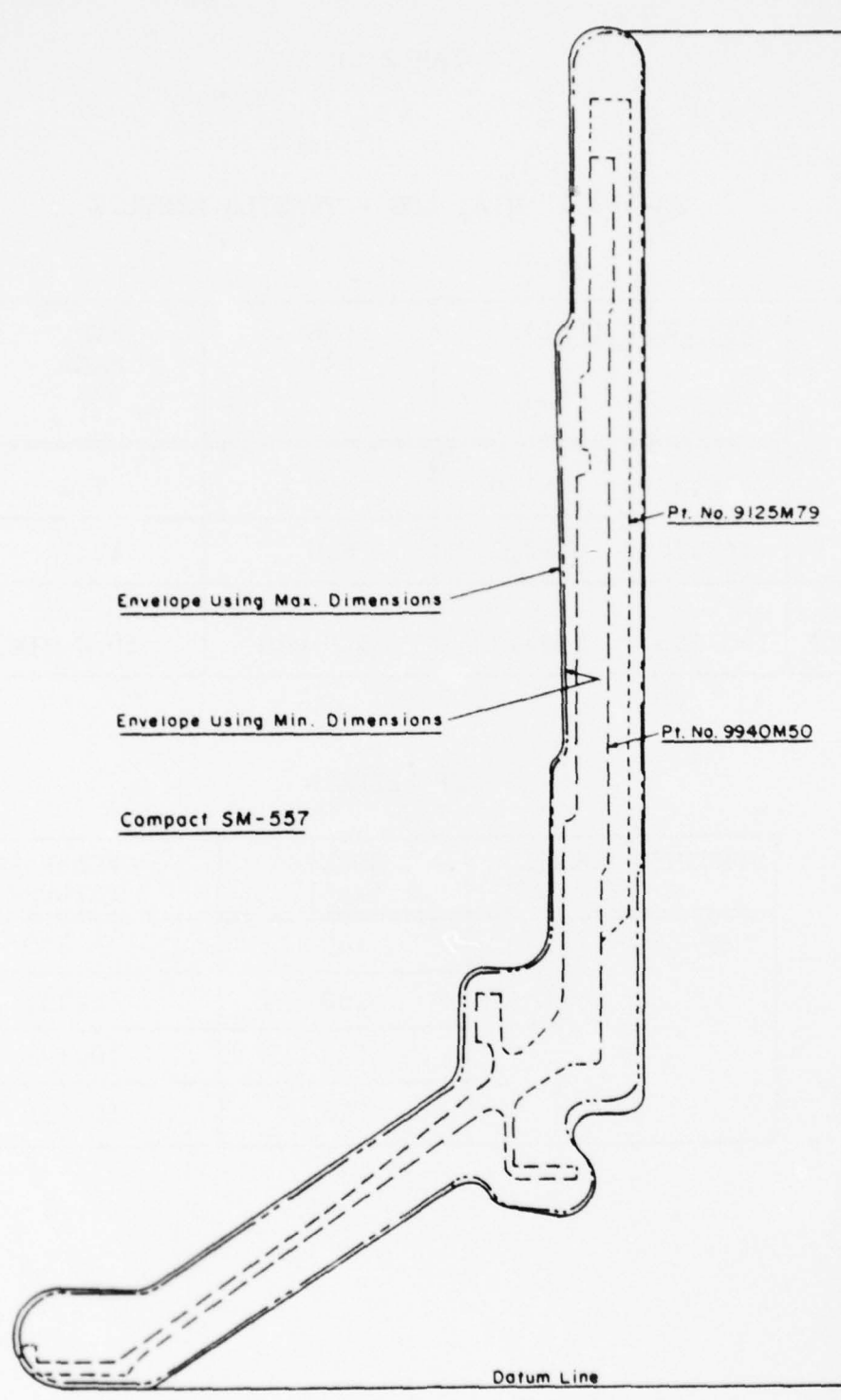


Figure 96. Target versus actual shape of Part SM-557.



TABLE 51

## SM-561 2" DIA. LOG - TENSILE RESULTS

	STRENGTH (KSI)		ELONG. (%)	RED. AREA (%)
	F <sub>tu</sub>	F <sub>ty</sub>		
	170.5	161.0	6.5	7.4
	168.7	162.0	8.0	12.7
SPEC RANGE	163-183	153-173	5.0 MIN.	10.0 MIN.

## LCF RESULTS

SPECIMEN SOURCE	STRESS (ksi)	CYCLES TO FAILURE
SM-561	140	5,850
	130	5,235
	120	10,549
	110	10,531

Low cycle fatigue results on compact SM-561 (Ceramic Mold) - 2" dia. are also given in Table 51. The data for SM-561 was lower than the values obtained on the sub-scale stub shafts and metallographic examination of specimens from SM-561 indicated that this compact was not fully dense throughout due to lower zone problems in the LAS.

The three full scale F-101 stub shafts were heat treated at Lindberg at 1475°F, 4 hours, water quench, aged at 1175°F for 8 hours and returned to G.E. Lynn.

Three thermocouples were used to monitor work-piece temperature. The solution temperature of 1475°F was held within  $\pm 15^\circ\text{F}$ . The water quench was affected within 45 seconds. The furnace was cooled to 1175°F and the parts were replaced for the aging cycle.

All three shafts were ultrasonically inspected at Evendale and found to meet the drawing requirements for this part. The parts were given a wet slurry polishing treatment prior to ultrasonic inspection to improve the surface finish. The two parts which were to be machined were also given a whole part density measurement and values of 0.1681 and 0.1682 lbs/in<sup>3</sup> were obtained which is in good agreement with the density of cast and wrought Ti-17 of  $0.1683 \pm .0001$  lbs/in<sup>3</sup>.

Gas analysis was conducted on the cut-up part after ultrasonic inspection and a high hydrogen content was found as indicated in Table 52. Other check analyses were also made in other areas of the shaft and high hydrogen was again found. The spin pit disc material was checked and found to have a hydrogen level only 3 ppm above the specification value of 125 ppm maximum. The compact SM-561 which was HIP in a ceramic mold also had a high hydrogen content. The spin pit discs were HIP as a log in a steel can and had a relatively low hydrogen content indicating that the source of hydrogen was in the ceramic mold containerization process. This hydrogen source probably originated in the secondary pressing media.

Samples from the stub shaft SM-557 were vacuum annealed in the laboratory at 1175°F and hydrogen was reduced to near the specification level. All three full scale stub shafts were then vacuum annealed

TABLE 52

## GAS ANALYSIS RESULTS

MATERIAL	CONDITION	ANALYSIS RESULTS - PPM	
		HYDROGEN	OXYGEN
Stub Shaft SM-557-1	As Received	347	1005
Stub Shaft SM-557-2	" "	336	1250
Stub Shaft SM-557-3	" "	314	1190
Stub Shaft SM-557-4	" "	365	1220
SM-561	As Received	270	1313
Spin Pit Disc	As Received	128	961
Stub Shaft SM-557-1	Lab H. T. (1)	76	973
Stub Shaft SM-557-2	Lab H. T. (1)	152	1351
Stub Shaft SM-557	Production H. T. (2)	170	1190
Specification	-	125 max.	1300 max.

Notes: (1) Vacuum annealed 1175°F, 8 hours in laboratory vacuum furnace.

(2) Vacuum annealed in production furnace (all three shafts degassed).

at 1175°F aging temperature for 8 hours and analysis indicated that hydrogen was reduced to 170 ppm. Although this value is above the specification limit, it was decided to proceed with part machining and testing on the full size stub shaft. However, the results indicate that caution must be exercised in evacuation of the compacts to avoid residual moisture in the ceramic material which would cause high hydrogen levels in the compacts after HIP.

Shafts numbered SM-555 and SM-556 were shipped to CMRC for target machining prior to finish machining at General Electric, Lynn. This consisted of machining of the ID bore as well as the aft surface of the large flange. From these true surfaces, General Electric would set up to machine the OD surface of the large flange. They use this as their datum surface throughout the final part machining.

As previously indicated, full scale stub shaft SM-557 was used for cut-up evaluation and testing. Tests included those normally conducted on a cast and wrought part to qualify a raw material and forging source.

Table 53 presents the tensile test results for specimens from the full scale shaft SM-557. The underlined values are below the specification limits. Typical strength values for cast and wrought Ti-17 forgings are shown for comparison at each temperature.

Low cycle fatigue data on specimens taken from the full scale stub shaft SM-557 are given in Table 54. The LCF results are shown in Figures 97 through 100. The low cycle fatigue results are similar to those obtained earlier on HIP cylinders and sub-scale shafts. That is, the smooth bar fatigue lives are well below cast and wrought beta processed forgings. Previous evaluations indicated that this behavior was a result of the influence of inclusions on the behavior of smooth bar specimens.

Table 55 shows the high cycle fatigue data for both smooth and notched specimens. These data are plotted in Figures 101 and 102. Typical data for cast and wrought Ti-17 forgings are 90 ksi for smooth bar fatigue and 18 ksi for  $K_t = 4.0$  notched bar fatigue. These results are consistent with those reported earlier in the program for the sub-scale disc testing. That is, smooth bar fatigue,



TABLE 53

## TENSILE PROPERTIES OF T1-17 SHAFT SM-557

Temp. Of	Specimen (1)		Strength (ksi)		Elong. (%)	R.A. (%)
	Location	Direction (2)	$F_{tu}$	$F_{ty}$		
75	Shaft	Axial	164.5	157.1	5.7	8.5
75	Rim	Tangential	165.7	156.8	7.0	10.1
75	Cone	Radial	166.9	159.3	8.0	11.1
75	Cone	Tangential	162.2	154.8	4.3	7.0
75	Shaft	Axial	163.8	156.0	9.2	15.9
75	Cone	Radial	162.4	154.6	7.2	10.8
Spec. Min.						
Typical (Beta Forged T1-17)			163.0	153.0	5.0	10.0
			170.0	160.0	8.0	15.0
400	Shaft	Axial	144.1	122.4	8.3	13.8
400	Shaft	Axial	137.7	121.4	4.3	5.9
400	Cone	Tangential	144.9	124.2	8.1	13.1
400	Shaft	Axial	143.2	123.9	6.6	10.4
400	Rim	Tangential	147.4	126.2	10.3	17.4
400	Cone	Tangential	144.8	124.9	9.3	14.9
Typical						
			151.0	130.0	-	-
600	Shaft	Axial	138.3	112.1	10.0	23.8
600	Cone	Tangential	138.7	113.5	9.6	17.1
600	Shaft	Axial	136.9	112.1	9.0	17.8
600	Rim	Tangential	137.6	112.2	9.2	17.0
600	Cone	Tangential	138.3	113.1	9.3	19.6
600	Cone	Radial	141.4	113.9	11.4	21.0
Typical						
			145.0	119.0	-	-

NOTES: (1) Nominal gage section: 0.25" diameter X 1.0" long  
 Strain rate through 0.2% yield: 0.005 in/in/min.  
 Head rate thence to failure: 0.05 in/min.

(2) Direction with respect to engine axis.

TABLE 54

## LOW CYCLE FATIGUE RESULTS

Ti-17 FULL-SCALE STUB SHAFT (SM-557)

Test Conditions: A=0.95, R=0.015, Freq.=30 CPM		
A. Test Temperature 75°F		
K <sub>t</sub>	Max. Stress (ksi)	Cycles to Failure
1.0	137.5	3,168
	135	4,958
	132	7,893
	130	4,266
	125	1,431
	120	7,664
	115	17,478
	115	5,234
2.0	90	8,502
	85	11,402
	80	5,501
	75	29,323
	70	12,338
	67	28,173
	65	30,995
	60	21,581
B. Test Temperature 600°F		
1.0	134	Failed on Loading
	130	881
	125	687
	120	5,844
	117	10,262
	115	2,285
	100	13,328
	100	6,026
	90	5,828
	85	21,690
2.0	90	4,388
	85	6,131
	85	3,082
	80	8,028
	75	12,060
	70	8,782
	65	24,052
	60	29,380

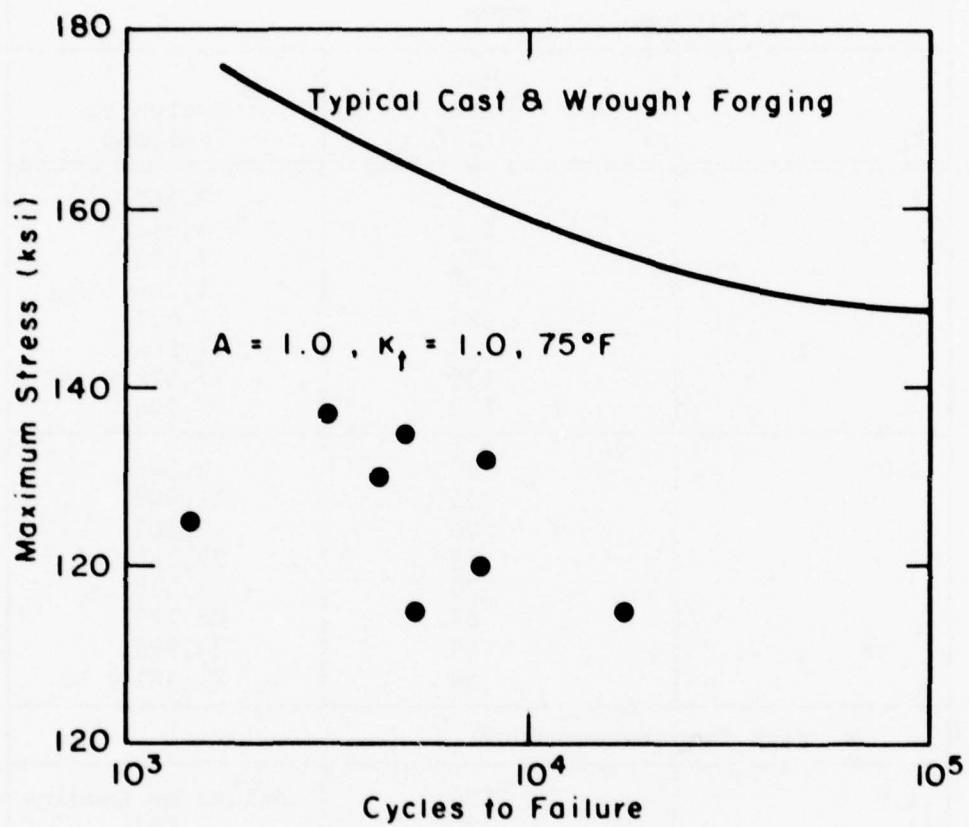


Figure 97. Low Cycle Fatigue Results - Ti-17 Full-Scale Stub Shaft (SM-557).

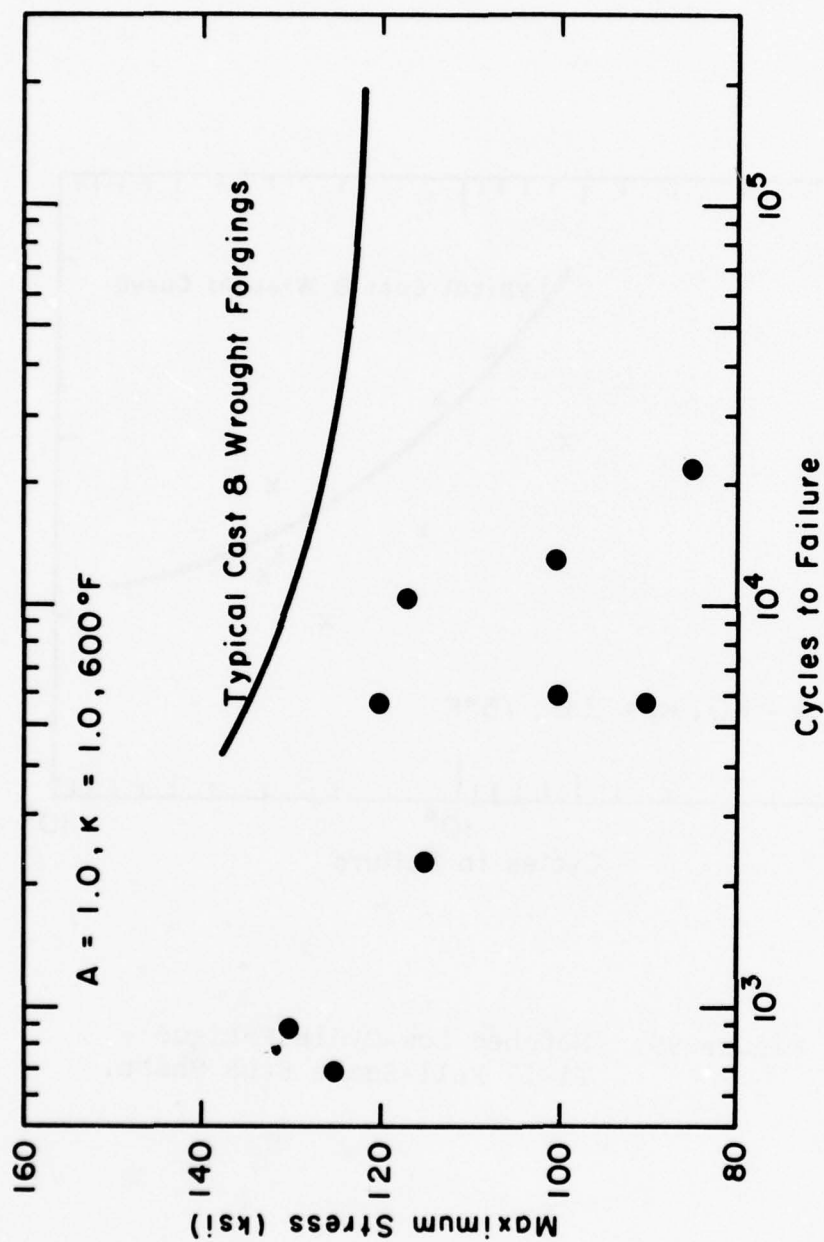


Figure 98. Low-Cycle Fatigue Results - Ti-17 Full-Scale Stub Shaft (SM-557).



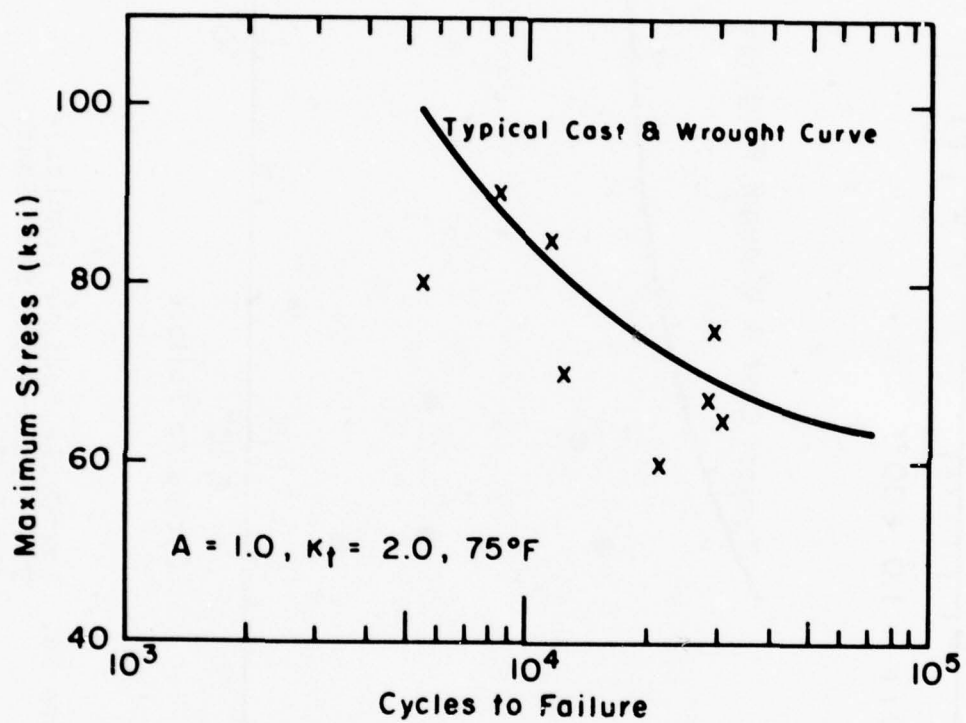


Figure 99. Notched Low-Cycle Fatigue -  
Ti-17 Full-Scale Stub Shaft.

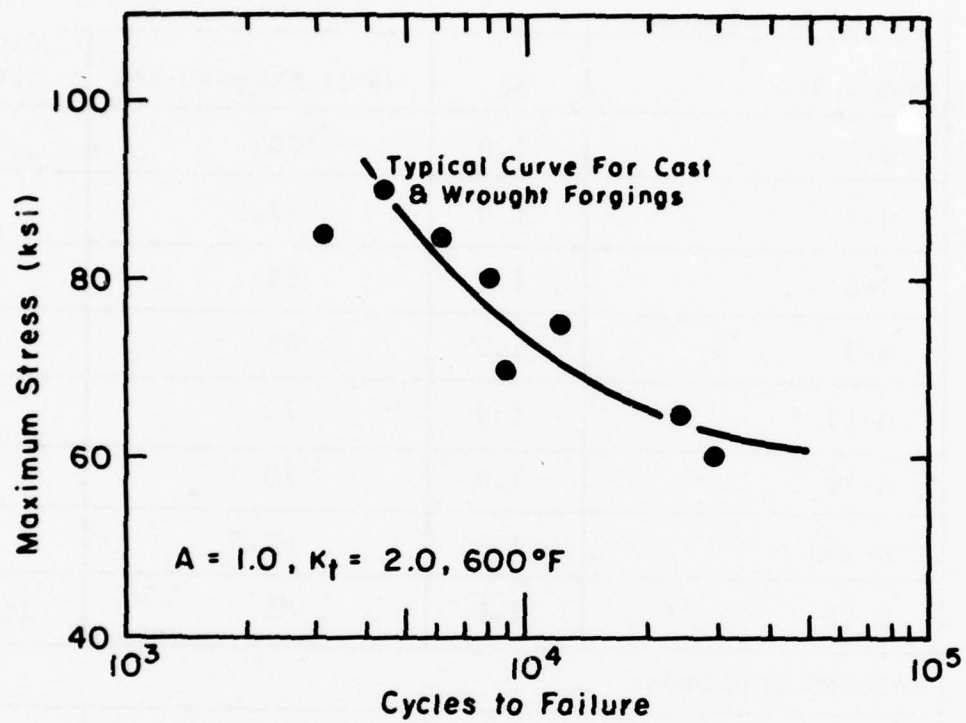


Figure 100. Notched Low-Cycle Fatigue -  
Ti-17 Full-Scale Stub Shaft.

TABLE 55

## HIGH-CYCLE FATIGUE OF Ti-17 SHAFT SM-557

A =  $\infty$ , ROTATING BEAM SPECIMEN

Smooth Specimens			
Spec. No.	K <sub>t</sub>	Max. Stress, ksi	Cycles to Failure
H-1	1.0	100	208,000
H-5	1.0	97.5	18,000
H-8	1.0	95	27,000
H-3	1.0	85	50,000
H-15	1.0	75	54,000
H-10	1.0	70	65,000
H-14	1.0	67.5	74,000
H-12	1.0	65	11,486,000
Notched Specimens			
H-11	4.0	30	106,000
H-2	4.0	28	166,000
H-4	4.0	26	213,000
H-16	4.0	25	433,000
H-7	4.0	24	789,000
H-13	4.0	22	1,074,000
H-9	4.0	20	2,678,000
H-6	4.0	18	12,224,000

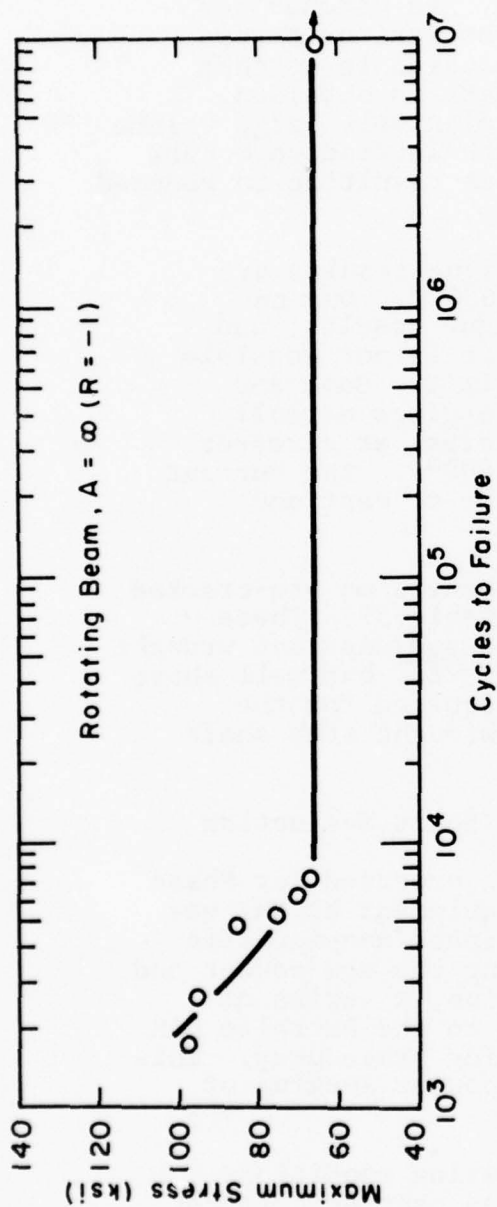


Figure 101. Smooth Bar High-Cycle Fatigue.

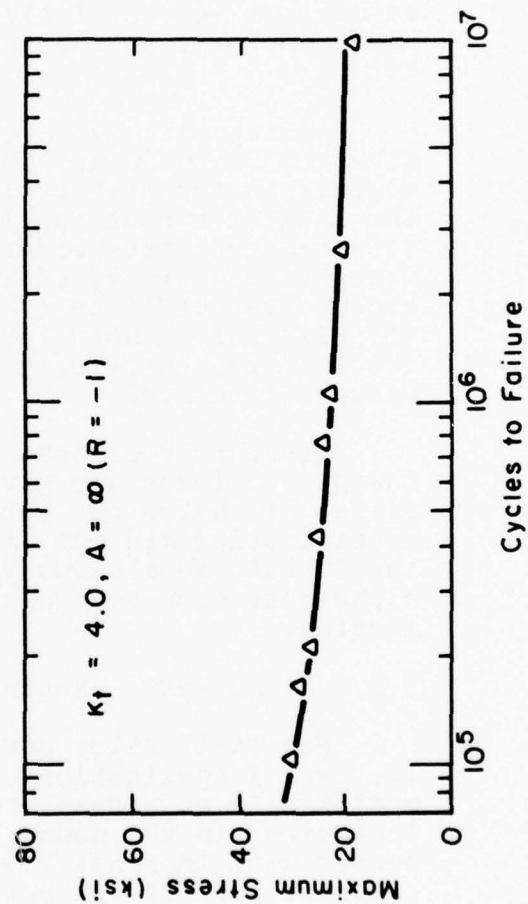


Figure 102. Notched Bar High-Cycle Fatigue - Rotating Beam.



both low and high cycle types, is reduced  $\sim 30\%$  in stress level for a given life, as compared to cast and wrought forgings. Notched fatigue at  $K_t = 2.0$  for LCF and  $K_t = 4.0$  for HCF, is about the same for the powder and cast and wrought products. The reduced smooth bar strength was attributed to the presence of inclusions in the powder products and confirmed by SEM/EDAX analysis. In notched bar fatigue, the notch localizes the maximum stress at one area, and unless an inclusion is at that location, normal fatigue strength is obtained. For smooth specimens, with a relatively large volume at maximum stress, fatigue crack initiation occurs preferentially at the inclusions resulting in reduced life.

Additional high cycle fatigue results are given in Table 56 at 750°F and 600°F. Due to scatter in the high cycle fatigue results, and the lack of runout specimens, it is not possible to estimate a true endurance limit. Cast and wrought beta processed Ti-17 forgings normally produce runout lives ( $>10^7$  cycles) at stresses of  $\sim 112$  ksi at both 750°F and 600°F. The current results are, therefore, inferior to cast and wrought forgings.

Fracture toughness test results on pre-cracked Charpy specimens are given in Table 57. These values are below the beta processed cast and wrought specification minimum of 50 ksi  $\sqrt{in}$ , but well above the 30 ksi in minimum value required for the alpha-beta processed cast and wrought stub shaft forging.

#### 3.2.1.5 Summary - Engine Stub Shaft Evaluation

New Ti-17 alloy powder was produced for Phase II, Task I application. REP equipment at NMI was modified in an attempt to eliminate non-metallic inclusions in the powder. Using the new powder and powder used in Phase I evaluation, a series of compacts were HIP in one cycle in the Battelle LAS with various handling and canning procedures. This work was supplemented by AFML powder swaging of all three Ti-17 powder lots.

None of the various processing conditions produced LCF behavior as good as cast and wrought material. However, the experimental results were

TABLE 56

## HIGH CYCLE FATIGUE RESULTS

Ti-17 FULL-SCALE STUB SHAFT (SM-557)

Test Conditions:  $K_t=1.0$ ,  $A=0.95$  ( $R=0.015$ )

A. Test Temperature 75°F		
Max. Stress (ksi)	Alt. Stress (ksi)	Cycles to Failure
120	58.5	15,000
115	56	119,000
112.5	54.8	448,000
110	53.6	3,861,000
105	51.2	47,000
105	51.2	46,000
B. Test Temperature 600°F		
115	56	94,000
110	53.6	17,000
105	51.2	31,000
95	46.3	31,000
85	41.4	116,000
75	36.5	63,000

TABLE 57

## PRE-CRACKED CHARPY TOUGHNESS RESULTS

Ti-17 F-101 HIP STUB SHAFT: S/N SM-557.

Spec. No.	w	w-a	a/w	f(a/w)	$K_C$ ksi $\sqrt{\text{in.}}$
C2	.3915	.202	.1895	5.05	42.2
C3	.3907	.212	.1787	4.68	49.2
C6	.3950	.211	.1840	4.80	47.3
C8	.3950	.2185	.1765	4.56	51.0

$$K_C = 8.35 f(a/w)$$

marred by problems in the HIP run which resulted in the "C" series (Ceramic Mold Material) being incompletely consolidated as evidenced by porosity in the microstructure. The LAS run experienced problems with temperature and time at temperature in the lower section of the autoclave. As a result, the "C" series had the poorest LCF behavior, falling below the Ti-6-4 data. The AFML swaged materials exhibited considerable scatter. The overall results of the tests, however, indicated that handling and processing procedures, other than the powder manufacture, did not have a marked effect on LCF behavior. The bulls-eye fracture appearance on LCF specimens indicate the continued presence of foreign material inclusions at the fatigue origins.

The original Phase II Plans were modified by substitution of 6" diameter discs rather than the full scale stub shaft at the request of F-101 Design Engineering. Due to heat treat problems, three discs were spin pit tested, two in a high strength condition and one in the normal specification range. The results of the Spin Pit tests indicated that the PM discs were in the expected burst speed/stress range for their mechanical property level with the exception of disc #1 which fractured at approximately 10% lower speed. The fracture origins were at pores or inclusions in the bore area. The lower speed failure of Disc #1 was attributed to a larger void or inclusion at the fracture origin. Crack growth rate data from one of the spin pit specimens indicate poorer crack growth behavior as compared to cast and wrought material. A possible cause could be the higher hydrogen content of the HIP material.

Shape trials were carried out to produce a full size stub shaft with a minimum of effort due to contract funding and timing runouts. Only minor shape changes were deemed necessary to produce the three full scale stub shafts after the first trial, based on experience gained in the Phase I effort. The second shape trial produced two stub shafts with machining envelopes adequate for producing finish machined parts. The third stub shaft (SM-557) was diverted to use for cut-up evaluation and testing since it was the most difficult to index for finish machining.

The results of the test evaluation on full scale stub shaft SM-557 were similar to the results found in the Phase I study on the sub-scale stub shaft. For the most part, all test data was comparable to cast and wrought data with the exception of low cycle fatigue results. The low cycle fatigue results show that smooth bar fatigue lives are well below cast and wrought beta processed forging data, while the notched bar data are comparable. The behavior is believed to be the result of the greater incidence of inclusions in the smooth bar LCF cross-section as opposed to the notch type, since it is less likely that the notch specimen, due to fixed orientation, would contain an inclusion site to act as a stress riser.

### 3.2.2 Task II - Airframe Keel Splice Former Evaluation

Based on the Phase I - Task II and III effort involving evaluation of Ti-6-4 HIP Parameters and shape making studies, it was concluded that the Phase II, Task II requirements of MIL-T-9047 would be met with HIP + annealed Ti-6-4 powder containing increased oxygen content to 0.166%. Three shape iterations were carried out in Phase I on the keel splice fitting. The final shape and final tooling modifications had been made for Phase II evaluation.

#### 3.2.2.1 Ti-6-4 Test Panels

The actual keel splice formers were too small to provide all of the test material required for testing under this contract. Therefore, two rectangular panels (S-1 and S-2) measuring 2 x 4 x 8 inches and a 3-7/8 inch round x 7-1/2 inch long cylinder (S-3) were HIP at 1750°F. Prior to testing, these test specimens were annealed for two hours at 1300°F and air cooled.

Density measurements were made on the samples as well as on a forged Ti-6-4 sample. Results are shown in Table 58.

Tensile coupons were removed from S-1 and S-2 shapes only. Round tensile specimens (.252 dia. 1" gage length) were machined and tested according to ASTM E8. The results are shown in Table 59. Although the tensile strengths are uniform, a difference in reduction of area is noted from specimens taken from



TABLE 58  
DENSITY OF Ti-6-4 TEST PANELS

Number	Material	Density
S-1	P.M. Rectangle No. 1	.1598 lb/in <sup>3</sup>
S-2	P.M. Rectangle No. 2	.1600 lb/in <sup>3</sup>
S-3	P.M. Cylinder	.1600 lb/in <sup>3</sup>
Reference	Forging	.1601 lb/in <sup>3</sup>

TABLE 59  
Ti-6-4 TENSILE TEST RESULTS

Specimen	Strength (ksi)		Percent Elongation In 1 Inch	Percent Reduction of Area
	F <sub>tu</sub>	F <sub>ty</sub>		
S1-1	136	126	17	23.8
S1-2	136	126	17	23.1
S1-3	137	128	17	42.5
S1-4	137	128	17	38.6
S2-1	136	126	16	29.6
S2-2	136	127	16	41.8

the same block (S-1). The properties meet the requirements of MIL-T-9047.

Notched fatigue specimens ( $K_t = 3$ ) were tested in a Sonntag SF-10-U machine at a cyclic rate of 30 Hertz and a stress ratio of 0.1. The data are shown in Table 60 and plotted in the form of a S-N curve in Figure 103. For comparison, the upper and lower fatigue limits of forged Ti-6Al-4V are given in Figure 103. The higher notched fatigue life of the HIP product is evident and may relate to the finer alpha morphology.

Compact tension specimens, 1.5 in. thick, were pre-cracked and tested in accordance with the requirements of ASMT E399-74 to determine fracture toughness. The data are listed in Table 61. The toughness is high and is commensurate with the values for beta-processed material of medium oxygen content (.14 - .17%). The data were uniform regardless of specimen orientation which is indicative of lack of marked texture. The fracture faces were exceedingly flat and smooth.

WOL\* type specimens were pre-cracked and subjected to constant amplitude sinusoidal loading over a range of stress intensities using a computer controlled MTS machine. The computer monitored the crack growth through feed back of the output of a compliance gauge mounted on the specimen. Data output was in the form  $BEC^{**}$  vs. N. The BEC data was converted to crack length from previously established compliance calibration curves. The  $da/dN$  vs.  $\Delta K$  data was curved fitted using an exponential variation of the Nth Order Constrained Regression Polynomial. Plots of the crack growth rate are shown in Figures 104, 105, and 106. The curves are very uniform and no perturbations can be seen which may be due to dense inclusions or porosity. The crack growth

---

\*WOL = Wedge Opening Loading

\*\*BEC = Compliance (C) normalized for thickness (B) and modulus (E).

TABLE 60

## Ti-6-4 FATIGUE TEST RESULTS\*

Specimen	Maximum Stress (ksi)	Cycles To Failure
S1-1	65.0	103,000
S1-2	60.0	90,000
S1-3	50.0	5,000,000**
S1-4	55.0	770,000
S1-5	60.0	244,000
S1-6	70.0	82,000
S1-7	75.0	46,000
S1-8	57.5	1,747,000
S1-9	52.5	7,671,000**

\*Tested at a cyclic rate of 1800 cpm and a stress ratio of 0.1

\*\*No Failure

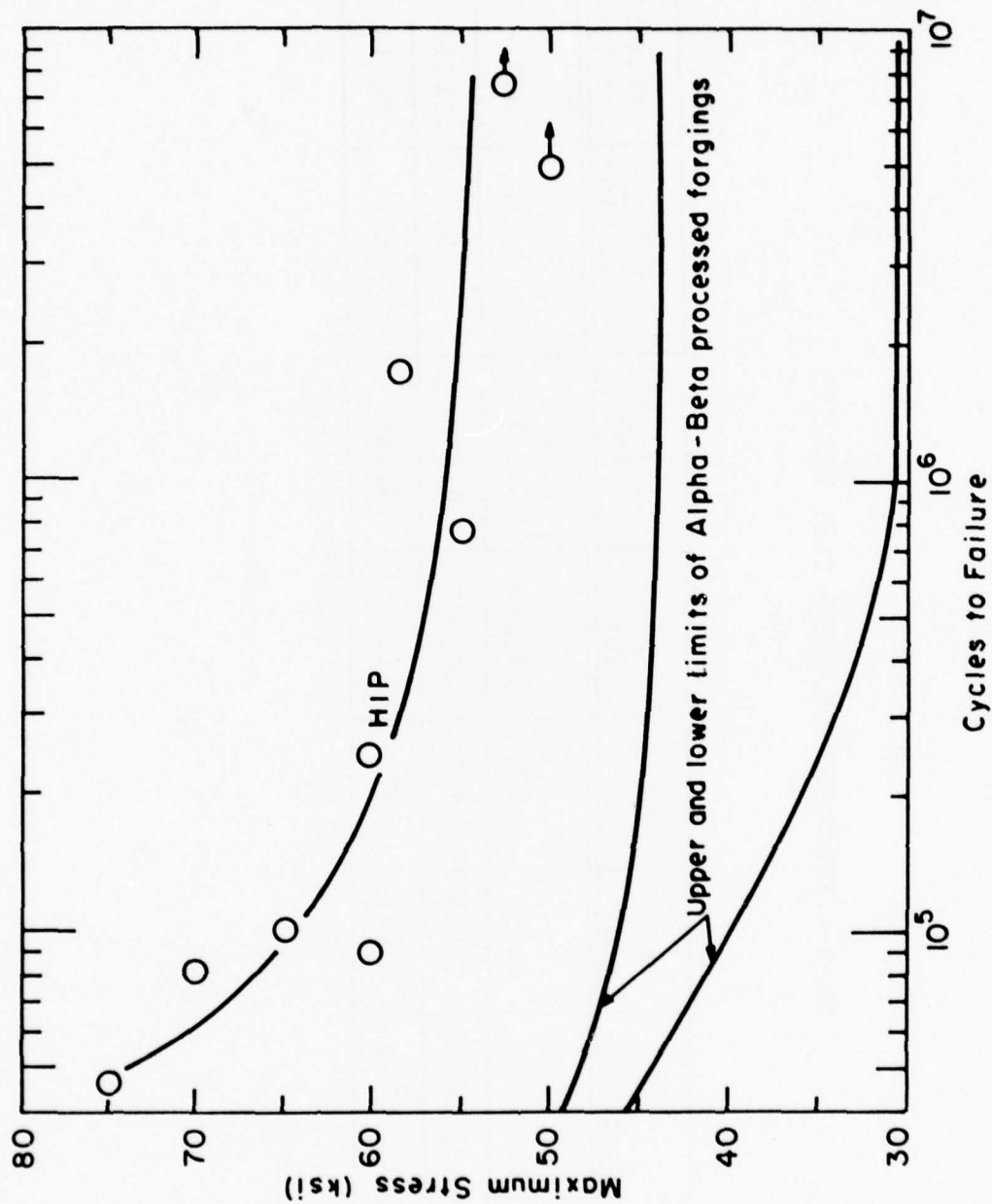


Figure 103. Notched fatigue strength of HIPed Ti-6Al-4V.  
(Forging data limits ref. AFML TR-73-301)



TABLE 61

## Ti-6-4 FRACTURE TOUGHNESS TEST RESULTS

Specimen	A (in)	B (in)	P <sub>Q</sub> (lbs)	$2.5 \left( \frac{KQ}{YS} \right)^2$	K <sub>IC</sub> (ksi $\sqrt{\text{in}}$ )	Validity of Test
S2, L-LT	1.495	1.500	21,340	0.951	78.2	Valid
S3, L-LT	1.474	1.500	20,905	0.890	75.7	Valid
S3, LT-L	1.483	1.500	21,655	0.968	78.9	Valid

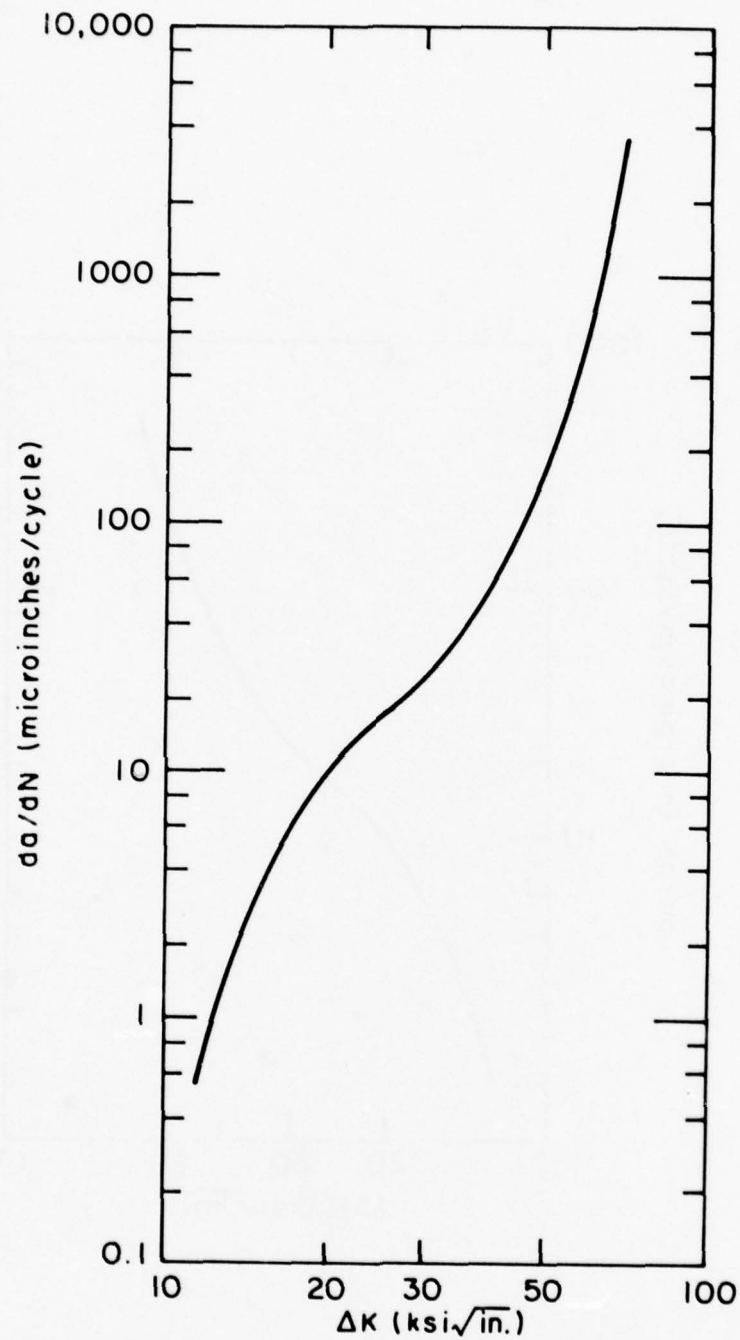


Figure 104. Crack growth rate for WOL specimen S1-1, L-T.

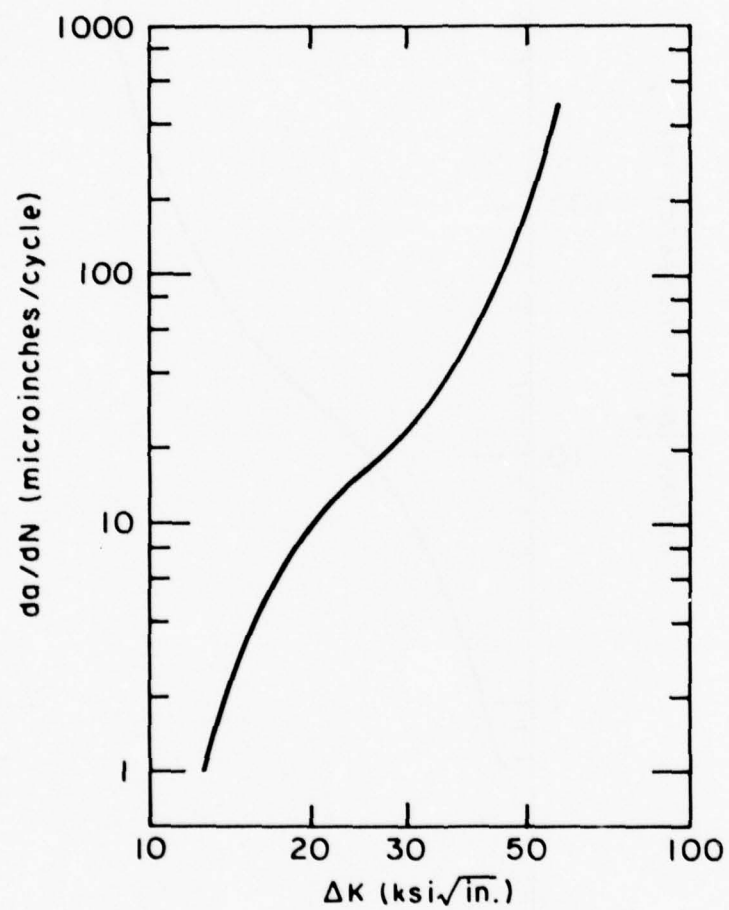


Figure 105. Crack growth rate for WOL specimen S1-2, L-T.

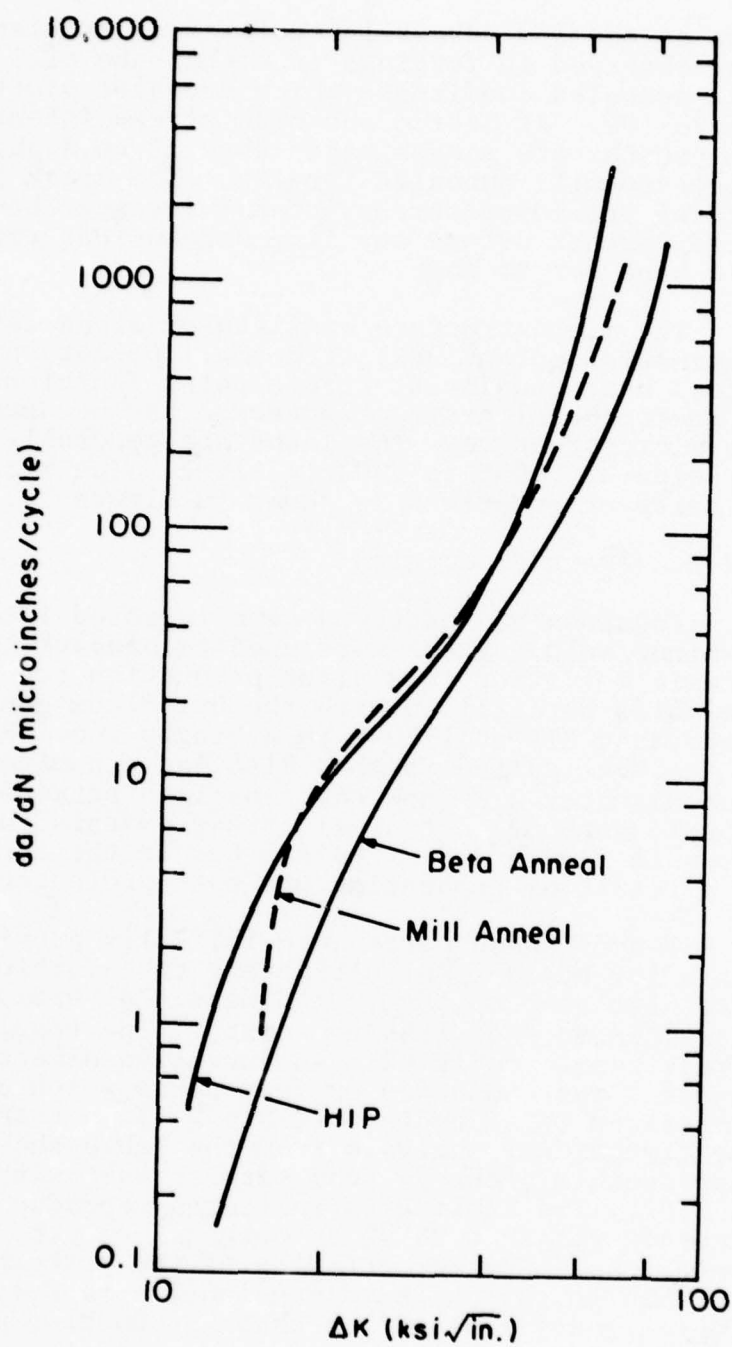


Figure 106. Crack growth rate for WOL specimen S2-1, LT-L.  
(Wrought mill anneal and beta anneal forging crack growth rate shown for comparison)



rate at the low stress intensities is greater than that observed in forgings in either the mill or beta annealed conditions which are also plotted in Figure 106. At medium and high stress intensities, the growth rate approximates that of an alpha-beta processed-mill annealed forging. The crack growth rate at the lower stress intensities must be investigated further before any firm conclusions regarding this behavior is made.

The microstructure consists of alpha laths (estimated content 98%) with small pockets of transformed beta usually at triple point junctions. No preferential grain orientation can be detected in the microstructure. The laths are generally .00025 in. wide by .0005 to .003 in. long. The microstructure in three orientations is shown in Figure 107.

#### 3.2.2.2 Part Production

Fourteen wax patterns were injected into an aluminum mold. These were used to prepare the ceramic molds for this pilot production run. All of the molds were filled with the 0.166% oxygen Ti-6-4 powder and HIP at 1750°F in a single run. Each of the keel splice formers also had a nominal 1/2 inch diameter x 3 inch test specimen attached as a prolongation. A typical part from this run is shown in Figure 108. The saw cut in the foreground is a result of separating the test prolongation.

Ten of these parts were initially provided to MCAIR for evaluation; ultimately two additional parts were also sent to them. A dimensional analysis was conducted on the first ten parts. The results are summarized in Table 62. An extensive dimensional analysis was conducted on four parts which are summarized in Appendix D (Table D-6) to this report. The dimensional analysis from the Table shows reproducible accuracy from part to part within 1.5 to 3.0%. The Table also indicates reproducible accuracy within 0 to 7% of original target dimensions. Further refining of the pattern is possible to narrow the dimensional spread even though program goals were met on these production parts.

One HIP keel splice former was chem-milled in a standard chem-mill bath as used at MCAIR. The parts were wired and hung in the bath and etched at a rate of 3 mils/minute/surface. Ten minutes were

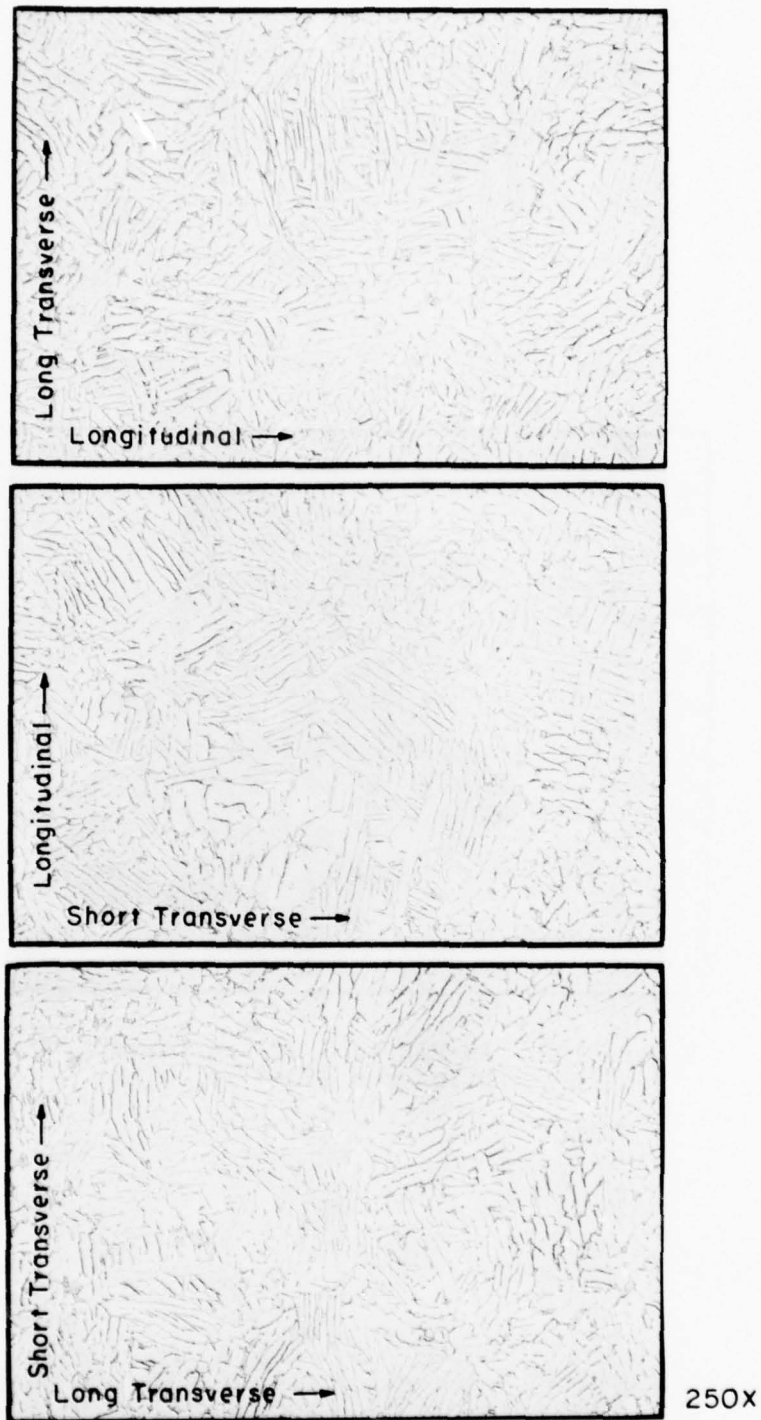


Figure 107. Microstructure of HIP shape.

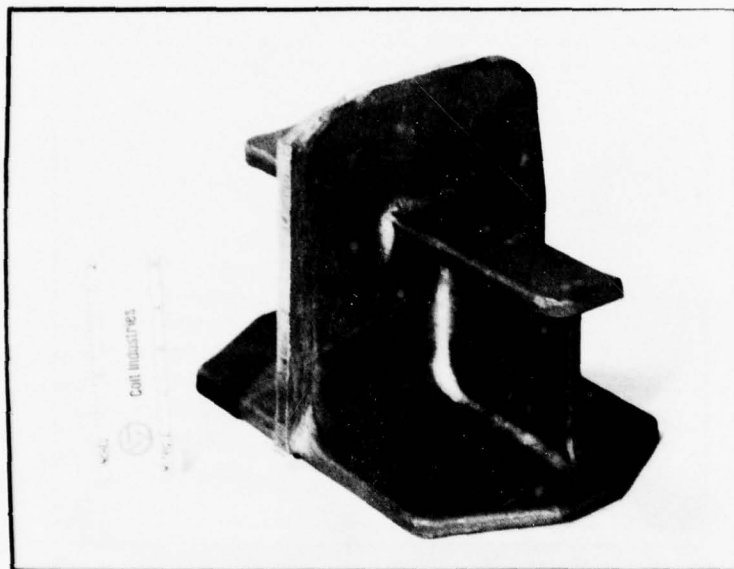
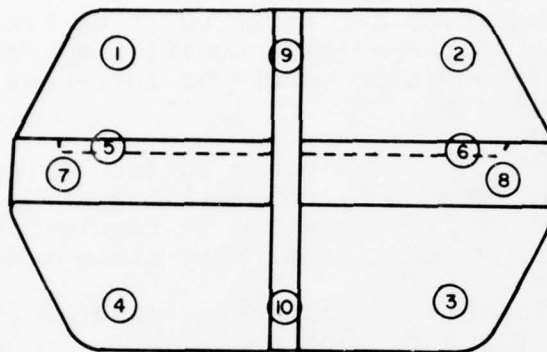


Figure 108. As-HIP keel splice former from pilot run (SM-417).

TABLE 62

DIMENSIONAL ANALYSIS OF HIP KEEL  
SPLICE FORMERS



	Thickness at Indicated Area, Inch									
	1	2	3	4	5	6	7	8	9	10
SM 409	.197	.199	.189	.195	.190	.193	.198	.194	.230	.222
SM 411	.197	.196	.194	.191	.189	.184	.196	.200	.232	.225
SM 412	.200	.197	.193	.201	.183	.182	.196	.197	.236	.230
SM 413	.191	.190	.192	.193	.185	.176	.190	.194	.230	.223
SM 414	.199	.195	.188	.191	.184	.182	.189	.194	.234	.233
SM 416	.196	.180	.188	.190	.189	.180	.192	.197	.238	.238
SM 418	.204	.197	.193	.196	.184	.177	.202	.200	.226	.224
SM 419	.201	.198	.195	.189	.186	.184	.196	.203	.230	.230
SM 421	.196	.193	.190	.189	.183	.175	.193	.186	.228	.229
SM 422	.192	.197	.188	.186	.185	.187	.194	.199	.238	.226
$\bar{x}$	.197	.194	.191	.192	.186	.182	.195	.196	.232	.228
$\sigma$	.004	.006	.003	.004	.003	.005	.004	.005	.004	.005



required to obtain the required dimensions on the larger platform sections of the component. After chem-milling, the part weighed .41 lbs which is comparable to the machined flyweight of a forged component. Only thickness dimensions were checked and these met engineering drawing requirements.

The deficiencies in the HIP part which must be corrected before chem-milling can be utilized are as follows:

- 1) Surfaces which are required to be flat must be flat in the as-HIP condition as any out-of-flat condition cannot be corrected by chem-milling.
- 2) Dimples, laps, and other surface irregularities are not removed by chem-milling and a liquid hone or similar process would be required to remove such irregularities if they are not deep.
- 3) Edge thickening or thinning must be avoided in the HIP component design.
- 4) Mid-planes of flat and parallel surfaces should be located during the mold design to obtain proper distances between such planes after chem-milling. In a machining operation, metal may be removed preferentially from one distance between such parallel surfaces; this option is not available in the chem-milling operation unless a masking operation (a cost factor) is used.

#### 3.2.2.3 Post-HIP Processing

Prior to machining, the parts were heat treated by annealing at 1300°F 2 hours, and air cooled. The prolongation and the parts were not heat treated together.

During machining, the numerical identification of the components were inadvertently lost. Both the forged and the HIP components were dimensionally checked prior to testing. The forged part thicknesses were generally less than those of the HIP specimens and were more uniform part to part. This is attributed to the NC machining of the production (forged) parts whereas the HIP components were conventionally machined. However, all parts were

within engineering drawing tolerance.

#### 3.2.2.4 Non-Destructive Evaluation

Radiography and penetrant inspections were the principal methods of non-destructive examination. The parts were X-rayed according to MCAIR process specification P.S. 21206 Quality Level 2-1T. This quality level is defined as follows:

Maximum penetrameter thickness, 2% (expressed as percentage of the material thickness)

Minimum perceptible hole diameter, 1T (expressed as multiple thickness of image quality indicator T)

Equivalent penetrameter sensitivity, 1.4%

All films were double loaded to minimize artifacts. The parts were shot in three orthogonal views before and after machining.

Examination of the film for the as-HIP condition showed dense inclusions always less than .030 in. dia. and areas of low density. The latter type of defect was thought to be surface depressions. The examination of the film for the fully machined condition showed a decrease in a number of inclusions, also the areas of low density were eliminated. No other abnormalities which would hinder performance were detected.

The parts were routinely inspected after machining using penetrant per MCAIR specification P.S. 21202, Class L. This class permits rounded indications, however, no linear indications are acceptable. All parts passed this penetrant inspection.

#### 3.2.2.5 Static Test

The HIP keel splice formers were match drilled to fit a test beam and assembled using Hi-Lok fasteners. The test set-up is shown in Figure 109 and installed in the machine in Figure 110. The HIP part was loaded at a rate of 1,000 lb/minute to failure. An autographic load-strain curve was used to detect yield load and maximum load was used as the failure point. The results are shown in Table 63. The higher yield and failure loads are attributed primarily to the dimensional variations as previous tests on the same powder

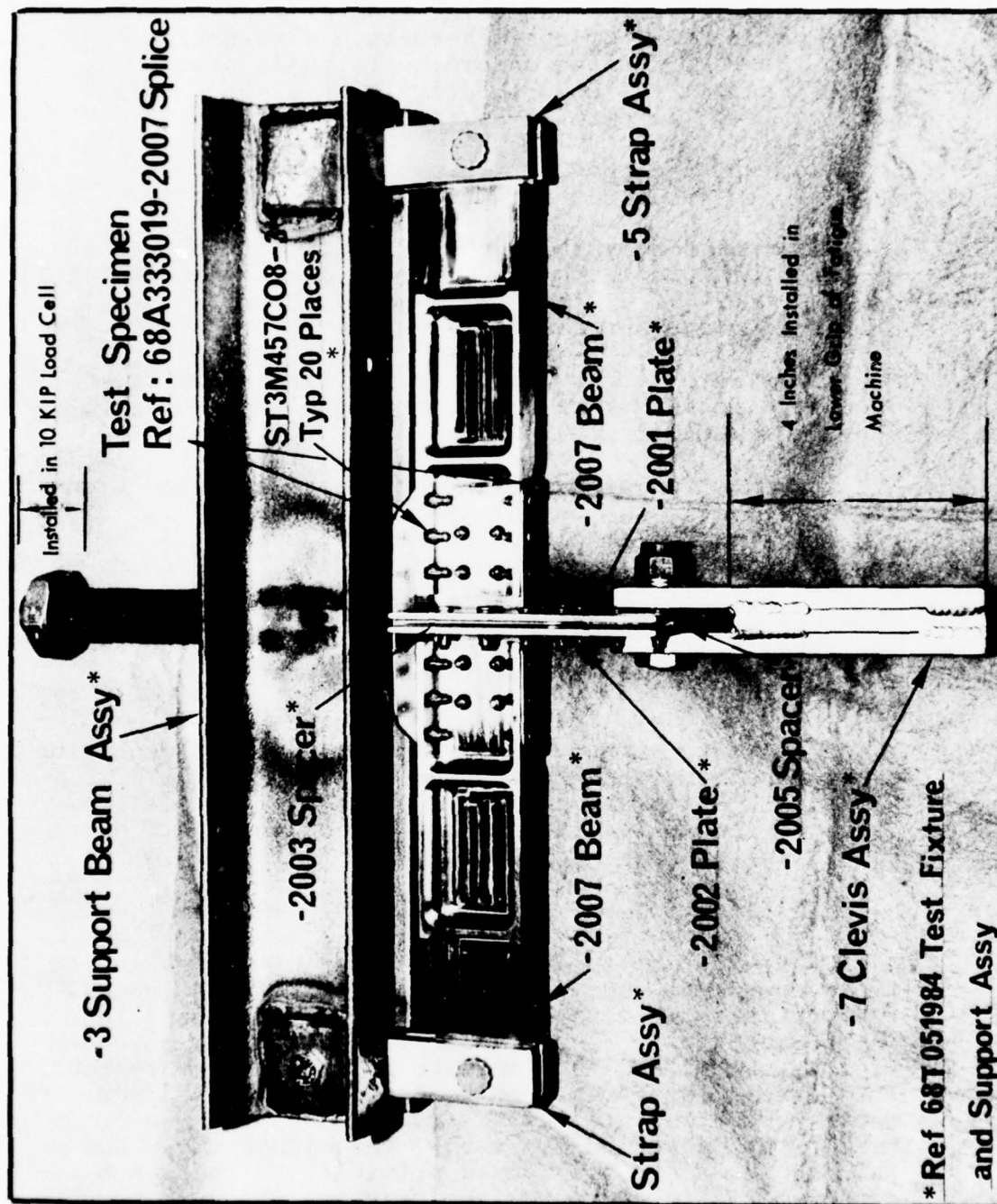


Figure 109. Test assembly.

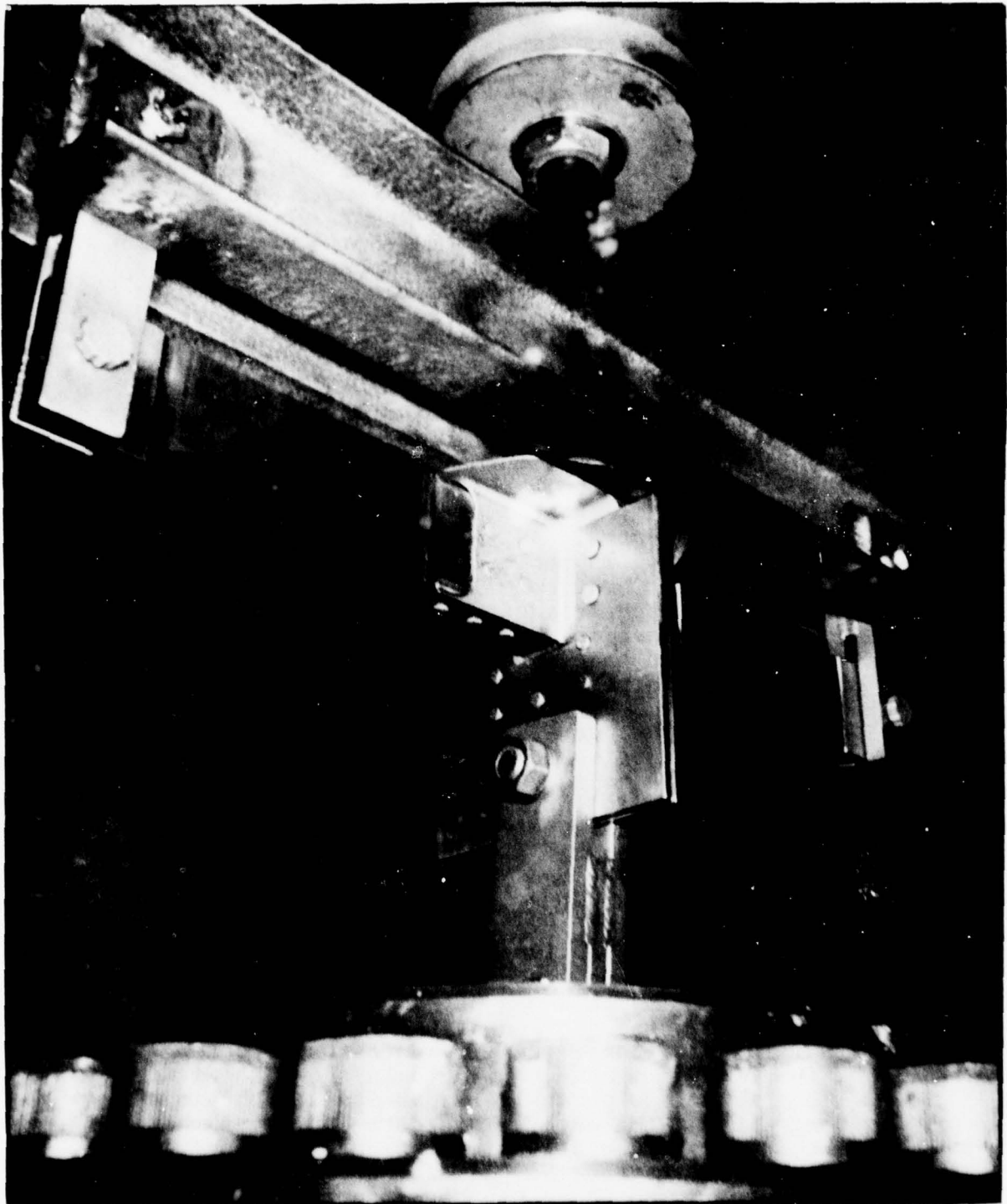


Figure 110. Set-up for spectrum fatigue testing of forged and hot isostatic pressed keel splice formers 68A333019-2007.



lot did not show any unusually high strengths. A typical failed part is shown in Figure 111.

#### 3.2.2.6 Spectrum Fatigue Tests

The same test set-up was used for the fatigue tests as for the static tests. The R-4 Horizontal Tail (F-15) spectrum was used for this series of tests. The design limit load was 2,200 lbs or 91.7% of the yield load of the forged component and 84.6% of the yield load of the HIP component. The results of the spectrum fatigue tests are listed in Table 64. Because the fixture holes were slightly elongated, oversize holes were made in the fixture and HIP component No. 3 and larger Hi-Lok (.189" diameter vs. .16" diameter) fasteners were used. In all cases, the HIP components showed longer life than the forged counterparts. "Life" was defined as the time necessary to form a crack and propagate it to an adjacent bolt hole. By this definition, both the crack initiation and crack growth behavior could be evaluated. A typical keel splice former after fatigue testing is shown in Figure 112. Fracture initiated at a bolt hole in the top narrow longitudinal flange and propagated to the adjacent bolt holes in the web in one direction and propagated to the edge of the narrow longitudinal flange in the opposite direction. In many instances, the crack proceeded beyond the first adjacent bolt hole and ended at or near the wide longitudinal flange; this can be attributed to the load spikes in the spectrum which rapidly extended the crack beyond the desired end point. Failure to stop the test when the crack reached this first bolt hole in the web did not significantly affect the results as frequent observations were made during this critical part of the test.

The test data given earlier in this report tended to indicate that the HIP specimens had a longer life and this was attributed to the dimensional variances (thickness) in the flange area. To illustrate this, the life data were plotted as a function of flange thickness as shown in Figure 113. A regression analysis was made to obtain a best fit for the data. This data indicates that within expected scatter for fatigue, the long life of HF3 (HIP-Fatigue-No. 3 X-Ray Film) specimen whose life was 23,360 hours can be directly attributed to

TABLE 63

STATIC TEST RESULTS  
FORGED AND "HIP"  
KEEL SPLICE FORMERS, 68A333019-2007

Specimen Number	Fabrication Method	Yield Load, lbs	Failure Load, lbs
1FS	Forged	2,400	4,000
2HS	HIP	2,600	4,140

TABLE 64

SPECTRUM FATIGUE DATA  
R-4 HORIZONTAL TAIL SPECTRUM (F-15)  
KEEL SPLICE FORMERS, 68A333019-2007  
DESIGN LIMIT LOAD, 2,200 LBS

Specimen Number	Fabrication Method	Hours to Failure	Average
2FF	Forged	11,255	8,594
3FF	Forged	10,400	
4FF	Forged	6,960	
5FF	Forged	5,760	
3HF	HIP	23,360	18,480
5HF	HIP	17,840	
6HF*	HIP	14,240	

\*Oversize hole and fasteners (.189" diameter in lieu of .169")

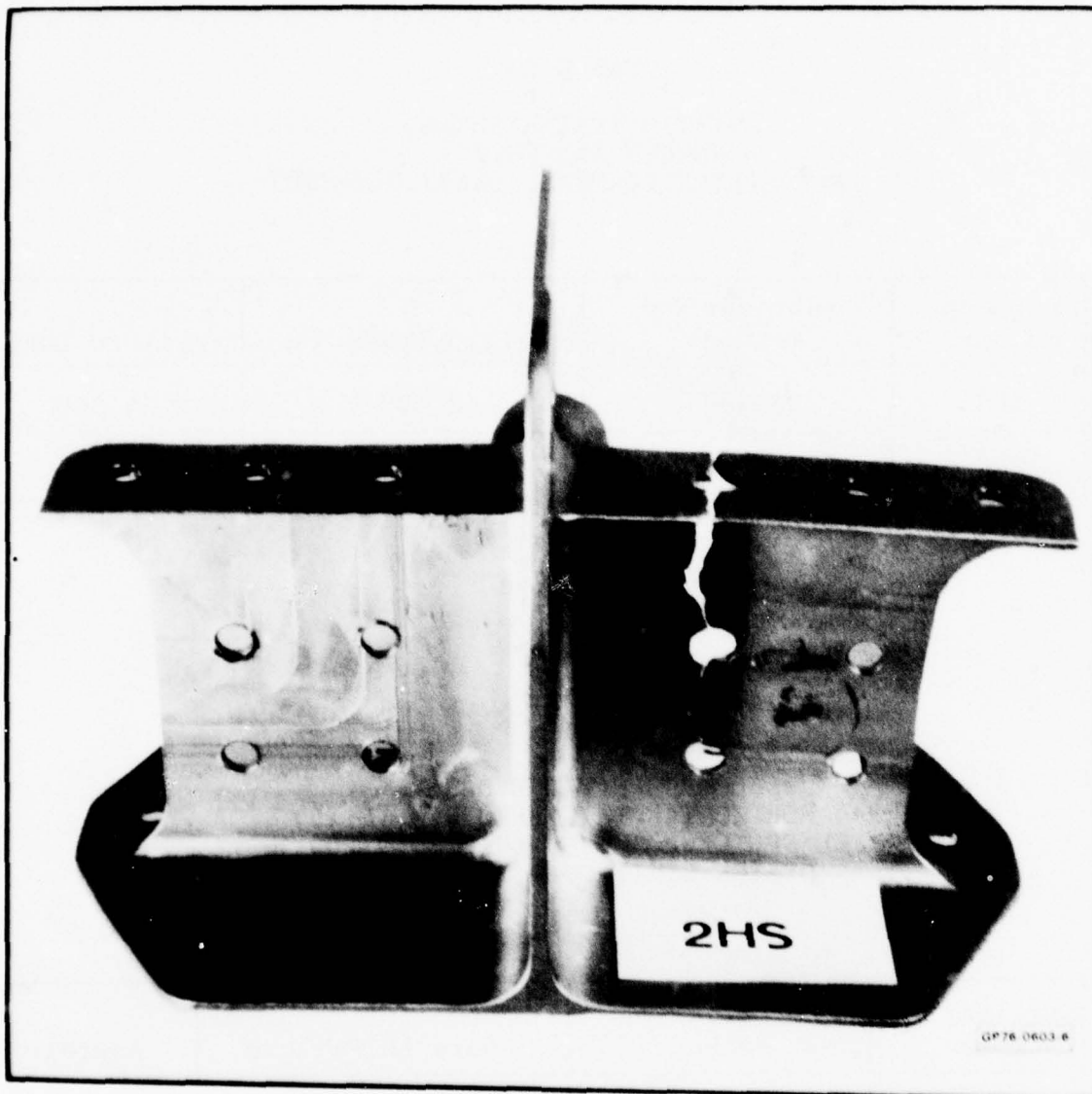


Figure 111. Hot isostatic pressed and machined keel splice former failed in static test.  
(Load at yield, 2,600 lb; at failure, 4,140 lb.)

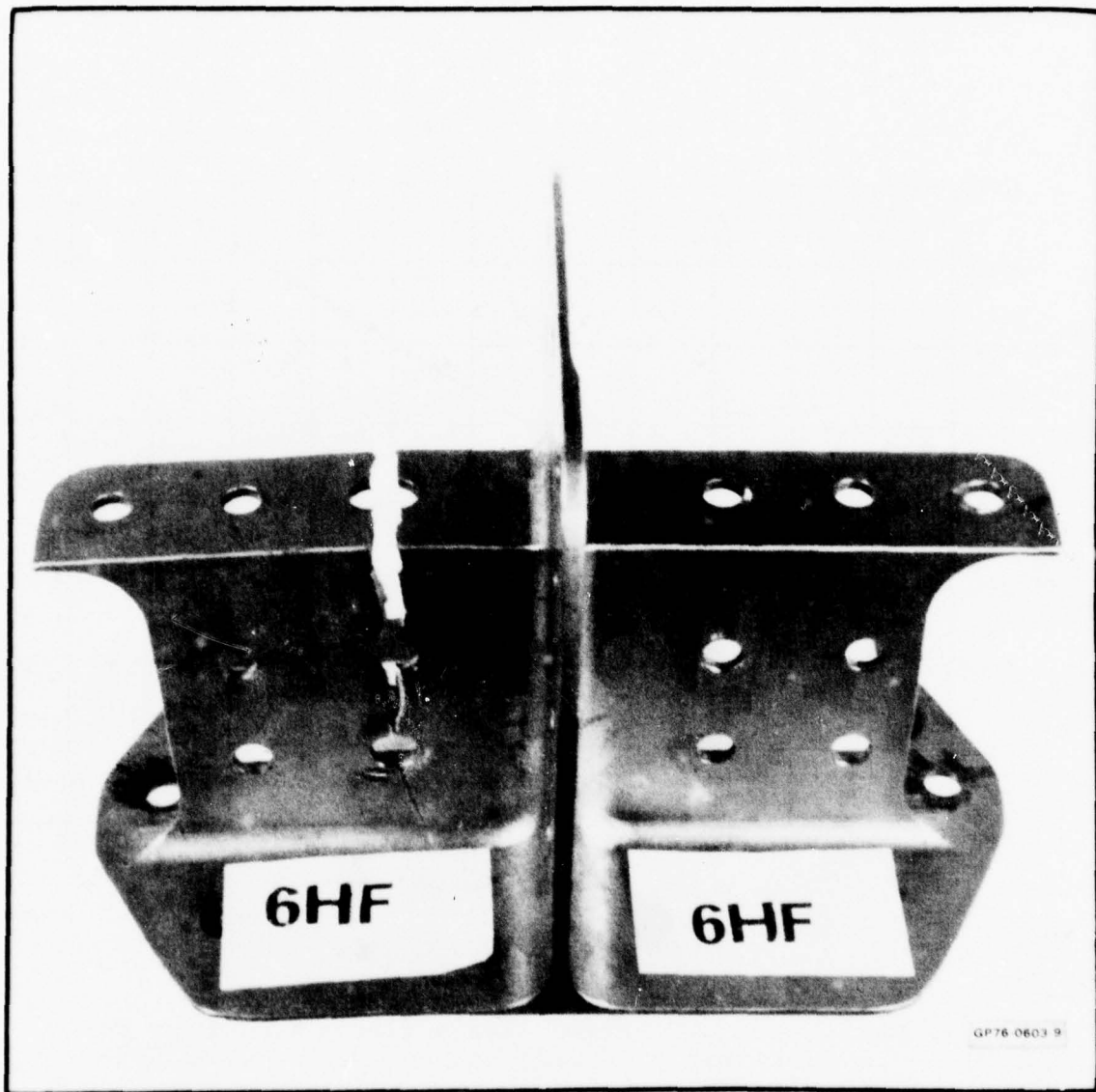
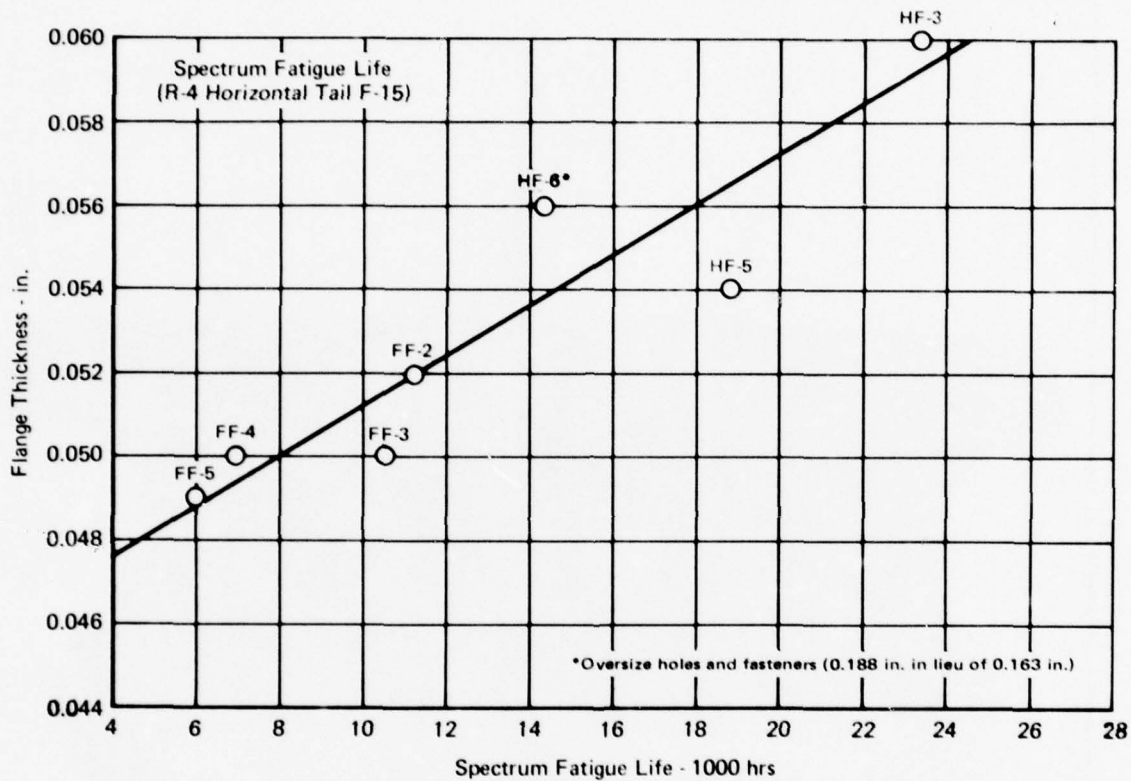


Figure 112. Hot isostatic pressed and machined keel splice former with enlarged holes failed in spectrum fatigue test; life, 14,240 hrs.





GP76-0603-23

Figure 113. Spectrum fatigue life - flange thickness relationship of keel splice former 68A333019-2007.

the oversize holes\* which effectively reduced the cross-sectional area of the flange. All of the forged specimens had lives reasonably close to their expected lives assuming scatter is inevitable.

The data thus indicates that the spectrum fatigue lives of the HIP keel splice formers are equivalent to that of wrought product.

### 3.2.2.7 Fractography

A scanning electron microscope (SEM) was used to examine the fracture characteristics of the HIP and the wrought products. Fracture surfaces of a compact tension specimen used for fracture toughness determination and the keel splice formers used for spectrum fatigue testing were used for the study.

#### 1) Compact Tension Specimen

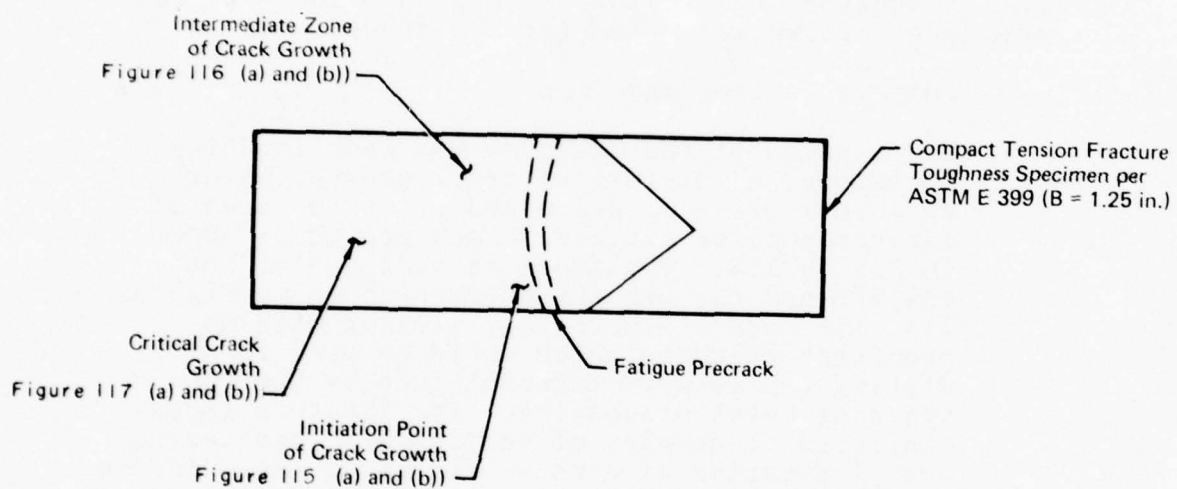
Examination of the fracture was made in three locations; a) at initial crack growth, b) at an intermediate location and c) in the area of catastrophic or critical crack growth as shown in Figure 114. The fracture surfaces of both the HIP and the wrought product shown in Figures 115, 116, and 117 were very similar with no prominent features which could be used to distinguish between material made by the two types of metal processing. The fracture faces consisted of dimples of varying size and tears, both indicative of ductile fracture. No evidence of cleavage or other abnormalities indicative of high or low density inclusions were detected.

#### 2) Keel Splice Former

The section examined was the area between the bolt hole and the edge of the narrow flange. Here also three areas were examined: a) at the early stage of crack growth, b) an intermediate

---

\*Holes enlarged to eliminate ovality induced in the beam holes during prior tests.



GP76-0603-14

Figure 114. Sketch of a compact tension fracture toughness specimen.

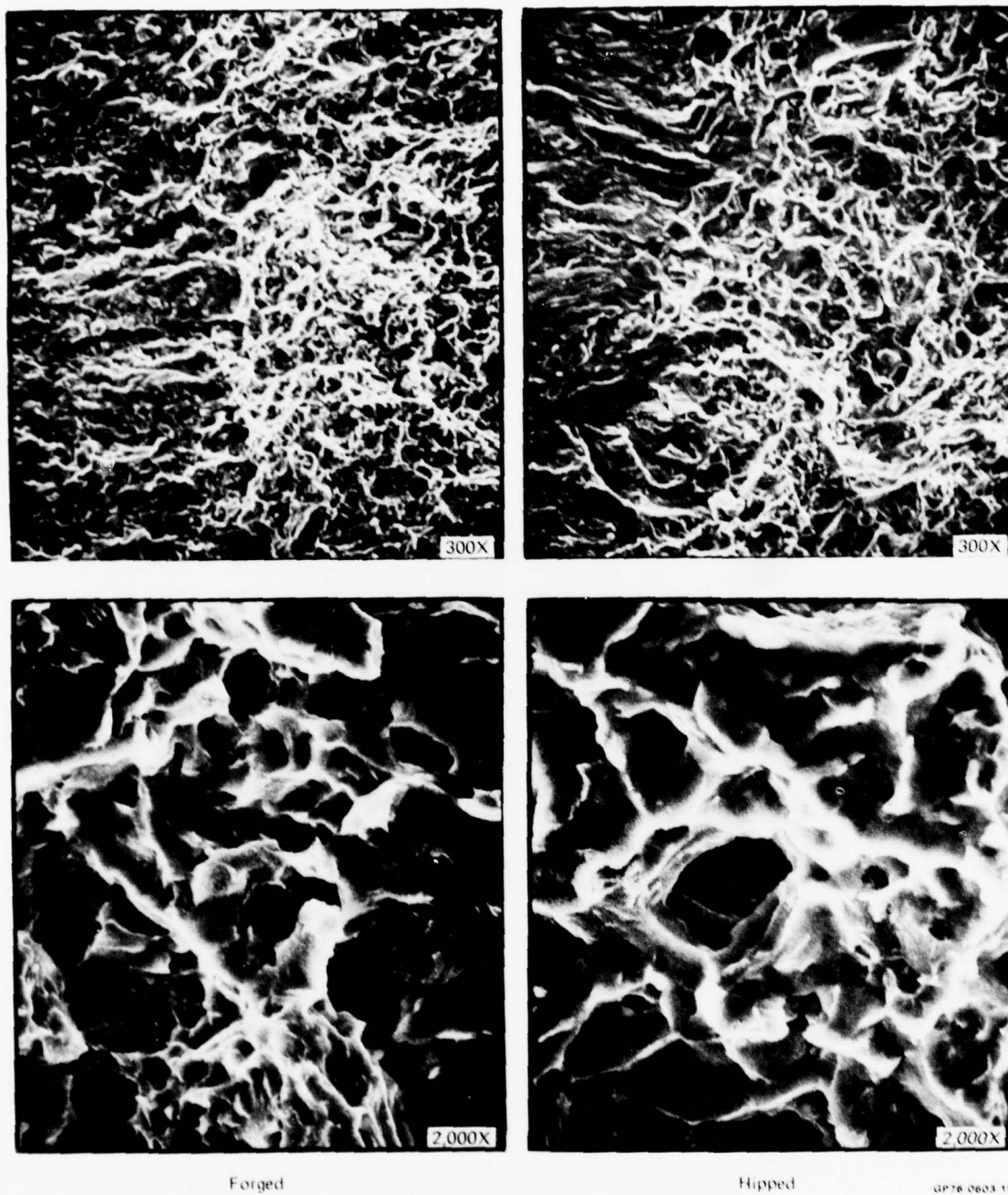


Figure 115. Low and high magnification views of (a) forged and (b) HIPed Ti-6Al-4V in area of initial crack growth showing dimples of mixed sizes and depth.



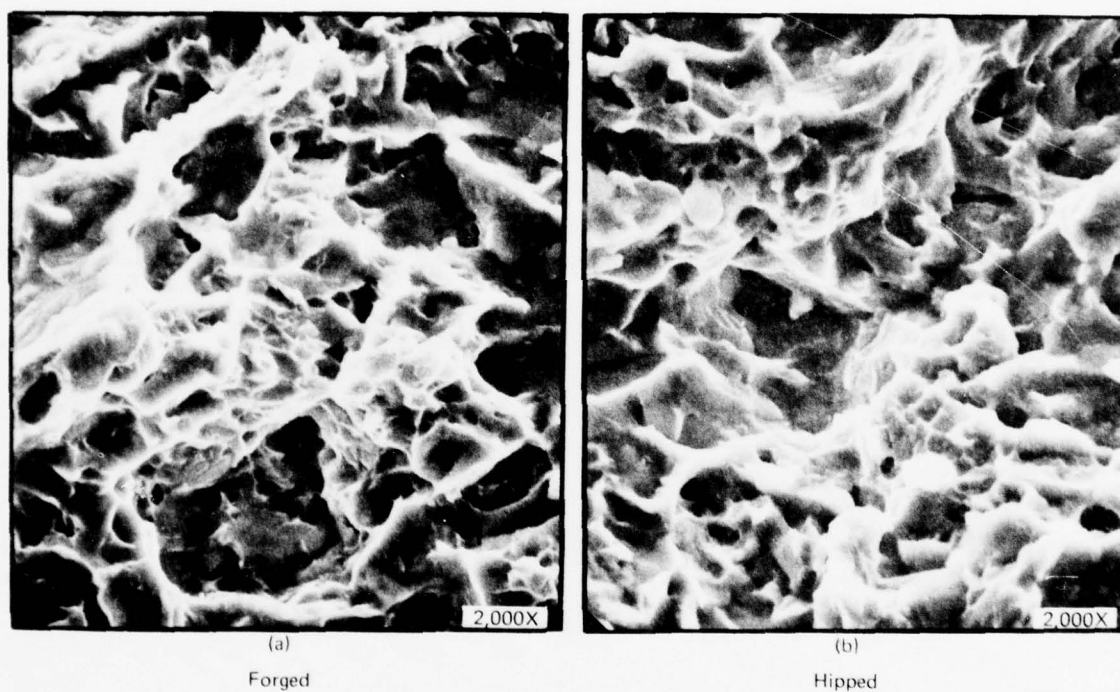
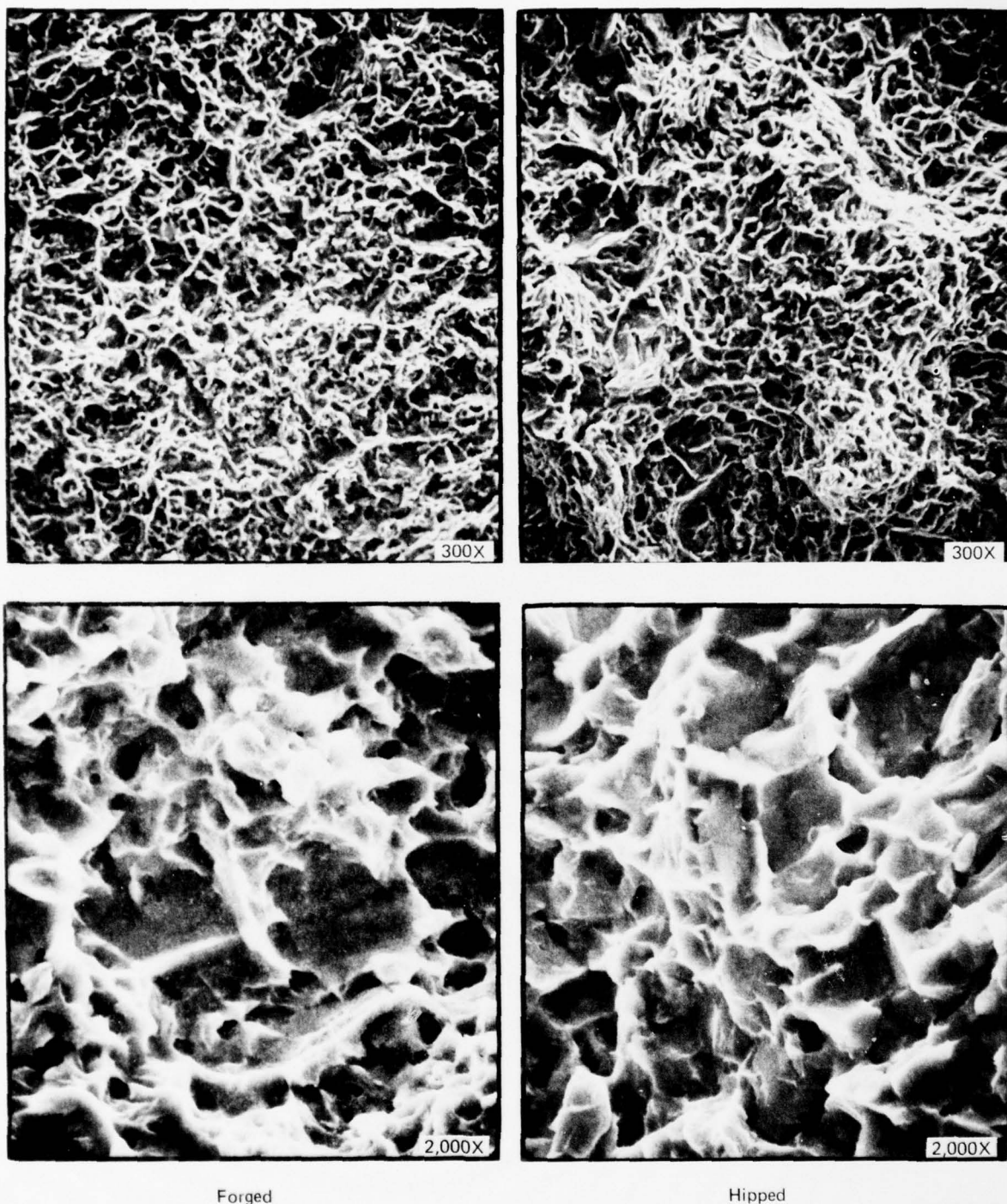


Figure 116. Fracture appearance at intermediate location in a compact tension specimen of (a) forged and (b) HIPed Ti-6Al-4V showing dimples of varying size and depth.



Forged

HIPed

GP76-0603-16

Figure 117. Low and high magnification views of (a) forged and (b) HIPed Ti-6Al-4V fracture in area of rapid crack growth showing dimples of varying size and depth.

area near the point of critical crack growth. The low magnification photos, Figures 118 and 119, show widely spaced "beach marks" in the HIP specimen (Figure 118) which, because of its longer life, should show a greater number of load spikes, especially those with magnitude of 111.8% of design limit load (DLL) which occur every 4,000 hours. High magnification fractographs are shown in Figures 120 and 121.

In the area of crack initiation of the HIP specimen (Figure 119), a prominent striation is visible which by its size should be indicative of a large load spike. The size and prominence of this striation would indicate that this spike is the result of the 111.8% DLL spike which was not prominent on low magnification. If this assumption is correct, it then follows that the crack initiation period on the HIP specimen was longer. The striation spacing on both sides of the load spike is nearly equal which is unusual. It would be expected that after such a large load spike, the crack growth would be retarded, resulting in smaller striation spacing until the crack front passes through the plastic zone created by the spike. Because of its short life, a large striation was not observed in the forged specimen in the early stages of crack growth (Figure 117).

In the midsection of the crack, a large striation is also detected in the HIP specimen. This is also assumed to be the 111.8% DLL spike which would be the second of four such spikes which would occur in the 17,840 hours of life. Not all such spikes would be visible in the fractograph as a portion of the total life (50-60%) would be expended in crack initiation. The striation spacing in this zone is larger in the forged specimen than in the HIP specimen. This is due to either (1) the dimensional variances resulting in lower stress intensities in the HIP specimen or (2) difference in total crack length, (opposite end of crack may be further from origin in the wrought specimen), with the former reason being more probable.

In the area of fast crack growth, the difference in striation spacing is the most prominent difference between the two types of fabrication. As noted above, this difference is most probably the result of the influence of dimensional variation resulting in differences in stress intensities.





45X

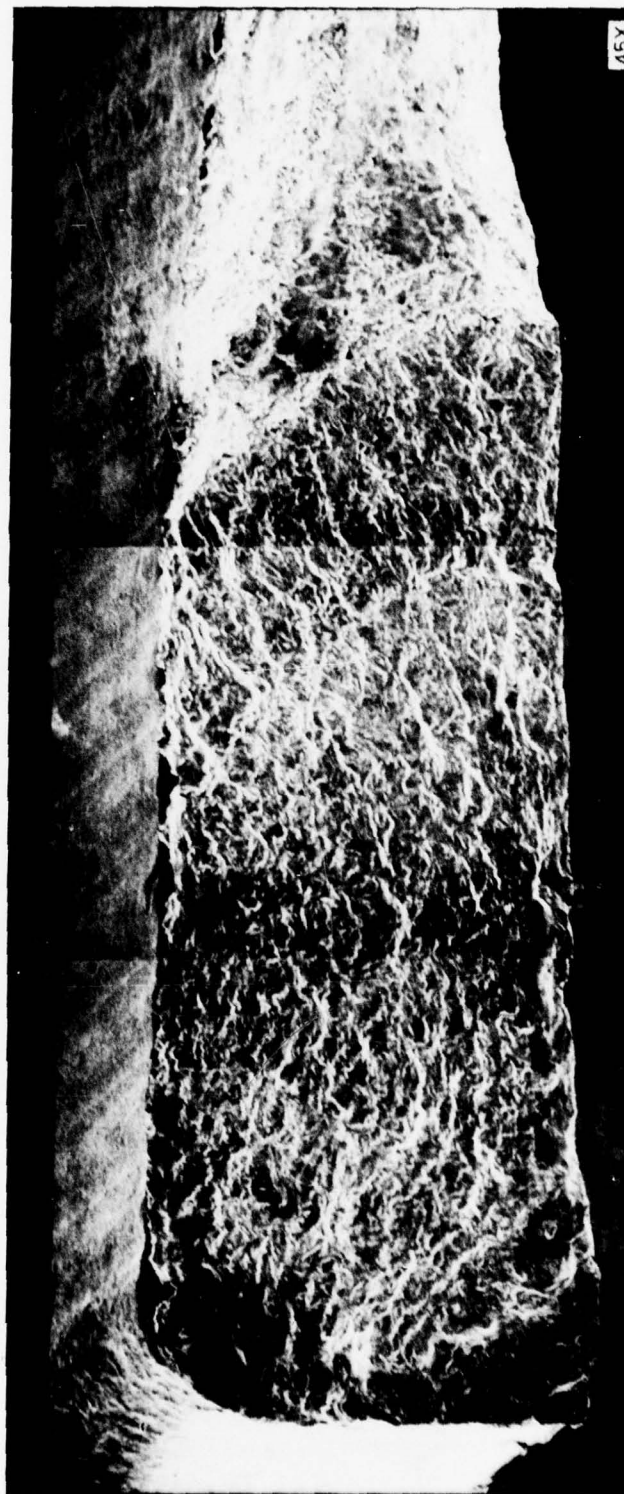
(c)

(b)

(a)

Figure 118. Fracture surface of a forged and machined keel splice former after spectrum fatigue test.  
(Life, 5,760 hrs. - Location: Bolt hole at top of narrow flange)





GP76 0603 18

(c)

(b)

(a)

Figure 119. Fracture surface of HIP keel splice former after spectrum fatigue test.

(Life, 17,840 hrs. - Location: Bolt hole at top of narrow flange)



(c)

(b)

(a)

Figure 120. Enlargement of fractograph in Areas A, B, and C of a forged keel splice former shown in Figure 116. (Reduced ~30% in printing)

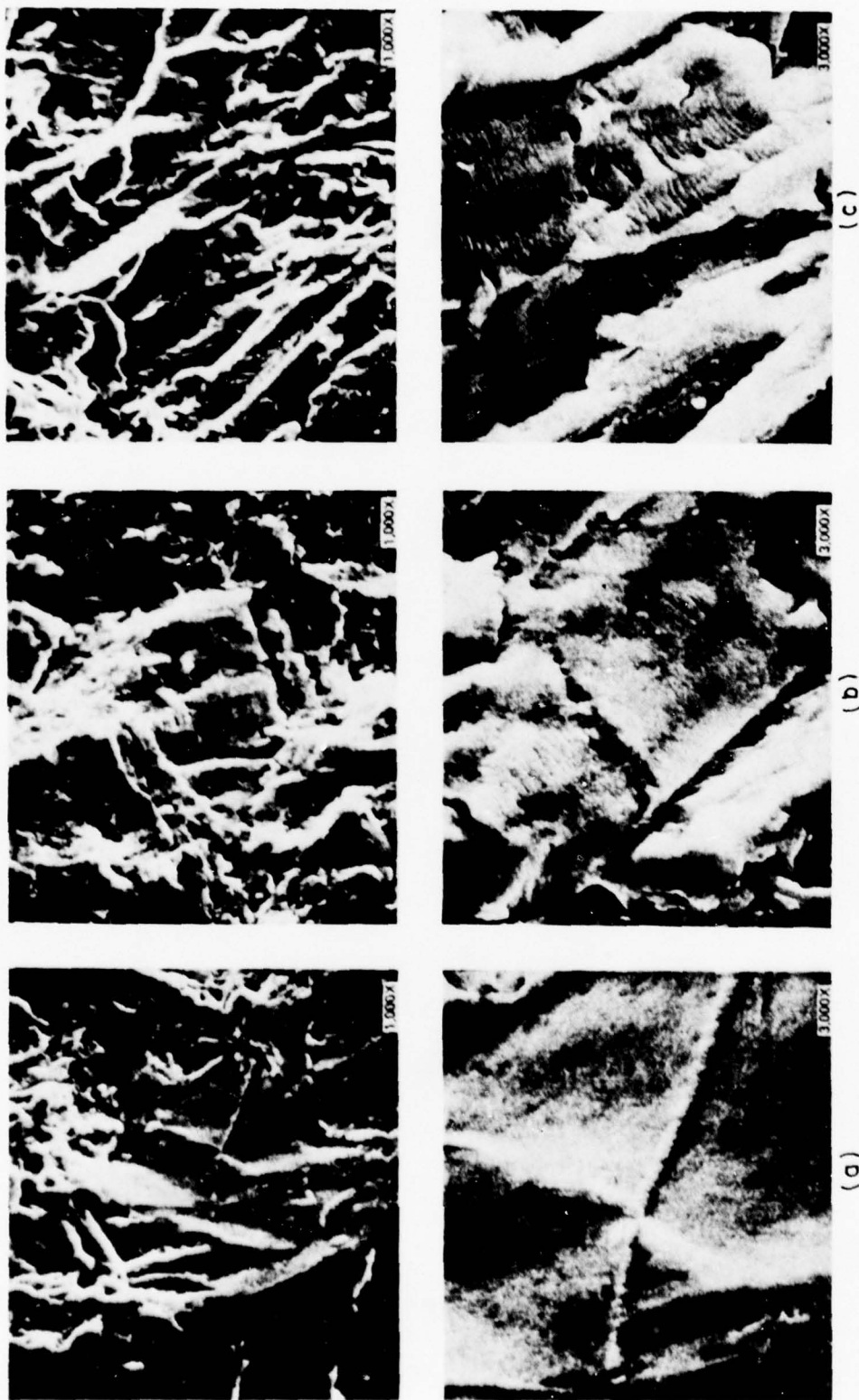


Figure 121. Enlargement of fractograph in Areas A, B, and C of a HIP keel splice former shown in Figure 117.  
(Reduced ~30% in printing)

The varying load, the difficulty of locating and identifying the load spikes and the dimensional differences in the keel splice formers complicates the results so that firm conclusions regarding crack initiation, crack growth, and retardation behavior cannot be made relative to the two types of fabrication. In earlier work, it was found that the notched fatigue life of the HIP specimens was higher; however, microstructural differences observed in this HIP batch were sufficiently different that it may be questionable if such superiority is carried through. In addition, the crack growth curves representative of the two types of fabrication were very similar with the possible exception at the low stress intensity portion of the  $da/dN$  vs.  $\Delta K$  curve. Thus, if any improved life is attributed to the HIP specimens, it should be primarily reflected in the crack initiation phase of the total life. Additional tests would be required to determine the effect of microstructural differences on the crack initiation, crack growth and retardation behavior of powder metallurgy - HIP components.

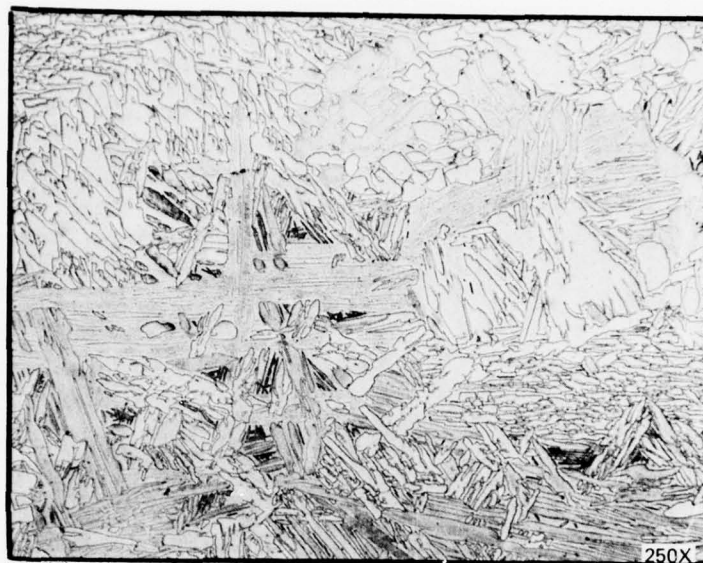
### 3.2.2.8 Prolongations

The keel splice formers were HIPed with integral prolongations approximately 3/8" dia. x 3-1/2" long, suitable for tensile test specimens. Although the prolongations and the keel splices were identified numerically before separation, the identity of the keel splices was inadvertently lost during machining. In addition, the keel splices and the prolongations were heat treated separately. This heat treatment consisted of 1300°F, two hours, air cool. The prolongations were machined to standard 3/8" diameter round threaded tensile specimens and tested according to the requirements of ASTM E8. The results are shown in Table 65. The tensile strengths were higher than obtained previously to qualify the powder lot and HIP cycle. In addition, the low yield strength for three of the specimens, (specimens 409, 411, and 421) and the low ductility of one specimen (409) also did not conform to previous results. A metallographic examination disclosed that the microstructures shown in Figures 122 and 123 were dissimilar from that previously observed. Instead of coarse alpha laths, the structure consisted of acicular or serrated alpha.



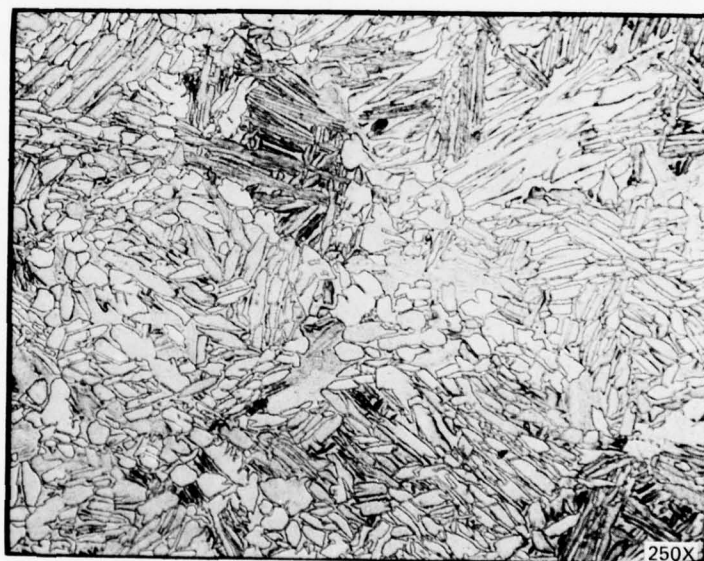
TABLE 65  
TENSILE TEST DATA FOR PROLONGATIONS FROM  
HIP KEEL SPLICE FORMERS

Identification	Strength (ksi)		% Elong. in 1 in.	Reduction of Area
	F <sub>tu</sub>	F <sub>ty</sub>		
SM-409	154	116	8	11
411	152	103	14	32
412	156	122	14	29
415	146	125	15	36
416	144	121	15	37
417	142	122	15	38
418	137	122	17	39
419	142	126	16	38
420	143	126	14	38
421	141	118	17	36
422	144	126	15	36



SM-409

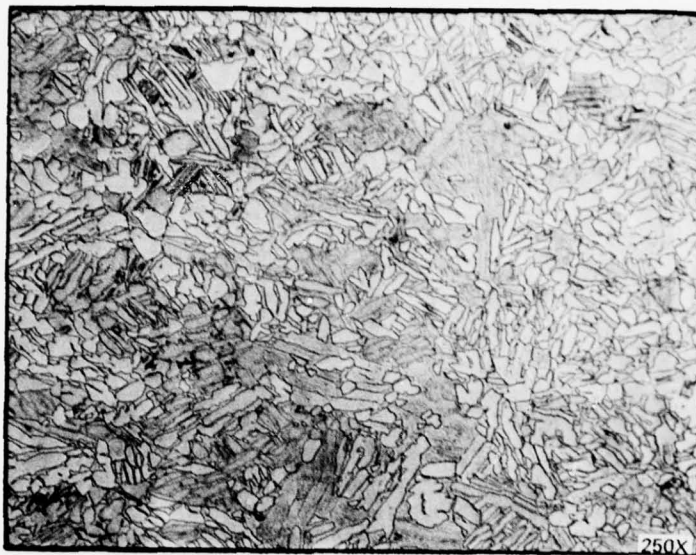
Properties:  $F_{tu}$  - 154 ksi      8% Elong.  
 $F_{ty}$  - 116 ksi      11.2% Red. of Area



SM-411

Properties:  $F_{tu}$  - 152 ksi      8% Elong.  
 $F_{ty}$  - 103 ksi      31.7% Red. of Area

Figure 122. 250X microstructure of prolongation from keel splice formers SM-409 and SM-411 annealed at 1300 F, 2 hours, air cooled.



SM-412

Properties:  $F_{tu}$  - 156 ksi    14% Elong.  
 $F_{ty}$  - 122 ksi    29.3% Red. of Area



SM-415

Properties:  $F_{tu}$  - 146 ksi    15% Elong.  
 $F_{ty}$  - 125 ksi    35.9% Red. of Area

Figure 123. 250X microstructure of prolongation from keel splice formers SM-412 and SM-415 annealed at 1300 F, 2 hours, air cooled.

To determine if the prolongation heat treatment was the cause of the anomalous results, sub-size flat tensile specimens were cut from the vertical divider of the keel splice former. The specimen geometry is shown in Figure 124. Prior to machining, the specimens were stress relieved at 1150°F for one hour to remove any cold working introduced during the test. The results are shown in Table 66. With one exception, the results approximated those obtained on the HIP cycle qualification, namely 137 ksi  $F_{tu}$  and 127 ksi  $F_{ty}$ . Geometry and gauge length differences prevented comparison of the elongation. Specimen No. HF-6, however, did show a low yield strength.

The microstructures of these specimens shown in Figure 125 suggest the reason for the variation of properties. The structure of HS-2 is typical of that previously observed and consists of coarse alpha laths. The structure of HF-5 is a mixture of primary alpha, coarse alpha laths and some finer acicular alpha. The structure of HF-6 is typical of beta processing and consists of Widmanstatten alpha with fine and coarse alpha laths and grain boundary alpha. The properties of HF-6 reflects this microstructure, namely a lower yield strength. This variation in microstructure is attributed to localized variations in the beta transus temperature due to chemistry variations from particle to particle. This phenomenon has been observed in the Ti-17 alloy as well, and an effort is being made to accurately establish the cause and, then, formulate a corrective or preventive action.

#### 3.2.2.9 Summary - Keel Splice Former

The PM approach to near-net shape part production has been fully demonstrated with the Ti-6-4 alloy. Keel splice former supplementary tests were evaluated and found to be equivalent to cast and wrought Ti-6-4.

A pilot lot of HIP shapes was produced and component tested. These were found to be equivalent to the current forged parts under both static and spectrum fatigue loading. All parts passed MCAIR NDI test standards. Dimensional analysis of the pilot run met all engineering drawing dimensional requirements with the minimum machining envelope goals of one pound per part total weight being attained.



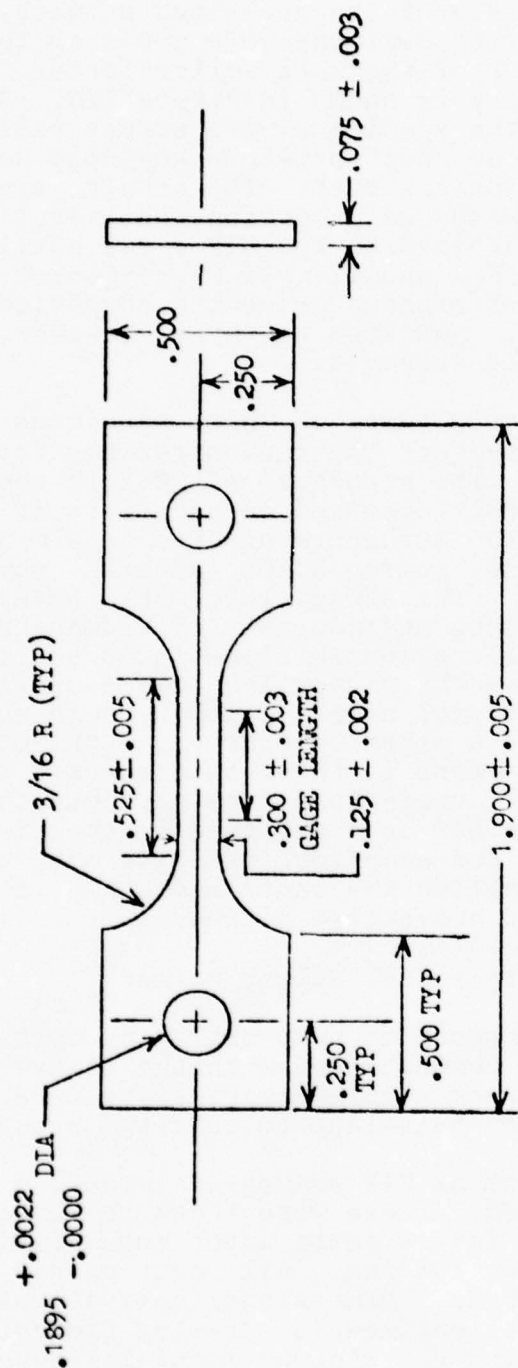


Figure 124. Tensile specimen geometry.

TABLE 66

TENSILE TEST DATA FOR SPECIMENS REMOVED  
FROM KEEL SPLICE FORMERS

Identification	Strength (ksi)		% Elongation in 0.3 in.
	F <sub>tu</sub>	F <sub>ty</sub>	
HS-2	137	126	22
HF-5	137	124	14
HF-6	141	117	18
FF-5	132	126	14
FF-6	140	132	14

Identification Code -: H-HIP, F-Forced (First Letter)  
F-Fatigue, S-Static Test (Second Letter)



(a) HS-2  
Static Test  
Specimen



(b) HS-5  
Spectrum Fatigue  
Specimen



(c) HS-6  
Spectrum Fatigue  
Specimen

GP76 0603 22

Figure 125. Microstructure of keel splice formers.

In addition, chem-milling evaluations on one keel splice under standard conditions used at MCAIR resulted in a finished part to engineering drawing requirements after only ten minutes in the bath. Although more control of surface and flatness would be required on the as-HIP part, chem-milling should be a viable cost effective process to replace the finish machining steps.

### 3.2.3 Task III - Economic Analysis and Final Material and Process Specifications

#### 3.2.3.1 Economic Analysis

##### Ti-17 Compressor Stub Shaft

The original goals of the contract were not completely realized with respect to the compressor stub shaft due to continuing problems with low cycle fatigue levels. Although shape making technology by the HIP ceramic mold process was successfully demonstrated, final machining and testing of the part was not carried to completion.

However, based on previous data and the weight and relative costs of material and processing, certain comparative values may be obtained. The original rationale for the contract was the high potential for cost savings through the application of PM processes to components which had poor material utilization rates as rough forgings. These include most disc forgings, compressor castings, and conical shafts. Titanium alloy applications in the F-101 engine are shown in Table 67. The approximate material utilization rates are given for a number of these parts. The fan discs and stages 1 and 2 compressor discs have integral conical shafts or spacers which add greatly to forging weight. The conical stub shaft requires several forging operations and because of this, material utilization is highly inefficient. Thus, the compressor stub shaft was chosen as a prime example of a component that could be produced by PM techniques to near-net shape with highly efficient material utilization rates. Savings would accrue both from lower input weight and reduced machining.



TABLE 67

## F-101 ENGINE TITANIUM COMPONENTS

Component Name	Material	Approx. Rough Forging Weight	Machined Forging Shipped Weight (sonic)	Final Part Weight	Material Utilization	
					Shipped Sonic Shape	Final Part
Stage 1 Fan Disc	Ti-17	350	109	52	3.2	6.7
Stage 2 Fan Disc	Ti-17	400	105	53	3.8	7.5
Forward Stub Shaft	Ti-6-4	59	17	6	3.5	9.8
Aft Stub Shaft	Ti-6-4	93	30	13	3.1	7.2
Fan Casing	Ti-6-4	242	220	95	1.1	2.5
Stage 1 Compressor Disc	Ti-17	120	77	31.6	1.6	3.8
Stage 2 Compressor Disc	Ti-17	120	77	31.6	1.6	3.8
Stage 3 Compressor Disc	Ti-17	105	55	11.8	1.9	8.9
Compressor Casing	Ti-6-4	310	236	52	1.3	6.8
*Compressor Stub Shaft	Ti-17	170	70	11.3	2.4	15.0
Compressor Aft Casing	Ti-6-4-2	520	180	52	2.9	10.0
TOTALS		2489	1176	383.3	2.1	7.4

\*Component selected for study on this program.

General Electric furnished an estimate of the economic impact of producing the F-101 compressor stub shaft in the Ti-17 alloy using the powder metallurgy techniques described in this report. Since the full-scale powder metallurgy stub shafts were not finish machined, General Electric considers this estimate to be tentative. The cost estimate was made as a ratio of projected costs for powder metallurgy product to current costs for cast and wrought product, each projected to the 250th unit of production.

The cost of the cast and wrought component at the 250th unit was extrapolated from the current quantity on a learning curve. This cost is for a targeted, qualified component delivered on the General Electric dock. The cost of the 250th powder metallurgy component is based on Crucible's estimate of the selling price of a targeted, qualified component delivered on the General Electric dock. The decreased cost of rough machining of the smaller powder metallurgy component was considered in the analysis. All costs are in early 1978 dollars, and do not take into account the recent increases in titanium billet costs, which would have more impact on the heavier cast and wrought component than on the lighter powder metallurgy component. The results of this analysis reveals that at the sonic shape, the powder metallurgy component would cost 68.5% of that of a cast and wrought component.

#### Keel Splice Former

A cost comparison analysis of the forged and HIP keel splice former was carried out by MCAIR. The guidelines for the cost analysis were as follows:

##### A. HIP

Powder Cost -	\$25 per lb./\$10 per lb.
Powder Amount -	Finished weight x 2.5
Shape -	Quote from Crucible based on buy of 162 pieces.
Machining -	Cost of rough cut eliminated from current actual cost of machining.
Tooling -	Included in shape cost.

##### B. Forging

Shape -	Actual procurement costs on last buy.
Machining -	Actual machining costs.
Tooling -	None (Dies available).

Technical requirements were taken from MIL-F-83142, "Forgings, Titanium Alloys, Premium Quality", for the forging analysis and Final Specification No. 5114-4, "Premium Quality, Powder Metallurgy As-Hot Isostatic Pressed (HIP) Ti-6-4 Titanium Base Alloy Parts" for the HIP parts.

The results of the cost analysis are shown in Table 68. The differences between the costs of HIP and forging are relatively small. Because the keel splice former is small and relatively simple, it is not an ideal part for demonstrating potential cost savings that can be accrued by the powder metallurgy HIP process.

Examination of the cost figures shows that machining is the most expensive processing step. By improving the HIP process to eliminate those factors which presently preclude chem-milling to size, there is a potential for a major cost reduction by eliminating or minimizing the need for machining. This combination of processes, HIP-Chem-Mill, should be further explored to fully derive the benefits of HIP method of fabrication.

TABLE 68

COST ANALYSIS FOR THE KEEL SPLICE FORMER  
68A333019-2007 FABRICATED BY FORGING AND  
BY POWDER-HIP PROCESS

	Forged and Machined	HIP and Machined (Powder @ \$25/lb.)	HIP and Machined (Powder @ \$10/lb.)
Material	\$53	\$66	\$49.50
Machining	\$98	\$78	\$78.00
Total	\$151	\$144	\$127.50

### 3.2.3.2 Final Material and Process Specifications

The preliminary specifications developed from the results of the Phase I effort on the Ti-17 alloy and the sub-scale stub shaft were reviewed for changes by G.E. based on the Phase II results.

Similarly, the preliminary specifications developed from the results of the Phase I effort on the Ti-6-4 alloy and the keel splice former were reviewed for changes again based on the Phase II effort.

The tentative specifications are given in Appendices F through I to this report and cover the material and processing areas as noted below:

- 1) Tentative Specification #5114-1 "Prealloyed Titanium Powder"
- 2) Tentative Specification #5114-2 "Hot Isostatic Pressing (HIP) of Titanium Alloy Powder"
- 3) Tentative Specification #5114-3 "Premium Quality Powder Metallurgy As-Hot Isostatic Pressed (HIP) Ti-17 Titanium Alloy Powder"
- 4) Tentative Specification #5114-4 "Premium Quality Powder Metallurgy As-Hot Isostatic Pressed (HIP) Ti-6-4 Titanium Base Alloy Parts"

These final specifications were reviewed and coordinated with both the users and the AFML.



## SECTION IV

### CONCLUSIONS AND RECOMMENDATIONS

#### 4.1 CONCLUSIONS

The ability to produce cost effective, high quality, near-net shapes of titanium engine and airframe components from a PM HIP process has been successfully demonstrated. Work conducted in achieving this objective established the following:

- 1) The REP powder, as received, contained tungsten, iron and non-metallic inclusions; the latter being detrimental to low cycle fatigue life.
- 2) All mold materials were found to be satisfactory for shape development, but SiO<sub>2</sub> was chosen for cost and availability.
- 3) Optimum HIP parameters established for the two alloys were:  
  
Ti-17      Heated autoclave, 1650°F temperature  
            at 15,000 psi with an 8 hour hold.  
  
Ti-6-4      Heated autoclave, 1750°F temperature  
            at 15,000 psi with an 8 hour hold.
- 4) Tensile and fracture toughness characteristics of alpha-beta HIP and beta HIP Ti-17 material compare favorably with wrought material specifications.
- 5) Post compaction thermal treatment is neither necessary nor beneficial.
- 6) All potential causes for degraded LCF behavior were evaluated, with inclusions from processing handling in the REP powder still remaining as the major reason for the poor LCF results.
- 7) The mechanical properties obtained on the compressor stub shaft were satisfactory. However, the LCF behavior was severely degraded due to non-metallic inclusions and would not be adequate for use at high stress levels.

- 8) Higher oxygen content powder (0.166%) was required for the Ti-6-4 alloy to meet mechanical property specifications.
- 9) The Ti-6-4 alloy did not display the fatigue problems encountered with the Ti-17 alloy.
- 10) The HIP Ti-17 stub shaft can be ultrasonically inspected to the required specifications.
- 11) The HIP keel splice former parts passed both radiographic and dye penetrant inspection to MCAIR quality specifications.
- 12) The PM approach to near-net shape part production has been fully demonstrated with both the Ti-17 and Ti-6-4 alloy components.
- 13) Chem-milling should be a viable cost effective process to replace the finish machining steps on the keel splice former.
- 14) The results of the cost analysis on PM HIP versus cast and wrought processes indicate that PM near-net shape processing is cost effective.

#### 4.2 RECOMMENDATIONS

The successful conclusion to the concept of PM near-net shape part production provided a firm foundation from which a final manufacturing process can be established. The following areas are recommended for further investigation to fully establish a low cost process for titanium engine aircraft and air-frame component manufacture:

- 1) Investigation of new or improved powder manufacturing techniques for titanium alloy to produce higher purity powder at lower cost.
- 2) Investigation of greater control of shape making technology to minimize or eliminate final machining steps.
- 3) Evaluate the effect of chem-milling in conjunction with improved shape surface texture for minimizing or eliminating finish machining steps.

- 4) Expand the application of PM near-net shape technology to additional aircraft engine and airframe components in future programs for more cost effective production capability with respect to bigger and more complex parts.

## APPENDIX A

SUMMARY OF ALL ELECTRODE SHIPPED TO  
NUCLEAR METALS FOR CONVERSION TO POWDER



TABLE A-1  
Ti-6-4 ELECTRODE SUMMARY

Code	lbs.	Length inches	Code	lbs.	Length inches	Code	lbs.	Length inches
AT1	6.68	8.54	AC1	6.77	8.67	AX1	6.71	8.60
	6.67	8.53		7.50	9.63		6.87	8.81
	6.75	8.65		5.94	7.61		6.73	8.60
	6.83	8.77		6.80	8.70		6.70	8.60
	6.67	8.53		6.77	8.65		6.74	8.63
	<u>33.60</u>			<u>33.78</u>			<u>33.75</u>	
AT2	6.87	8.78	AC2	6.892	8.83	AX2	6.86	8.80
	6.91	8.82		6.85	8.78		6.83	8.71
	6.89	8.80		6.92	8.84		6.82	8.70
	6.89	8.80		6.87	8.80		6.86	8.80
	6.865	8.80		6.88	8.83		6.83	8.73
	<u>34.425</u>			<u>34.412</u>			<u>34.20</u>	
AT3	6.92	8.85	AC3	6.86	8.82	AX3	6.88	8.83
	6.86	8.75		6.98	8.90		6.89	8.82
	6.86	8.78		6.98	8.90		6.91	8.85
	6.92	8.85		6.96	8.90		<u>20.68</u>	
	6.87	8.78		7.00	8.94			
	<u>34.43</u>			<u>34.78</u>				
AT4	6.69	8.56	AC4	6.74	8.61	AX4	6.81	8.72
	6.71	8.60		6.65	8.50		6.81	8.72
	6.62	8.48		6.70	8.57		6.875	8.80
	6.66	8.54		6.68	8.54		6.966	8.93
	6.70	8.58		6.65	8.50		6.77	8.68
	<u>33.38</u>			<u>33.42</u>			6.507	8.34
							6.36	8.14
							<u>47.098</u>	
AT5	6.95	8.90	AC5	7.00	8.92	AX5	6.96	8.93
	6.94	8.88		7.00	8.94		7.00	8.98
	6.91	8.90		6.75	8.65		6.97	8.92
	6.95	8.87		7.03	9.04		7.00	8.96
	7.03	9.00		6.98	8.94		7.06	9.04
	<u>34.78</u>			<u>34.76</u>			<u>34.99</u>	
AT6	7.78	9.98	AC6	6.68	8.55	AX6	6.60	8.46
	7.79	9.99		6.65	8.51		7.13	9.12
	7.78	9.98		6.56	8.38		6.52	8.34
	7.81	10.00		6.70	8.58		6.50	8.34
	<u>31.16</u>			6.64	8.50		6.57	8.42
				<u>33.23</u>			<u>33.32</u>	

Total weight: 610.195 lbs.

TABLE A-2  
Ti-17 ELECTRODE SUMMARY

<u>Code</u>	<u>lbs.</u>	<u>Length</u> <u>inches</u>	<u>Code</u>	<u>lbs.</u>	<u>Length</u> <u>inches</u>	<u>Code</u>	<u>lbs.</u>	<u>Length</u> <u>inches</u>
BT1	6.70	8.13	BC1	6.70	8.10	BX1	6.75	8.22
	6.77	8.24		6.91	8.40		<u>6.79</u>	8.20
	6.73	8.17		6.91	8.40		13.54	
	6.73	8.17		6.99	8.48			
	<u>6.73</u>	8.17		<u>6.92</u>	8.37			
	33.66			34.43				
BT2	7.82	9.48	BC2	7.90	9.57	BX2	7.78	9.38
	7.82	9.50		7.56	9.18		7.77	9.40
	7.82	9.48		7.96	9.64		7.79	9.44
	<u>7.90</u>	9.57		<u>7.85</u>	9.50		<u>7.75</u>	9.40
	31.36			31.27			31.09	
BT3	6.83	8.28	BC3	8.19	9.90	BX3	6.86	8.30
	6.82	8.26		8.20	9.94		6.81	8.23
	6.83	8.30		8.18	9.90		6.82	8.25
	6.81	8.25		<u>8.27</u>			6.86	8.29
	<u>6.83</u>	8.25		32.84			<u>6.73</u>	8.15
	34.12						34.08	
BT4	6.63	8.06	BC4	8.27	10.00	BX4	6.59	8.00
	6.63	8.05		8.16	9.90		6.59	7.98
	6.70	8.16		8.17	9.93		6.63	8.10
	6.70	8.12		<u>8.17</u>	9.93		6.61	8.05
	<u>6.75</u>	8.20		32.77			<u>6.62</u>	8.03
	33.41						33.04	
BT5	6.80	8.20	BC5	8.20	9.94	BX5	6.72	8.18
	6.75	8.18		8.23	10.00		6.80	8.26
	6.62	8.04		8.22	8.94		6.82	8.30
	6.74	8.18		<u>8.23</u>	10.00		6.73	8.14
	<u>6.78</u>	8.20		32.88			<u>6.94</u>	8.45
	33.69						34.01	
BT6	6.75	8.18	BC6	8.24	10.00	BX6	6.88	8.33
	6.78	8.23		8.19	9.90		6.81	8.24
	6.80	8.26		8.27	10.00		6.77	8.20
	6.88	8.30		<u>8.25</u>	10.00		6.79	8.24
	<u>6.79</u>	8.20		32.95			<u>6.86</u>	8.30
	34.00						34.11	

Total weight: 577.25

APPENDIX B

TEST DATA FOR Ti-17

TABLE B-1

ROOM TEMPERATURE PROPERTIES OF SUB-TRANSUS  
HIP Ti-17 ALLOY (BCL AUTOCLAVE)

Compact	Condition	Evaluation*	Strength (ksi)		Modulus (psi x 10 <sup>6</sup> )	El (%)	RA (%)	Charpy, Kq (ksi $\sqrt{\text{in.}}$ )
227	As-HIP	C	F <sub>tu</sub>	F <sub>ty</sub>	17.4 17.6 -	16.0 10.0 12.8	40.1 15.4 26	- - 48.0
	PCTT	C	163.3	157.5				
	PCTT	G	161.0 167.1	156.0 160.9				
233	As-HIP	C	162.1	156.3	15.2 17.0 -	15.0 13.0 14.5	32.5 36.5 35	- - 44.0
	PCTT	C	165.3	159.3				
	PCTT	G	168.6	161.9				
236	As-HIP	C	163.6	157.2	17.8 -	15.0 14.5	39.5 35	- 49.8
	As-HIP	G	165.2	158.7				
248	As-HIP	C	167.0	160.0	16.5 16.4 -	14.0 14.0 10.5	38.0 21.8 27.3	- - 44.0
	PCTT	C	166.2	154.5				
	PCTT	G	171.7	165.9				
250	As-HIP	C	167.4	161.7	15.7 16.0 -	15.0 11.0 12.2	32.3 16.5 29.6	- - 48.2
	PCTT	C	168.0	156.9				
	As-HIP	G	164.5	159.3				
252	As-HIP	C	166.6	158.4	16.1 -	15.0 12.2	32.5 34.7	- 46.8
	As-HIP	G	164.3	157.9				
Average $\sigma^2$ $\sigma$	As-HIP		164.9	158.6	16.5 1.0 1.0	14.3 1.7 1.3	34.9 13.0 3.6	48.3 2.3 1.5
			3.3	2.6				
			1.8	1.6				
Average $\sigma^2$ $\sigma$	PCTT		166.8	159.3	16.8 0.5 0.7	12.3 3.1 1.8	25.5 68.6 8.3	45.3 5.3 2.3
			10.8	15.4				
			3.3	3.9				

Wrought Ti-17  
Specification $\alpha - \beta$ 163 min  
153 min7 min  
15 min

30 min

\*C, CMRC - single value  
G, GE - Avg. of 2 values



TABLE B-2

ROOM TEMPERATURE PROPERTIES OF SUB-TRANSUS  
HIP Ti-17 ALLOY (CSMD AUTOCLAVE)

Compact	Condition	Evaluation*	Strength (ksi)		Modulus (psi x 10 <sup>6</sup> ) E	E1 (%)	RA (%)	Charpy, Kq (ksi $\sqrt{\text{in.}}$ )
			F <sub>tu</sub>	F <sub>ty</sub>				
254 #	As-HIP PCTT	C	112.5	-	13.5	<1	<1	-
		C	128.0	122.0	13.7	<1	<1	-
256 #	As-HIP PCTT	C	150.9	135.8	14.8	4.0	3.6	-
		C	151.9	141.9	12.2	4.0	6.0	-
264 #	As-HIP PCTT	C	156.3	148.2	15.6	3.0	7.8	-
		G						
265 #	As-HIP PCTT	C	109.8	-	13.3	<1	<1	-
		G	124.5	121.4	13.0	<1	<1	-
269 #	As-HIP As-HIP	C	150.3	144.3	15.4	1.0	3.2	-
		G						
270	As-HIP PCTT As-HIP	C	163.8	156.3	16.3	15.0	36.5	-
		C	161.7	151.2	15.7	9.0	15.0	-
		G	164.8	157.5		12.2	34.0	46.4

Wrought Ti-17  
Specification $\alpha - \beta$ 163  
min153  
min7  
min15  
min30  
min\*C, CMRC - single value  
G, GE - Avg. of 2 values

# Contained considerable porosity, i.e., 2% or more.

TABLE B-3

ROOM TEMPERATURE PROPERTIES OF  
BETA-HIP Ti-17 ALLOY

Compact	Condition	Evaluation*	Strength (ksi)		Modulus (psi x 10 <sup>6</sup> ) E	El (%)	RA (%)	Charpy, K <sub>q</sub> (ksi√in.)
			F <sub>tu</sub>	F <sub>ty</sub>				
237	As-HIP	C	161.0	151.8	15.8	5.0	9.6	-
	As-HIP	G	163.6	156.0	-	5.3	8.5	59.2
	PCTT	C	161.7	153.6	16.7	5.0	11.2	-
238	As-HIP	C	161.8	153.3	16.4	8.0	16.0	-
	PCTT	C	160.5	150.9	16.5	5.0	11.3	-
	PCTT	G	167.0	161.2	-	3.5	6	49.8
243	As-HIP	C	164.7	155.1	16.4	8.0	13.4	-
	PCTT	C	163.0	153.0	16.7	5.0	10.2	-
	PCTT	G	171.4	165.2	-	4.3	6	49.3
261	As-HIP	C	166.4	153.0	15.9	10.0	16.2	-
	PCTT	C	164.0	153.9	16.6	5.0	10.5	-
	PCTT	G	170.0	162.1	-	5.0	9.8	54.0
274	As-HIP	C	164.3	154.2	16.0	8.0	11.6	-
	As-HIP	G	164.7	156.7	-	9.4	24.2	54.8
	PCTT	C	162.3	151.8	16.2	6.0	10.8	-
275	As-HIP	C	164.8	155.1	16.3	13.0	27.8	-
	As-HIP	G	165.0	157.1	-	9.8	25.8	53.6
Average $\sigma_2$ $\sigma$	As-HIP		164.1	154.7	16.1	8.5	17.0	55.9
			2.8	3.2	0.1	6.0	52.0	8.7
			1.7	1.8	0.3	2.5	7.2	2.9
Average $\sigma_2$ $\sigma$	PCTT		165.0	156.5	16.5	4.9	9.5	51.0
			16.2	30.0	0.04	0.5	4.8	6.7
			4.0	5.5	0.2	0.7	2.2	2.6
Wrought Ti-17 Specification			163 min	153 min		5 min	10 min	50 min
			$\beta$					

\*C, CMRC - single value  
G, GE - Avg. of 2 values

TABLE B-4

LOW-CYCLE FATIGUE RESULTS  
 $A=1.0$ ,  $K_t=1.0$ , LOAD CONTROL

No.	Stress (ksi)	Cycles to Failure	Observation of Fracture Origin
233	150	6,559	Fe-rich particle
	140	7,573	Inclusion of Fe, Mn, K, Ca, Si, Cr (?)
237	150	6,858	Inclusion of Fe, Mn, K, Ca, Si
	140	10,115	N/A*
236	150	11,971	N/A*
	130	20,887	High Al at failure origin
227	140	14,502	N/A
	130	16,262	N/A
250	130	8,896	Inclusion of Fe, Ca, Si, Mn
	120	5,147	Inclusion, N/A
252	140	16,659	Inclusion, N/A
	130	45,510	Inclusion, analysis pending
270	140	10,593	Inclusion, N/A
	130	8,864	Inclusion, analysis pending
275	140	24,445	N/A
	130	23,444	Inclusion, analysis pending

---

\*N/A, not analyzed

TABLE B-5

HIGH-CYCLE FATIGUE RESULTS  
 $A = \infty$ ,  $K_t = 1.0$ , ROTATING BEAM

No.	Stress (ksi)	<u>Cycles to Failure</u> (x 1000)	Remarks
227	90	44	
	70	2,741	
233	90	52	
	75	393	
236	85	50	
	77.5	64	
237	80	1,386	
	75	> 44,000	Did not fail
250	80	46	
	65	62	
252	70	261	
	60	> 46,000	Did not fail
	SL 75	5,314	
270	80	192	
	67.5	9,263	Si-rich inclusion at fracture origin
275	90	192	
	70	9,943	
	SL 85	12,070	



APPENDIX C  
TEST DATA FOR T1-6-4

TABLE C-1  
TENSILE PROPERTIES OF ANNEALED  
ELI Ti-6-4 (CMRC)

Compact	Type of Cycle	Condition	Strength (ksi)		Modulus (psi x 10 <sup>6</sup> ) E	E1 (%)	RA (%)
			F <sub>tu</sub>	F <sub>ty</sub>			
277	CSMD	As-HIP	120.8	110.8	16.4	20.0	46.3
		PCTT	118.5	111.0	16.2	12.0	24.6
281	CSMD	As-HIP	121.5	112.4	16.2	19.0	45.5
		PCTT	119.0	109.8	15.9	16.0	25.4
284	CSMD	As-HIP	120.5	110.4	16.7	20.0	46.1
		PCTT	121.0	109.6	16.7	17.0	38.1
279	BCL	As-HIP	122.5	114.0	15.9	18.0	45.6
		PCTT	119.4	109.4	16.4	17.0	44.3
287	BCL	As-HIP	122.5	113.6	15.9	18.0	45.6
		PCTT	117.9	109.2	16.4	19.0	45.6
293	BCL	As-HIP	122.7	113.6	16.3	18.0	45.5
		PCTT	118.7	109.2	16.5	18.0	43.8
Average σ <sup>2</sup> σ			121.75 0.88 0.94	112.47 2.39 1.55	16.2 0.09 0.3	18.8 0.96 0.98	45.8 0.12 0.34
Specification			130 min	120 min		10 min	

TABLE C-2

## TENSILE PROPERTIES OF ANNEALED ELI Ti-6-4 (MCAIR)

Compact Identification	Condition	Strength (ksi)		Modulus (psi x 10 <sup>6</sup> ) E	Elongation (%)	Reduction of Area (%)
		F <sub>tu</sub>	F <sub>ty</sub>			
277	AS-HIP	124.0	112.0	16.9	17	43.1
		124.0	112.0	17.1	17	43.9
279	PCTT*	122.0	109.0	17.0	12	22.9
		122.0	110.0	16.9	11	20.3
281	AS-HIP	128.0	117.0	17.1	17	45.0
		127.0	117.0	17.5	16	43.7
284	PCTT	122.0	109.0	17.1	17	43.7
		124.0	109.0	17.2	16	40.9
287	AS-HIP	121.0	108.0	17.7	17	44.0
		126.0	112.0	17.3	17	43.4
293	PCTT	127.0	117.0	17.6	17	44.1
		123.0	109.0	17.7	16	43.6
294	AS-HIP	124.0	112.0	17.1	16	43.7
		124.0	112.0	17.2	16	43.2
297	PCTT	124.0	109.0	16.9	15	39.2
		124.0	110.0	17.1	16	42.4
298	AS-HIP	128.0	118.0	17.1	17	43.7
		127.0	117.0	17.2	18	42.1
299	PCTT	122.0	110.0	17.0	18	42.5
		122.0	110.0	16.7	17	43.9
300	AS-HIP	127.0	117.0	17.3	17	43.5
		127.0	117.0	17.1	17	43.2
301	PCTT	124.0	113.0	16.6	18	44.7
		122.0	109.0	17.0	18	43.4
Average	AS-HIP	125.6	114.3	-	16.7	43.5
		4.6	10.5	-	0.3	0.5
σ <sub>L</sub>	AS-HIP	2.2	3.2	-	0.6	0.7

\*PCTT, Post-Compaction Thermal Treatment consisting of 2 hours diffusion anneal at HIP temperature.





TABLE D-1

DIMENSIONAL ANALYSIS OF SUB-SCALE STUB SHAFT  
FIRST ITERATION - SM-295

Dimension No.	Target Dimension	Compact SM-295
1	8.40 DIA.	8.405 DIA.
2	6.10 DIA.	5.880 DIA.
3	4.30 DIA.	4.060 DIA.
4	6.20 DIA.	6.125 DIA.
5	1.80 DIA.	1.640 DIA.
6	3.25 DIA.	3.015 DIA.
7	5.20	4.805
8	3.70	3.687
9	5.35	5.217
10	6.20	6.060

TABLE D-2

DIMENSIONAL ANALYSIS OF SUB-SCALE STUB SHAFT  
SECOND ITERATION - SM-324

Dimension No.	Target Dimension	Compact SM-324
1	8.40 DIA.	8.443 DIA.
2	6.10 DIA.	6.050 DIA.
3	4.30 DIA.	4.400 DIA.
4	6.20 DIA.	6.100 DIA.
5	1.80 DIA.	1.990 DIA.
6	3.25 DIA.	3.445 DIA.
7	5.20	4.050
8	3.70	2.820
9	5.35	4.415
10	6.20	5.150

TABLE D-3

DIMENSIONAL ANALYSIS OF SUB-SCALE STUB SHAFT  
THIRD ITERATION - SM-337

Dimension No.	Target Dimension	Compact SM-337
1	8.40 DIA.	8.400 DIA.
2	6.10 DIA.	6.080 DIA.
3	4.30 DIA.	4.480 DIA.
4	6.20 DIA.	6.200 DIA.
5	1.80 DIA.	2.23 DIA.
6	3.25 DIA.	3.540 DIA.
7	5.20	5.090
8	3.70	3.820
9	5.35	5.360
10	6.20	6.110

Table D-4

DIMENSIONAL ANALYSIS OF SUB-SCALE STUB SHAFT  
FOURTH ITERATION - SM-357

Dimension No.	Target Dimension	Compact SM-357
1	8.40 DIA.	8.480 DIA.
2	6.10 DIA.	6.050 DIA.
3	4.30 DIA.	4.320 DIA.
4	6.20 DIA.	6.200 DIA.
5	1.80 DIA.	2.250 DIA.
6	3.25 DIA.	3.380 DIA.
7	5.20	4.510
8	3.70	3.550
9	5.35	5.060
10	6.20	5.950

TABLE D-5

DIMENSIONAL ANALYSIS OF SUB-SCALE STUB SHAFT  
FIFTH ITERATION - (SM-368, -384, and -385)

Dimension No.	Target Dimension	SM-368	<u>Compacts</u> SM-384	SM-385
1	8.40 DIA.	8.500 DIA.	8.510 DIA.	8.500 DIA.
2	6.10 DIA.	5.980 DIA.	6.000 DIA.	5.990 DIA.
3	4.30 DIA.	-	-	-
4	6.20 DIA.	6.200 DIA.	6.270 DIA.	6.240 DIA.
5	1.80 DIA.	2.120 DIA.	2.140 DIA.	2.260 DIA.
6	3.25 DIA.	3.320 DIA.	3.330 DIA.	3.340 DIA.
7	5.20	-	-	-
8	3.70	-	-	-
9	5.35	5.950	5.980	6.010
10	6.20	6.910	6.890	6.890

TABLE D-6

DETAILED DIMENSIONAL ANALYSIS  
OF A PRODUCTION RUN OF FOUR KEEL SPLICE FORMERS

Dimension No.	Target Dimension	Compact SM-376	Compact SM-377	Compact SM-378	Compact SM-379
1	5/16 R	5/16 R	5/16 R	5/16 R	5/16 R
2	1.180	1.090	1.090	1.100	1.155
3	.710	.560	.680	.680	.680
4	3.020	3.040	3.040	3.052	3.065
5	5.165	4.960	4.965	4.950	4.950
6	27°56'	28°	28°	28°	28°
7	3/8 R	11/32	11/32 R	11/32 R	11/32 R
8	2.330	2.300	2.320	2.310	2.310
9	1.820	1.825	1.795	1.810	1.820
10	3.760	3.800	3.810	3.810	3.780
11	.224	.170	.185	.193	.200
12	1/8 R	1/8 R	1/8 R	1/8 R	1/8 R
13	5/16 R	5/16 R	5/16 R	5/16 R	5/16 R
14	.880	.890	.885	.885	.870
15	3.320	3.375	3.365	3.375	3.360
16	2.125	2.163	2.150	2.158	2.121
17	.180	.160	.163	.169	.175
18	1.180	1.140	1.120	1.130	1.190
19	1/8 R	1/8 R	1/8 R	1/8 R	1/8 R
20	.174	.165	.167	.172	.168
21	9°56'	10°	10°	10°	10°
22	1/2 R	7/16 R	7/16 R	7/16 R	1/2 R
23	.180	.160	.156	.167	.160
24	2.120	1.940	1.935	1.930	1.950



TABLE D-7  
 DIMENSIONAL ANALYSIS OF FULL-SIZE STUB SHAFT  
 FIRST ITERATION - SM-494

Dimension No.	Target Dimension	Compact SM-494
1	16.42 DIA.	16.80
2	13.72 DIA.	14.12
3	.78	.59
4	14.32 DIA.	14.68
5	3.29	3.21
6	4.16	4.25
7	7.70 DIA.	7.70
8	6.05 DIA.	6.06
9	5.84	5.75
10	5.77 DIA.	5.78
11	10.00	10.20
12	5.51 DIA.	5.53
13	13.49	13.75
14	3.76 DIA.	4.475
15	4.65	5.00
16	4.30	4.74
17	2.71	3.14
18	5.20	5.43
19	4.66	4.42
20	1.89	2.37
21	7.53 DIA.	7.37
22	1.94	2.30

TABLE D-8

DIMENSIONAL ANALYSIS OF FULL-SIZE STUB SHAFTS  
FINAL ITERATION - (SM-555, -556, and -557)

Dimension No.	"Z" Dimension	Target Dimension	Compact SM-555		Compact SM-556		Compact SM-557	
			Min. Envelope	Max. Envelope	Min. Envelope	Max. Envelope	Min. Envelope	Max. Envelope
1	.390	8.210	7.995	8.070	8.088	8.199	7.950	8.008
2	.780	7.700	.895	1.026	.906	.945	.885	.949
3	.780	7.300	.885	1.006	.894	.949	.867	.912
4	1.100	6.597	6.525	6.670	6.658	6.829	6.471	6.536
5	2.000	5.358	5.269	5.427	5.380	5.522	5.140	5.202
6	2.900	4.119	3.923	4.035	4.084	4.205	3.788	3.831
7	3.400	3.850	3.732	3.769	3.820	3.871	3.689	3.730
8	3.800	3.850	3.732	3.781	3.838	3.885	3.702	3.744
9	4.160	3.500	4.069	4.105	4.159	4.188	3.983	3.994
10	4.700	3.025	2.900	2.932	2.984	3.033	2.854	2.881
11	5.500	3.025	2.889	2.921	2.981	3.032	2.834	2.865
12	5.740	3.025	5.866	5.955	6.005	6.113	5.819	5.889
13	6.300	2.885	2.736	2.765	2.834	2.894	2.705	2.721
14	7.800	2.885	2.757	2.774	2.823	2.851	2.739	2.762
15	9.300	2.885	2.765	2.793	2.827	2.847	2.765	2.790
16	9.900	2.885	9.999	10.069	10.134	10.247	9.907	9.982
17	10.500	2.755	2.634	2.658	2.690	2.708	2.639	2.669
18	12.500	2.755	2.652	2.690	2.711	2.753	2.635	2.691
19	13.490	2.315	13.075	13.114	13.316	13.346	12.953	13.018
20	12.500	1.880	1.939	1.909	2.058	1.997	1.986	1.963
21	10.000	1.880	1.935	1.912	2.038	2.016	1.984	1.966
22	7.800	1.880	1.933	1.916	2.025	2.033	1.981	1.968
23	4.820	1.880	5.509	5.443	5.411	5.335	5.082	5.024
24	4.200	2.155	2.045	1.985	2.325	2.282	2.012	1.964
25	3.230	2.155	-	-	3.096	3.076	3.001	2.857
26	2.710	2.600	"Z"-2.692 2.740	2.699	"Z"-2.837 2.799	2.739	"Z"-2.500 2.720	2.680
27	2.200	2.330	"Z"-2.194	2.448	"Z"-2.306	2.473	"Z"-2.025	2.438
28	1.890	2.750	1.938	1.904	2.039	2.016	1.699	1.649
29	1.890	3.250	1.912	1.860	1.991	1.954	1.741	1.703
30	2.190	High Point	2.213	2.141	2.225	2.231	2.012	1.964
31	2.000	4.107	4.147	3.997	4.247	4.153	"Z"-1.805 4.088	4.019
32	1.500	4.795	4.876	4.712	4.974	4.897	4.542	4.424
33	1.000	5.484	5.629	5.426	5.693	5.584	5.301	5.220
34	.500	6.172	6.396	6.120	6.374	6.258	6.050	5.959
35	0	Drop Off Point	.192 (310°)	.028 (150°)	.089 (150°)	.049 (30°)	.026 (240°)	.005 (30°)
36	0	7.700	.154 (270°)	.007 (150°)	.034 (150°)	.001 (30°)	.047 (120°)	.004 (240°)

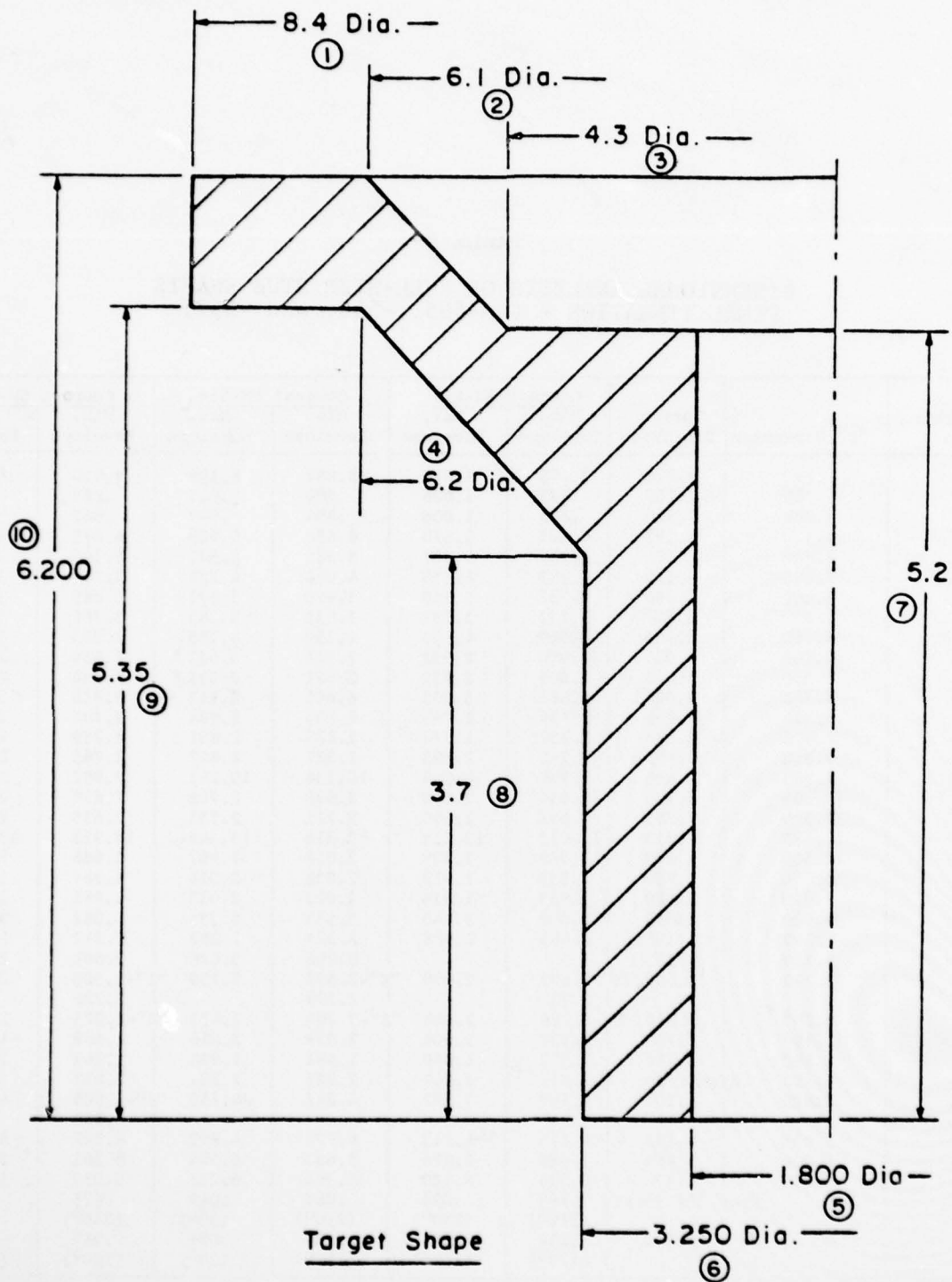


Figure D-1. Dimensional Reference Points - Sub-Scale Stub Shaft.

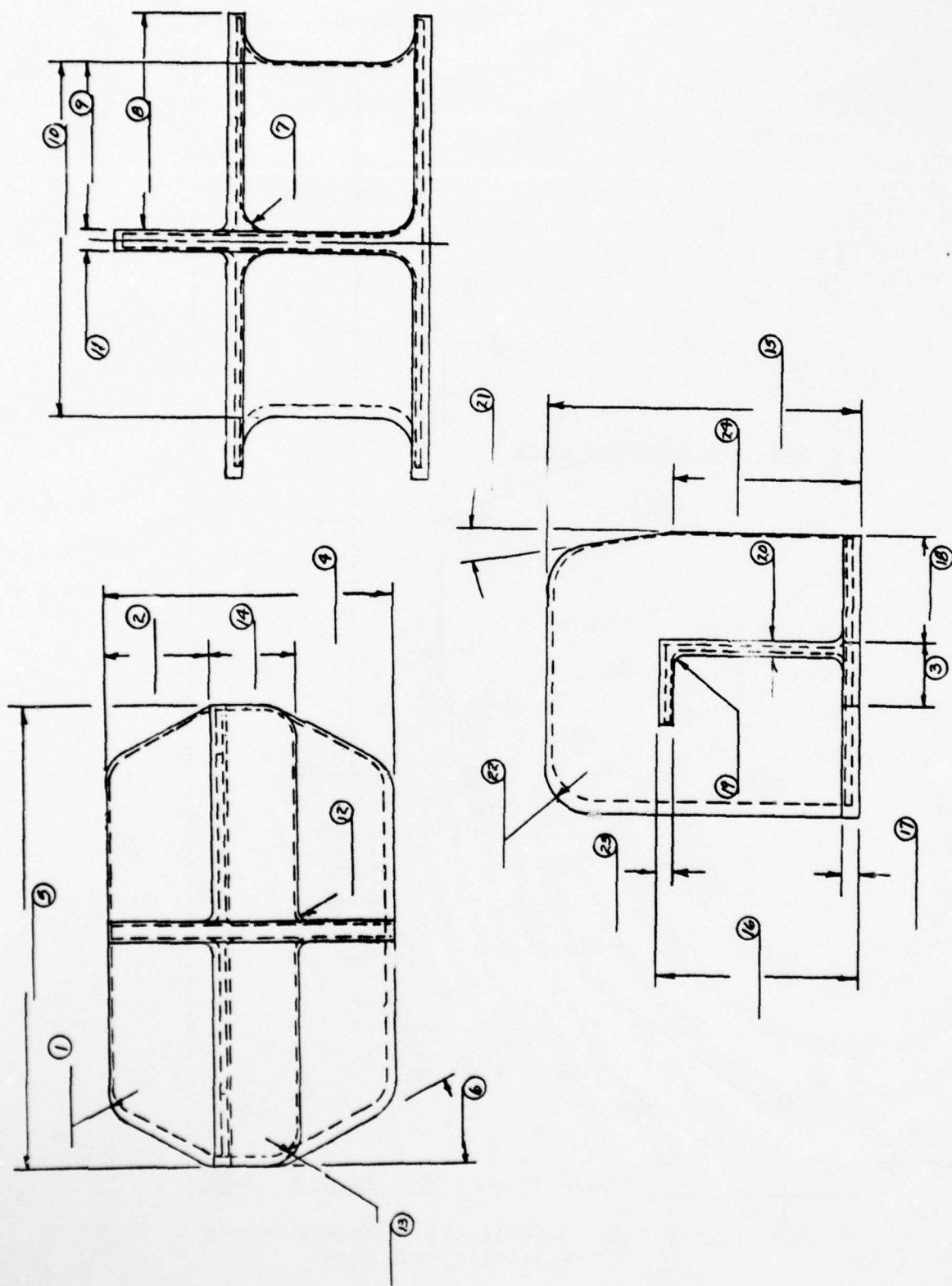


Figure D-2. Dimensional Reference Points - Keel Splice Former.



AD-A078 039

COLT INDUSTRIES INC PITTSBURGH PA CRUCIBLE MATERIALS--ETC F/6 11/6  
CONSOLIDATION OF TITANIUM POWDER TO NEAR NET SHAPES.(U)  
MAY 78 J H SCHWERTZ , V K CHANDHOK

F33615-74-C-5114

UNCLASSIFIED

AFML-TR-78-41

NL

4 OF 4

AD  
A078039



END  
DATE  
FILMED  
1-80  
DDC

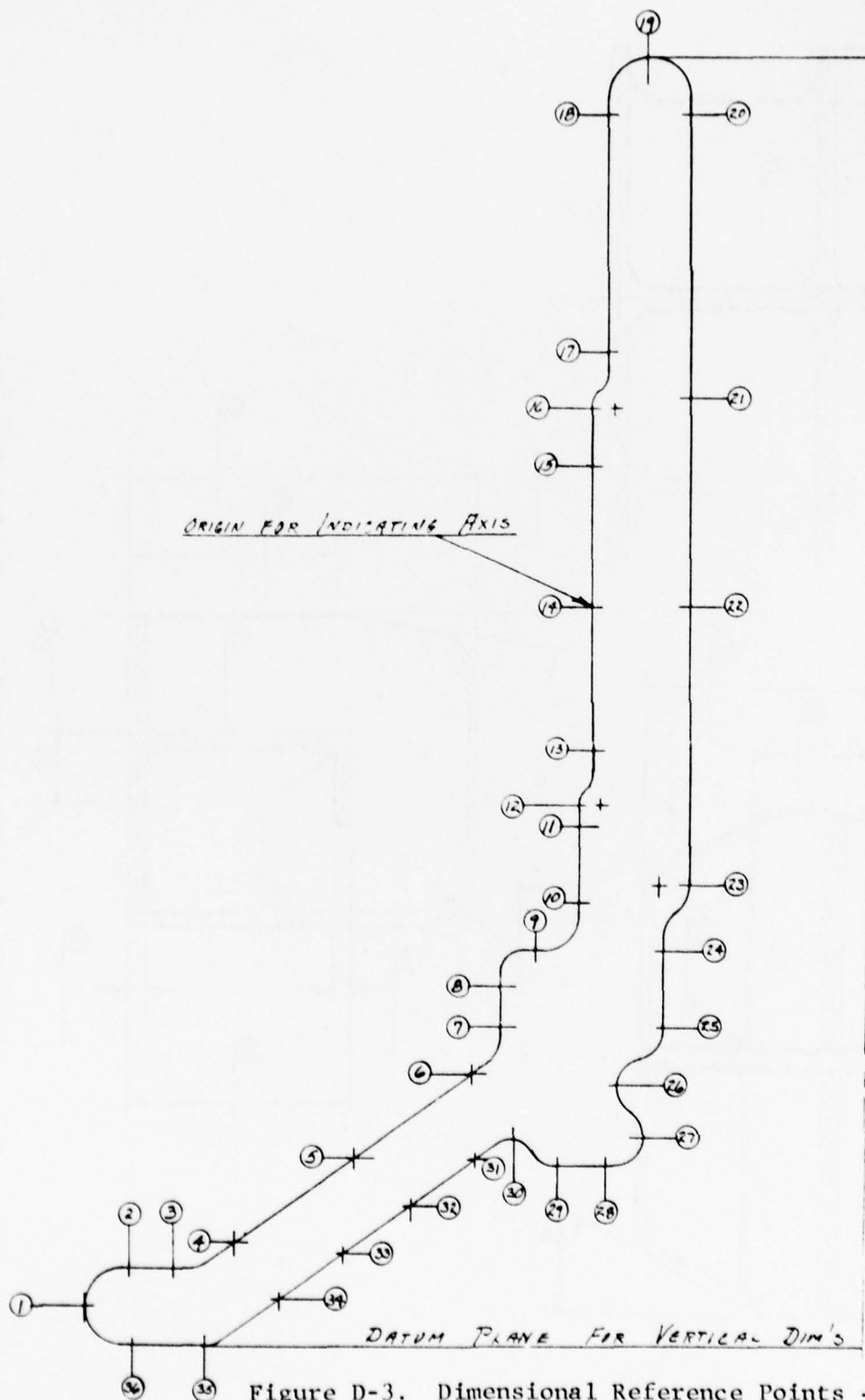


Figure D-3. Dimensional Reference Points - Full-Size Stub Shaft.

APPENDIX E  
CRACK GROWTH DATA FOR Ti-17

TABLE E-1

# CRACK GROWTH DATA (ROOM TEMPERATURE)

METCUT RESEARCH ASSOCIATES INC.  
COMPACT TENSION CRACK GROWTH (H/W=0.6 ONLY)

PROJECT NUMBER \_\_\_\_\_ 100-25114  
TEST NUMBER \_\_\_\_\_ 2  
MATERIAL \_\_\_\_\_ TI 17  
TEST MACHINE \_\_\_\_\_ SFLU, 5:1 M  
TEST FREQUENCY \_\_\_\_\_ 30 HZ

SPECIMEN NUMBER \_\_\_\_\_ CF-3  
TEST TEMPERATURE \_\_\_\_\_ 75°F  
RELATIVE HUMIDITY \_\_\_\_\_ 55-63%  
TEST ENVIRO. \_\_\_\_\_ LAB AIR  
STRESS RATIO \_\_\_\_\_ A= 0.90

SPECIMEN SIZE (IN) \_\_\_\_\_ 2H= 2.410 \_\_\_\_\_ W= 1.999 \_\_\_\_\_ B= 1.007 \_\_\_\_\_ A1= 0.687

TOT CYCLES NT (10 <sup>3</sup> )	CRACK LGTH A (IN)	LOAD RNG (LBS)	STR INT RNG ksi (√in.)	CRACK GROWTH RATE DA/DN
0.000	0.775	1800.0	8.99	*****
6.000	0.785	1800.0	9.09	1.58 X10 -6
12.000	0.792	1800.0	9.18	1.25 X10 -6
18.000	0.804	1800.0	9.32	2.00 X10 -6
24.000	0.813	1800.0	9.41	1.33 X10 -6
30.000	0.821	1800.0	9.52	1.50 X10 -6
36.000	0.835	1800.0	9.68	2.17 X10 -6
42.000	0.842	1800.0	9.77	1.25 X10 -6
48.000	0.855	1800.0	9.93	2.08 X10 -6
54.000	0.865	1800.0	10.07	1.75 X10 -6
60.000	0.876	1800.0	10.21	1.83 X10 -6
66.000	0.888	1800.0	10.38	2.00 X10 -6
72.000	0.900	1800.0	10.55	2.00 X10 -6
78.000	0.911	1800.0	10.71	1.92 X10 -6
84.000	0.928	1800.0	10.96	2.75 X10 -6
90.000	0.943	1800.0	11.18	2.42 X10 -6
96.000	0.959	1800.0	11.45	2.75 X10 -6
102.000	0.974	1800.0	11.69	2.50 X10 -6
108.000	0.992	1800.0	12.01	3.00 X10 -6
114.000	1.009	1800.0	12.32	2.83 X10 -6
120.000	1.027	1800.0	12.67	3.08 X10 -6
126.000	1.053	1800.0	13.19	4.25 X10 -6
130.000	1.068	1800.0	13.52	3.87 X10 -6
134.000	1.084	1800.0	13.87	3.88 X10 -6
138.000	1.103	1800.0	14.31	4.63 X10 -6
142.000	1.124	1800.0	14.86	5.37 X10 -6
146.000	1.144	1800.0	15.42	5.12 X10 -6
149.000	1.161	1800.0	15.89	5.50 X10 -6
152.000	1.181	1800.0	16.51	6.67 X10 -6
155.000	1.202	1800.0	17.23	7.17 X10 -6
157.000	1.217	1800.0	17.76	7.50 X10 -6
159.000	1.233	1800.0	18.35	8.00 X10 -6
161.000	1.245	1800.0	18.83	6.00 X10 -6
163.000	1.265	1800.0	19.64	9.75 X10 -6
165.000	1.287	1800.0	20.62	1.10 X10 -5
166.000	1.298	1800.0	21.15	1.10 X10 -5
167.000	1.314	1800.0	21.95	1.60 X10 -5
168.000	1.325	1800.0	22.55	1.15 X10 -5
169.000	1.340	1800.0	23.35	1.45 X10 -5
170.000	1.357	1800.0	24.37	1.75 X10 -5
171.000	1.377	1800.0	25.59	1.95 X10 -5
172.000	1.421	1800.0	28.67	4.40 X10 -5



TABLE E-2

# CRACK GROWTH DATA (ROOM TEMPERATURE)

METCUT RESEARCH ASSOCIATES INC.  
COMPACT TENSION CRACK GROWTH (H/W=0.6 ONLY)

PROJECT NUMBER 100-25114  
TEST NUMBER 1  
MATERIAL TI 17  
TEST MACHINE SF1U, 5:1 M  
TEST FREQUENCY 30 HZ

SPECIMEN NUMBER CF-1  
TEST TEMPERATURE 75°F  
RELATIVE HUMIDITY 59-65%  
TEST ENVIRO. LAB AIR  
STRESS RATIO A= 0.90

SPECIMEN SIZE (IN) 2H= 2.405 W= 1.999 B= 1.004 A1= 0.704

TOT CYCLES NT (10 <sup>3</sup> )	CRACK LGTH A (IN)	LOAD RNG (LBS)	STR INT RNG ksi ( $\sqrt{\text{in.}}$ )	CRACK GROWTH RATE DA/DN
0.000	0.807	880.0	4.58	*****
20.000	0.810	880.0	4.60	1.75 X10 <sup>-7</sup>
50.000	0.816	880.0	4.63	1.83 X10 <sup>-7</sup>
90.000	0.824	880.0	4.68	2.00 X10 <sup>-7</sup>
130.000	0.833	880.0	4.74	2.25 X10 <sup>-7</sup>
170.000	0.840	880.0	4.78	1.87 X10 <sup>-7</sup>
210.000	0.852	880.0	4.85	2.75 X10 <sup>-7</sup>
250.000	0.861	880.0	4.91	2.38 X10 <sup>-7</sup>
290.000	0.872	880.0	4.98	2.63 X10 <sup>-7</sup>
330.000	0.879	880.0	5.03	1.87 X10 <sup>-7</sup>
370.000	0.891	880.0	5.11	3.12 X10 <sup>-7</sup>
410.000	0.902	880.0	5.19	2.63 X10 <sup>-7</sup>
450.000	0.912	880.0	5.26	2.50 X10 <sup>-7</sup>
490.000	0.926	880.0	5.36	3.62 X10 <sup>-7</sup>
530.000	0.937	880.0	5.44	2.63 X10 <sup>-7</sup>
570.000	0.947	880.0	5.52	2.50 X10 <sup>-7</sup>
610.000	0.961	880.0	5.63	3.62 X10 <sup>-7</sup>
650.000	0.972	880.0	5.72	2.75 X10 <sup>-7</sup>
690.000	0.989	880.0	5.86	4.12 X10 <sup>-7</sup>
730.000	1.002	880.0	5.98	3.25 X10 <sup>-7</sup>
770.000	1.017	880.0	6.11	3.75 X10 <sup>-7</sup>
810.000	1.033	880.0	6.27	4.12 X10 <sup>-7</sup>
850.000	1.053	880.0	6.47	4.88 X10 <sup>-7</sup>
890.000	1.073	880.0	6.68	5.00 X10 <sup>-7</sup>
930.000	1.096	880.0	6.95	5.88 X10 <sup>-7</sup>
960.000	1.112	880.0	7.14	5.33 X10 <sup>-7</sup>
990.000	1.133	880.0	7.40	6.83 X10 <sup>-7</sup>
1020.000	1.156	880.0	7.72	7.67 X10 <sup>-7</sup>
1040.000	1.173	880.0	7.97	8.25 X10 <sup>-7</sup>
1060.000	1.193	880.0	8.29	1.02 X10 <sup>-6</sup>
1080.000	1.214	880.0	8.64	1.05 X10 <sup>-6</sup>
1090.000	1.226	880.0	8.86	1.20 X10 <sup>-6</sup>
1100.000	1.236	880.0	9.05	1.00 X10 <sup>-6</sup>
1110.000	1.249	880.0	9.30	1.30 X10 <sup>-6</sup>
1120.000	1.261	880.0	9.55	1.20 X10 <sup>-6</sup>
1130.000	1.276	880.0	9.88	1.55 X10 <sup>-6</sup>
1140.000	1.289	880.0	10.17	1.30 X10 <sup>-6</sup>
1150.000	1.308	880.0	10.62	1.90 X10 <sup>-6</sup>
1158.000	1.325	880.0	11.06	2.12 X10 <sup>-6</sup>
1164.000	1.338	880.0	11.41	2.17 X10 <sup>-6</sup>
1176.000	1.354	880.0	11.85	2.58 X10 <sup>-6</sup>
1180.000	1.370	880.0	12.34	2.75 X10 <sup>-6</sup>
1184.000	1.398	880.0	13.26	4.38 X10 <sup>-6</sup>

TABLE E-3

# CRACK GROWTH DATA (TEST TEMPERATURE 600°F)

METCUT RESEARCH ASSOCIATES INC.  
COMPACT TENSION CRACK GROWTH (H/W = 0.6 ONLY)

PROJECT NUMBER 100-25114  
TEST NUMBER 3  
MATERIAL TI 17  
TEST MACHINE SF10  
TEST FREQUENCY 30 HZ

SPECIMEN NUMBER CF-2  
TEST TEMPERATURE 600°F  
RELATIVE HUMIDITY 54-70%  
TEST ENVIRO. LAB AIR  
STRESS RATIO A= 0.90

SPECIMEN SIZE (IN) 2H= 2.410 W= 2.000 B= 1.006 A1= 0.687

TOT CYCLES NT (10 <sup>3</sup> )	CRACK LGTH A (IN)	LOAD RNG (LBS)	STR INT RNG ksi ( $\sqrt{\text{in.}}$ )	CRACK GROWTH RATE DA/DN
0.000	0.767	990.0	4.89	*****
10.000	0.771	990.0	4.92	4.00 X10 -7
20.000	0.774	990.0	4.94	3.50 X10 -7
30.000	0.778	990.0	4.96	3.00 X10 -7
45.000	0.784	990.0	4.99	4.00 X10 -7
60.000	0.787	990.0	5.02	2.67 X10 -7
80.000	0.796	990.0	5.07	4.25 X10 -7
100.000	0.803	990.0	5.11	3.25 X10 -7
120.000	0.811	990.0	5.17	4.50 X10 -7
140.000	0.817	990.0	5.20	2.50 X10 -7
160.000	0.822	990.0	5.24	2.75 X10 -7
180.000	0.831	990.0	5.30	4.50 X10 -7
200.000	0.840	990.0	5.36	4.75 X10 -7
220.000	0.847	990.0	5.41	3.50 X10 -7
240.000	0.856	990.0	5.47	4.25 X10 -7
260.000	0.867	990.0	5.55	5.50 X10 -7
280.000	0.873	990.0	5.60	3.00 X10 -7
300.000	0.879	990.0	5.64	3.00 X10 -7
320.000	0.890	990.0	5.72	5.25 X10 -7
340.000	0.899	990.0	5.80	5.00 X10 -7
360.000	0.908	990.0	5.86	4.25 X10 -7
380.000	0.919	990.0	5.95	5.50 X10 -7
400.000	0.929	990.0	6.04	5.00 X10 -7
420.000	0.939	990.0	6.12	4.75 X10 -7
440.000	0.949	990.0	6.21	5.25 X10 -7
460.000	0.958	990.0	6.29	4.50 X10 -7
480.000	0.967	990.0	6.37	4.75 X10 -7
500.000	0.979	990.0	6.48	5.75 X10 -7
520.000	0.989	990.0	6.58	5.25 X10 -7
540.000	0.999	990.0	6.67	4.75 X10 -7
560.000	1.011	990.0	6.79	6.00 X10 -7
580.000	1.028	990.0	6.97	8.50 X10 -7
600.000	1.043	990.0	7.14	7.75 X10 -7
620.000	1.058	990.0	7.31	7.25 X10 -7
640.000	1.072	990.0	7.48	7.00 X10 -7
660.000	1.088	990.0	7.68	8.00 X10 -7
680.000	1.110	990.0	7.97	1.10 X10 -6
695.000	1.121	990.0	8.13	7.33 X10 -7
710.000	1.137	990.0	8.37	1.10 X10 -6
725.000	1.154	990.0	8.63	1.10 X10 -6
740.000	1.173	990.0	8.94	1.27 X10 -6
750.000	1.186	990.0	9.18	1.35 X10 -6
760.000	1.200	990.0	9.42	1.35 X10 -6
770.000	1.217	990.0	9.75	1.70 X10 -6
780.000	1.233	990.0	10.08	1.60 X10 -6
790.000	1.250	990.0	10.45	1.70 X10 -6
800.000	1.270	990.0	10.91	2.00 X10 -6
806.000	1.283	990.0	11.22	2.08 X10 -6
812.000	1.300	990.0	11.68	2.92 X10 -6
818.000	1.315	990.0	12.09	2.50 X10 -6
824.000	1.336	990.0	12.71	3.50 X10 -6
828.000	1.335	990.0	13.31	4.75 X10 -6
831.000	1.372	990.0	13.87	5.50 X10 -6
834.000	1.386	990.0	14.39	4.83 X10 -6
837.000	1.403	990.0	15.03	5.67 X10 -6

APPENDIX F

TENTATIVE SPECIFICATION NO. 5114-1

PREALLOYED TITANIUM POWDER

## APPENDIX F

### TENTATIVE SPECIFICATION NO. 5114-1

#### PREALLOYED TITANIUM POWDER

#### 1. SCOPE

1.1 Form: This specification covers prealloyed titanium powder.

1.1.1 This specification contains the following classes:

Class A - Spherical Powder

Class B - Non-spherical Powder

1.2 Application: For consolidating into forging billet, preforms, or for direct consolidation to a near-net shape component.

1.3 Definitions: For purposes of this specification, the following definitions shall apply.

Powder Heat - The blend of powders produced from one or more powder lots of a single original melted heat.

Powder Lot - Powder produced during a single cycle of the powder production equipment or consecutive cycles using same input stock conducted at essentially the same parameters, and screened to the specified size.

Purchaser - The procuring activity that issued the procurement document invoking this specification.

#### 2. APPLICABLE DOCUMENTS

The following publications form a part of this specification to the extent specified herein. The latest revision of each specification shall apply.

2.1 SAE Publications: Available from Society of Automotive Engineers, Inc., 400 Commonwealth Drive, Warrendale, Pennsylvania 15096

#### 2.1.1 Aerospace Material Specifications

AMS 2350 - Standards and Test Methods

AMS 2635 - Radiographic Inspections

AMS 2249 - Chemical Check Analysis Limits - Titanium and Titanium Alloys



- 2.2 ASTM Publications: Available from American Society for Testing Materials, 1916 Race Street, Philadelphia, Pennsylvania 19103

ASTM B214 - Sieve Analysis of Granular Metal Powders

ASTM B243 - Definition of Terms, Powder Metallurgy

ASTM B215 - Sampling Finished Lots of Metal Powders

- 2.3 Government Publications: Available from Commanding Officer, Naval Publications and Forms Center, 5801 Tabor Avenue, Philadelphia, Pennsylvania 19120

2.3.1 Federal Standards

Federal Test Method Standard 151 - Metals; Test Methods

2.3.2 Military Standards

MIL Std 794 - Parts and Equipment, Procedure for Packaging and Packing of.

3. TECHNICAL REQUIREMENTS

- 3.1 Material: Shall be a prealloyed powder, produced in hydrogen, an inert atmosphere, or vacuum. The powder shall not contain greater than 1% of splat material or agglomerated masses. The powder shall conform to the composition requirements of 3.3 and shall have particle size distribution as shown in 3.4.1. The source, quality, and production process of the feed material shall be subject to approval by the purchaser. Chemistry and processing history of this feed material shall be reported (4.5).

3.2 Physical Characteristics:

Class A - Powder shall be essentially spherical and have a minimum tap density of 55% of theoretical. This must reproduce within  $\pm 1\frac{1}{2}\%$  on three tests.

Class B - Powder is largely non-spherical or does not meet minimum density requirements for Class A.

- 3.3 Composition: Shall conform to those in Table E-1, by weight, determined by approved methods.

- 3.3.1 Check Analysis: Composition variations shall meet the requirements of AMS 2249.

- 3.3.2 Powder from each powder lot shall meet the oxygen and nitrogen limits before blending to form a powder heat.
- 3.3.3 A powder heat which does not meet the requirements of 3.3 shall not be used.
- 3.4 Properties: The powder shall conform to the following requirements:
- 3.4.1 Particle Size: The particles shall all pass through a 35 mesh (500 $\mu$ m) sieve with a normal size distribution for the powder production process used. This particle size determination shall be performed per ASTM B214, or other approved method.)
- 3.5 Quality
- 3.5.1 Initial Qualification: A new vendor or process must qualify his powder for use in the following manner.
- 3.5.1.1 A randomly selected sample of about 0.75 lbs (330 grms) to 1.0 lbs (454 grms) from each powder heat shall be hot compacted using a method which will not contaminate the powder particles during consolidation. A theoretical density minimum of 98.5% is required.
- 3.5.1.2 Each compact shall be divided such that eighteen (18) square inches with a thickness of 0.200 + .015" - .025" may be evaluated by radiographic means. (Also, a portion shall be used for oxygen analysis - see paragraph 3.2). The eighteen (18) square inches shall be radiographed, per ASM 2635, and evaluated for low and high density inclusions.
- 3.5.2 Production Quality Control: Each lot of powder shall be examined for contaminants and results reported for informational purposes.
- 3.5.2.1 The powder shall be uniform in color and quality, dry, and free from foreign material 35 mesh (500 $\mu$ m) screen size. Level of 35 mesh screen size contaminants shall be as agreed between vendor and purchaser.
- 3.5.2.2 The powder shall pass through a magnetic separating device a minimum of two times. Quantity of magnetic material removed shall be reported for informational purposes only.

4. QUALITY ASSURANCE PROVISIONS

- 4.1 Responsibility for Inspection: The vendor of the powders shall supply all samples and shall be responsible for performing all agreed tests. Results of such tests shall be reported to the purchaser as required in 4.5. Purchaser reserves the right to perform such confirmatory testing as he deems necessary to assure that the powder conforms to the requirements of this specification.
- 4.2 Classification of Tests: Tests to determine conformance to all technical requirements of this specification are classified as acceptance or routine control tests.
- 4.2.1 For direct U. S. Military procurement, qualification test material and supporting test data shall be submitted to the cognizant qualification agency as directed by the request for procurement, the procuring activity, or the contracting officer (see 4.4).
- 4.3 Sampling: Sufficient material shall be taken, per ASTM B215 for each powder lot or heat to perform each test in duplicate.
- 4.4 Approval: The purchaser may, at his discretion, request a sample of powder for evaluation, prior to the vendor commencing powder production for use.
- 4.4.1 Production Process: The process to be used shall have been initially qualified per 3.5.1. The vendor shall use materials, processing techniques, and routine inspection methods on production powder which are essentially the same as those used on approved sample or identified previous production orders, which are identified by powder heat or lot number(s). If any change is necessary in materials, in processing technique, or in routine inspection methods, vendor shall submit for reapproval a statement of the proposed changes, and when requested, submit a sample of the powder produced by the revised process. No powder produced by the revised process shall be shipped (except samples for purchaser approval) prior to receipt of reapproval.
- 4.5 Reports
- 4.5.1 Certificate of Conformance: The powder vendor shall furnish with each shipment, three copies of a certificate of conformance which shall include:

- a) The results of the test of chemical composition for each powder heat or lot in the shipment, including chemistry and processing history of feed stock.
- b) The results of the tests for particle size and distribution for each powder heat or lot in the shipment.
- c) A statement that each powder heat or lot in the shipment conforms to the other technical requirements of this specification.
- d) Purchase order number, material specification number, vendor product designation, heat or lot number, and quantity.

4.6 Resampling and Retesting: If any sample used in the above tests fails to meet the specification requirements, disposition of the powder will be based on the results of testing three additional samples for each non-conforming sample. Failure of any retest samples to meet the specified requirements shall be cause for rejection of the powder represented and no additional testing shall be permitted. Results of all tests, non-conforming as well as conforming retest, shall be reported. Acceptance of the powder lot(s), determined to be non-conforming by the original test, but acceptable by the retest, shall be at the discretion of the purchaser.

## 5. PREPARATION FOR DELIVERY

### 5.1 Packaging and Identification

5.1.1 Packaging: The powder shall be packaged in containers of the size ordered, or those required to assure acceptance and safe transport to the point of delivery. When required, a heat or lot of powder may be packaged in a multiplicity of small containers, as long as heat or lot identity is maintained.

Each container shall be thoroughly cleansed immediately prior to filling, and sealed immediately after filling to protect the contents from contamination during shipment and during storage under normal dry storage conditions. Seals used on the containers shall be so designed that they must be destroyed in order for the container to be opened.

5.1.2 Identification: Each container shall be permanently and legibly marked to give at least the following information:



Ti-17 Powder (5114-1)

Manufacturer's identification \_\_\_\_\_

Quantity \_\_\_\_\_

Heat or Lot Number \_\_\_\_\_

Container No. (If more than one per lot) \_\_\_\_ of \_\_\_\_

- 5.1.3 Individual containers may be packed in an exterior shipping container capable of protecting the materials from damage during transit and storage.

- 5.1.4 Each exterior shipping container shall be legibly marked with the following information in such a manner that the markings will not smear or be obliterated during normal handling and use:

Ti-17 Powder (5114-1)

Manufacturer's identification \_\_\_\_\_

Purchase Order Number \_\_\_\_\_

Quantity \_\_\_\_\_

Heat or Lot Number \_\_\_\_\_

Containers \_\_\_\_\_ Thru \_\_\_\_\_ of \_\_\_\_\_ Total

- 5.1.5 Containers shall be prepared for shipment in accordance with commercial practice to assure carrier acceptance and safe transportation to the point of delivery. Packaging shall conform to carrier rules and regulations applicable to the mode of transportation.
- 5.1.6 For direct U. S. Military procurement, packaging shall be in accordance with MIL-Std-794, Level A or Level C, as specified in the request for procurement. Commercial packaging per 5.1.5 will be acceptable if it meets the requirements of Level C.

6. ACKNOWLEDGEMENT

A vendor shall mention this specification number (latest revision) in all quotations and when acknowledging purchase orders.

7. REJECTIONS

Powder not conforming to this specification or to authorized modification will be subject to rejection.

8.     NOTES

8.1     Definitions: For definitions of terms used herein,  
          refer to ASTM B243.

8.2     For direct U. S. Military procurement, purchase documents should specify (at minimum) the following:

- a) Title, number, and date of specification.
- b) Size of container desired (if shipped by commercial carrier must conform to 5.1.1).
- c) Quantity of powder desired.
- d) Applicable level of packaging (see 5.1.6).

TABLE F-1  
COMPOSITION OF ALLOYS

	1	2	3	4	5	6	7	8	9	10
	6-4 (Std)	6-4 (ELI)	3-2-1/2	6-2-4-2	6-2-4-6	Ti-17	Corona 5	Beta I	Beta III	6-6-2
Al	5.5-6.75	5.5-6.5	2.5-3.5	5.5-6.5	5.5-6.5	4.5-5.5	4-5	2-4		5-6
V	3.5-4.5	3.5-4.5	2-3					12.5-14.5		5-6
Sn				1.75-2.25	1.8-2.2	1.5-2.5			3.75-5.25	1.5-2.5
Zr				3.5-4.5	3.6-4.4	1.5-2.5			4.5-7.5	
Mo				1.75-2.25	5.5-6.5	3.5-4.5	4-6		10-13	
Cr						3.5-4.5	1.25-1.75	10-12		
Fe	.3 max	.15 max	.25 max	.25 max	.15 max	.3 max	.25 max	.35 max	.35 max	.35-1.0
O	.2 max	.13 max	.12 max	.12 max	.12 max	.08-.13	.18 max	.2 max	.18 max	
C	.1 max	.08 max	.05 max	.1 max	.04 max	.05 max	.05 max	.05-.1	.1 max	.05 max
N	.05 max	.05 max	.02 max	.05 max	.02 max	.04 max	.04 max	.05-.08	.05 max	.20 max
H	.015 max	.015 max	.015 max	.015 max	.015 max	.0125 max	.015 max	.015 max	.02 max	.04 max
Cu						.1 max				.35-1.0
Mn						.1 max				
All other, total	.3 max	.3 max	.3 max	.3 max	.3 max	.2 max	.3 max	.3 max	.3 max	.3 max
Ti	Bal	Bal	Bal	Bal	Bal	Bal	Bal	Bal	Bal	Bal

APPENDIX G

TENTATIVE SPECIFICATION NO. 5114-2

HOT ISOSTATIC PRESSING (HIP) OF TITANIUM ALLOY POWDER



## APPENDIX G

### TENTATIVE SPECIFICATION NO. 5114-2

#### HOT ISOSTATIC PRESSING (HIP) OF TITANIUM ALLOY POWDER

##### 1. SCOPE

1.1 Scope: This specification presents requirements for hot isostatic pressing of titanium alloy powder forging preforms and HIP parts.

1.1.1 Classification: This specification contains the following classes:

Class A - HIP parts

Class B - Forging Preforms

The requirements specified herein apply to all classes unless otherwise specified.

1.2 Definitions: For purposes of this specification, the following definitions shall apply:

Part Lot - Parts produced in the same autoclave cycle and from same heat of powder.

Purchaser - The procurement activity that issued the procurement document invoking this specification.

Working Zone - The volume of the heated region of an autoclave which may be occupied by parts or material to be hot isostatically pressed.

##### 2. APPLICABLE DOCUMENTS

2.1 The following documents shall form a part of this specification to the extent specified herein. Unless a specific issue is specified, the latest revision shall apply.

American Society for Testing and Materials

ASTM E230 Temperature-Electromotive Force (EMF)  
Tables for Thermocouples

3. EQUIPMENT

3.1 Autoclave

3.1.1 Autoclaves shall be of the inert gas pressurization type, internally heated, cold wall pressure vessel.

3.2 Fixtures

3.2.1 Suitable jigs, trays, baskets, hangers, racks or other fixtures shall be provided as necessary for proper handling and positioning of materials to be hot isostatic pressed. All fixtures shall be made of material which is compatible with the material to be treated, or adequately isolated to assure that undesirable reactions or mechanical distortion do not occur.

3.3 Containers

3.3.1 Powder containers shall be made from materials demonstrated to have no adverse effect on the titanium.

3.4 Temperature Measurement and Control Devices

3.4.1 Temperature Measurement

3.4.1.1 Temperature measuring and recording devices shall be provided for the autoclave. The devices shall be of the potentiometric type, shall use thermocouple sensors, and shall provide permanent records of the temperature during the entire treatment.

3.4.2 Temperature Control

3.4.2.1 A sufficient number of suitable automatic temperature control devices shall be provided and properly arranged in the autoclave to assure the required temperature control in the working zone. The devices shall be of the potentiometric type and shall use thermocouple sensors.

3.5 Pressure Measurement Devices

3.5.1 Pressure measurement devices shall be accurate to within + or - two percent at the maximum operating pressure and shall be capable of continuously monitoring and recording the pressure in the autoclave throughout the process.

4.     PROCEDURE

4.1     General

- 4.1.1   All processing equipment and significant processing parameters shall be approved by the Purchaser. Once a technique for producing a specific part or preform has been established and approved, no changes shall be made without prior approval of the Purchaser.
- 4.1.2   All hot isostatic pressing facilities shall be qualified in accordance with Section 5 of this specification prior to production.

4.2     Cleaning

- 4.2.1   All containers and fixtures shall be properly cleaned to remove all loose particles and all surface contaminants which may be detrimental to the material being treated or to autoclave components.

4.3     Container Filling

- 4.3.1   Leak Check: All HIP containers shall be leak tested by an appropriate procedure.
- 4.3.2   Filling and Sealing: Powder or powder-filled molds shall be loaded into the container and the loaded container outgassed and sealed by a method approved by the Purchaser.

4.4     Loading of Autoclave

- 4.4.1   All material to be treated shall be located within the working zone in such a manner as to facilitate pressurization of the chamber and assure uniform heating and cooling of the material.

4.5     Instrumentation

- 4.5.1   A minimum of three thermocouples shall accompany the material during treatment. They shall be located in the hottest, coldest and average temperature regions of the working zone which is in use as determined by the temperature uniformity qualification test. The thermocouples shall be in close proximity to the containers. An alternate instrumentation plan may be used with prior approval of the Purchaser.

4.6     Time, Temperature and Pressure

- 4.6.1   The autoclave heat-up, pressurization and cooling cycles shall be approved by the Purchaser.

4.7 Pressure Environment

4.7.1 Equipment: All pressure indicating equipment shall be adjusted in accordance with the instrument manufacturer's instructions.

4.7.2 Pressure: The chamber pressure during treatment shall be 15,000 psi minimum for two hours minimum at temperature. During heat-up, treatment, and cool down, the chamber pressure shall be continuously recorded. The specific pressure/time conditions shall be subject to approval by the Purchaser.

4.8 Thermal Treatment

4.8.1 The times and temperatures for the thermal cycle shall be as agreed upon between Purchaser and vendor. The temperatures shall be continuously measured and recorded with respect to time during the entire thermal cycle. The use of multi-point recorders with a periodic print out of five minutes maximum per thermocouple is permitted.

4.9 Density

4.9.1 Class A: HIP parts shall have a density greater than 99.8 percent of a HIP test sample fabricated from the same powder heat or master powder blend. The powder pressing and forging processes used on the test sample shall be by methods agreed upon by the Purchaser and the vendor.

Class B: As-compacted preforms shall have a density greater than 99.6 percent of a compacted plus forged test sample fabricated from the same powder heat or master powder blend. The powder compaction and forging processes used on the test sample shall be by methods agreed upon by the Purchaser and the vendor.

4.10 Microstructure

4.10.1 HIP parts or preforms shall have a uniform microstructure with no outlining of prior particle boundaries or evidence of voids.

4.11 Decanning

4.11.1 HIP containers shall be completely removed by a method approved by the Purchaser.

4.12 Re-HIP

4.12.1 Re-HIP is permitted, provided re-HIP is not specifically prohibited by the procurement document.



#### 4.13 Inspections and Tests

- 4.13.1 All inspections or tests required by the drawing or applicable specifications shall be performed. The results of these inspections or tests shall meet the requirements of the drawing or applicable specifications.
- 4.13.2 Sample parts or representative material shall be evaluated with respect to microstructure and density to the requirements of the drawing or applicable specification.

#### 4.14 Records

- 4.14.1 All records and test results for each hot isostatic pressing treatment shall be maintained for Purchaser surveillance. These records shall include at least the following information:

- (a) Purchaser identification of parts or material treated
- (b) Part or material alloy designation
- (c) Autoclave identification
- (d) Pre-cleaning procedures
- (e) Loading procedures including fixture materials and part placement
- (f) Instrumentation procedures including thermocouple type and placement
- (g) Pressure records
- (h) Temperature records
- (i) Post cleaning procedures
- (j) Powder container material and container removal procedures
- (k) Pressure media
- (l) Metallographic evaluation results
- (m) Visual inspection results

- 4.14.2 Records shall be maintained to provide traceability for each serialized part. Each part shall be traceable to a particular hot isostatic pressure treatment, date, time, autoclave, and location and raw material source.

#### 5. QUALITY ASSURANCE PROVISIONS

##### 5.1 General

- 5.1.1 All qualifications shall be the responsibility of the hot isostatic pressing vendor. The vendor shall be responsible for all testing and shall sign all necessary forms which certify that qualification in accordance with this specification has been attained.
- 5.1.2 Procedures for equipment qualifications, if other than those required by this specification, are subject to approval by the Purchaser.
- 5.1.3 The Purchaser reserves the right to observe any of the qualification tests required by this specification to determine conformance to this specification.
- 5.2 Autoclave Qualification
- 5.2.1 Temperature Uniformity: All autoclaves shall be qualified for working zone temperature uniformity prior to use for production hot isostatic pressing. All autoclaves shall be requalified at least every three months after the initial qualification. All autoclaves shall be requalified after any alterations to the equipment which may affect temperature uniformity. Requalification may be on a working load.
- 5.2.1.1 When approaching thermal equilibrium, per 5.2.2, none of the load temperature readings shall exceed the selected control temperature by more than 25 F (14 C). After thermal equilibrium is reached, the maximum temperature variation of any load test thermocouple shall not deviate from the selected control temperature by more than  $\pm 25$  F ( $\pm 14$  C).
- 5.2.2 Qualification Procedure: Temperature uniformity tests shall be conducted with the autoclave containing a representative production load of parts or material and at a typical production pressure. The test shall be made using calibrated test thermocouples and a potentiometer type measuring instrument with a minimum sensitivity of 0.02 millivolt. The outputs of the test thermocouples shall be properly corrected as determined by the thermocouple calibrations. A minimum of three test thermocouples or one per each cubic foot (28 dm<sup>3</sup>) of working zone, whichever is greater, but no more than eight, shall be used for determining the temperature uniformity. When more than three thermocouples are required, the additional thermocouple locations shall be symmetrically distributed within the working zone. The initial qualification shall be performed at the lowest and highest operating temperatures of the autoclave. Requalifications shall be performed at a convenient temperature within the operating range. The temperature of all test and auto-

clave control thermocouples shall be recorded at five minute intervals starting immediately after application of power to the autoclave. In order that the recurrent temperature pattern of the autoclave can be established, temperature measurements shall be continued after the control thermocouple indicates thermal stability at the hold temperature, through the hold cycle, and until 1000 F has been reached on the cooling cycle.

5.3 Temperature Measurement and Control Qualification

5.3.1 Instruments: All instruments used for temperature measurement shall have an indicated temperature accuracy of  $\pm 0.25$  percent of the maximum operating temperature over the entire operating temperature range. All instruments used for temperature control shall have an indicated temperature accuracy of  $\pm 0.5$  percent of the maximum operating temperature over the entire operating temperature range. The indicated temperature accuracy of each instrument shall be determined in accordance with the equipment manufacturer's recommendations and using a known EMF input of suitable accuracy. After the initial qualification, all instruments shall be requalified at least every 30 days, unless otherwise agreed upon by the vendor and the Purchaser.

5.3.2 Thermocouples: Prior to each use, all thermocouples shall be capable of meeting the temperature - electromotive force requirements of ASTM E230 for special grade wire as determined by suitable test methods and requalification intervals.

5.4 Pressure Indicating Instrument Qualification

5.4.1 All pressure indicating instruments shall be checked in accordance with the equipment manufacturer's recommendations. The equipment's performance shall be within the limits supplied by the equipment manufacturer. After the initial qualification, each instrument shall be requalified at least every six months.

5.5 Process Qualification

5.5.1 Prior to production processing, process procedures shall be submitted to the Purchaser for approval.

5.5.2 Process procedures shall include the following information:

- (a) Purchaser identification of parts or material treated
- (b) Part and alloy designation
- (c) Autoclave identification
- (d) Pre-cleaning procedures
- (e) Loading procedures including fixture materials and part placement
- (f) Instrumentation procedures including thermocouple type and placement
- (g) Pressure records
- (h) Temperature records
- (i) Post cleaning procedures
- (j) Powder container material and container removal procedures
- (k) Pressure media
- (l) Metallographic evaluation procedure
- (m) Visual inspection procedure

## 5.6 Records

5.6.1 All records and test results shall be maintained for Purchaser surveillance. A card shall be affixed to the autoclave and other necessary components after qualification to indicate compliance with this specification. The card shall contain the following minimum information:

- (a) Type of equipment
- (b) Equipment manufacturer where applicable
- (c) Equipment model and serial number where applicable
- (d) Equipment location
- (e) Statement indicating compliance with this specification
- (f) Signature of vendor's qualifying agent



APPENDIX H

TENTATIVE SPECIFICATION NO. 5114-3

PREMIUM QUALITY, POWDER METALLURGY AS-HOT ISOSTATIC  
PRESSED (HIP) Ti-17 TITANIUM BASE ALLOY PARTS

## APPENDIX H

### TENTATIVE SPECIFICATION NO. 5114-3

#### PREMIUM QUALITY, POWDER METALLURGY AS-HOT ISOSTATIC PRESSED (HIP) Ti-17 TITANIUM BASE ALLOY PARTS

#### 1. SCOPE

1.1 Scope: This specification presents requirements for Ti-17 titanium base alloy powder metallurgy as-HIP parts.

1.1.1 Classification: This specification contains the following classes:

<u>Class</u>	<u>HIP Processing Temperature</u>	<u>LCF &amp; Fracture Toughness</u>
A	Alpha-Beta	Not Required
B	Alpha-Beta	Required
C	Beta	Not Required
D	Beta	Required

The requirements specified herein apply to all classes unless otherwise specified.

1.2 Definitions: For purposes of this specification, the following definitions shall apply:

Purchaser - The procuring activity that issued the procurement document invoking this specification.

Capability - The words "shall be capable of" or "capability test" indicate characteristics or properties required in the product but for which testing of each lot is not required. However, if such testing is performed by the Purchaser, material not conforming to the requirements shall be subject to rejection.

HIP - An acronym for hot-isostatic-pressing.

Macroetch - Etching of a metal surface for acceptance of gross structural details and defects for observation.

Premium Quality - Material which is produced under special process and quality control, used primarily for critical rotating parts.

"A" - Ratio - Alternating stress divided by the mean stress.

Lot - A group of HIP parts processed at the same time with identical process conditions and raw material source.

## 2. APPLICABLE DOCUMENTS

- 2.1 The following documents shall form a part of this specification to the extent specified herein. Unless a specific issue is specified, the latest revision shall apply.

### GENERAL SPECIFICATIONS

5114-1 Pre-Alloy Titanium Powder

5114-2 Hot Isostatic Pressing (HIP) of Titanium Alloy Powder

### AMERICAN SOCIETY FOR TESTING AND MATERIALS

ASTM E8 Tension Testing of Metallic Materials

ASTM E399 Plane-Strain Fracture Toughness Testing of Metallic Materials

### AEROSPACE MATERIAL SPECIFICATIONS

AMS 2249 Chemical Check Analysis Limits-Titanium and Titanium Alloys

AMS 2645G Fluorescent Penetrant Inspection

## 3. REQUIREMENTS

### 3.1 Raw Material

- 3.1.1 Parts shall be produced from powder of a titanium base alloy known as Ti-17 meeting the requirements of 5114-1.

### 3.1.2 Chemical Composition, Percent

Aluminum -----	4.50-5.50	Hydrogen -----	0.0125 Max.
Zirconium ----	1.50-2.50	Copper -----	0.10 Max.
Tin -----	1.50-2.50	Manganese -----	0.10 Max.
Molybdenum ---	3.50-4.50	Other Elements,	
Chromium -----	3.50-4.50	Each -----	0.10 Max.*
Carbon -----	0.05 Max.	Other Elements,	
Iron -----	0.30 Max.	Total -----	0.20 Max.*
Oxygen -----	0.08-0.13	Titanium -----	Remainder
Nitrogen -----	0.04 Max.		

\*Determination not required for routine acceptance.

- 3.1.2.1 The analysis made by the manufacturer to determine the percentages of elements required by this specification shall conform to the requirements of 3.1.2 and shall be reported in a certificate of test.

### 3.2 Powder Process Requirements

- 3.2.1 Powder shall be obtained only from sources approved by the Purchaser.
- 3.2.2 HIP shapes shall be processed according to the requirements of Specification 5114-2.
- 3.2.3. First Article: Before production has commenced, reports of mechanical and metallurgical tests (4.2.1) of the first item tested to confirm the HIP technique shall be made available to the Purchaser or his authorized representative for approval. The approval of the first article sample authorizes the commencement of production but does not relieve the supplier of responsibility for compliance with all applicable provisions of this specification.
- 3.2.4 Design Documentation: Part drawings shall indicate:  
(a) configuration and dimensions of the finished shape, (b) alloy composition to be used, (c) location from which specimens shall be cut for first-article tests, (d) final heat treatment, and (e) required reference points or surfaces for NDE or machining.



- 3.2.5 Surface Contamination Control: The part drawing shall dimensionally define the limits for the contamination-free, heat treated end-product, meeting all the requirements of this specification. At the same time it shall provide excess metal volumes sufficient to assure that no contaminated zones remain after removal of excess metal.
- 3.2.6 Each HIP shape or a portion thereof shall be etched prior to inspection for chemical segregation, voids and inclusions. Etching of semi-finished or finished machined parts shall be as specified by the Purchaser. Segregation, inclusions, or voids visible after etching, shall be cause for rejection. Etching procedures shall be approved by the Purchaser. Examination of etched surfaces may be done at magnification of 1-10X.

### 3.3 Heat Treatment

- 3.3.1 All heat treat temperatures refer to metal temperature. All times refer to time at temperature for the heaviest section.

- 3.3.2 Classes A and B: Solution treat at 1575 F for four hours and rapid air cool to room temperature, re-heat to 1475 F, hold four hours and water quench. Age at a temperature in the range 1100-1250 F for eight hours and air cool to room temperature. Rapid air cooling and water quenching from the solution temperature shall begin within 45 seconds from the time the parts are removed from the furnace.

#### Classes C and D

Solution Heat Treatment: Solution heat treat at a temperature of  $1475\text{ F} \pm 15$  ( $802\text{ C} \pm 8$ ) for four hours and water quench to room temperature. Water quenching from the solution temperature shall begin within 45 seconds from the time the parts are removed from the furnace.

Aging Treatment: Heat to a temperature within the range of 1100 F to 1250 F ( $592$  to  $677\text{ C}$ ); hold for eight hours at a selected temperature within  $\pm 15\text{ F}$  ( $\pm 8\text{ C}$ ), and air cool.

- 3.3.3 Rough machined parts may be stress relieved at  $1020\text{ F} \pm 25$  ( $549\text{ C} \pm 14$ ) for a minimum of two hours and air cooled prior to final machining.

- 3.3.4 The hydrogen content of finished parts shall not exceed 0.0125 percent.
- 3.3.5 There shall be no visual evidence of oxide discoloration, cracks, or residual container material on finished parts.

3.4 Mechanical Properties

- 3.4.1 Tensile specimens shall meet the room temperature tensile shown below.

Classes A and B:

Strength (ksi)	$F_{tu}$	---- 163,000
		---- 183,000

Strength (ksi)	$F_{ty}$	---- 153,000
		---- 173,000

Elongation (% in 4D), Min.- 7

Reduction of Area, % Min. - 15

Classes C and D:

Strength (ksi)	$F_{tu}$	---- 163,000
		---- 183,000

Strength (ksi)	$F_{ty}$	---- 153,000
		---- 173,000

Elongation (% in 4D), Min.- 5

Reduction of Area, % Min. - 10

- 3.4.2 Room Temperature Fracture Toughness and Low Cycle Fatigue (Classes B and D)

- 3.4.2.1 Plane strain fracture toughness tests shall be conducted and all test results and test specimen thicknesses used shall be reported to the Purchaser in the certificate of test. The plane strain fracture toughness shall meet a minimum value of 40 kpsi  $\sqrt{\text{in.}}$  for Class B, and 50 kpsi  $\sqrt{\text{in.}}$  for Class D.

- 3.4.3 Room Temperature Low-Cycle Fatigue (Classes B and D)

3.4.3.1 Low-cycle fatigue tests shall be conducted and the number of cycles to failure shall be reported to the Purchaser in the certificate of test. Tests shall be conducted at a stress ratio (alternating/mean stress) of  $.95 + .05$  with a maximum stress level (mean stress plus alternating stress) of 90,000 psi (621 MPa) at a cyclic rate of 10 to 30 cycles per minute. When specifically required by the drawing test specimens shall have a minimum of 6000 cycles.

3.5 Metallographic Inspection

3.5.1 HIP parts shall exhibit a substantially uniform micro-structure.

3.5.2 The hardness at .005 inch from the surface shall not exceed the core hardness by more than 40 points Knoop (100 gram load).

3.6 Vendor's Certificate of Test

3.6.1 The vendor shall certify all chemical and mechanical tests herein specified. A certificate of test, in triplicate, on each lot supplied to this specification shall be mailed by the vendor to the machining vendor with or preceding the shipment. This certificate shall give the numerical results of all required tests and inspections and shall show that the results are in accordance with the requirements of this specification. If a heat appears in more than one lot of parts, the numerical results of the tests shall be recorded in the certificate of test for each of the lots of parts in which it appears. In addition, the certificate shall show the following information:

- (a) Purchase order number
- (b) Powder heat number
- (c) Serial number for each HIPing
- (d) Lot number for each HIPing
- (e) Heat treat lot number for each HIPing
- (f) Hydrogen content of finished HIPings, as determined on representative parts
- (g) Testing source for tensile, fracture, toughness, and low-cycle fatigue specimens if applicable
- (h) Specific heat treatment cycle used
- (i) Quantity
- (j) Specification number, CLASS, and revision number

### 3.7 Material Identification Record

3.7.1 A material identification record shall be submitted by the machining vendor to the Purchaser and shall include the following information:

- (a) HIPing vendor's certificate of test
- (b) Heat treat vendor
- (c) Specification number, CLASS, and revision number

### 3.8 Marking

3.8.1 The type of marking and location shall be as specified on the drawing.

## 4. QUALITY ASSURANCE PROVISIONS

### 4.1 General

4.1.1 The certificate of test for each lot or lots within a shipment shall report the data required by this specification for the number of sample items or test specimens as required by this specification, or as additionally directed by the Purchaser.

4.1.2 Unless otherwise specified, all testing shall be conducted in accordance with ASTM. All parts are subject to cut up upon receipt by the Purchaser and shall have the required properties throughout the product. The vendor shall inform the Purchaser of the test procedures used. Once these procedures are established, they shall not be changed without approval of the Purchaser.

### 4.2 Chemical Analysis

4.2.1 Chemical analyses shall be conducted in accordance with standard ASTM methods, or by methods agreed upon between Purchaser and vendor.

4.2.2 Chemical check analysis limits shall be in accordance with AMS 2249.

### 4.3 Mechanical Properties

#### 4.3.1 General

4.3.1.1 The number and frequency of mechanical property tests shall be in accordance with a Quality Control Plan approved by the Purchaser. The location of test specimens shall be as specified by the Purchaser. The machining and testing sources for all test specimens shall be subject to approval by the Purchaser.



#### 4.3.2 Tensile

- 4.3.2.1 Tensile specimens, taken per 4.3.1, shall be tested in accordance with the applicable requirements of ASTM E8.
- 4.3.2.2 For referee tensile tests, a strain rate of .005 inch per inch (0.005 mm per mm) per minute through the 0.2 percent yield strength shall be used.

#### 4.3.3 Fracture Toughness

- 4.3.3.1 Compact tension type fracture toughness specimens, taken per 4.3.1, shall be tested in accordance with the applicable requirements of ASTM E399. Thickness of test specimens shall be one inch (25.4 mm) unless otherwise specified. For HIPings less than one inch in thickness, fracture toughness test methods shall be as agreed between vendor and purchaser.

#### 4.3.4 Low-Cycle Fatigue

- 4.3.4.1 Low cycle fatigue test specimens, taken per 4.3.1, shall be machined to the configuration and dimensions shown in Figure 1-C with a  $K_t = 2.0$  stress concentration in the gage section. The notch shall be made using low stress grinding techniques to prevent the formation of high residual stresses in the surfaces.

#### 4.4 Fluorescent Penetrant Inspection

- 4.4.1 After completion of all processing operation, all parts shall be fluorescent penetrant inspected per AMS 2645G, in accordance with limits specified on the drawing.
- 4.4.2 Rework of fluorescent penetrant indications shall fall within the blend limits of the applicable drawings. All blends shall be smooth in contour with no sharp breaks or scratches within them. If no blend limits are shown on the drawing, all rework shall fall within the applicable drawing dimensions. Such reworked areas shall be macroetched prior to reinspection by fluorescent penetrant inspection. Etching procedures shall be approved by the Purchaser.
- 4.4.3 No rework of fluorescent penetrant indications is permitted on the pressure faces or root radii of dovetail serrations.
- 4.4.4 When specified on the drawing, finish machined parts shall be etched on all surface areas prior to fluorescent penetrant inspection, by procedures approved by the Purchaser.

4.5     Ultrasonic Inspection

- 4.5.1   All parts shall be ultrasonic inspected by a method and with limits as agreed upon between purchaser and vendor.

4.6     Metallographic Inspection

- 4.6.1   Representative heat treated parts from each lot to each part number shall be examined per a Quality Control Plan approved by the Purchaser.
- 4.6.2   Microstructure shall be determined on polished and etched specimens at 100X magnification.
- 4.6.3   Evidence of an oxide case (white layer) shall be determined on polished and etched specimens at 500X magnification. A maximum alpha case thickness of 0.005" is permitted on as-HIP surfaces.
- 4.6.4   A microhardness traverse may be performed by the Purchaser to determine the depth of surface contamination.

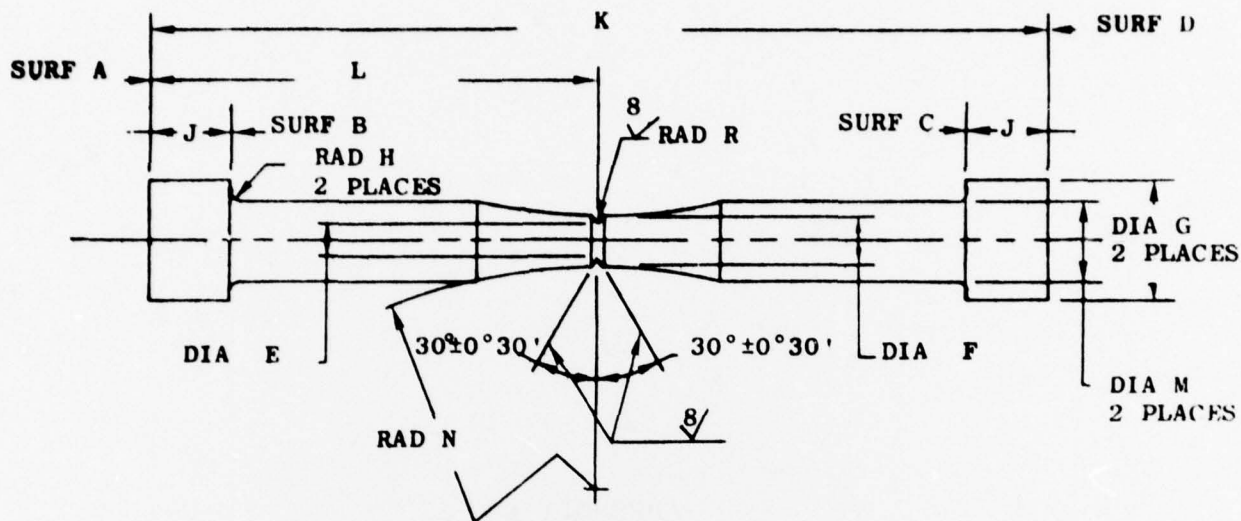
5.     PREPARATION FOR DELIVERY

5.1     Packing

- 5.1.1   All parts shall be suitable packed to prevent damage or loss in shipment.

5.2     Marking

- 5.2.1   Each shipment shall be legibly marked with the purchase order number, manufacturer's name, part name and drawing number.



$K_t$	R Inches	R mm
1.5	.0910	2.311
1.6	.0721	1.831
1.7	.0591	1.501
1.8	.0489	1.242
1.9	.0422	1.072
2.0	.0363	0.922
2.1	.0316	0.803
2.4	.0225	0.572
2.5	.0204	0.518
2.6	.0184	0.467
2.9	.0142	0.361
3.0	.0131	0.333
3.1	.0120	0.305
3.4	.0096	0.244
3.5	.0090	0.229
3.6	.0084	0.213

NOTES:

1. All dimensions are in inches, with SI Units in millimeters.
2. Unless otherwise specified, all surfaces are 32.
3. Remove burrs and sharp edges with .015 inch (0.381 mm) max. radius or chamfer (except notch).
4. Diameter "G" to be concentric within .001 inch (0.025 mm); all other diameters to be concentric within .0005 inch (0.013 mm).
5. Remove notch edges with  $.005 \pm .001$  inch ( $0.127 \pm 0.025$  mm) radius.
6. Surfaces A, B, C, and D to be perpendicular to centerline within .001 inch (0.025 mm).
7. Notch and radius "N" to be stress free ground.
8. Lathe centers permitted, .20 inch (5.08 mm) max. depth.
9. Notch radius to be "R"  $\pm .0005$  inch ( $\pm 0.013$  mm).

E	F	G	H	J	K	L	M	N
.249	.353	.748	.030	.340	3.90	1.995	.499	2.95
.251	.355	.750	.050	.360	4.10	2.005	.501	3.05

SI UNITS

6.325	8.966	18.999	0.76	8.64	99.1	50.67	12.675	74.9
6.375	9.017	19.050	1.27	9.14	104.1	50.93	12.725	77.5

Figure H-1. Notched Low-Cycle Fatigue Test Specimen.

APPENDIX I

TENTATIVE SPECIFICATION NO. 5114-4

PREMIUM QUALITY, POWDER METALLURGY AS-HOT ISOSTATIC  
PRESSED (HIP) Ti-6-4 TITANIUM BASE ALLOY PARTS



## APPENDIX I

### TENTATIVE SPECIFICATION NO. 5114-4

#### PREMIUM QUALITY, POWDER METALLURGY AS-HOT ISOSTATIC PRESSED (HIP) Ti-6-4 TITANIUM BASE ALLOY PARTS

#### 1. SCOPE

1.1 Scope: This specification presents requirements for Ti-6-4 titanium base alloy powder metallurgy as-HIP parts.

1.1.1 Classification: This specification contains the following classes:

Class A - Standard Ti-6-4 Composition per 5114-1

Class B - ELI Ti-6-4 Composition per 5114-1

1.1.2 Condition: Shapes shall be supplied in the following conditions as specified (6.4):

Condition H - As-HIP

Condition A - Annealed

Condition ST - Solution heat treated

Condition STA - Solution heat treated and aged

Condition DA - Duplex annealed

The requirements specified herein apply to all classes unless otherwise specified.

1.2 Definitions: For purposes of this specification, the following definitions shall apply:

Purchaser - The procuring activity that issued the procurement document involving this specification.

Capability - The words "shall be capable of" or "capability test" indicate characteristics or properties required in the product but for which testing of each lot is not required. However, if such testing is performed by the Purchaser, material not conforming to the requirements shall be subject to rejection.

HIP - An acronym for hot-isostatic-pressing.

Macroetch - Etching of a metal surface for acceptance of gross structural details and defects for observation.

Premium Quality - Material which is produced under special process and quality control, used primarily for critical rotating parts.

"A" - Ratio - Alternating stress divided by the mean stress.

Lot - A group of HIP parts processed at the same time with identical process conditions and raw material source.

## 2. APPLICABLE DOCUMENTS

- 2.1 The following documents shall form a part of this specification to the extent specified herein. Unless a specific issue is specified, the latest revision shall apply.

### GENERAL SPECIFICATIONS

5114-1 Pre-Alloyed Titanium Powder

5114-2 Hot Isostatic Pressing (HIP) of Titanium Alloy Powder

### AMERICAN SOCIETY FOR TESTING AND MATERIALS

ASTM E8 Tension Testing of Metallic Materials

ASTM E399 Plane-Strain Fracture Toughness Testing of Metallic Materials

### AEROSPACE MATERIAL SPECIFICATIONS

AMS 2249 Chemical Check Analysis Limits-Titanium and Titanium Alloys

AMS 2645G Fluorescent Penetrant Inspection

3. REQUIREMENTS

- 3.1 Raw Material: Parts shall be produced from Class A powder of a titanium base alloy known as Ti-6-4 meeting the requirements of 5114-1.
- 3.2 Powder Process Requirements
- 3.2.1. Powder shall be obtained only from sources approved by the Purchaser.
- 3.2.2. HIP shapes shall be processed according to the requirements of Specification 5114-2.
- 3.3 First Article: Before production has commenced, reports of mechanical and metallurgical tests (4.2.1) of the first item tested to confirm the HIP technique shall be made available to the Purchaser or his authorized representative for approval. The approval of the first article sample authorizes the commencement of production but does not relieve the supplier of responsibility for compliance with all applicable provisions of this specification.
- 3.4 Design Documentation: Part drawings shall indicate:  
(a) configuration and dimensions of the finished shape, (b) alloy composition to be used, (c) location from which specimens shall be cut for first-article tests, (d) final heat treatment, and (e) required reference points or surfaces for NDE or machining.
- 3.5 Surface Contamination Control: The part drawing shall dimensionally define the limits for the contamination-free, heat treated end-product, meeting all the requirements of this specification. At the same time it shall provide excess metal volumes sufficient to assure that no contaminated zones remain after removal of excess metal.
- 3.6 Heat Treatment: Shapes of titanium alloys ordered in the as-HIP condition shall be capable of meeting the requirements of Table H-1 after solution heat treatment and aging or the requirements of Table H-2 after annealing. Parts ordered annealed shall conform to the requirements of Table H-2 as received and shall be capable of meeting the requirements of Table H-1 after solution heat treatment and aging. Parts ordered solution heat treated shall be capable of meeting the requirements of Table H-1 as received. Heat treatment shall be performed on the entire part, not on a localized area. All heat treatments shall be in accordance with the requirements of MIL-H-81200.

3.7 Metallographic Inspection

3.7.1 HIP parts shall exhibit a substantially uniform micro-structure.

3.7.2 The hardness at .005 inch from the surface shall not exceed the core hardness by more than 40 points Knoop (100 gram load).

3.8 Vendor's Certificate of Test

3.8.1 The vendor shall certify all chemical and mechanical tests herein specified. A certificate of test, in triplicate, on each lot supplied to this specification shall be mailed by the vendor to the machining vendor with or preceding the shipment. This certificate shall give the numerical results of all required tests and inspections and shall show that the results are in accordance with the requirements of this specification. If a heat appears in more than one lot of parts, the numerical results of the tests shall be recorded in the certificate of test for each of the lots of parts in which it appears. In addition, the certificate shall show the following information:

- (a) Purchase order number
- (b) Powder heat number
- (c) Serial number for each HIPing
- (d) Lot number for each HIPing
- (e) Heat treat lot number for each HIPing
- (f) Hydrogen content of finished HIPings, as determined on representative parts
- (g) Testing source for tensile, fracture, toughness, and low-cycle fatigue specimens if applicable
- (h) Specific heat treatment cycle used
- (i) Quantity
- (j) Specification number, CLASS, and revision number

3.9 Material Identification Record

3.9.1 A material identification record shall be submitted by the machining vendor to the Purchaser and shall include the following information:

- (a) HIPing vendor's certificate of test
- (b) Heat treat vendor
- (c) Specification number, CLASS, and revision number



### 3.10 Marking

- 3.10.1 The type of marking and location shall be as specified on the drawing.

## 4. QUALITY ASSURANCE PROVISIONS

### 4.1 General

- 4.1.1 The certificate of test for each lot or lots within a shipment shall report the data required by this specification for the number of sample items or test specimens as required by this specification, or as additionally directed by the Purchaser.
- 4.1.2 Unless otherwise specified, all testing shall be conducted in accordance with ASTM. All parts are subject to cut up upon receipt by the Purchaser and shall have the required properties throughout the product. The vendor shall inform the Purchaser of the test procedures used. Once these procedures are established, they shall not be changed without approval of the Purchaser.

### 4.2 Chemical Analysis

- 4.2.1 Chemical analyses shall be conducted in accordance with standard ASTM methods, or by methods agreed upon between Purchaser and vendor.
- 4.2.2 Chemical check analysis limits shall be in accordance with AMS 2249.

### 4.3 Mechanical Properties

#### 4.3.1 General

- 4.3.1.1 The number and frequency of mechanical property tests shall be in accordance with a Quality Control Plan approved by the Purchaser. The location of test specimens shall be as specified by the Purchaser. The machining and testing sources for all test specimens shall be subject to approval by the Purchaser.

#### 4.3.2 Tensile

- 4.3.2.1 Tensile specimens, taken per 4.3.1, shall be tested in accordance with the applicable requirements of ASTM E8.
- 4.3.2.2 For referee tensile tests, a strain rate of .005 inch per inch (0.005 mm per mm) per minute through the 0.2 percent yield strength shall be used.

#### 4.3.3 Fracture Toughness

4.3.3.1 Compact tension type fracture toughness specimens, taken per 4.3.1, shall be tested in accordance with the applicable requirements of ASTM E399. Thickness of test specimens shall be one inch (25.4 mm) unless otherwise specified. For HIPings less than one inch in thickness, fracture toughness test methods shall be as agreed between vendor and purchaser.

#### 4.3.4 Low-Cycle Fatigue

4.3.4.1 Low cycle fatigue test specimens, taken per 4.3.1, shall be machined to the configuration and dimensions shown in Figure H-1 with a  $K_t = 2.0$  stress concentration in the gage section. The notch shall be made using low stress grinding techniques to prevent the formation of high residual stresses in the surfaces.

#### 4.4 Fluorescent Penetrant Inspection

4.4.1 After completion of all processing operation, all parts shall be fluorescent penetrant inspected per AMS 2645G, in accordance with limits specified on the drawing.

4.4.2 Rework of fluorescent penetrant indications shall fall within the blend limits of the applicable drawings. All blends shall be smooth in contour with no sharp breaks or scratches within them. If no blend limits are shown on the drawing, all rework shall fall within the applicable drawing dimensions. Such reworked areas shall be macro-etched prior to reinspection by fluorescent penetrant inspection. Etching procedures shall be approved by the Purchaser.

4.4.3 No rework of fluorescent penetrant indications is permitted on the pressure faces or root radii of dovetail serrations.

4.4.4 When specified on the drawing, finish machined parts shall be etched on all surface areas prior to fluorescent penetrant inspection, by procedures approved by the Purchaser.

#### 4.5 Ultrasonic Inspection

4.5.1 All parts shall be ultrasonic inspected by a method and with limits as agreed upon between purchaser and vendor.

#### 4.6 Metallographic Inspection

4.6.1 Representative heat treated parts from each lot to each part number shall be examined per a Quality Control Plan approved by the Purchaser.

- 4.6.2 Microstructure shall be determined on polished and etched specimens at 100X magnification.
- 4.6.3 Evidence of an oxide case (white layer) shall be determined on polished and etched specimens at 500X magnification. A maximum alpha case thickness of 0.005" is permitted on as-HIP surfaces.
- 4.6.4 A microhardness traverse may be performed by the Purchaser to determine the depth of surface contamination.
- 5. PREPARATION FOR DELIVERY
  - 5.1 Packing
    - 5.1.1 All parts shall be suitably packed to prevent damage or loss in shipment.
  - 5.2 Marking
    - 5.2.1 Each shipment shall be legibly marked with the purchase order number, manufacturer's name, part name and drawing number.

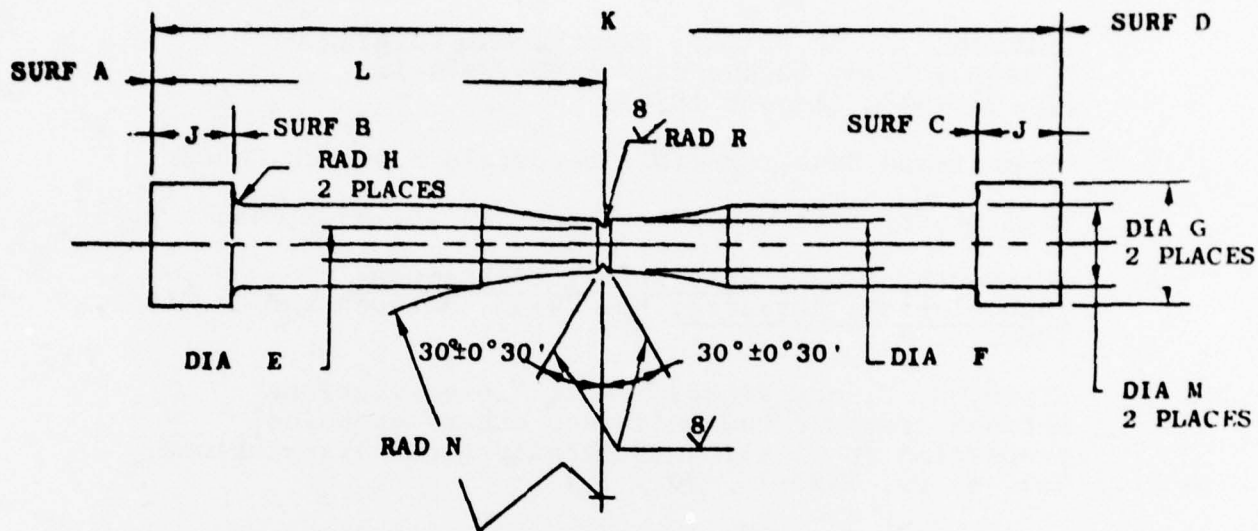
TABLE I-1  
PROPERTIES OF HEAT TREATED PARTS

<u>Composition</u>	<u>Strength (min)</u>		<u>Elong. (min)</u> <u>%</u>	<u>R.A. (min)</u> <u>%</u>
	<u>F<sub>tu</sub></u> <u>(ksi)</u>	<u>F<sub>ty</sub></u> <u>(ksi)</u>		
Ti-6-4	160	150	10	15
Ti-6-4 (ELI)	150	140	12	20

TABLE I-2  
PROPERTIES OF ANNEALED PARTS

<u>Composition</u>	<u>Strength (min)</u>		<u>Elong. (min)</u> <u>%</u>	<u>R.A. (min)</u> <u>%</u>
	<u>F<sub>tu</sub></u> <u>(ksi)</u>	<u>F<sub>ty</sub></u> <u>(ksi)</u>		
Ti-6-4	130	120	10	25
Ti-6-4 (ELI)	120	110	10	27





$K_t$	R Inches	R mm
1.5	.0910	2.311
1.6	.0721	1.831
1.7	.0591	1.501
1.8	.0489	1.242
1.9	.0422	1.072
2.0	.0363	0.922
2.1	.0316	0.803
2.4	.0225	0.572
2.5	.0204	0.518
2.6	.0184	0.467
2.9	.0142	0.361
3.0	.0131	0.333
3.1	.0120	0.305
3.4	.0096	0.244
3.5	.0090	0.229
3.6	.0084	0.213

NOTES:

1. All dimensions are in inches, with SI Units in millimeters.
2. Unless otherwise specified, all surfaces are 32/.
3. Remove burrs and sharp edges with .015 inch (0.381 mm) max. radius or chamfer (except notch).
4. Diameter "G" to be concentric within .001 inch (0.025 mm); all other diameters to be concentric within .0005 inch (0.013 mm).
5. Remove notch edges with .003 ± .001 inch (0.127 ± 0.025 mm) radius.
6. Surfaces A, B, C, and D to be perpendicular to centerline within .001 inch (0.025 mm).
7. Notch and radius "N" to be stress free ground.
8. Lathe centers permitted, .20 inch (5.08 mm) max. depth.
9. Notch radius to be "R" ± .0005 inch (± 0.013 mm).

E	F	G	H	J	K	L	M	N
.249	.353	.748	.030	.340	3.90	1.995	.499	2.95
.251	.355	.750	.030	.360	4.10	2.005	.501	3.05

SI UNITS

6.325	8.966	18.999	0.76	8.64	99.1	50.67	12.675	74.9
6.375	9.017	19.050	1.27	9.14	104.1	50.93	12.725	77.5

Figure I-1. Notched Low-Cycle Fatigue Test Specimen.

#### REFERENCES

1. Kulkarni, K. M. et al., "Isothermal Forging of Titanium Alloy Bulkheads," AFML-TR-74-138, AD #923-548L (August 1974).
2. Unpublished Data, Crucible Materials Research Center.
3. Preliminary Data under Contract F33615-74-C-1449.
4. Duckworth, W. E., Statistical Techniques in Technological Research, pp. 24-35, Methuen and Co. Ltd., 1968.
5. Hirth, J. P. and Froes, F. H., "Interrelations between fracture toughness and other mechanical properties in Ti alloys," Metallurgical Transactions, Vol. 8, pp. 1165-76, July 1977.
6. Sprague, R. A., "Low-Cycle Fatigue Properties of Titanium Alloys," presented at the New York University Titanium Metallurgy Course, September 1969.
7. Pierce et al., "Some Observations Pertaining to Simple Fracture Toughness Screening Tests for Titanium," AFML-TR-70-311, AD #725-750, July 1969 - August 1970, WPAFB, Ohio.
8. Eylon, D. and Birla, N., "Fatigue Origins in Beta III Powder Compacts," Metallurgical Transactions "A", Volume 8A, pp. 367, February 1977.